A POSTERIORI ERROR ANALYSIS OF FINITE ELEMENT METHOD FOR PARABOLIC INTERFACE PROBLEMS

by

JHUMA SEN GUPTA

DEPARTMENT OF MATHEMATICS
INDIAN INSTITUTE OF TECHNOLOGY GUWAHATI
GUWAHATI-781039, INDIA

April, 2015

A POSTERIORI ERROR ANALYSIS OF FINITE ELEMENT METHOD FOR PARABOLIC INTERFACE PROBLEMS

A thesis submitted

in partial fulfillment of the requirements

for the degree of

DOCTOR OF PHILOSOPHY

by

Jhuma Sen Gupta

(Roll No. 09612311)

DEPARTMENT OF MATHEMATICS

INDIAN INSTITUTE OF TECHNOLOGY GUWAHATI

GUWAHATI - 781039, INDIA

April, 2015

To my beloved parents
Baba (Himangshu Sen Gupta)
and
Maa (Dharitri Sen Gupta)

Certificate

It is certified that the work contained in this thesis entitled **"A posteriori error analysis of finite element method for parabolic interface problems"** by **Jhuma Sen Gupta,** a student of Department of Mathematics, Indian Institute of Technology Guwahati, for the award of the degree of Doctor of Philosophy has been carried out under my supervision and that this work has not been submitted elsewhere for a degree.

April, 2015

Dr. Rajen Kumar Sinha
Professor
Department of Mathematics
Indian Institute of Technology Guwahati

Acknowledgement

This journey would not have been possible without the support and help of numerous people. It is my pleasure to write a note of thanks to all those who contributed in many ways to the successful completion of my PhD and made it an unforgettable experience for me.

First and foremost, I feel it a great privilege to express my deepest and the most sincere gratitude to my supervisor Prof. Rajen Kumar Sinha for his invaluable guidance, enduring support and constant encouragement throughout this work. I am particularly grateful to him for listening to my countless queries with patience and providing insightful comments which helped to make my Ph.D experience productive and stimulating. I am much indebted to him for spending his precious time into reading this thesis and providing the valuable suggestions and advice which helped to make this thesis worthwhile. I am also thankful to him for making me feel free to express my views and for sharing an excellent rapport with me. Apart from academics, he taught me many things that helped me broaden my perspective in life.

I would like to thank the doctoral committee members Prof. D. C. Dalal, Prof. S. Natesan and Dr. K.V. Srikanth for their useful comments and suggestions during the progress of my work. I express my sincere thanks to all the faculty members of the Department of Mathematics for their help and cooperations.

Words fail me to express my deepest gratitude to Dr. Anjan K. Chakrabarty whose dedicated teaching, priceless advices and enormous help during my M.Sc brought me here. I will forever be thankful to him for his motivation and encouragement to pursue research at IIT. His emphasis on mathematical rigor and incredible understanding helped me to broaden my knowledge in the subject. I again owe my thankfulness to him for his help on various occasions at IIT Guwahati.

I take this opportunity to thank the Head, Department of Mathematics, IIT Guwahati for providing me the necessary facilities during my research work. I also thank the Ministry of Human and Resource Development, Govt. of India, for offering me financial assistance to carry out my research work. I express my thanks to our lab assistants Santanu da and Pranpratim da for their help. Sridhar da, Phatik da, Saurav da and Manoj da also deserve special thanks

for their assistance in all official matters.

My special thanks to the senior research mate Murali da for helping me in the computational work. It would be unfair if I donot acknowledge some of my friends with whom I shared my research experiences and lived many memorable moments. I take this opportunity to say heartful thanks to Namita di, Chitralekha and Deepanwita. We spent many enjoyable moments together inside and outside the campus which I will always treasure. I convey a special thanks to Gayatri, Saloni and Bini who helped me in various ways at IIT Guwahati. I am also thankful to my current and former colleagues: Manideepa di, Rajbhavan da, Dishari, Neelam, Pratibha, Tanushree, Tamal as well as many others for their help and cooperation at IIT Guwahati.

I also expand my thanks to Prof. R. K. Sinha and Rupa (ma'am) for their affection and love which gave me homely feeling during my stay at IIT Guwahati.

Words can never be enough to express my deepest sense of gratitude towards my family. Last, but far from least, I especially thank my parents Baba and Maa for their never ending encouragement, great moral support and inspiration which helped me to reach up to this stage. I would also like to express my deepest appreciation and love to my precious younger sister Dula (Bonu) for cheering me all time. The endless thanks goes to Dadumoni for all the blessings he has showered onto me. I thank my well wishers and all people who have helped me directly or indirectly in this journey whose name I may have inadvertently forgotten. Above all, I thank the almighty God for everything.

April, 2015

With regards,

(**Jhuma Sen Gupta**)

Department of Mathematics

Indian Institute of Technology Guwahati

"A mathematician's nightmare is a sequence n_ϵ that tends to 0 as ϵ becomes infinite."

Paul R. Halmos

Abstract

The primary aim of this thesis is to study *a posteriori* error analysis of parabolic interface problems in a bounded convex polygonal domain in $\mathbb{R}^2$. Interface problems arise in various applications ranging from material science to fluid dynamics when two distinct materials or fluids with different conductivities or densities or diffusion coefficients are involved. Due to the discontinuity of the coefficient along the interface, the solution has a lower regularity in the entire domain. Therefore, it is not so straightforward to extend the analysis of the parabolic problem to the parabolic interface problems. This thesis attempts to extend *a posteriori* error analysis of parabolic problems to the parabolic interface problems.

A residual-based *a posteriori* error estimates for both the spatially discrete and the fully discrete approximations are considered and analyzed. The residual-based *a posteriori* error analysis relies on the approximation properties of the Clément-type interpolation operator introduced by Scott and Zhang [92]. However, to obtain $O(h^2)$ convergence with the piecewise linear elements for such type of operator, one requires the global H^2 regularity of the solution. But, as the solution of the parabolic interface problem is only in $H^1(\Omega)$ globally and hence, the standard approximation properties do not apply directly for the interface problems. Therefore, new approximation properties for the Clément-type interpolation operator are derived in this thesis. An appropriate elliptic reconstruction operator along with the new approximation results are used to derive *a posteriori* error bounds for the parabolic interface problems. Almost optimal order *a posteriori* error estimates are obtained in the $L^\infty(L^2)$-norm for the the spatially discrete approximation.

The fully discrete space-time finite element discretizations based on the backward Euler, the Crank-Nicolson (CN) and the two-step backward differentiation formula (BDF-2) approximations are also studied in this thesis. The CN approximation is one of the most popular time-stepping method but it has the lack of smoothing property of the solution operator, whereas the two-step BDF method exhibits the smoothing property of the solution. The essential ingredients in both the CN and BDF-2 error analysis are the continuous piecewise quadratic space-time reconstructions and the new Clément-type interpolation estimates. Op-

timal order in time and almost optimal order in space *a posteriori* estimates are derived in the $L^\infty(L^2)$-norm.

In addition, we have also extended our analysis to treat the semilinear parabolic interface problems. *A posteriori* error analysis for both the backward Euler and the Crank-Nicolson approximations are presented. An appropriate modifications of elliptic reconstruction and use of the new interpolation results are used to derive *a posteriori* estimates which are of optimal order in time and almost optimal in space.

Finally, numerical experiments for a two dimensional test problem are performed to study the asymptotic behaviour of the various error estimators for the linear parabolic interface problems.

Contents

List of Symbols

$\mathbb{N}$	The set of natural numbers
$\mathbb{Z}_+$	The set of non-negative integers
$\mathbb{R}^n$	n-dimensional Euclidean space
$\bar{A}$	The closure of a set $A \subset \mathbb{R}^2$
A°	The interior of a set $A \subset \mathbb{R}^2$
∂A	The boundary of a set A
$m(A)$	The standard Lebesgue measure of a set $A \subset \mathbb{R}^2$
$\operatorname{card} A$	The cardinality of a set A
Ω	Bounded convex polygonal domain in $\mathbb{R}^n$
$\partial\Omega$	Lipschitz boundary of Ω
Ω_1	Subdomain of Ω
$\partial\Omega_1 := \Gamma$	Boundary of Ω_1 (interface)
u	The exact solution of the parabolic interface problem
β	Diffusion coefficient
f	Forcing term
u_0	Initial function
$[v]$	Jump of a quantity v across the interface Γ
$\mathbf{n}$	Unit outward normal to the interface Γ
$D^\alpha\phi$	One of the partial derivative of order $\lvert\alpha\rvert$ of $\phi : \mathbb{R}^n \to \mathbb{R}$
$\operatorname{supp}\phi$	Support of a function ϕ
$C^m(\bar{\Omega}), m \in \mathbb{Z}_+$	The space of m times continuously differentiable function on $\bar{\Omega}$
$C_0^m(\Omega), m \in \mathbb{Z}_+$	The space of all C^m functions with compact support in Ω
$C_0^\infty(\Omega)$	The space of all infinitely differentiable functions with compact support in Ω

$L^p(\mathcal{M})$	The Lebesgue spaces of order $p\,(1 \leq p \leq \infty)$ over a Lebesgue measurable set $\mathcal{M}$
$\|\cdot\|_{L^p(\mathcal{M})}$	Norm on $L^p(\mathcal{M})$
$\langle\cdot,\cdot\rangle_{\mathcal{M}}$	Standard L^2 inner product on $\mathcal{M}$
$W^{m,p}(\mathcal{M})$	The Sobolev Spaces of order $(m,p), m \in \mathbb{N}$ and $1 \leq p \leq \infty$ over a Lebesgue measurable set $\mathcal{M}$
$\|\cdot\|_{W^{m,p}(\mathcal{M})}$	Norm on $W^{m,p}(\mathcal{M})$
$\|\cdot\|_{W^{m,p}(\mathcal{M})}$	Semi-norm on $W^{m,p}(\mathcal{M})$
$H^m(\Omega)$	Sobolev Hilbert space $W^{m,2}(\Omega)$ $(m \in \mathbb{N})$
$\|\cdot\|_{H^m(\Omega)}$	Norm on $H^m(\Omega)$
$\|\cdot\|_{H^m(\Omega)}$	Semi-norm on $H^m(\Omega)$
$H_0^m(\Omega)$	The completion of $C_0^\infty(\Omega)$ in H^m-norm
$L^p(0,T;\mathbf{B})$	The standard Bochner space with $\mathbf{B}$ is a Banach space $(1 \leq p \leq \infty)$
$\|\cdot\|_{L^p(0,T;\mathbf{B})}$	Norm on $L^p(0,T;\mathbf{B})$
$C(0,T;\mathbf{B})$	The space of continuous function $\phi : [0,T] \to \mathbf{B}$
$\|\cdot\|_{C(0,T;\mathbf{B})}$	Norm on $C(0,T;\mathbf{B})$
$a(\cdot,\cdot)$	Bilinear form
α_0	Continuity constant for $a(\cdot,\cdot)$
γ_0	Coercivity constant for $a(\cdot,\cdot)$
$\mathcal{T}_h$	Shape regular, conforming triangulation of $\bar{\Omega}$ for the spatially discrete finite element approximation
$\mathcal{T}_h^*$	Set of all interface triangles
$\mathcal{T}_h \setminus \mathcal{T}_h{}^*$	Set of all non-interface triangles
S_K	Patch of a triangle K
$\mathcal{E}_h$	Set of all internal edges of the triangles in $\mathcal{T}_h$
$\mathcal{E}_h^*$	Set of all edges of the interface triangles in $\mathcal{T}_h{}^*$

$\mathcal{E}_h \setminus \mathcal{E}_h^*$	Set of all internal edges of the non-interface triangles in $\mathcal{T}_h \setminus \mathcal{T}_h{}^*$
Σ_h	Union of all internal edges in $\mathcal{E}_h$
$\mathbb{S}_h$	Finite element space for the spatially discrete approximation
$\mathbb{P}_1(K)$	The space of polynomials of degree at most 1 over K
Π_0^h	L^2-projection operator corresponding to the finite element space $\mathbb{S}_h$
$\mathcal{A}_h$	Discrete elliptic operator corresponding to the bilinear form $a(\cdot,\cdot)$ for the spatially discrete approximation
$\mathscr{J}_h$	The Clément-type interpolation operator corresponding to the finite element space $\mathbb{S}_h$
$\mathcal{R}_h$	Elliptic reconstruction operator for the spatially discrete approximation
$\mathbf{R}_h(u_h)$	Element residual associated with the spatially discrete approximation
$\mathbf{J}_h(u_h)$	Jump residual associated with the spatially discrete approximation
$\varepsilon(t)$	Elliptic reconstruction error
$\rho(t)$	Parabolic error
$\mathscr{O}_{\mathrm{S},h}(u_h(t))$	Elliptic reconstruction error estimator in the L^2-norm for the spatially discrete approximation
$\mathscr{M}_{\mathrm{S},h}(u_h(t))$	Spatial error estimator for the spatially discrete approximation
$\mathcal{T}_n$	Shape regular, conforming triangulation of $\bar{\Omega}$ for the fully discrete finite element approximation
$\mathbb{S}^n$	The finite element space for the fully discrete approximation
$\mathcal{E}_n$	Set of all internal edges of the triangles in $\mathcal{T}_n$
Σ_n	Union of all internal edges in $\mathcal{E}_n$
$U(t)$	Continuous, piecewise linear approximation in time of $u(t)$
Π_0^n	L^2-projection operator corresponding to the finite element space $\mathbb{S}^n$
$\mathcal{A}_h^n$	Discrete elliptic operator corresponding to the bilinear form $a(\cdot,\cdot)$ for the fully discrete approximation

$\mathscr{J}_n$	The Clément-type interpolation operator corresponding to the finite element space $\mathbb{S}^n$
$\mathcal{R}^n$	Elliptic reconstruction operator for the fully discrete approximation of linear parabolic interface problem
$\Theta(t)$	Linear space-time reconstruction of the fully discrete approximate solution
$\mathbf{R}_n$	Element residual for the fully discrete backward Euler approximation
$\mathbf{J}_n$	Jump residual for the fully discrete backward Euler approximation
$\mathscr{O}_{\mathrm{BE},1,n}$	Elliptic reconstruction error estimator for the fully discrete backward Euler approximation in the H^1-norm
$\mathscr{O}_{\mathrm{BE},2,n}$	Elliptic reconstruction error estimator for the fully discrete backward Euler approximation in the L^2-norm
$\mathscr{M}_{\mathrm{BE},n}$	Space-mesh error estimator for the fully discrete backward Euler approximation
$\mathscr{T}_{\mathrm{e,BE},n}$	Temporal error estimator for the fully discrete backward Euler approximation
$\mathscr{D}_{\mathrm{BE},n}$	Data approximation error estimator for the fully discrete backward Euler approximation
$\tilde{\Phi}(t)$	Continuous piecewise linear approximation of $f(t)$
$\tilde{U}(t)$	Crank-Nicolson reconstruction
$\tilde{\rho}(t)$	Parabolic error for the fully discrete Crank-Nicolson approximation
$\tilde{\sigma}(t)$	Time reconstruction error for the fully discrete Crank-Nicolson approximation
$\mathscr{O}_{\mathrm{CN},n}$	Elliptic reconstruction error estimator for the fully discrete Crank-Nicolson approximation
$\mathscr{M}_{\mathrm{CN},n}$	Space-mesh error estimator for the fully discrete Crank-Nicolson approximation
$\mathscr{T}_{\mathrm{re,CN},n}$	Temporal reconstruction error estimator for the fully discrete Crank-Nicolson approximation
$\mathscr{S}_{\mathrm{CN},n}$	Space-error estimator for the fully discrete Crank-Nicolson approximation

$\mathscr{T}_{\mathrm{e,CN},n}$	Temporal error estimator for the fully discrete Crank-Nicolson approximation
$\mathscr{C}_{\mathrm{CN},n}$	Coarsening error estimator for the fully discrete Crank-Nicolson approximation
$\mathscr{D}_{\mathrm{CN},n,1}, \mathscr{D}_{\mathrm{CN},n,2}$	Data approximation error estimators for the fully discrete Crank-Nicolson approximation
$\hat{\Phi}(t)$	Piecewise linear approximation of $f(t)$
$\hat{U}(t)$	BDF-2 reconstruction
$\hat{\rho}(t)$	Parabolic error for the fully discrete BDF-2 approximation
$\hat{\sigma}(t)$	Time reconstruction error for the fully discrete BDF-2 approximation
$\mathscr{O}_{\mathrm{BDF},n}$	Elliptic reconstruction error estimator for the fully discrete BDF-2 approximation
$\mathscr{M}_{\mathrm{BDF},n}$	Space-mesh error estimator for the fully discrete BDF-2 approximation
$\mathscr{T}_{\mathrm{re,BDF},n}$	Temporal reconstruction error estimator for the fully discrete BDF-2 approximation
$\mathscr{S}_{\mathrm{BDF},n}$	Space-error estimator for the fully discrete BDF-2 approximation
$\mathscr{T}_{\mathrm{e,BDF},n}$	Temporal error estimator for the fully discrete BDF-2 approximation
$\mathscr{C}_{\mathrm{BDF},n}$	Coarsening error estimator for the fully discrete BDF-2 approximation
$\mathscr{D}_{\mathrm{BDF},n,i}\,(i=1,2)$	Data approximation error estimators for the fully discrete BDF-2 approximation
$\mathcal{R}_b^n$	Elliptic reconstruction operator for the fully discrete backward Euler approximation of the semilinear problem
$\mathcal{R}_c^n$	Elliptic reconstruction operator for the fully discrete Crank-Nicolson approximation of the semilinear problem

$\bar{\rho}(t)$	Parabolic error for the fully discrete backward Euler approximation of the semilinear problem
$\bar{\varepsilon}(t)$	Elliptic reconstruction error for the fully discrete backward Euler approximation of the semilinear problem
$\breve{\Phi}(t)$	Piecewise linear approximation in time of $f(t,u)$
$\bar{\Theta}(t)$	Linear space-time reconstruction for the backward Euler approximation of the semilinear problem
$\breve{U}(t)$	Crank-Nicolson reconstruction for the semilinear problem
$\breve{\varepsilon}(t)$	Elliptic reconstruction error for the fully discrete Crank-Nicolson approximation of the semilinear problem
$\breve{\rho}(t)$	Parabolic error for the fully discrete Crank-Nicolson approximation of the semilinear problem
$\breve{\sigma}(t)$	Time reconstruction error for the fully Crank-Nicolson approximation of the semilinear problem
$\breve{\Theta}(t)$	Linear space-time reconstruction for the Crank-Nicolson approximation of the semilinear problem
$\mathscr{O}_{\mathrm{SBE},n}$	Elliptic reconstruction error estimator for the fully discrete backward Euler approximation of the semilinear problem
$\mathscr{M}_{\mathrm{SBE},n}$	Space-mesh error estimator for the fully discrete backward Euler approximation of the semilinear problem
$\mathscr{T}_{\mathrm{e,SBE},n}$	Temporal error estimator for the fully discrete backward Euler approximation of the semilinear problem
$\mathscr{D}_{\mathrm{SBE},n,i}\,(i=1,2)$	Data approximation error estimators for the fully discrete backward Euler approximation of the semilinear problem
$\mathscr{O}_{\mathrm{SCN},n}$	Elliptic reconstruction error estimator for the fully discrete Crank-Nicolson approximation of the semilinear problem

$\mathscr{M}_{\mathrm{SCN},n}$	Space-mesh error estimator for the fully discrete Crank-Nicolson approximation of the semilinear problem
$\mathscr{T}_{\mathrm{re,SCN},n}$	Temporal reconstruction error estimator for the fully discrete Crank-Nicolson approximation of the semilinear problem
$\mathscr{S}_{\mathrm{SCN},n}$	Space-error estimator for the fully discrete Crank-Nicolson approximation of the semilinear problem
$\mathscr{T}_{\mathrm{e,SCN},n}$	Temporal error estimator for the fully discrete Crank-Nicolson approximation of the semilinear problem
$\mathscr{C}_{\mathrm{SCN},n}$	Coarsening error estimator for the fully discrete Crank-Nicolson approximation of semilinear problem
$\mathscr{D}_{\mathrm{SCN},n,i}, i \in \{1,2,3,4\}$	Data approximation error estimators for the fully discrete Crank-Nicolson approximation of the semilinear problem
$\mathcal{C}_P$	Poincare's constant
$\mathcal{C}_G$	Gronwall's constant
$\mathcal{C}_R$	Elliptic regularity constant
$\mathcal{C}_L$	Lipschitz constant
$\mathcal{C}_{I,k}, k \in \{1,\ldots,4\}$	Interpolation constants

List of Figures

List of Tables

1 Introduction

The main objective of this thesis is to study *a posteriori* error analysis of the finite element method for the parabolic interface problems. This chapter introduces the problem and serves to provide some necessary background for the work to follow. It also contains a brief survey of the relevant literature and motivation for the present work. Finally, the organization of the thesis is described in the last section of this chapter.

1.1 Problem Statement

Let Ω be a bounded convex polygonal domain in $\mathbb{R}^2$ with Lipschitz boundary $\partial\Omega$, and let Ω_1 be a subdomain of Ω with C^2 boundary $\partial\Omega_1 := \Gamma$ (see, Fig. 1.1). The interface Γ divides the domain Ω into two subdomains Ω_1 and $\Omega_2 := \Omega \setminus \Omega_1$. Consider the linear parabolic interface problem of the form

$$u_t(x,t) - \mathrm{div}(\beta(x)\nabla u(x,t)) = f(x,t) \quad \text{in} \quad \Omega \times (0,T] \tag{1.1.1}$$

with prescribed initial and boundary conditions

$$u(x,0) = u_0(x) \quad \text{in} \quad \Omega; \qquad u = 0 \quad \text{on} \quad \partial\Omega \times [0,T] \tag{1.1.2}$$

and jump conditions on the interface

$$[u] = 0, \quad \left[\beta \frac{\partial u}{\partial \mathbf{n}}\right] = 0 \quad \text{across} \quad \Gamma \times [0,T], \tag{1.1.3}$$

where $u_t = \frac{\partial u}{\partial t}$, $[v]$ denotes the jump of a quantity v across the interface Γ, i.e., $[v](x) = v_1(x) - v_2(x)$, $x \in \Gamma$ with $v_i(x) = v(x)|_{\Omega_i}$, $i = 1, 2$, and $T < +\infty$. The symbol $\mathbf{n}$ denotes the unit outward normal to the boundary $\partial\Omega_1 := \Gamma$. The diffusion coefficient $\beta(x)$ is assumed to be positive and piecewise constant on each subdomain, i.e.,

$$\beta(x) = \beta_i \quad \text{for} \quad x \in \Omega_i, \ i = 1, 2.$$

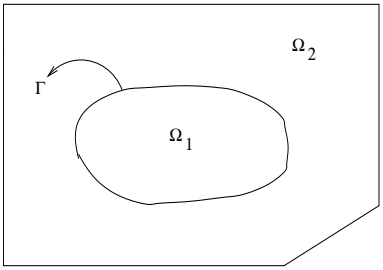

Figure 1.1: *Domain Ω with subdomains Ω_1, Ω_2 and the interface Γ.*

The initial data $u_0(x)$ and the forcing term $f(x,t)$ are real valued functions and are assumed to be smooth. Further, the interface is assumed to be of arbitrary shape but is of class C^2 for our purpose.

Interface problems arise in various physical applications such as in material science, fluid dynamics, solid mechanics, electrodynamics, biomedical and chemical engineering and so on. The study of parabolic interface problems is motivated by the models of heat conduction in composite materials (cf. Ladyženskaja *et al.* [61]), heat-mass transfer problem (cf. Jovanović and Vulkov [57]), transport of a dissolved species in two-phase incompressible flow problems (cf. Reusken and Nguyen [90]), viscoplasticity and plasticity with hardening as well as perfect plasticity (cf. Carstensen [31]), eddy current in electromagnetic field theory (cf. Aldroubi and Renardy [7], Lumer and Weis [73] and MacCamy and Suri [75]) and cellular signal transduction (cf. Cangiani and Natalini [30]). Other interesting models include simulation of the electric potential [66], water flow in porous media with a source at the interface [80], air-vapour-heat transport through textile materials [106], electrokinetic flows [25] and solute dynamics across arterial walls [29]. In particular, the case $[u] = 0$ and $\left[\beta \frac{\partial u}{\partial \mathbf{n}}\right] = 0$ models the transport of a dissolved species in two-phase incompressible flow problems, see [90].

Interface problems are often referred to as differential equations with discontinuous coefficients. The discontinuity in the coefficient is because of the physical phenomena described above separating two materials or two states. Because of the discontinuity of the coefficients along the interface Γ, the interface problems usually lead to non-smooth solutions. Due to the inherent complexity of these problems and low global regularity of solutions, the convergence analysis (both *a priori* and *a posteriori* error analysis) of these problems has remained a major part of the mathematical study up to the present day. *A posteriori* error analysis of time-dependent problems has attracted much attention in recent years from both the theoretical and numerical point of view. The theory of *a posteriori* error analysis of finite element method for interface problems is a

challenging issue in the past few years and yet to be thoroughly explored. Therefore, an attempt has been made in this thesis to address some of these aspects such as $L^\infty(L^2)$-norm *a posteriori* error analysis for the various space-time discretization methods for the parabolic interface problems by means of the energy technique.

1.2 Notations and Prerequisites

In this section, we introduce some standard notations, function spaces and recall some basic results to be used in this thesis. All functions considered here are real valued. For the purpose of introducing notations, we assume that Ω is a polygonal domain in $\mathbb{R}^n$ with boundary $\partial\Omega$. Let $x = (x_1, x_2, \ldots, x_n)$ be an n-tuple with $dx := dx_1 dx_2 \ldots dx_n$. By the order of α, where $\alpha = (\alpha_1, \alpha_2, \ldots, \alpha_n)$ with $\alpha_i \in \mathbb{Z}_+$ (the set of non-negative integers) we mean $|\alpha| := \alpha_1 + \alpha_2 + \cdots + \alpha_n$. Then $D^\alpha\phi$ denotes one of the $|\alpha|^{\text{th}}$ order partial derivatives of ϕ and is given by

$$D^\alpha\phi := \frac{\partial^{|\alpha|}\phi}{\partial x_1^{\alpha_1}\,\partial x_2^{\alpha_2}\ldots\partial x_n^{\alpha_n}}.$$

By the support of a function ϕ on Ω we mean

$$\operatorname{supp}\phi := \overline{\{x \in \Omega \mid \ \phi(x) \neq 0\}}.$$

We say that ϕ has a compact support in Ω if $\operatorname{supp}\phi$ is a compact set in Ω.

Function Spaces. For any non-negative integer m, $C^m(\bar{\Omega})$ is defined as the space of m times continuously differentiable functions on $\bar{\Omega}$. Let $C_0^m(\Omega)$ be the space of all $C^m(\Omega)$ functions with compact support in Ω. Further, $C_0^\infty(\Omega)$ is the space of all infinitely differentiable functions with compact support in Ω.

Given a Lebesgue measurable set $\mathcal{M} \subset \mathbb{R}^n$ and $1 \leq p \leq \infty$, the Lebesgue spaces $L^p(\mathcal{M})$ refer to the linear space of equivalence classes of measurable functions ϕ on $\mathcal{M}$ such that $\|\phi\|_{L^p(\mathcal{M})} < \infty$, where

$$\begin{aligned} \|\phi\|_{L^p(\mathcal{M})} &:= \left(\int_{\mathcal{M}} |\phi(x)|^p dx\right)^{\frac{1}{p}}, \quad 1 \leq p < \infty, \\ \|\phi\|_{L^\infty(\mathcal{M})} &:= \operatorname*{ess\,sup}_{x\in\mathcal{M}} |\phi(x)| < \infty, \quad p = \infty. \end{aligned}$$

In particular, $L^2(\mathcal{M})$ is a Hilbert space with respect to the norm $\|\cdot\|_{L^2(\mathcal{M})} = \|\cdot\|_{\mathcal{M}}$ induced by the inner product $\langle\phi,\psi\rangle_{\mathcal{M}} = \int_{\mathcal{M}} \phi(x)\psi(x)dx$.

We now introduce the notion of Sobolev spaces. Let $m > 0$ be an integer and $1 \leq p \leq \infty$. The Sobolev space $W^{m,p}(\mathcal{M})$ is defined as a linear spaces of functions (or

equivalence classes of functions) in $L^p(\mathcal{M})$ such that all distributional derivatives up to order m are also in $L^p(\mathcal{M})$, i.e.,

$$W^{m,p}(\mathcal{M}) := \{\phi \in L^p(\mathcal{M}) \mid D^\alpha \phi \in L^p(\mathcal{M}) \text{ for all } |\alpha| \leq m\}.$$

The spaces $W^{m,p}(\mathcal{M})$ are Banach spaces with norms

$$\|\phi\|_{W^{m,p}(\mathcal{M})} := \left(\sum_{|\alpha| \leq m} \|D^\alpha \phi\|^p_{L^p(\mathcal{M})} \right)^{\frac{1}{p}} \quad \text{for} \quad 1 \leq p < \infty,$$

and

$$\|\phi\|_{W^{m,\infty}(\mathcal{M})} := \max_{|\alpha| \leq m} \|D^\alpha \phi(x)\|_{L^\infty(\mathcal{M})} \quad \text{for} \quad p = \infty.$$

Also, the semi-norms on $W^{m,p}(\mathcal{M})$ are defined as

$$|\phi|_{W^{m,p}(\mathcal{M})} := \sum_{|\alpha|=m} \|D^\alpha \phi\|_{L^p(\mathcal{M})}.$$

For $p = 2$, we denote the spaces $W^{m,2}(\mathcal{M})$ by $H^m(\mathcal{M})$ with the norm $\|\cdot\|_{H^m(\mathcal{M})}$ and the semi-norm $|\cdot|_{H^m(\mathcal{M})}$. For simplicity of notations, whenever $\mathcal{M} = \Omega$, we will denote $\|\cdot\|_{L^2(\Omega)}$ by $\|\cdot\|$ and $\|\cdot\|_{H^1(\Omega)}$ by $\|\cdot\|_1$.

The Sobolev space $H^m(\Omega)$ is a Hilbert space with the norm induced by the inner product defined by

$$\langle \phi, \psi \rangle_m := \sum_{|\alpha| \leq m} \int_\Omega D^\alpha \phi D^\alpha \psi \quad \forall \phi, \psi \in H^m(\Omega).$$

The space $H^m_0(\Omega)$ is defined as the completion of $C^\infty_0(\Omega)$ in the H^m-norm. In addition, the function space $H^1_0(\Omega)$ is characterized by the elements from $H^1(\Omega)$ which vanish on the boundary of Ω, where the boundary values are to be interpreted in the sense of trace.[1]

For $1 \leq p \leq \infty$, we also define the standard Bochner spaces $L^p(0, T; \mathbf{B})$, where $\mathbf{B}$ is a real Banach space with norm $\|\cdot\|_{\mathbf{B}}$, consisting of all measurable functions $\phi : (0, T) \longrightarrow \mathbf{B}$ for which

$$\begin{aligned} \|\phi\|_{L^p(0,T;\mathbf{B})} &:= \left(\int_0^T \|\phi(t)\|^p_{\mathbf{B}} \right)^{\frac{1}{p}} < \infty \quad \text{for} \quad 1 \leq p < \infty, \\ \|\phi\|_{L^\infty(0,T;\mathbf{B})} &:= \operatorname*{ess\,sup}_{t \in (0,T)} \|\phi(t)\|_{\mathbf{B}} < \infty \quad \text{for} \quad p = \infty. \end{aligned}$$

[1] The trace is a continuous (bounded) linear operator $\gamma : H^1(\Omega) \longrightarrow L^2(\partial\Omega)$ with $\gamma(u) = u|_\gamma$.

Here and in the subsequent chapters, we shall also use the following space. For a given Banach space $\mathbf{B}$, we define $H^1(0,T;\mathbf{B})$ as the space consisting of all measurable functions $\phi : (0,T) \longrightarrow \mathbf{B}$ for which

$$\|\phi\|_{H^1(0,T;\mathbf{B})} := \left(\int_0^T \|\phi(t)\|_{\mathbf{B}}^2 dt + \int_0^T \|\phi_t(t)\|_{\mathbf{B}}^2 dt\right)^{\frac{1}{2}} < \infty.$$

When no risk of confusion exists we shall write $L^2(\mathbf{B})$ for $L^2(0,T;\mathbf{B})$ and $L^\infty(\mathbf{B})$ for $L^\infty(0,T;\mathbf{B})$. Furthermore, $C(0,T;\mathbf{B})$ is defined as the space of continuous functions $\phi : [0,T] \longrightarrow \mathbf{B}$ with norm $\|\phi\|_{C(0,T;\mathbf{B})} := \max_{t\in[0,T]} \|\phi(t)\|_{\mathbf{B}} < \infty$. For a complete discussion on Sobolev Spaces, one may refer to Adams and Fourier [1], Dautray and Lions [36] and Grisvard [50].

In addition, we shall also work on the spaces $X := H_0^1(\Omega) \cap H^2(\Omega_1) \cap H^2(\Omega_2)$ and $Y := L^2(\Omega) \cap H^1(\Omega_1) \cap H^1(\Omega_2)$ endowed with the norms

$$\|\phi\|_X := \|\phi\|_{H_0^1(\Omega)} + \|\phi\|_{H^2(\Omega_1)} + \|\phi\|_{H^2(\Omega_2)}$$

and

$$\|\phi\|_Y := \|\phi\|_{L^2(\Omega)} + \|\phi\|_{H^1(\Omega_1)} + \|\phi\|_{H^1(\Omega_2)},$$

respectively.

Inequalities. We recall some important inequalities for our subsequent use (see, Hardy *et al.* [53]). From time to time we shall also refer to the following well-known inequalities.

Young's inequality: If a, b are non-negative integers, and $\epsilon > 0$ then

$$ab \leq \frac{a^2}{2\,\epsilon} + \frac{\epsilon\, b^2}{2}.$$

An important consequence of the Young's inequality is the celebrated Hölder's inequality. The discrete version of the Hölder's inequality is stated below.

Hölder's inequality: Let $p > 1$ and q be such that $\frac{1}{p} + \frac{1}{q} = 1$. Then, for any real numbers $a_i, b_i, i = 1, 2, \ldots, n$,

$$\sum_{i=1}^n |a_i\, b_i| \leq \left(\sum_{i=1}^n |a_i|^p\right)^{\frac{1}{p}} \left(\sum_{i=1}^n |b_i|^q\right)^{\frac{1}{q}}.$$

In particular, for $p = q = 2$, the above inequality is known as the Cauchy-Schwarz inequality in $\mathbb{R}^n$.

The integral analogue of the Hölder's inequality is as follows: Let $p, q \in [1, \infty)$ be such that $\frac{1}{p} + \frac{1}{q} = 1$. Suppose $\phi, \psi : \Omega \longrightarrow \mathbb{R}$ are Lebesgue measurable. Then

$$\|\phi\,\psi\|_{L^1(\Omega)} \leq \|\phi\|_{L^p(\Omega)}\, \|\psi\|_{L^q(\Omega)}.$$

For $p = q = 2$, the above inequality is known as the Cauchy-Schwarz inequality in integral form which will be of frequent use.

Lemma 1.2.1 (Poincaré inequality, [24]). *Let Ω be a bounded domain in $\mathbb{R}^n$. Then there exists a positive constant $\mathcal{C}_P = \mathcal{C}_P(\Omega)$ such that*

$$\|\phi\| \leq \mathcal{C}_P \|\nabla\phi\| \quad \forall \phi \in H_0^1(\Omega).$$

An important consequence of the Poincaré's inequality is that $\|\nabla(\cdot)\|$ defines a norm on $H_0^1(\Omega)$.

Next, we state the following discrete version of Gronwall's lemma.

Lemma 1.2.2 (Discrete Gronwall's lemma, [87]). *Let (x_n), (y_n), and (z_n) be non-negative real sequences and satisfy*

$$x_n \leq y_n + \sum_{0 \leq k \leq n} z_k \, x_k \qquad \text{for } n \geq 0,$$

then

$$x_n \leq y_n + \sum_{0 \leq k \leq n} y_k \, z_k \, \exp\left(\sum_{k<j<n} z_j\right) \qquad \text{for } n \geq 0.$$

The following lemma is proved to be convenient for later use (see, Lakkis and Makridakis [62]).

Lemma 1.2.3. *For $a = (a_0, a_1, \ldots, a_n) \in \mathbb{R}^{n+1}$, $b = (b_0, b_1, \ldots, b_n) \in \mathbb{R}^{n+1}$ and $c \in \mathbb{R}$, and if*

$$\|a\|^2 \leq c^2 + a \cdot b$$

then

$$\|a\| \leq |c| + \|b\|,$$

where for any $x = (x_0, x_1, \ldots, x_n), y = (y_0, y_1, \ldots, y_n) \in \mathbb{R}^{n+1}$, $\|x\| := \left(\sum_{i=0}^{n} |x_i|^2\right)^{\frac{1}{2}}$ denotes the standard Euclidean vector norm, and $x \cdot y$ denotes the standard inner product on $\mathbb{R}^{n+1}$.

Hereafter, we assume that Ω is a bounded polygonal domain in $\mathbb{R}^2$ with Lipschitz boundary $\partial\Omega$.

Existence, Uniqueness and Regularity Results. The existence and uniqueness of the solutions for both the elliptic and parabolic interface problems are investigated by numerous authors, see Babuška [8], Chen and Zou [33], Gilbarg and Trudinger [47],

Girault and Raviart [48], Hackbusch [51], Kellogg [58], Marti [77] and references therein. For a more general interface problems, the existence and uniqueness results can be found in Ladyženskaja *et al.* [61] and Lumer and Weis [73]. Due to the discontinuity of the coefficient β along the interface Γ, the solution u in general possess low global regularity even if the coefficients are very smooth in individual subdomains. We now recall from [33, 61] the following regularity result associated with the elliptic interface problem.

Theorem 1.2.1. *Assume that $f_1 \in L^2(\Omega)$. Then the problem*

$$-\text{div}(\beta(x)\nabla v(x)) = f_1(x) \quad in \quad \Omega$$

with Dirichlet boundary condition

$$v = 0 \quad on \quad \partial\Omega$$

and jump conditions on the interface

$$[v] = 0, \qquad \left[\beta\frac{\partial v}{\partial \boldsymbol{n}}\right] = 0 \quad across \quad \Gamma$$

has a unique solution $v \in X$ and satisfies the following a priori estimate

$$\|v\|_X \leq \mathcal{C}_R \, \|f_1\|.$$

Concerning the regularity of the solution for the parabolic interface problem (1.1.1) – (1.1.3), we have the following result.

Theorem 1.2.2 (Chen and Zou, [33])**.** *Let $f \in H^1(0,T;L^2(\Omega))$ and $u_0 \in H_0^1(\Omega)$. Then the problem* (1.1.1) – (1.1.3) *has a unique solution $u \in L^2(0,T;X) \cap H^1(0,T;Y)$.*

Framework for the Finite Element Method. For the purpose of the finite element approximation of the interface problem (1.1.1)–(1.1.3), we begin by writing the problem in weak form: Find $u \in L^\infty(0,T;H_0^1(\Omega))$ satisfying

$$\begin{aligned} (1.2.1) \qquad \langle u_t(t),\varphi\rangle + a(u(t),\varphi) &= \langle f(t),\varphi\rangle \ \ \forall \varphi \in H_0^1(\Omega), \quad \text{a.e. } t \in (0,T], \\ u(0) &= u_0, \end{aligned}$$

where $a(\cdot,\cdot) : H_0^1(\Omega) \times H_0^1(\Omega) \longrightarrow \mathbb{R}$ is a bilinear form defined by

$$a(v,w) = \langle \beta\nabla v, \nabla w\rangle \quad \forall v, w \in H_0^1(\Omega)$$

with ∇ denotes the spatial gradient and $f : \Omega \times [0,T] \longrightarrow \mathbb{R}$.

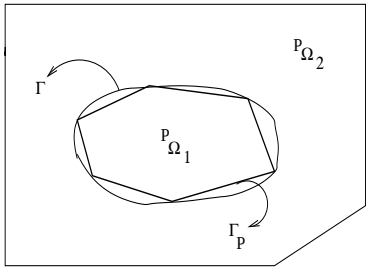

Figure 1.2: *Polygonal domain P_{Ω_1} and P_{Ω_2} with polygonal boundary Γ_P of P_{Ω_1}.*

The bilinear form $a(\cdot,\cdot)$ is bounded and coercive on $H_0^1(\Omega)$, i.e., $\exists \alpha_0, \gamma_0 > 0$ such that

$$|a(v,w)| \leq \alpha_0 \, \|v\|_1 \|w\|_1 \quad \forall v, w \in H_0^1(\Omega), \tag{1.2.2}$$

and

$$a(v,v) \geq \gamma_0 \, \|v\|_1^2 \quad \forall v \in H_0^1(\Omega). \tag{1.2.3}$$

Discretization of the Domain Ω. In order to describe the triangulation of the domain Ω, we first approximate the domain Ω_1 by a polygon P_{Ω_1} with boundary Γ_P such that all the vertices of the polygon lie on the interface Γ. Thus, Γ_P (see, Fig. 1.2) now splits the domain Ω into two subdomains P_{Ω_1} and P_{Ω_2}, where P_{Ω_2} is a polygon approximating the domain Ω_2. For the purpose of the spatially discrete approximations, let $\mathcal{T}_h = \{K\}$ be a family of shape regular conforming triangulations of $\bar{\Omega}$. We shall make the following assumptions on $\mathcal{T}_h$ (cf. [33]).

SA1. If $K_1, K_2 \in \mathcal{T}_h$ and $K_1 \neq K_2$, then either $K_1 \cap K_2 = \emptyset$ or $K_1 \cap K_2$ share a common edge or a common vertex. We also assume that each triangle is either in P_{Ω_1} or in P_{Ω_2} or intersects the interface Γ in at most two vertices.

SA2. Let $h := \max\{h_K \mid h_K = \mathrm{diam}(K),\ K \in \mathcal{T}_h\}$. For $K \in \mathcal{T}_h$, the patch S_K is given by $S_K := (\cup_{i \in \mathcal{I}_K} \bar{K}_i)^\circ$, where $\mathcal{I}_K := \{i \in \mathbb{N} \mid \partial K_i \cap \partial K \neq \emptyset,\ \ K_i \in \mathcal{T}_h\}$. We assume that the patch S_K is uniformly bounded, i.e., there exists a constant $C > 0$ such that

$$\max_{K \in \mathcal{T}_h} \{\mathrm{card}\, \mathcal{I}_K\} \leq C, \tag{1.2.4}$$

where $\mathrm{card}\, \mathcal{I}_K$ refers to the cardinality of the set $\mathcal{I}_K$.

Next, we introduce some notations. We split the triangulation $\mathcal{T}_h$ into three disjoint sets. The first one refers to the set of all interface triangles, denoted by $\mathcal{T}_h^*$, and the

other two refers to the set of all non-interface triangles denoted by $\mathcal{T}_{h,\Omega_1}$ and $\mathcal{T}_{h,\Omega_2}$ with $\mathcal{T}_h \setminus \mathcal{T}_h{}^* := \mathcal{T}_{h,\Omega_1} \cup \mathcal{T}_{h,\Omega_2}$, where

$$\begin{aligned} \mathcal{T}_h^* &:= \{K \in \mathcal{T}_h \mid K \cap \Gamma_P \neq \emptyset\}, \\ \mathcal{T}_{h,\Omega_i} &:= \{K \in \mathcal{T}_h \mid K \subsetneq P_{\Omega_i}\} \quad \text{for} \quad i = 1, 2. \end{aligned}$$

Let $\mathcal{E}_h := \{E\}$ be the set of all internal edges of the triangles $K \in \mathcal{T}_h$. Similarly, we split the set $\mathcal{E}_h$ into three disjoint sets $\mathcal{E}_h^*$, $\mathcal{E}_{h,\Omega_1}$ and $\mathcal{E}_{h,\Omega_2}$, where $\mathcal{E}_h^*$ refers to the set of all edges of the interface triangles in $\mathcal{T}_h{}^*$ and $\mathcal{E}_{h,\Omega_i}(i = 1, 2)$ denotes the set of all edges of the non-interface triangles in $\mathcal{T}_{h,\Omega_i}$. Set $\mathcal{E}_h \setminus \mathcal{E}_h^* = \mathcal{E}_{h,\Omega_1} \cup \mathcal{E}_{h,\Omega_2}$. Let $\Sigma_h := \cup_{E \in \mathcal{E}_h} E$ and the norm $\|\cdot\|_{\Sigma_h} := \|\cdot\|_{L^2(\Sigma_h)}$. The pictorial representations of the splitting of $\mathcal{T}_h$ and $\mathcal{E}_h$ are shown in Fig. 1.3.

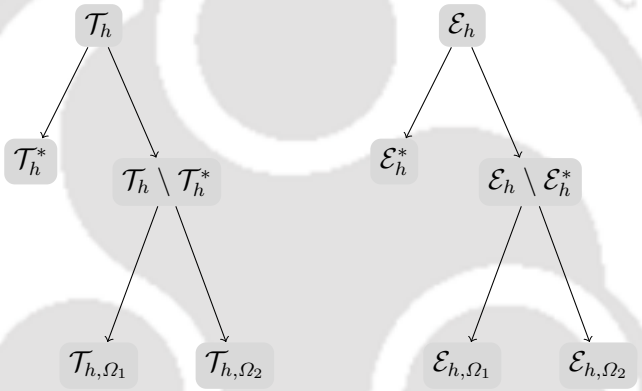

Figure 1.3: *Pictorial representations of the splitting of $\mathcal{T}_h$ and $\mathcal{E}_h$.*

For a shape regular triangulation $\mathcal{T}_h$ of Ω, consider the finite element space

$$\mathbb{S}_h := \left\{\chi \in H_0^1(\Omega) \;\middle|\; \chi|_K \in \mathbb{P}_1(K) \quad \text{for all} \quad K \in \mathcal{T}_h\right\},$$

where $\mathbb{P}_1(K)$ is the space of polynomials of degree at most 1 over K.

Spatially Discrete Finite Element Approximation. We define the spatially discrete finite element approximation $u_h : [0, T] \longrightarrow \mathbb{S}_h$ of u as follows: Find $u_h(t) \in \mathbb{S}_h$ such that

$$\begin{aligned} \langle u_{h,t}, \chi_h\rangle + a(u_h, \chi_h) &= \langle f, \chi_h\rangle \quad \forall \chi_h \in \mathbb{S}_h, \quad \text{a.e. } t \in (0, T], \\ u_h(\cdot, 0) &= I_h u_0, \end{aligned} \tag{1.2.5}$$

where I_h is some chosen projection operator from $H_0^1(\Omega)$ into the finite dimensional subspace $\mathbb{S}_h$.

Next, we rewrite the elliptic operator in a compact form which will be used subsequently for the rest of the dissertation.

Representation of bilinear form: Let $v_h \in \mathbb{S}_h$. Then the bilinear form $a(\cdot,\cdot)$ can be rewritten using Green's formula as

$$\begin{aligned} a(v_h,\varphi) &= \sum_{K\in\mathcal{T}_h} \langle -\mathrm{div}(\beta\nabla v_h),\varphi\rangle_K \; + \; \sum_{E\in\mathcal{E}_h} \langle j[\beta v_h],\varphi\rangle_E \\ &= \langle (v_h)_{\mathrm{el}},\varphi\rangle \; + \; \langle j[\beta v_h],\varphi\rangle_{\Sigma_h} \quad \forall \varphi \in H_0^1(\Omega)\ , \end{aligned} \tag{1.2.6}$$

where $j[\beta v_h]$ denotes the spatial jump of $\beta\,\nabla v_h$ across an element side $E \in \mathcal{E}_h$ and is defined as

$$j[\beta v_h]|_E(x) := \lim_{\epsilon\to 0} \left(\beta\nabla v_h(x \; + \epsilon\eta_E) \; - \beta\nabla v_h(x \; - \epsilon\eta_E)\right)\cdot\eta_E, \tag{1.2.7}$$

where η_E is an arbitrary unit normal vector to E at the point x. The quantity $(v_h)_{\mathrm{el}}$ in (1.2.6) denotes the regular part of the distribution $-\mathrm{div}(\beta\,\nabla v_h)$, and is defined as a piecewise continuous function such that

$$\langle (v_h)_{\mathrm{el}},\varphi\rangle := \sum_{K\in\mathcal{T}_h} \langle -\mathrm{div}(\beta\nabla v_h),\varphi\rangle_K \;\; \forall\varphi\in H_0^1(\Omega). \tag{1.2.8}$$

Now, we shift our attention to introduce the space-time finite element discretizations of the domain for the fully discrete approximations. We shall use the same symbols as in the spatially discrete case with the index "h" is replaced by "n" to describe the situation at each time level.

Space-time Discretizations of the Domain. Let $\mathcal{P} := \{(t_{n-1},t_n]\}_{n=1}^N$ be a partition of $[0,T]$ with $I_n := (t_{n-1},t_n]$ and $k_n := t_n - t_{n-1}$ be the time steps. Let $\mathcal{T}_n = \{K\}(0 \le n \le N)$ be the triangulations of $\bar{\Omega}$ at the time level t_n. In the context of fully discrete case, we shall make the following assumptions on $\mathcal{T}_n$. The first two assumptions are similar to the assumptions **SA1** and **SA2** (as described in spatially discrete case) with $\mathcal{T}_h$ is replaced by $\mathcal{T}_n$ and h is replaced by h_n. The third one is on the compatibility of triangulations $\mathcal{T}_n$.

FA1. If $K_1, K_2 \in \mathcal{T}_n$ and $K_1 \neq K_2$, then either $K_1 \cap K_2 = \emptyset$ or $K_1 \cap K_2$ share a common edge or a common vertex. We also assume that each triangle is either in P_{Ω_1} or in P_{Ω_2} or intersects the interface Γ in at most two vertices.

FA2. Let $h_n := \max\{h_K \mid h_K = \mathrm{diam}(K),\ K \in \mathcal{T}_n\}$. For $K \in \mathcal{T}_n$, the patch S_K is given by $S_K := (\cup_{i\in\mathcal{I}_K}\bar{K}_i)^\circ$, where $\mathcal{I}_K := \{i \in \mathbb{N} \mid \partial K_i \cap \partial K \neq \emptyset, \quad K_i \in \mathcal{T}_n\}$.

We assume that the patch S_K is uniformly bounded, i.e., there exists a constant $C > 0$ such that

$$\max_{K \in \mathcal{T}_n} \{\text{card}\, \mathcal{I}_K\} \leq C, \tag{1.2.9}$$

where $\text{card}\, \mathcal{I}_K$ refers to the cardinality of the set $\mathcal{I}_K$.

FA3. Two simplicial decompositions $\mathcal{T}_{n-1}$ and $\mathcal{T}_n$ of $\bar{\Omega}$ are said to be compatible if they are derived from the same macro triangulation $\mathcal{T} = \mathcal{T}_0$ by an admissible refinement procedure which preserves shape regularity (cf. [24] and [91]) and assures that for any elements $K \in \mathcal{T}_{n-1}$ and $K' \in \mathcal{T}_n$, either $K \cap K' = \emptyset$, $K \subset K'$, or $K' \subset K$. There is a natural partial ordering on a set of compatible triangulations, namely $\mathcal{T}_{n-1} \leq \mathcal{T}_n$ if $\mathcal{T}_n$ is a refinement of $\mathcal{T}_{n-1}$. Then for a given pair of of successive compatible triangulations $\mathcal{T}_{n-1}$ and $\mathcal{T}_n$, we define naturally the finest common coarsening $\hat{\mathcal{T}}_n := \mathcal{T}_n \wedge \mathcal{T}_{n-1}$ with local mesh sizes are given by $\hat{h}_n := \max\{h_{n-1}, h_n\}$. These conditions allow us to bound the elliptic errors which lie in two adjacent finite element spaces, i.e., finite element spaces defined on meshes at adjacent time steps. For a more detailed discussions on compatible triangulations, we refer to Appendices A and B of [62].

We shall also need the following notations for future use. For $0 \leq n \leq N$, $\mathcal{E}_n$ be the set of all edges $\{E\}$ of the triangles $K \in \mathcal{T}_n$ which do not lie on $\partial\Omega$, and $\Sigma_n := \cup_{E \in \mathcal{E}_n} E$. Furthermore, we will also use the sets $\hat{\Sigma}_n := \Sigma_n \cap \Sigma_{n-1}$ and $\check{\Sigma}_n := \Sigma_n \cup \Sigma_{n-1}$.

1.3 Background and Motivation

This section reports a brief survey of the relevant literature regarding the interface problems and elucidates the motivation for the present study. Interface problems occur in a wide variety of applications in science and engineering and naturally arise when two dissimilar materials interact across an interface. Due to the irregular geometry of the interface and the discontinuity of the coefficient along the interface, the analytical solutions are rarely available for interface problems. Therefore, numerical approximation is the only way to approach such problems. There are several numerical methods in the literature designed for the interface problems. In practice, a discretization procedure such as finite difference methods (FDM) and finite element methods (FEM) are adapted. We first detail a brief account of the literature concerning the FDM for interface problems.

Finite Difference Methods. There has been a considerable research to solve interface problems using FDM, see [5, 21, 54, 65, 67, 70] and references therein. LeVeque in [65] has proposed an immersed interface method with the second order accuracy for

the elliptic interface problems using uniform rectangular grid. In [70], Li *et al.* has considered the elliptic interface problem in polar coordinates, where they have transformed the interface problem with a nonsmooth or discontinuous solution to a problem with a smooth solution. Then, a second order finite difference scheme is developed for the elliptic interface problem in polar coordinates. The authors of [71] have used a first order finite difference scheme for elliptic interface problem to capture the boundary conditions across an interface. The resulting linear system is symmetric and same as the one obtained for the standard Poisson equation in the absence of interface. Further, this method has been extended to achieve second order accuracy for the elliptic interface problem in [54]. An implicit finite difference scheme for one dimensional heat equation with a stationary interface has been developed by Akrivis *et al.* in [5] to obtain second-order accuracy in space and time. For two-dimensional parabolic interface problems, the convergence of the finite difference scheme has been studied by Bojović in [21]. For a more detailed discussion on FDM for interface problem, we refer to [67, 68] and the references quoted therein.

Finite Element Methods. FEM is a powerful and general class of numerical technique for finding approximate solutions of differential equations over a given domain. The advantage of finite element method over other numerical techniques lies in its capability to handle complex geometry in a systematic way and it has a rigorous mathematical foundation. The error analysis of FEM is grouped into two categories: *A priori error analysis* and *a posteriori error analysis* .

A priori error analysis. The *a priori* error analysis of interface problems by means of FEM has been investigated by several authors. To begin with, we first present a brief account of the literature on the elliptic interface problems. The *a priori* error analysis of elliptic interface problems can be traced back to the work of Babuška in [8]. Subsequently, it has been studied thoroughly by several authors Barrett and Elliott [16], Bramble and King [22], Chen and Zou [33], Nielsen [81], Cai *et al.* [27] and references therein. In [8], the author has converted the problem to an equivalent minimization problem and obtained sub-optimal order error estimates in the H^1-norm. The word "optimal order" refers to the classical terminology in the approximation theory (see, [97]). Then, under some regularity assumptions (both the solution and the normal derivative of the solution are assumed to be continuous and fourth order differentiable on each subdomain) on the solution operator, Barrett and Elliott in [16] have shown the convergence of finite element solution to the true solution at an optimal rate in both the H^1 and L^2-norms on each individual subdomain. Subsequently, Bramble and King in [22] have approximated the smooth domain by a polygonal domain and then the

boundary data are transferred to the polygonal boundaries. The discontinuous Galerkin finite element method is then applied to the perturbed problem defined on polygonal subdomains and optimal order error estimates for rough as well as smooth boundary data for the nonhomogeneous second order elliptic interface problems are obtained. Later, with reasonable regularity assumption on the true solution, the convergence of finite element method is studied in [33] and [81]. The authors of [33] have obtained almost optimal order convergence in both the H^1 and L^2-norms. In [81], Nielsen has proved optimal order convergence in the H^1-norm for the elliptic interface problem in the presence of arbitrary small ellipticity. While deriving the estimates, the author has assumed that the interface triangles follow exactly the interface Γ. The discontinuous Galerkin FEM has been studied by Cai *et al.* in [27] for bounded polygonal domain in $\mathbb{R}^2$. A quasi-optimal *a priori* error estimates is derived under the assumption that solutions are only in $H^{1+\epsilon}(\Omega)$ with $\epsilon \in (0,1)$.

Up to now, all literature presented above are about the elliptic interface problems. We shall now concentrate on the *a priori* error analysis of finite element approximation of the parabolic interface problem $(1.1.1) - (1.1.3)$. The first contribution in this direction is given by Chen and Zou in [33]. In this article, the authors have considered finite element method in which domain Ω_1 is approximated by a polygonal domain and then the fully discrete backward Euler approximation has been studied. Nearly optimal order estimates in both the L^2 and H^1-norms are obtained with low global regularity of the solution. Later, Huang and Zou in [55] have proved some new *a priori* estimates for both the elliptic and parabolic interface problems. These new estimates contain explicitly the coefficient β and it helps to reflect the physical behaviours of the solutions. Recently, a new isoparametric type of disctretizations is proposed by Sinha and Deka in [93]. Both the spatially discrete and the fully discrete backward Euler approximations are analyzed and optimal order convergence are shown to hold in the $L^2(H^1)$ and $L^2(L^2)$ norms. Later, the same authors have extended their work to obtain optimal order convergence in the $L^\infty(L^2)$ and $L^\infty(H^1)$ norms in [37].

Next, We shall shift our attention to the semilinear parabolic interface problem, i.e., when the forcing term f is a function of x, t, and u. The study of semilinear interface problems is motivated by models of mass transfer of substances through semipermeable membranes. Such models arise from various applications in biomedical and chemical engineering, e.g., modeling of electrokinetic flows, solute dynamics across arterial walls, and cellular signal transduction, for instance, see [25] and [29]. The existence, uniqueness and regularity of the solution of the semilinear parabolic interface problems have been investigated by Feng and Shen in [45]. Although a good number of articles and books

are devoted to the linear interface problems, but the literature seems to lack on error analysis of semilinear interface problems in the *a priori* framework. Sinha and Deka [95] have studied both the elliptic and parabolic semilinear interface problems in the framework of Brezzi - Rappaz -Raviart [26]. Optimal energy-norm error estimates are derived for the semilinear elliptic and parabolic interface problems in [95]. For a more detailed discussion on the finite element error analysis of semilinear parabolic problems (in absence of an interface), we refer to [34, 97, 98] and references cited therein.

The reference [68] offers an excellent review of *a priori* error analysis of interface problems by means of both FDM and FEM, and also contains a comprehensive list of literature. For further works on *a priori* error analysis of interface problems, one may refer to Ženíšek [105], Hansbo [52], Li *et al.* [69], Sinha and Deka [94], Gong *et al.* [49], Jovanović and Vulkov [56], Massjung [78], Falk and Walker [43], Peterseim [85], Wei *et al.* [102] and references therein.

An priori error estimate predicts a bound of the form

$$\|u - U\|_{\mathcal{X}} \leq \mathcal{C}(u,\ \text{data})h^r, \tag{1.3.1}$$

where u and U, respectively, are the exact and finite element solution of a given problem. $\mathcal{C}(u,\ \text{data})$ is a positive constant depends on the exact solution u and the given data. Also, h denotes the discretization parameter; r refers to the order of accuracy of the underlying finite element space and $\mathcal{X}$ denotes a specified norm. Observe that the bound (1.3.1) rely on the exact solution which is unknown for most of the partial differential equations. Thereby, the *a priori* error analysis investigates the convergence properties of the proposed discretizations and proves the asymptotic convergence of the error as the discretization parameter goes to zero. As *a priori* error estimate does not provide a quantitative information on the size of the error and therefore, this automatically brings to a new diverse error estimation method called *a posteriori* error estimation technique.

A posteriori error analysis. An *a posteriori* error analysis leads to a bound for the error $e := u - U$ in terms of the approximate solution U, the given data and the mesh parameter h, i.e., *a posteriori* error estimate is a bound of the form

$$\|u - U\|_{\mathcal{X}} \leq \eta(U, \text{data})h^r, \tag{1.3.2}$$

where $\mathcal{X}$ denotes a specified norm. An estimator $\eta(U, \text{data})h^r$ is a computable quantity which decreases with optimal order with respect to the mesh parameter h requiring the lowest possible regularity permitted by the problem. In contrast to the *a priori* error analysis, the concept of *a posteriori* error analysis provides techniques for the automatic choice of suitable discretizations leading to efficient approximation algorithms. In

the recent years, there has been a growing popularity of *a posteriori* error estimation technique in engineering and scientific computation community because of its ability to control the error in the quantity of physical interest. Moreover, *a posteriori* error estimation is central to the design of adaptive algorithms to control and minimize the error.

A posteriori error analysis and adaptive meshing procedure have attracted many researchers, and a variety of different *a posteriori* error estimates have been proposed and analyzed for the parabolic problems. Most of the error estimates can be classified into residual and recovery types. In residual type error estimates, various residual quantities such as element and jump residuals are used to bound the error. Whereas in recovery type, a gradient recovery (postprocessing) operator is applied to the finite element solution and then compared with the gradients of the exact solution to assess the error. *A posteriori* error estimates have also been derived based on the use of hierarchic bases or equilibrated residuals. In this thesis, we shall restrict ourself only to the residual-based *a posteriori* error estimates.

In order to put the results of this thesis into a proper perspective, we present a brief literature regarding *a posteriori* error analysis for both the elliptic and parabolic problems. The research on *a posteriori* error analysis and adaptive mesh refinement for the finite element methods for one dimensional elliptic boundary value problems began in the late 1970's. The pioneering work on this topic is due to Babuška and Rheinboldt [9, 10]. The theory of *a posteriori* error estimation technique is well accepted in the context of finite element method of elliptic problems. Some comprehensive summary of works can be found in chronicle order; Babuška and Rheinboldt [11], Bank and Weiser [13], Eriksson and Johnson [39], Verfürth [100], Dörfler and Rumpf [38], Ainsworth and Oden [2], Rannacher [88], and references therein. However, *a posteriori* error analysis of the FEM for the parabolic problems has been a topic of research since early '80s. The first significant contribution towards the *a posteriori* error analysis of parabolic problem is due to Eriksson and Johnson in [40] and subsequent ones in [41, 42]. Eriksson and his co-worker have obtained optimal order estimates in the $L^\infty(L^2)$-norm using the parabolic duality technique. However, their method hinges on the parabolic regularizing effect which fails to provide estimate in the $L^2(H^1)$-norm and this motivates one to consider the standard energy technique. Moreover, the energy technique is the more versatile method for the finite element error analysis as it is directly based on the variational formulation of the problem. The extant literature on *a posteriori* error analysis for the parabolic problems by means of the energy argument can be found in [18, 32, 86, 101]. An optimal order *a posteriori* error estimate of residual-type in the $L^2(H^1)$-norm has

been derived by Picasso in [86]. Subsequently in [101], Verfürth has derived optimal order estimate in the $L^2(H^1)$-norm and sub-optimal estimate in the $L^\infty(L^2)$-norm for the parabolic problem using the energy argument.

In the context of parabolic problems, it has been observed in [86, 101] that energy method for *a posteriori* error analysis yields suboptimal rates in the $L^\infty(L^2)$-norm. Since energy method is the most elementary technique for estimating the error in the *a priori* error analysis and therefore, this raises a natural question that whether this method can be applied to *a posteriori* analysis for the parabolic problems to obtain optimal bounds in the $L^\infty(L^2)$-norm. Recently, Makridakis and Nochetto in [76] have successfully addressed this issue by introducing a novel elliptic reconstruction operator $\mathcal{R}_h : \mathbb{S}_h \longrightarrow H_0^1(\Omega)$. This reconstruction operator is a *a posteriori* dual analogue of Wheeler's elliptic projection operator [103] introduced in the context of *a priori* error analysis to restore the optimality in the $L^\infty(L^2)$-norm. The idea behind the introduction of elliptic reconstruction operator is to extend the traditional energy method in *a priori* error analysis to *a posteriori* error analysis to obtain optimal order estimates in the $L^\infty(L^2)$-norm.

To restore the optimality, the usual strategy is to split the total error $e := u - U$ into two parts $e := (u - \mathcal{R}_h U) + (\mathcal{R}_h U - U)$ such that

- parabolic error $u - \mathcal{R}_h U$ satisfies a variant of original partial differential equation with a righthand side which can be bounded *a posteriori* in an optimal way,
- and well established theory of *a posteriori* error bounds for elliptic problems can be used to obtain the spatial (reconstruction) error $\mathcal{R}_h U - U$.

Though a large number of literature available on *a posteriori* error analysis for non-interface problems, there seems a little existing work in the literature which provides *a posteriori* bounds for the interface problems. References and reviews of *a posteriori* error analysis for the elliptic interface problems can be found in [19, 27, 28]. Bernardi and Verfürth [19] have studied residual-based *a posteriori* error estimates for the elliptic interface problem and derived the error bounds in the H^1-norm. A new recovery based *a posteriori* error bounds are derived in [28] for the conforming linear finite element approximation to the elliptic interface problems. Recently, Cai *et al.* [27] have used discontinuous Galerkin method to study both the residual and recovery-based *a posteriori* error estimates for the elliptic interface problems. In the context of parabolic interface problems, a residual-based *a posteriori* error estimate has been investigated by Berrone in [20]. Both the upper and lower bounds are derived in the $L^2(H^1)$-norm. The author has used the idea of bubble function technique to derive the lower bound.

It is noteworthy that *a posteriori* error analysis for interface problems available in the literature (cf. [19, 20, 27, 28]) are concerned with only in the H^1-norm error estimates.

Due to the low global regularity of the solution of the parabolic interface problems, the extension of the standard *a posteriori* error analysis of the finite element method for the parabolic problems to the parabolic interface problems is not straightforward. To the best of our knowledge the $L^\infty(L^2)$-norm *a posteriori* error estimates for the parabolic interface problems are yet to be explored. Therefore, an attempt has been made in this thesis to extend the $L^\infty(L^2)$-norm *a posteriori* error analysis of the purely parabolic problems to the parabolic interface problems. To begin with, we first study residual-based *a posteriori* error estimates for the spatially discrete finite element approximation of the linear parabolic interface problem $(1.1.1)-(1.1.3)$. For purely parabolic problems (in the absence of an interface), it is known that (cf. [101]) the energy method for *a posteriori* error analysis yields suboptimal rates of convergence in the $L^\infty(L^2)$-norm. In order to recover the optimality, Makridakis and Nochetto in [76] have introduced the idea of elliptic reconstruction technique for the spatially discrete case and then later prolonged to the fully discrete case in [62] for the parabolic problems. The error analysis mainly uses the approximation properties of the Clément-type interpolation operator of Scott and Zhang [92]. However, for a higher order approximation properties of such type of operator, the analysis of [92] require $u \in H^r(\Omega), r \geq 2$. For instance, to obtain $O(h^2)$ convergence with piecewise linear element one requires $u \in H^2(\Omega)$. But, due to the discontinuity of the coefficient along the interface Γ, the solution of the parabolic interface problem $(1.1.1)-(1.1.3)$ is only in $H^1(\Omega)$ globally (Theorem 1.2.2) and hence, the standard approximation properties do not apply directly for interface problems. As a consequence, it is not straightforward to extend the analysis of [76] to the present problem. Therefore, new approximation properties for a Clément-type interpolation operator are established (Theorem 2.2.2). The Sobolev embedding and extension theorems are used in a crucial way to derive these new approximation results.

For the purpose of *a posteriori* error analysis, we decompose the total error as

$$\begin{aligned} e(t) &:= u(t) - u_h(t) \\ &= \{u(t) - \mathcal{R}_h u_h(t)\} + \{\mathcal{R}_h u_h(t) - u_h(t)\} \\ &:= \rho(t) + \varepsilon(t), \end{aligned}$$

where $\mathcal{R}_h$ is an elliptic reconstruction operator defined in (2.3.1). Here, $\varepsilon(t) := \mathcal{R}_h u_h(t) - u_h(t)$ represents the elliptic reconstruction error and $\rho(t) := u(t) - \mathcal{R}_h u_h(t)$ refers to the parabolic error. Then *a posteriori* error bound for the main error (Theorem 2.3.2) in a suitable norm is obtained by combining the bounds on the reconstruction error $\varepsilon(t)$

(Lemma 2.3.1) along with the parabolic error $\rho(t)$ (Lemma 2.3.2). We wish to emphasize that no *a posteriori* error bounds are available in the literature with respect to the L^2-norm for the elliptic interface problems. Therefore, these new interpolation estimates for the Clément-type operator are used to derive a reconstruction error estimates in the L^2-norm (Lemma 2.3.1). We use the standard duality technique to derive the reconstruction error bounds. On the other hand, the parabolic error $\rho(t)$ is estimated by an appropriate use of error equation (2.3.19) and the standard energy argument.

Our next aim is to study the fully discrete backward Euler approximation for (1.1.1)−(1.1.3). For purely parabolic problems, *a posteriori* error estimates for the fully discrete backward Euler approximation has been studied by Picasso [86], Verfürth [101] and Lakkis and Makridakis [62]. The authors of [86, 101] have employed piecewise linear elements in the space discretizations and the backward Euler approximation in the time discretizations to obtain optimal order *a posteriori* bounds in the $L^2(H^1)$-norm. However, the effect of mesh change is not considered in their error analysis. Subsequently, Lakkis and Makridakis [62] have studied the fully discrete backward Euler approximation via reconstruction approach and obtained optimal order estimates in the $L^\infty(L^2)$-norm. Further, their analysis also reflects the effect of mesh change behaviour. Motivated by the above discussions, we have studied the fully discrete backward Euler approximation for the parabolic interface problem (1.1.1)−(1.1.3) and obtained optimal order estimates in the $L^2(H^1)$-norm and almost optimal order bound in the $L^\infty(L^2)$-norm. Analogues to the spatially discrete case, we split the total error $e(t) := u(t) - U(t)$ into two parts as

$$\begin{aligned} e(t) &:= u(t) - U(t) \\ &= \{u(t) - \Theta(t)\} + \{\Theta(t) - U(t)\}, \end{aligned}$$

where U and Θ are given by (3.2.6) and (3.2.7), respectively. In the above, $\{\Theta(t) - U(t)\}$ and $\{u(t) - \Theta(t)\}$ refer to the elliptic reconstruction error and parabolic error, respectively, which in turn bounded separately to obtain *a posteriori* error bounds for the main error (Theorem 3.2.2). The reconstruction error $\{\Theta(t) - U(t)\}$ can be handled in a manner similar to the spatial discrete case. Whereas, the *a posteriori* bound for the parabolic error $\{u(t) - \Theta(t)\}$ relies on the energy argument and an appropriate use of error equation (see, (3.2.11) in Lemma 3.2.2). An *a posteriori* error bound for the parabolic error comprises of several error bounds namely, the *spatial error* (Lemma 3.2.3), the *temporal error* (Lemma 3.2.4) and the *data approximation error* (Lemma 3.2.5).

To obtain higher order accuracy in time, our next objective is to study the fully dis-

crete Crank-Nicolson approximation for the parabolic interface problem (1.1.1)−(1.1.3). For a continuous, piecewise linear approximation in time, Verfürth [101] has obtained suboptimal order *a posteriori* bounds for the heat equation for the Crank-Nicolson approximation with the standard energy argument. Later, Akrivis *et al.* in [4] have introduced a continuous, piecewise quadratic polynomial so-called Crank-Nicolson reconstruction to recover optimality for the time discretizations for the parabolic problems. The authors of [4] have not considered the mesh change effect while deriving the *a posteriori* bound. Subsequently, the effect of mesh change has been considered by Bänsch *et al.* in [15] for the Crank-Nicolson approximation for the parabolic problems. The energy argument is employed to establish optimal order *a posteriori* error estimate in the $L^\infty(L^2)$-norm.

Following the idea of [4, 15], we have defined a quadratic (in time) space-time reconstruction $\tilde{U}$ for the parabolic interface problem (1.1.1) − (1.1.3) to restore the second order convergence in time. The reconstruction $\tilde{U}$ is such that

- $\tilde{U}$ is continuous on $[0, T]$ and
- the difference $\tilde{U} - \Theta(t)$ is an *a posteriori* quantity and can be bounded in an optimal way, i.e., of $O(k_n^2)$.

A traditional way to write the error as sum of the terms,

$$\begin{aligned} e(t) &:= u(t) - U(t) \\ &= \{u(t) - \tilde{U}(t)\} + \{\tilde{U}(t) - \Theta(t)\} + \{\Theta(t) - U(t)\} \\ &:= \tilde{\rho}(t) + \tilde{\sigma}(t) + \varepsilon(t), \end{aligned}$$

which are then treated separately to obtain main *a posteriori* error bound (Theorem 4.2.2). The term $\tilde{\rho}(t)$ denotes the parabolic error and can be bounded by an *a posteriori* quantity using the energy argument. The bound on the parabolic error comprises of the following errors: The *temporal error* (Lemma 4.2.3), the *space-mesh error* (Lemma 4.2.4), the *space error* (Lemma 4.2.5), the *data approximation error* (Lemma 4.2.6), and the *coarsening error* (Lemma 4.2.7). The third term $\varepsilon(t)$ represents the elliptic reconstruction error and can be handled in a similar fashion like the fully discrete backward Euler case, whereas $\tilde{\sigma}(t)$ accounts for the time reconstruction error.

Our next goal is to consider approximations at equidistant time level of parabolic interface problem (1.1.1)−(1.1.3) in which the time derivative is replaced by the two-step backward differentiation formula (BDF-2) approximation. Although the Crank-Nicolson approximation is one of the most popular time-stepping method for the parabolic problems, it has the lack of smoothing property of the solution operator [15, 74, 97]. However,

it is known that multistep methods are widely used in numerical computations for non-stationary problems. Among the abundance of methods, the BDF-2 method seems to of particular interest, for details we refer to [17, 23, 79, 97]. Especially, the BDF-2 method is stable for constant time steps and is of second order accurate in time. In contrast to the Crank-Nicolson approximation, this method exhibits the smoothing property of solution [17, 63]. For purely parabolic problems (in the absence of an interface), *a posteriori* error estimate for the BDF-2 approximation has been studied by Akrivis *et al.* in [3]. The mesh change effect has not been taken into account in their analysis. Therefore, an attempt has been made to extend the BDF-2 *a posteriori* analysis of the parabolic problems to the parabolic interface problems with mesh chang effect. Motivated by the discussions in [3], a quadratic (in time) space-time reconstruction $\hat{U}$ is introduced for the BDF-2 approximation for the parabolic interface problems. A quadratic reconstruction operator along with the elliptic reconstruction and new approximation properties of a Clément-type interpolation operator are used to obtain *a posteriori* error bound in the $L^\infty(L^2)$-norm. The main key features of our analysis is that we have incorporated the effect of mesh modification strategy in the error analysis unlike the work of Akrivis *et al.* in [3]. The derivation of *a posteriori* error bound is based on the energy technique in the reconstruction framework.

Finally, we now shift our attention to study the semilinear parabolic interface problems. To discretize the problem in time we have considered both the backward Euler and the Crank-Nicolson approximations, and in space the standard piecewise linear finite elements. The forcing term $f(x,t,u)$ is assumed to satisfy the Lipschitz condition with respect to the third argument, i.e., there exists a constant $\mathcal{C}_L > 0$ such that

$$|f(x,t,v) - f(x,t,w)| \leq \mathcal{C}_L |v-w| \quad \forall v, w \in \mathbb{R}. \tag{1.3.3}$$

The aim of this work is to extend our *a posteriori* error analysis of the linear parabolic interface problem to the semilinear case. More precisely, the backward Euler and the Crank-Nicolson *a posteriori* error analysis are carried out for the semilinear interface problem using the energy technique in the reconstruction framework. Other worth mentioning technicalities for our analysis are new approximation results of the Clément-type interpolation operator and the discrete version of Gronwall's lemma (Lemma 1.2.2). Optimal order estimates in time and nearly optimal order estimates in space in the $L^\infty(L^2)$-norm are obtained for both the backward Euler and the Crank-Nicolson approximation (Theorem 6.2.1 and Theorem 6.3.2). For *a posteriori* analysis of non-interface semilinear parabolic problems, one may refer to the articles [59] and [60].

1.4 Organization of the Thesis

This thesis contains the following chapters and is organized as follows.

Chapter 1 introduces the problem and provides the necessary notations and prerequisites. It also contains a brief overview of the existing literature. The motivation for the present study and the contributions made in this thesis are also highlighted.

Chapter 2 is devoted to the *a posteriori* error analysis for the spatially discrete finite element approximation for the linear parabolic interface problem (1.1.1) – (1.1.3) using the elliptic reconstruction technique. New interpolation approximation properties for the Clément-type interpolation operator [92] are established. The energy method is used to derive *a posteriori* error estimates with almost optimal order convergence in the $L^\infty(L^2)$-norm.

Chapter 3 provides the *a posteriori* error analysis for the fully discrete backward Euler approximation for the problem (1.1.1) – (1.1.3). The main tools in deriving *a posteriori* estimates are new Clément type interpolation estimates and an appropriate elliptic reconstruction operator. Optimal *a posteriori* error bounds in the $L^2(H^1)$ norm and a nearly optimal error estimate in the $L^\infty(L^2)$ norm are established using the energy argument.

In Chapter 4, we derive *a posteriori* error estimates for the fully discrete Crank-Nicolson approximation for the interface problem (1.1.1) – (1.1.3). A quadratic space-time reconstruction plays a central role in the error analysis. We establish *a posteriori* error estimates of almost optimal order in space and second order in time with respect to the $L^\infty(L^2)$-norm.

A posteriori error analysis for the space-time BDF-2 approximation for the linear parabolic interface problem (1.1.1)−(1.1.3) is discussed in Chapter 5. A quadratic space-time BDF-2 reconstruction is introduced for the problem and nearly optimal order *a posteriori* error bounds are derived in the $L^\infty(L^2)$-norm.

In Chapter 6, we address the *a posteriori* error analysis for the semilinear parabolic interface problems. In time discretization both the backward Euler and the Crank-Nicolson approximations are considered whereas in space we have considered the standard piecewise linear finite elements. Our analysis shows that the method yields optimal order estimates in time and almost optimal order estimates in space in the $L^\infty(L^2)$-norm. The main technical tools used are the energy argument combined with elliptic reconstruction technique.

In Chapter 7, we perform numerical experiments to study the asymptotic behaviour of the various error estimators for a test problem. Numerical results validate the optimality

of the derived estimators.

Finally in Chapter 8, we discuss the critical evaluation of the results presented in this thesis. This chapter concludes with a brief discussion on the possible extensions and future work.

For clarity of presentation we have repeatedly mention the equations (1.1.1) – (1.1.3) and the relevant preliminary materials at the beginning of each chapter.

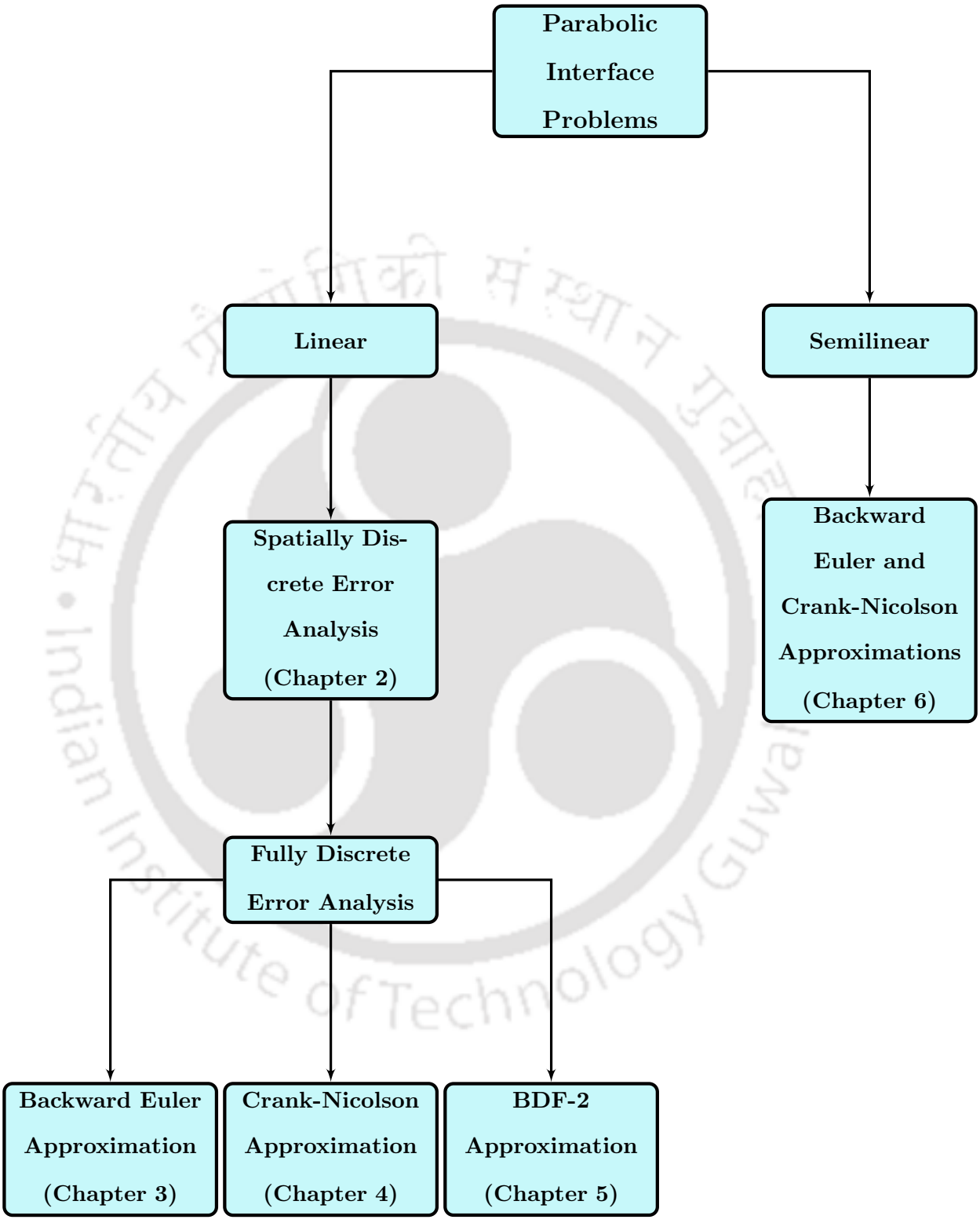

Figure 1.4: *Schematic strategy of the thesis.*

2

Spatially Discrete Error Analysis

In this chapter, we derive residual-based *a posteriori* error estimates for the spatially discrete finite element approximation of the linear parabolic interface problem (1.1.1) – (1.1.3). The salient features of the *a posteriori* error analysis includes: (i) an appropriate introduction of an elliptic reconstruction operator, and (ii) new approximation results of the Clément-type interpolation operator. We close this chapter by presenting an almost optimal order *a posteriori* error estimate in the $L^\infty(L^2)$-norm. The interface is assumed to be of arbitrary shape but is of class C^2.

2.1 Introduction

To begin with we first recall the parabolic interface problem of the form

$$u_t(x,t) - \mathrm{div}(\beta(x)\nabla u(x,t)) = f(x,t) \quad \text{in} \quad \Omega \times (0,T] \tag{2.1.1}$$

with prescribed initial and boundary conditions

$$u(x,0) = u_0(x) \quad \text{in} \quad \Omega; \qquad u = 0 \quad \text{on} \quad \partial\Omega \times [0,T] \tag{2.1.2}$$

and jump conditions on the interface

$$[u] = 0, \quad \left[\beta \frac{\partial u}{\partial \mathbf{n}}\right] = 0 \quad \text{across} \quad \Gamma \times [0,T], \tag{2.1.3}$$

where Ω is a bounded convex polygonal domain in $\mathbb{R}^2$ with Lipschitz boundary $\partial\Omega$, Ω_1 is a subdomain of Ω with C^2 boundary $\partial\Omega_1 := \Gamma$ (interface) and $\Omega_2 := \Omega \setminus \Omega_1$. Here, $[v]$ denotes the jump of a quantity v across the interface Γ, i.e., $[v](x) = v_1(x) - v_2(x)$, $x \in \Gamma$ with $v_i(x) = v(x)|_{\Omega_i}$, $i = 1, 2$ and $T < +\infty$. The symbol $\mathbf{n}$ denotes the unit outward normal to the boundary $\partial\Omega_1 := \Gamma$. The diffusion coefficient $\beta(x)$ is assumed to be positive and piecewise constant on each subdomain, i.e.,

$$\beta(x) = \beta_i \quad \text{for} \quad x \in \Omega_i,\ i = 1, 2.$$

The initial function $u_0(x)$ and the forcing term $f(x,t)$ are real valued functions and assumed to be smooth.

As a first step towards finite element approximation of (2.1.1) – (2.1.3), we recall the bilinear form $a(\cdot,\cdot) : H_0^1(\Omega) \times H_0^1(\Omega) \longrightarrow \mathbb{R}$ defined by

$$a(v,w) = \langle \beta \nabla v, \nabla w \rangle \quad \forall v, w \in H_0^1(\Omega). \tag{2.1.4}$$

The bilinear form $a(\cdot,\cdot)$ is bounded and coercive on $H_0^1(\Omega)$, i.e., $\exists \alpha_0, \gamma_0 > 0$ such that

$$|a(v,w)| \leq \alpha_0 \, \|v\|_1 \|w\|_1 \quad \forall v, w \in H_0^1(\Omega), \tag{2.1.5}$$

and

$$a(v,v) \geq \gamma_0 \, \|v\|_1^2 \quad \forall v \in H_0^1(\Omega). \tag{2.1.6}$$

Then the weak formulation of (2.1.1)−(2.1.3) is stated as follows: Find $u \in L^\infty(0,T; H_0^1(\Omega))$ satisfying

$$\begin{aligned} \langle u_t(t), \varphi \rangle + a(u(t), \varphi) &= \langle f(t), \varphi \rangle \ \ \forall \varphi \in H_0^1(\Omega), \quad \text{a.e. } t \in (0,T], \\ u(0) &= u_0. \end{aligned} \tag{2.1.7}$$

Additionally, we also recall the finite element space $\mathbb{S}_h$ corresponding to the triangulation $\mathcal{T}_h$ (as described in Chapter 1) as

$$\mathbb{S}_h := \left\{ \chi \in H_0^1(\Omega) \;\middle|\; \chi|_K \in \mathbb{P}_1(K) \quad \text{for all} \ \ K \in \mathcal{T}_h \right\},$$

where $\mathbb{P}_1(K)$ is the space of polynomials of degree at most 1 over K. The spatially discrete finite element approximation $u_h : [0,T] \longrightarrow \mathbb{S}_h$ of u is defined as

$$\begin{aligned} \langle u_{h,t}, \chi_h \rangle \ + \ a(u_h, \chi_h) &= \langle f, \chi_h \rangle \quad \forall \chi_h \in \mathbb{S}_h, \quad \text{a.e. } t \in (0,T], \\ u_h(\cdot, 0) &= I_h u_0, \end{aligned} \tag{2.1.8}$$

where I_h is a chosen projection operator from $H_0^1(\Omega)$ into the finite dimensional subspace $\mathbb{S}_h$.

Next, we recall the representation of bilinear form $a(\cdot,\cdot)$ from Chapter 1. Using Green's formula the bilinear form can be represented in more compact form as

$$a(v_h, \varphi) = \langle (v_h)_{\text{el}}, \varphi \rangle \ + \ \langle j[\beta v_h], \varphi \rangle_{\Sigma_h} \quad \forall \varphi \in H_0^1(\Omega), \tag{2.1.9}$$

where the symbols $j[\beta v_h]$ and $(v_h)_{\text{el}}$ are defined in (1.2.8) and (1.2.7), respectively.

We now define the L^2 projection operator for the subsequent use. Let $\Pi_0^h : L^2(\Omega) \longrightarrow \mathbb{S}_h$ be defined by

$$\langle \Pi_0^h v\, , \chi_h \rangle \;=\; \langle v,\; \chi_h \rangle \;\text{ for }\; v \in L^2(\Omega) \;\text{ and }\; \forall \chi_h \in \mathbb{S}_h. \tag{2.1.10}$$

Let $\mathcal{A}_h : H_0^1(\Omega) \longrightarrow \mathbb{S}_h$ be the discrete elliptic operator associated with the bilinear form $a(\cdot,\cdot)$ and be such that for $v \in H_0^1(\Omega)$,

$$\langle \mathcal{A}_h v,\; \chi_h \rangle = a(v, \chi_h) \qquad \forall \chi_h \in \mathbb{S}_h. \tag{2.1.11}$$

For purely parabolic problem, *a posteriori* error analysis for the spatially discrete approximation has been studied by Makridakis and Nochetto in [76] . They have used elliptic reconstruction in conjunction with the energy technique to derive optimal order *a posteriori* error bound in the $L^\infty(L^2)$-norm. The *a posteriori* error analysis in [76] relies on the approximation properties of the Clément-type interpolation operator [92]. The approximation properties for such type of operator are proved in [92] (Theorem 4.1, [92]) under suitable regularity assumptions on functions. In particular, for $O(h^2)$ approximation results using the linear finite elements, the analysis of [92] demands functions to be in $H^2(\Omega)$. However, in the present case, due to the discontinuity of the diffusion coefficient β along the interface Γ the solution has a lower regularity in the entire domain Ω, usually one has only $u \in H_0^1(\Omega)$. Thus, the existing approximation results do not apply directly. Therefore, the extension of *a posteriori* analysis of purely parabolic problems to the parabolic interface problems is not straightforward.

In this chapter, an attempt has been made to extend the *a posteriori* error analysis of the spatially discrete approximation of the parabolic problems [76] to the parabolic interface problem (2.1.1) – (2.1.3). The new approximation results for the Clément-type interpolation operator are established to deal with the interface problems. Other key technical tools used are an appropriate elliptic reconstruction operator and the energy argument.

The rest of this chapter is organized as follows. In Section 2.2, we establish new approximation results for the Clément-type interpolation operator. In Section 2.3, elliptic reconstruction operator is introduced and *a posteriori* error estimate of nearly optimal order in the $L^\infty(L^2)$-norm is derived.

2.2 Clément-type Interpolation Error Estimates

In this section, we shall prove new approximation properties of the Clément-type interpolation operator in a bounded convex polygonal domain $\Omega \subseteq \mathbb{R}^2$. Clément-type operators were introduced by Scott and Zhang in [92] for nonsmooth functions.

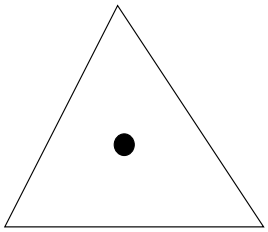

(a) z is an interior point of an element K.

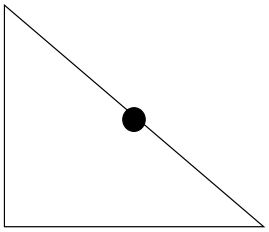

(b) z is an interior point of an edge E.

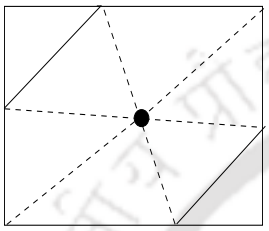

(c) z is a common boundary point of some edges (marked with broken line) and z is an interior point of Ω.

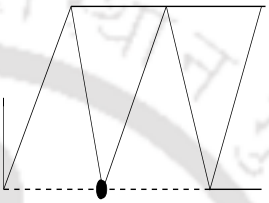

(d) z is a common boundary point of some edges (marked with broken line) and z is a boundary point of Ω.

Figure 2.1: *Choice of subdomain* $\mathcal{F}_z$.

We now follow Scott-Zhang [92] to define the Clément-type interpolation operator. Let $\mathcal{N}_h$ be the set of all interpolation nodes of the triangulation $\mathcal{T}_h$. For each $z \in \mathcal{N}_h$, define

$$\mathcal{F}_z := \begin{cases} K, & \text{if } z \text{ is an interior point of } K \in \mathcal{T}_h, \\ E, & \text{if } z \text{ is an interior point of an edge E of the triangle } K \in \mathcal{T}_h, \\ E_0, & \text{any edge } E_0 \text{ containing } z, \text{ if } z \text{ is a common boundary point of some edges} \\ & \text{and } z \text{ is an interior point of the domain } \Omega, \\ \tilde{E}_0, & \text{any edge } \tilde{E}_0 \text{ containing } z \text{ and } \tilde{E}_0 \subset \partial\Omega, \text{ if } z \text{ is a common boundary} \\ & \text{point of some edges and } z \text{ is a boundary point of the domain } \Omega. \end{cases}$$

Let $\{\phi_z\}_{z\in\mathcal{N}_h}$ be the nodal basis for $\mathbb{S}_h$, i.e., $\phi_{z_i}(z_j) = \delta_{i,j}$, where $\delta_{i,j}$ is the Kronecker delta. Let $\{\psi_z\}_{z\in\mathcal{N}_h}$ be a dual basis of $\{\phi_z\}_{z\in\mathcal{N}_h}$, where $\psi_z : \mathcal{F}_z \longrightarrow \mathbb{R}$ and

$$\int_{\mathcal{F}_z} \psi_{z_i}\phi_{z_j} = \delta_{i,j},$$

where z_i and z_j are nodes associated with $\mathcal{F}_z$.

The Clément-type interpolation operator $\mathscr{J}_h : X \longrightarrow \mathbb{S}_h$ is defined by

$$\mathscr{J}_h v = \sum_{z \in \mathcal{N}_h} \phi_z \int_{\mathcal{F}_z} \psi_z(\xi) v(\xi) d\xi. \tag{2.2.1}$$

Remark 2.2.1. (i) The first two cases shown in Fig. $2.1(a) - 2.1(b)$ do not arise for the fitted finite element discretizations.

(ii) We wish to emphasize the fact that for $\mathscr{J}_h : W^{l,p}(\Omega) \longrightarrow \mathbb{S}_h$, the following estimates hold (cf. [92]): For $v \in W^{l,p}(\Omega)$,

$$\|v - \mathscr{J}_h v\|_{W^{m,p}(K)} \leq C h_K^{l-m} |v|_{W^{l,p}(S_K)}, \quad K \in \mathcal{T}_h, \ 0 \leq m \leq l \leq 2, \tag{2.2.2}$$

where

$$l \geq 1 \ \text{ if } \ p = 1 \quad \text{and} \quad l > \frac{1}{p} \ \text{ otherwise,}$$

and the patch

$$S_K := (\cup_{i \in \mathcal{I}_K} \bar{K}_i)^\circ, \qquad \mathcal{I}_K := \{i \in \mathbb{N} \mid \partial K_i \cap \partial K \neq \emptyset, \ \ K_i \in \mathcal{T}_h\}.$$

Here, for an $A \subseteq \mathbb{R}^2$, A° and ∂A denote the closure, interior and boundary of A, respectively with respect to the Euclidean norm on $\mathbb{R}^2$.

We now state the following approximation properties. The proof of the theorem essentially uses (2.2.2) and the trace theorem on reference triangle.

Theorem 2.2.1. *Let $\mathscr{J}_h : X \longrightarrow \mathbb{S}_h$ be the standard Clément-type interpolation operator defined by (2.2.1). Then, for the finite element polynomial space of degree ≤ 1, the following interpolation estimates hold for $v \in H_0^1(\Omega)$:*

$$\|v - \mathscr{J}_h v\| \leq \mathcal{C}_{I,1} \, h \, \|v\|_1, \tag{2.2.3}$$

and

$$\|v - \mathscr{J}_h v\|_{\Sigma_h} \leq \mathcal{C}_{I,2} \, h^{\frac{1}{2}} \, \|v\|_1, \tag{2.2.4}$$

where the constants $\mathcal{C}_{I,k}$, $k \in \{1, 2\}$ are positive and depend only on the shape-regularity of the family of triangulations.

Proof. To prove (2.2.3), it is enough to obtain the result for individual elements and then sum up to obtain the result for the entire domain.

Let $K \in \mathcal{T}_h$. Then for $v \in H_0^1(\Omega)$, using (2.2.2) (with $m = 0, p = 2$ and $l = 1$), we have

$$\|v - \mathscr{J}_h v\|_{L^2(K)} \leq C \, h_K \, |v|_{H^1(S_K)}.$$

Summing up over all the triangles in $\mathcal{T}_h$, we have

$$\|v - \mathscr{J}_h v\| \leq C\, h \sum_{K \in \mathcal{T}_h} |v|_{H^1(S_K)}, \tag{2.2.5}$$

which together with (1.2.4), it now leads to

$$\|v - \mathscr{J}_h v\| \leq \mathcal{C}_{I,1}\, h \|v\|_1, \tag{2.2.6}$$

where $\mathcal{C}_{I,1}$ is a positive constant independent of h and this proves (2.2.3).

For the second estimate (2.2.4), we now recall some classical finite element estimates from [35]. Consider an arbitrary triangle $K \in \mathcal{T}_h$ and an arbitrary edge $E \in \mathcal{E}_h$ of K. Let

$$\begin{aligned} F_K \;&:\; \hat{K} \longrightarrow K \\ &\quad\; \hat{Y} \;\mapsto\; B_K \hat{Y} + b_K \end{aligned}$$

be an invertible affine transformation which maps the reference triangle $\hat{K}$ with vertices $(0,0)$, $(1,0)$ and $(0,1)$ onto K and the horizontal edge $\hat{E}$ of $\hat{K}$ onto E of K. In the above, B_K (an invertible 2×2 matrix) and b_K (a vector in $\mathbb{R}^2$) are obtained by using

$$F_K(\hat{a}_i) = a_i, \;\; 1 \leq i \leq 3,$$

where $\hat{a}_i$ and a_i are the vertices of the triangles $\hat{K}$ and K, respectively. Then

$$\|B_K\| \leq C h_K \quad \text{and} \quad |\det(B_K)| = \frac{m(K)}{m(\hat{K})} \leq C h_K^2. \tag{2.2.7}$$

Here, $\|B_K\| := \sup \left\{ \frac{\|B_K x\|_{\mathbb{R}^2}}{\|x\|_{\mathbb{R}^2}} \;:\; x(\neq 0) \in \mathbb{R}^2 \right\}$, $\|x\|_{\mathbb{R}^2}$ is the standard Euclidean vector norm in $\mathbb{R}^2$ and m denotes the standard Lebesgue measure in $\mathbb{R}^2$.

Let $\phi \in H^1(K)$ and let $\hat{\phi} = \phi \circ F_K \in H^1(\hat{K})$. Then, we employ the transformation rule for integrals (cf. [35]) to have

$$\|\hat{\phi}\|_{L^2(\hat{K})} \leq C |\det(B_K)|^{-\frac{1}{2}} \, \|\phi\|_{L^2(K)} \leq C h_K^{-1} \, \|\phi\|_{L^2(K)}, \tag{2.2.8}$$

and

$$\|\nabla \hat{\phi}\|_{L^2(\hat{K})} \leq C \, \|B_K\| \, |\det(B_K)|^{-\frac{1}{2}} \, \|\nabla \phi\|_{L^2(K)} \leq C \, \|\nabla \phi\|_{L^2(K)}. \tag{2.2.9}$$

A standard trace theorem on the reference triangle $\hat{K}$ implies

$$\|\phi\|_{L^2(E)} \leq C h_K^{\frac{1}{2}} \, \|\hat{\phi}\|_{H^1(\hat{K})}. \tag{2.2.10}$$

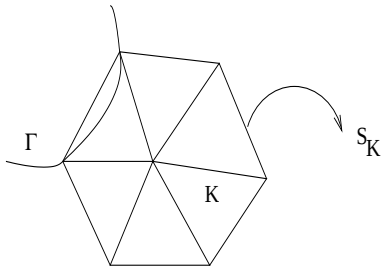

Figure 2.2: *A typical patch S_K of a triangle K.*

Invoking the transformation rule for the integrals (2.2.8) and (2.2.9) in (2.2.10), we obtain

$$\|\phi\|_{L^2(E)} \leq C\left\{h_K^{-\frac{1}{2}}\|\phi\|_{L^2(K)} + h_K^{\frac{1}{2}}\|\nabla\phi\|_{L^2(K)}\right\}. \tag{2.2.11}$$

We are now ready to derive the approximation properties of the Clément-type interpolation operator over edges.

For $E \in \mathcal{E}_h$, using (2.2.11) and (2.2.2), we obtain

$$\begin{aligned} \|v - \mathscr{J}_h v\|_{L^2(E)} &\leq C\left\{h_K^{-\frac{1}{2}}\|v - \mathscr{J}_h v\|_{L^2(K)} + h_K^{\frac{1}{2}}\|\nabla(v - \mathscr{J}_h v)\|_{L^2(K)}\right\} \\ &\leq Ch_K^{\frac{1}{2}}|v|_{H^1(S_K)}. \end{aligned} \tag{2.2.12}$$

Taking summation over all edges, we have

$$\begin{aligned} \|v - \mathscr{J}_h v\|_{\Sigma_h} &= \sum_{E\in\mathcal{E}_h}\|v - \mathscr{J}_h v\|_{L^2(E)} \\ &\leq C\sum_{K\in\mathcal{T}_h} h_K^{\frac{1}{2}}|v|_{H^1(S_K)} \\ &\leq \mathcal{C}_{I,2}\, h^{\frac{1}{2}}\|v\|_1, \end{aligned} \tag{2.2.13}$$

where in the last inequality, we have used (1.2.4) and we thus complete the proof of the theorem. □

In view of (2.2.2), we observe that to obtain $O(h^2)$ approximation properties for such type of operator one requires $v \in W^{2,p}(S_K)$ for all $K \in \mathcal{T}_h$. But, this need not be true for interface problems. This is because even for $K \in \mathcal{T}_h \setminus \mathcal{T}_h^*$, the patch S_K may contain an interface triangle (see, Fig. 2.2) and hence, $v \notin W^{2,p}(S_K)$. Therefore, one can not apply the approximation properties (2.2.2) directly while dealing with the interface problems. It is known that the solution of the interface problem $u \in X$, i.e., u has good regularity in the individual subdomains Ω_1 and Ω_2 ($u \in H^2(\Omega_i)$), but $u \notin H^2(\Omega)$. Therefore,

this local higher regularity along with the classical error estimate (2.2.2), the Sobolev embedding theorem and extension results are used to derive nearly $O(h^2)$ (up to $|\log h|$ factor) new approximation results for such type of operator.

Theorem 2.2.2. *Let $\mathscr{J}_h : X \longrightarrow \mathbb{S}_h$ be the standard Clément-type interpolation operator defined by (2.2.1). Then, for the finite element polynomial space of degree ≤ 1, the following interpolation estimates hold for $v \in X$:*

$$\|v - \mathscr{J}_h v\| \leq \mathcal{C}_{I,3}\, h^2\, |\log h|^{\frac{1}{2}}\, \|v\|_X, \tag{2.2.14}$$

and

$$\|v - \mathscr{J}_h v\|_{\Sigma_h} \leq \mathcal{C}_{I,4}\, h^{\frac{3}{2}}\, |\log h|^{\frac{1}{2}}\, \|v\|_X, \tag{2.2.15}$$

where the constants $\mathcal{C}_{I,k}$, $k \in \{3,4\}$ depend only on the shape-regularity of the family of triangulations.

Proof. Let $v \in X$. Then by the Sobolev embedding theorem, $v \in W^{1,p}(\Omega)$ for all $p > 2$ (cf. [33]). Let $v_i = v|_{\Omega_i}$ for $i = 1, 2$ and $v_1 = v_2$ on Γ. Then $v_i \in H^2(\Omega_i)$. As the interface Γ is of class C^2, one can have continuous extension of the functions $v_i \in H^2(\Omega_i)$ onto the whole domain Ω and obtain a function $\tilde{v}_i \in H^2(\Omega)$ such that $\tilde{v}_i|_{\Omega_i} = v_i$ for $i = 1, 2$ and

$$\|\tilde{v}_i\|_{H^2(\Omega)} \leq C\|v\|_{H^2(\Omega_i)} \quad \text{for } i = 1, 2. \tag{2.2.16}$$

The existence of such kind of extension can be found in Stein (cf. [96]).

We note that in order to derive (2.2.14), it is enough to derive the estimate over each triangles.

Clément-type estimates for triangles: To establish the approximation properties of the Clément-type interpolation operator for triangles, we consider the following two cases: Firstly, for the non-interface triangles ($K \in \mathcal{T}_h \setminus \mathcal{T}_h^*$) and then for the interface ones ($K \in \mathcal{T}_h^*$).

Clément-type estimates for non-interface triangles: Let $K \in \mathcal{T}_h \setminus \mathcal{T}_h^*$. Then, either $K \in \mathcal{T}_{h,\Omega_1}$ or $K \in \mathcal{T}_{h,\Omega_2}$. Suppose that $K \in \mathcal{T}_{h,\Omega_1}$. Then, using (2.2.2), we obtain

$$\begin{aligned} \|v - \mathscr{J}_h v\|_{L^2(K)} &= \|\tilde{v}_1 - \mathscr{J}_h \tilde{v}_1\|_{L^2(K)} \\ &\leq Ch_K^2 |\tilde{v}_1|_{H^2(S_K)}. \end{aligned} \tag{2.2.17}$$

Similarly, for $K \in \mathcal{T}_{h,\Omega_2}$, we have

$$\|v - \mathscr{J}_h v\|_{L^2(K)} \leq Ch_K^2 |\tilde{v}_2|_{H^2(S_K)}. \tag{2.2.18}$$

Summing up over all non-interface triangles in $\mathcal{T}_h \setminus \mathcal{T}_h^*$, using (2.2.17) and (2.2.18), we obtain

$$\begin{aligned}\sum_{K\in\mathcal{T}_h\setminus\mathcal{T}_h^*} \|v - \mathscr{J}_h v\|_{L^2(K)} &= \sum_{K\in\mathcal{T}_{h,\Omega_1}} \|v - \mathscr{J}_h v\|_{L^2(K)} + \sum_{K\in\mathcal{T}_{h,\Omega_2}} \|v - \mathscr{J}_h v\|_{L^2(K)} \\ &\leq Ch^2 \left\{ \sum_{K\in\mathcal{T}_{h,\Omega_1}} |\tilde{v}_1|_{H^2(S_K)} + \sum_{K\in\mathcal{T}_{h,\Omega_2}} |\tilde{v}_2|_{H^2(S_K)} \right\}. \qquad (2.2.19)\end{aligned}$$

An application of (1.2.4), (2.2.16) together with (2.2.19) yields

$$\begin{aligned}\sum_{K\in\mathcal{T}_h\setminus\mathcal{T}_h^*} \|v - \mathscr{J}_h v\|_{L^2(K)} &\leq Ch^2 \left\{ |\tilde{v}_1|_{H^2(\Omega)} + |\tilde{v}_2|_{H^2(\Omega)} \right\} \\ &\leq Ch^2 \|v\|_X. \qquad (2.2.20)\end{aligned}$$

Clément-type estimates for interface triangles: Let $K \in \mathcal{T}_h^*$. Then, using the Hölder's inequality and the fact that $m(K) \leq Ch_K^2$, we obtain for $p > 2$ that

$$\begin{aligned}\|v - \mathscr{J}_h v\|_{L^2(K)}^2 &\leq \left(\int_K \left(|v - \mathscr{J}_h v|^2 \right)^{\frac{p}{2}} dx \right)^{\frac{2}{p}} \left(\int_K dx \right)^{1-\frac{2}{p}} \\ &\leq C(h_K^2)^{1-\frac{2}{p}} \|v - \mathscr{J}_h v\|_{L^p(K)}^2.\end{aligned}$$

An application of (2.2.2) yields

$$\|v - \mathscr{J}_h v\|_{L^2(K)} \leq Ch_K^{2-\frac{2}{p}} \|v\|_{W^{1,p}(S_K)}, \ p > 2. \tag{2.2.21}$$

Summing up over all the interface triangles in $\mathcal{T}_h^*$ and using (1.2.4), we obtain for $p > 2$

$$\begin{aligned}\sum_{K\in\mathcal{T}_h^*} \|v - \mathscr{J}_h v\|_{L^2(K)} &\leq Ch^{2-\frac{2}{p}} \sum_{K\in\mathcal{T}_h^*} \|v\|_{W^{1,p}(S_K)} \\ &\leq Ch^{2-\frac{2}{p}} \|v\|_{W^{1,p}(\Omega)}. \qquad (2.2.22)\end{aligned}$$

Now, we recall the Sobolev embedding theorem (cf. Ren and Wei [89]) in two dimensions

$$H^1(\Omega_i) \hookrightarrow L^p(\Omega_i) \ \text{ with } p > 2,$$

i.e.,

$$\|v\|_{L^p(\Omega_i)} \leq Cp^{\frac{1}{2}} \|v\|_{H^1(\Omega_i)} \ \ \forall v \in H^1(\Omega_i), i = 1, 2 \ \text{ and } \ p > 2. \tag{2.2.23}$$

Then a simple calculation yields

$$\|v\|_{W^{1,p}(\Omega)} \leq C p^{\frac{1}{2}} \|v\|_X, \ p > 2. \tag{2.2.24}$$

Going back to (2.2.22), we now obtain

$$\sum_{K \in \mathcal{T}_h^*} \|v - \mathscr{J}_h v\|_{L^2(K)} \leq C h^{2-\frac{2}{p}} p^{\frac{1}{2}} \|v\|_X, \quad p > 2. \tag{2.2.25}$$

Now, summing up over all triangles in $\mathcal{T}_h$ and using (2.2.20) and (2.2.25), we obtain

$$\begin{aligned} \|v - \mathscr{J}_h v\|_{L^2(\Omega)} &= \sum_{K \in \mathcal{T}_h} \|v - \mathscr{J}_h v\|_{L^2(K)} \\ &= \sum_{K \in \mathcal{T}_h \setminus \mathcal{T}_h^*} \|v - \mathscr{J}_h v\|_{L^2(K)} + \sum_{K \in \mathcal{T}_h^*} \|v - \mathscr{J}_h v\|_{L^2(K)} \\ &\leq C \left\{ h^2 + h^{2-\frac{2}{p}} p^{\frac{1}{2}} \right\} \|v\|_X. \end{aligned}$$

Taking $p = |\log h|$ for small h in the above, we finally obtain

$$\|v - \mathscr{J}_h v\| \leq \mathcal{C}_{I,3} \ h^2 \ |\log h|^{\frac{1}{2}} \ \|v\|_X,$$

where the constant $\mathcal{C}_{I,3}$ is independent of h, and this completes the proof of (2.2.14).

To prove the second estimate (2.2.15), we proceed as follows.

Clément-type interpolation estimates for edges: Analogous to the previous case, here also the proof proceeds by considering two cases: Clément-type estimates for edges $E \in \mathcal{E}_h \setminus \mathcal{E}_h^* := \mathcal{E}_{h,\Omega_1} \cup \mathcal{E}_{h,\Omega_2}$ and $E \in \mathcal{E}_h^*$.

Clément-type estimates for edges $E \in \mathcal{E}_{h,\Omega_1} \cup \mathcal{E}_{h,\Omega_2}$: Let $E \in \mathcal{E}_{h,\Omega_1}$ be any edge of a triangle $K \in \mathcal{T}_{h,\Omega_1}$. Then, using (2.2.11) and (2.2.2) we obtain

$$\begin{aligned} \|v - \mathscr{J}_h v\|_{L^2(E)} &\leq C \left\{ h_K^{-\frac{1}{2}} \|v - \mathscr{J}_h v\|_{L^2(K)} + h_K^{\frac{1}{2}} \|\nabla(v - \mathscr{J}_h v)\|_{L^2(K)} \right\} \\ &\leq C \left\{ h_K^{-\frac{1}{2}} \|\tilde{v_1} - \mathscr{J}_h \tilde{v_1}\|_{L^2(K)} + h_K^{\frac{1}{2}} \|\nabla(\tilde{v_1} - \mathscr{J}_h \tilde{v_1})\|_{L^2(K)} \right\} \\ &\leq C \left\{ h_K^{-\frac{1}{2}} \, h_K^2 |\tilde{v_1}|_{H^2(S_K)} + h_K^{\frac{1}{2}} \, h_K |\tilde{v_1}|_{H^2(S_K)} \right\} \\ &\leq C \, h_K^{\frac{3}{2}} \, |\tilde{v_1}|_{H^2(S_K)}. \end{aligned} \tag{2.2.26}$$

Similarly, for a triangle $K \in \mathcal{T}_{h,\Omega_2}$ and an edge $E \in \mathcal{E}_{h,\Omega_2}$, we have

$$\|v - \mathscr{J}_h v\|_{L^2(E)} \leq C \, h_K^{\frac{3}{2}} \, |\tilde{v_2}|_{H^2(S_K)}. \tag{2.2.27}$$

Use of (2.2.26), (2.2.27) and (2.2.16) leads to

$$\begin{aligned}\sum_{E\in\mathcal{E}_h\setminus\mathcal{E}_h^*}\|v-\mathscr{J}_h v\|_{L^2(E)} &= \sum_{E\in\mathcal{E}_{h,\Omega_1}}\|v-\mathscr{J}_h v\|_{L^2(E)}+\sum_{E\in\mathcal{E}_{h,\Omega_2}}\|v-\mathscr{J}_h v\|_{L^2(E)}\\ &\le Ch^{\frac{3}{2}}\left\{\sum_{K\in\mathcal{T}_{h,\Omega_1}}|\tilde{v_1}|_{H^2(S_K)}+\sum_{K\in\mathcal{T}_{h,\Omega_2}}|\tilde{v_2}|_{H^2(S_K)}\right\}\\ &\le Ch^{\frac{3}{2}}\{\|\tilde{v_1}\|_{H^2(\Omega)}+\|\tilde{v_2}\|_{H^2(\Omega)}\}\\ &\le Ch^{\frac{3}{2}}\|v\|_X, \qquad (2.2.28)\end{aligned}$$

where in the third step, we have used (1.2.4).

Clément-type estimates for edges $E\in\mathcal{E}_h^*$: Let $E\in\mathcal{E}_h^*$ be any arbitrary edge of an interface triangle $K\in\mathcal{T}_h^*$. Then, in view of (2.2.11), we have

$$\|v-\mathscr{J}_h v\|_{L^2(E)}\le C\left\{h_K^{-\frac{1}{2}}\|v-\mathscr{J}_h v\|_{L^2(K)}+h_K^{\frac{1}{2}}\|\nabla(v-\mathscr{J}_h v)\|_{L^2(K)}\right\}. \qquad (2.2.29)$$

Arguing as in (2.2.21), we obtain

$$\|\nabla(v-\mathscr{J}_h v)\|_{L^2(K)}\le Ch_K^{1-\frac{2}{p}}\|v\|_{W^{1,p}(S_K)},\ \ p>2, \qquad (2.2.30)$$

which together with (2.2.21) and (2.2.29) yields

$$\|v-\mathscr{J}_h v\|_{L^2(E)} \le Ch_K^{\frac{3}{2}-\frac{2}{p}}\|v\|_{W^{1,p}(S_K)},\ \ p>2. \qquad (2.2.31)$$

Now, summing up over all the edges $E\in\mathcal{E}_h^*$ of the interface triangles, using (1.2.4) and (2.2.24) we obtain for $p>2$

$$\begin{aligned}\sum_{E\in\mathcal{E}_h^*}\|v-\mathscr{J}_h v\|_{L^2(E)} &\le Ch^{\frac{3}{2}-\frac{2}{p}}\sum_{K\in\mathcal{T}_h^*}\|v\|_{W^{1,p}(S_K)}\\ &\le Ch^{\frac{3}{2}-\frac{2}{p}}\|v\|_{W^{1,p}(\Omega)}\\ &\le Ch^{\frac{3}{2}-\frac{2}{p}}p^{\frac{1}{2}}\|v\|_X,\ p>2. \qquad (2.2.32)\end{aligned}$$

To complete the proof of (2.2.15), we use (2.2.28), (2.2.32) and take $p=|\log h|$ to obtain

$$\begin{aligned}\|v-\mathscr{J}_h v\|_{\Sigma_h} &= \sum_{E\in\mathcal{E}_h}\|v-\mathscr{J}_h v\|_{L^2(E)}\\ &\le C\left\{h^{\frac{3}{2}}+h^{\frac{3}{2}-\frac{2}{p}}p^{\frac{1}{2}}\right\}\|v\|_X\\ &\le \mathcal{C}_{I,4}\,h^{\frac{3}{2}}\,|\log h|^{\frac{1}{2}}\,\|v\|_X, \qquad (2.2.33)\end{aligned}$$

where the constant $\mathcal{C}_{I,4}$ is independent of h and depends on the shape-regularity of the family of triangulations. □

Remark 2.2.2. (*i*) For the purely parabolic problems, the following approximation properties are well-known for the Clément-type interpolation operator (see, [62]): For $v \in H^2(\Omega)$ and $0 \leq j \leq 2$, there exists interpolation constants $\mathcal{C}_j$, $\tilde{\mathcal{C}}_j$ such that

$$\|v - \mathscr{J}_h v\| \leq \mathcal{C}_j h^j |v|_{H^j(\Omega)}, \tag{2.2.34}$$

and

$$\|v - \mathscr{J}_h v\|_{\Sigma_h} \leq \tilde{\mathcal{C}}_j h^{j-\frac{1}{2}} |v|_{H^j(\Omega)}. \tag{2.2.35}$$

The main difference between the approximation properties (2.2.34)−(2.2.35) and (2.2.14)−(2.2.15) is that in the former one needs H^2 regularity to obtain $O(h^2)$ convergence with piecewise linear elements, whereas in the later only global H^1 regularity is used to obtain $O(h^2|\log h|)$ approximation properties for the Clément-type of operator. The low global regularity on the solution results into the appearance of the factor $|\log h|^{\frac{1}{2}}$ in (2.2.14) and (2.2.15).

(*ii*) In Chen and Zou [33], similar approximation properties (cf. Lemma 2.1 of [33]) are established for the standard linear interpolation operator in $C(\Omega)$ in the context of *a priori* error analysis for interface problems. In the proof, the authors of [33] have directly used the standard finite element interpolation results to obtain an estimate over non-interface triangles. Whereas, in the present scenario, to obtain an estimate oner non-interface triangles one can not apply the standard estimates (2.2.2) directly because for some $K \in \mathcal{T}_h \backslash \mathcal{T}_h^*$ and $v \in H^2(K)$ need not imply $v \in H^2(S_K)$, S_K refers to the corresponding patch of a triangle K. We use extension results together with the embedding results to overcome this difficulty.

2.3 Abstract Error Analysis

In this section, we derive an abstract *a posteriori* error bound for the quantity

$$\|u - u_h\|_{L^\infty(L^2)} := \max_{t\in[0,T]} \|u(t) - u_h(t)\|.$$

In the error analysis for the spatially discrete approximation of (2.1.1) − (2.1.3), we employ the elliptic reconstruction technique of [76]. This elliptic reconstruction operator for *a posteriori* error analysis may be thought of as a counterpart of the Wheeler's projection introduced in the context of *a priori* error analysis of parabolic problems.

Definition 2.3.1 (Elliptic reconstruction)**.** *Let $u_h \in \mathbb{S}_h$ be the spatially discrete finite element solution of the problem* (2.1.1) − (2.1.3)*. Then we define the elliptic reconstruction $\mathcal{R}_h u_h \in H_0^1(\Omega)$ of $u_h \in \mathbb{S}_h$ to be the solution of the following elliptic problem in the*

weak form as

$$a(\mathcal{R}_h u_h, \varphi) = \langle f - u_{h,t}, \varphi \rangle \quad \forall \varphi \in H_0^1(\Omega). \tag{2.3.1}$$

Remark 2.3.1. (*i*) The existence and uniqueness of the solution of elliptic problem (2.3.1) follows from the well established theory of elliptic interface problems and hence, the elliptic reconstruction is well defined. Further in view of (2.1.8), this definition may be expressed by saying that u_h is the finite element solution of the elliptic problem (2.3.1) with exact solution $\mathcal{R}_h u_h$. Therefore, $u_h - \mathcal{R}_h u_h$ can be bounded in various norms by *a posteriori* error estimator for elliptic problems.

(*ii*) For a.e. $t \in [0, T]$, we note that $u_h - \mathcal{R}_h u_h$ is orthogonal to the finite dimensional subspace $\mathbb{S}_h$ with respect to the bilinear form $a(\cdot, \cdot)$, i.e.,

$$a(u_h - \mathcal{R}_h u_h,\ \chi_h) = 0 \quad \forall \chi_h \in \mathbb{S}_h. \tag{2.3.2}$$

The property (2.3.2) is called the Galerkin orthogonality and plays a pivotal role in the derivation of residual-based *a posteriori* error estimates.

(*iii*) To motivate the Definition 2.3.1, we rewrite the spatially discrete approximation (2.1.8) as

$$a(u_h, \chi_h) \ = \ \langle f - u_{h,t}, \chi_h \rangle \quad \forall \chi_h \in \mathbb{S}_h, \quad \text{a.e. } t \in (0, T]. \tag{2.3.3}$$

Then the elliptic reconstruction is defined with the help of (2.3.3). This idea of the definition of elliptic reconstruction might be useful to deal with more general type of linear parabolic interface problems.

Unlike for the purely parabolic problems, *a posteriori* error estimates for the elliptic interface problems are not readily available in the literature with respect to the L^2 norm. Therefore, we shall derive *a posteriori* bounds for the elliptic reconstruction error in both the H^1 and L^2 norms. The proof uses the standard energy argument and relies on the approximation properties of the Clément-type operator derived in the previous section. Optimal order estimate in the H^1-norm and almost optimal order estimate in the L^2-norm are derived for the reconstruction error.

Lemma 2.3.1. *Let $\mathcal{R}_h u_h$ be the exact solution of the elliptic problem (2.3.1) and let u_h be its finite element approximation. Then we have the following reconstruction error bounds:*

$$\begin{aligned}
\|\mathcal{R}_h u_h - u_h\|_1 &\leq \frac{\mathcal{C}_{I,1}}{\gamma_0}\, h\, \|f - u_{h,t} - (u_h)_{\mathrm{el}}\| \ + \ \frac{\mathcal{C}_{I,2}}{\gamma_0}\, h^{\frac{1}{2}}\, \|j[\beta u_h]\|_{\Sigma_h}, \\
\|\mathcal{R}_h u_h - u_h\| &\leq \mathcal{C}_{I,5}\, h^2\, |\log h|^{\frac{1}{2}}\, \|f - u_{h,t} - (u_h)_{\mathrm{el}}\| \ + \ \mathcal{C}_{I,6}\, h^{\frac{3}{2}}\, |\log h|^{\frac{1}{2}}\, \|j[\beta u_h]\|_{\Sigma_h},
\end{aligned}$$

where $\mathcal{C}_{I,5} := \mathcal{C}_{I,3}\mathcal{C}_R$ *and* $\mathcal{C}_{I,6} := \mathcal{C}_{I,4}\mathcal{C}_R$. *In the above,* $\mathcal{C}_{I,i}(i = 1, ..., 4)$ *refer to the interpolation constants and* $\mathcal{C}_R$ *is the elliptic regularity constant.*

Proof. First, we prove the error estimate in the H^1 norm. For all $\varphi \in H_0^1(\Omega)$, using (2.3.1) and (2.1.9) we have

$$\begin{aligned} a(\mathcal{R}_h u_h - u_h, \varphi) &= \langle f - u_{h,t}, \varphi\rangle - a(u_h, \varphi) \\ &= \langle f - u_{h,t}, \varphi\rangle - \langle (u_h)_{\text{el}}, \varphi\rangle - \langle j[\beta u_h], \varphi\rangle_{\Sigma_h}. \end{aligned} \tag{2.3.4}$$

Application of the Galerkin orthogonality (2.3.2), the Cauchy-Schwarz inequality and Theorem 2.2.1 now leads to

$$\begin{aligned} a(\mathcal{R}_h u_h - u_h, \varphi) &= \langle f - u_{h,t} - (u_h)_{\text{el}}, \varphi - \mathscr{J}_h\varphi\rangle - \langle j[\beta u_h], \varphi - \mathscr{J}_h\varphi\rangle_{\Sigma_h} \\ &\leq \|f - u_{h,t} - (u_h)_{\text{el}}\| \, \|\varphi - \mathscr{J}_h\varphi\| + \|j[\beta u_h]\|_{\Sigma_h} \|\varphi - \mathscr{J}_h\varphi\|_{\Sigma_h} \\ &\leq \left\{ \mathcal{C}_{I,1} \, h \, \|f - u_{h,t} - (u_h)_{\text{el}}\| + \mathcal{C}_{I,2} \, h^{\frac{1}{2}} \, \|j[\beta u_h]\|_{\Sigma_h} \right\} \|\varphi\|_1. \end{aligned} \tag{2.3.5}$$

Choose $\varphi = \mathcal{R}_h u_h - u_h$ in (2.3.5) and then use the coercivity property of the bilinear form $a(\cdot, \cdot)$ to complete the proof of the first estimate.

For the L^2-error estimate, we apply the well-known duality argument. Let $w : [0, T] \longrightarrow X$ be the solution of the following elliptic problem

$$\begin{aligned} a(v, w(t)) &= \langle \mathcal{R}_h u_h - u_h, v\rangle \quad \forall v \in H_0^1(\Omega), \quad \text{a.e. } t \in [0, T], \\ w &= 0 \quad \text{on} \quad \partial\Omega, \\ [w] &= 0, \quad \left[\beta \frac{\partial w}{\partial \mathbf{n}}\right] = 0 \quad \text{across} \quad \Gamma, \end{aligned} \tag{2.3.6}$$

and w satisfies the regularity estimate (cf. Theorem 1.2.1)

$$\|w\|_X \leq \mathcal{C}_R \, \|\mathcal{R}_h u_h - u_h\|, \tag{2.3.7}$$

where $\mathcal{C}_R$ is a regularity constant depending on the domain Ω. Set $v = \mathcal{R}_h u_h - u_h$ in (2.3.6). Then use the Galerkin orthogonality property (2.3.2) to obtain

$$\begin{aligned} \|\mathcal{R}_h u_h - u_h\|^2 &= a(\mathcal{R}_h u_h - u_h, w - \mathscr{J}_h w) \\ &= a(\mathcal{R}_h u_h, w - \mathscr{J}_h w) - \langle (u_h)_{\text{el}}, w - \mathscr{J}_h w\rangle \\ &\quad - \langle j[\beta u_h], w - \mathscr{J}_h w\rangle_{\Sigma_h}. \end{aligned} \tag{2.3.8}$$

Again, using (2.3.1) and the Cauchy-Schwarz inequality, we have

$$\|\mathcal{R}_h u_h - u_h\|^2 \leq \|f - u_{h,t} - (u_h)_{\text{el}}\| \, \|w - \mathscr{J}_h w\| + \|j[\beta u_h]\|_{\Sigma_h} \, \|w - \mathscr{J}_h w\|_{\Sigma_h}. \tag{2.3.9}$$

To this end, use Theorem 2.2.2 and (2.3.7) to have

$$\begin{aligned}
&\|\mathcal{R}_h u_h - u_h\|^2 \\
&\quad \leq \left\{ \mathcal{C}_{I,3}\, h^2\, |\log h|^{\frac{1}{2}} \|f - u_{h,t} - (u_h)_{\mathrm{el}}\| + \mathcal{C}_{I,4}\, h^{\frac{3}{2}}\, |\log h|^{\frac{1}{2}}\, \|j[\beta u_h]\|_{\Sigma_h} \right\} \|w\|_X \\
&\leq \left\{ \mathcal{C}_{I,5} h^2 |\log h|^{\frac{1}{2}} \|f - u_{h,t} - (u_h)_{\mathrm{el}}\| + \mathcal{C}_{I,6} h^{\frac{3}{2}} |\log h|^{\frac{1}{2}} \|j[\beta u_h]\|_{\Sigma_h} \right\} \|\mathcal{R}_h u_h - u_h\|, \qquad (2.3.10)
\end{aligned}$$

which yields the second estimate and this completes the rest of the proof. □

Remark 2.3.2. As a consequence of the second estimate of Lemma 2.3.1, one can immediately have an almost optimal order *a posteriori* error estimate for the elliptic interface problems in the L^2-norm.

Corollary 2.3.1. *Differentiating (2.3.1) with respect to t and assuming $f_t \in L^2(0,T;L^2(\Omega))$, it follows that*

$$a((\mathcal{R}_h u_h)_t, \varphi) = \langle (f - u_{h,t})_t, \varphi \rangle \quad \forall \varphi \in H_0^1(\Omega). \qquad (2.3.11)$$

Also, in view of (2.3.2) we have

$$a((\mathcal{R}_h u_h - u_h)_t, \chi_h) = 0 \quad \forall \chi_h \in \mathbb{S}_h. \qquad (2.3.12)$$

In order to bound $\|(\mathcal{R}_h u_h - u_h)_t\|$ we employ the standard duality trick. Consider the dual elliptic problem with the forcing term $(\mathcal{R}_h u_h - u_h)_t$. For a.e. $t \in [0,T]$, let $w \in X$ be the solution of

$$\begin{aligned}
a(v, w(t)) &= \langle (\mathcal{R}_h u_h - u_h)_t, v \rangle \quad \forall v \in H_0^1(\Omega), \quad \text{a.e. } t \in [0,T], \qquad (2.3.13)\\
w &= 0 \quad \text{on} \quad \partial\Omega, \\
[w] &= 0, \quad \left[\beta \frac{\partial w}{\partial \boldsymbol{n}}\right] = 0 \quad \text{across} \quad \Gamma.
\end{aligned}$$

Further, w satisfies the following regularity estimate with constant $\mathcal{C}_R$ depending on the domain Ω

$$\|w\|_X \leq \mathcal{C}_R \|(\mathcal{R}_h u_h - u_h)_t\|. \qquad (2.3.14)$$

Invoking (2.3.11), (2.3.12) and arguing the same way as in (2.3.8) – (2.3.10)*, we have the following bound for the time derivative of the reconstruction error.*

$$\|\varepsilon_t(t)\| \leq \mathcal{C}_{I,5}\, h^2\, |\log h|^{\frac{1}{2}}\, \|(f - u_{h,t} - (u_h)_{\mathrm{el}})_t\| + \mathcal{C}_{I,6}\, h^{\frac{3}{2}}\, |\log h|^{\frac{1}{2}}\, \|j[\beta u_{h,t}]\|_{\Sigma_h}. \qquad (2.3.15)$$

Residuals. For $\varphi \in H_0^1(\Omega)$, the residuals associated with equation (2.1.8) is defined as

$$\begin{aligned}\langle \mathbf{R}_{\text{es}}, \varphi\rangle &= \langle u_{h,t}, \varphi\rangle + a(u_h, \varphi) - \langle f, \varphi\rangle \\ &= \langle u_{h,t}, \varphi\rangle + \langle (u_h)_{\text{el}}, \varphi\rangle + \langle\, j[\beta u_h], \varphi\rangle_{\Sigma_h} - \langle f, \varphi\rangle \\ &= \langle u_{h,t} + (u_h)_{\text{el}} - f, \varphi\rangle + \langle\, j[\beta u_h], \varphi\rangle_{\Sigma_h} \\ &= \langle \mathbf{R}_h(u_h(t)), \varphi\rangle + \langle \mathbf{J}_h(u_h(t)), \varphi\rangle_{\Sigma_h}.\end{aligned}$$

Therefore, we associate with (2.1.8) two residual functions namely, the *element residual* and the *jump residual*.

The *element residual* is defined as

$$\mathbf{R}_h(u_h(t)) := u_{h,t} + (u_h)_{\text{el}} - f,$$

and the *jump residual* is defined as

$$\mathbf{J}_h(u_h(t)) := j[\beta u_h].$$

Further, we define

$$\begin{aligned}\mathbf{R}_{h,t}(u_h(t)) &:= \frac{\partial}{\partial t}\left\{u_{h,t}(t) + (u_h)_{\text{el}} - f(t)\right\}. \\ \mathbf{J}_{h,t}(u_h(t)) &:= \frac{\partial}{\partial t}\left\{\mathbf{J}_h(u_h(t))\right\} \\ &:= j[\beta u_{h,t}].\end{aligned}$$

In the above, the equalities are to be understood in the sense of distributions.

Residual-based spatially discrete estimators: We define the following estimators.

The *elliptic reconstruction error estimator* as

$$\mathscr{O}_{\text{S},h}(u_h(t)) := \mathcal{C}_{I,5}\, h^2\, |\log h|^{\frac{1}{2}}\, \|\mathbf{R}_h(u_h(t))\| \;+\; \mathcal{C}_{I,6}\, h^{\frac{3}{2}}\, |\log h|^{\frac{1}{2}}\, \|\mathbf{J}_h(u_h(t))\|_{\Sigma_h}, \tag{2.3.16}$$

and *the spatial error estimator* as

$$\mathscr{M}_{\text{S},h}(u_h(t)) := \mathcal{C}_{I,5}\, h^2\, |\log h|^{\frac{1}{2}}\, \|\mathbf{R}_{h,t}(u_h(t))\| + \mathcal{C}_{I,6}\, h^{\frac{3}{2}}\, |\log h|^{\frac{1}{2}}\, \|\mathbf{J}_{h,t}(u_h(t)\|_{\Sigma_h}. \tag{2.3.17}$$

In order to derive the *a posteriori* error bound, we split the total error $e(t)$ by considering the reconstruction $\mathcal{R}_h u_h \in H_0^1(\Omega)$ as an intermediate object as follows: For a.e. $t \in [0, T]$,

$$\begin{aligned}e(t) &:= u(t) - u_h(t) \\ &= \rho(t) + \varepsilon(t),\end{aligned} \tag{2.3.18}$$

where $\rho(t) := u(t) - \mathcal{R}_h u_h(t)$ refers to the parabolic error and $\varepsilon(t) := \mathcal{R}_h u_h(t) - u_h(t)$ represents the elliptic reconstruction error.

The following lemma allows us to bound the parabolic error $\rho(t)$ in the $L^\infty(L^2)$-norm.

Lemma 2.3.2. *Let u be the exact solution of (2.1.1)−(2.1.3) and let u_h be its finite element approximation obtained by (2.1.8). Then, the following a posteriori bound holds for the parabolic error ρ:*

$$\max_{t\in[0,T]} \|\rho(t)\| \;\leq\; \|\rho(0)\| \;+\; 2\int_0^t \mathscr{M}_{\mathrm{S},h}(u_h(s))ds.$$

Proof. In order to bound $\rho(t)$, we have the following error equation

$$\begin{aligned} \langle \rho_t(t), \varphi\rangle + a(\rho(t),\varphi) &= -\langle \mathcal{R}_h u_{h,t}(t), \varphi\rangle - a(\mathcal{R}_h u_h(t),\varphi) + \langle f(t),\varphi\rangle \\ &= -\langle \varepsilon_t(t),\varphi\rangle \quad \forall \varphi \in H_0^1(\Omega), \end{aligned} \tag{2.3.19}$$

where in the above, we have used (2.3.1) and (2.1.7). Setting $\varphi = \rho$ in (2.3.19), applying the coercivity property of the bilinear form $a(\cdot,\cdot)$ and the Cauchy-Schwarz inequality we obtain

$$\frac{1}{2}\frac{d}{dt}\|\rho(t)\|^2 + \frac{\gamma_0}{2}\|\rho(t)\|_1^2 \leq \|\varepsilon_t(t)\|\,\|\rho(t)\|. \tag{2.3.20}$$

We integrate (2.3.20) from 0 to t. Then, use (2.3.15) to have

$$\begin{aligned} \|\rho(t)\|^2 + \gamma_0\int_0^t \|\rho(s)\|_1^2 ds &\leq \|\rho(0)\|^2 + 2\int_0^t \mathscr{M}_{\mathrm{S},h}(u_h(s))\,\|\rho(s)\|ds \\ &\leq \max_{t\in[0,T]}\|\rho(t)\|\left\{\|\rho(0)\| + 2\int_0^t \mathscr{M}_{\mathrm{S},h}(u_h(s))ds\right\}, \end{aligned} \tag{2.3.21}$$

and the desired bound for $\rho(t)$ now follows. □

The main result concerning $L^\infty(L^2)$-norm *a posteriori* estimate is presented below.

Theorem 2.3.2. *Let u be the exact solution of (2.1.1)−(2.1.3) and let u_h be its finite element approximation obtained by (2.1.8) . Then the following a posteriori error bound holds:*

$$\max_{t\in[0,T]}\|u(t) - u_h(t)\| \leq \|u_0 - I_h u_0\| + \mathscr{O}_{\mathrm{S},h}(u_h(0)) + \mathscr{O}_{\mathrm{S},h}(u_h(t)) + 2\int_0^t \mathscr{M}_{\mathrm{S},h}(u_h(s))ds.$$

In the above, the estimators $\mathscr{O}_{\mathrm{S},h}(u_h(t))$ and $\mathscr{M}_{\mathrm{S},h}(u_h(t))$ are defined in (2.3.16) and (2.3.17), respectively.

Proof. Since $e(t) = \rho(t) - \varepsilon(t)$, we use Lemma 2.3.1, Lemma 2.3.2 and the triangle inequality to obtain

$$\|e(t)\| \leq \|\rho(0)\| + 2\int_0^t \mathscr{M}_{\mathrm{S},h}(u_h(s))ds + \mathscr{O}_{\mathrm{S},h}(u_h(t)), \tag{2.3.22}$$

which together with

$$\|\rho(0)\| \leq \|u_0 - I_h u_0\| + \mathscr{O}_{\mathrm{S},h}(u_h(0)), \tag{2.3.23}$$

completes the rest of the proof. □

3

Fully Discrete Backward Euler Error Analysis

In this chapter, we shall extend the spatially discrete *a posteriori* error analysis to the fully discrete backward Euler approximation for the linear parabolic interface problem (1.1.1) – (1.1.3). The space discretization uses the standard linear finite element spaces that are allowed to change in time and the time discretization is based on the backward Euler approximation. An appropriate adaption of elliptic reconstruction operator introduced in Chapter 2 plays a major role in the analysis. The main ingredients in deriving *a posteriori* estimates are Clément-type interpolation estimates and a linear space-time reconstruction of the finite element solution. We use only the energy argument to establish *a posteriori* error estimates with optimal order convergence in the $L^2(H^1)$-norm and almost optimal order in the $L^\infty(L^2)$-norm.

3.1 Introduction

We shall begin by rewriting the parabolic interface problem. Let Ω be a bounded convex polygonal domain in $\mathbb{R}^2$ with Lipschitz boundary $\partial\Omega$. Let Ω_1 be a subdomain of Ω with C^2 boundary $\partial\Omega_1 := \Gamma$. The interface Γ divides the domain Ω into two subdomains Ω_1 and $\Omega_2 := \Omega \setminus \Omega_1$. Consider the linear parabolic interface problem of the form

$$u_t(x,t) - \mathrm{div}(\beta(x)\nabla u(x,t)) = f(x,t) \quad \text{in} \quad \Omega \times (0,T] \tag{3.1.1}$$

with prescribed initial and boundary conditions

$$u(x,0) = u_0(x) \quad \text{in} \quad \Omega; \qquad u = 0 \quad \text{on} \quad \partial\Omega \times [0,T] \tag{3.1.2}$$

and jump conditions on the interface

$$[u] = 0, \quad \left[\beta \frac{\partial u}{\partial \mathbf{n}}\right] = 0 \quad \text{across} \quad \Gamma \times [0,T], \tag{3.1.3}$$

where $[v]$ denotes the jump of a quantity v across the interface Γ, i.e., $[v](x) = v_1(x) - v_2(x)$, $x \in \Gamma$ with $v_i(x) = v(x)|_{\Omega_i}$, $i = 1, 2$ and $T < +\infty$. The symbol $\mathbf{n}$ denotes the unit outward normal to the boundary $\partial\Omega_1 := \Gamma$. The diffusion coefficient $\beta(x)$ is assumed to be positive and piecewise constant on each subdomain, i.e.,

$$\beta(x) = \beta_i \quad \text{for} \quad x \in \Omega_i,\ i = 1, 2.$$

The initial function $u_0(x)$ and the forcing term $f(x, t)$ are real valued functions and assumed to be smooth.

To present the finite element method for the problem (3.1.1) – (3.1.3), we now introduce its weak formulation. Let $u \in L^\infty(0, T; H_0^1(\Omega))$ be the solution of the following problem

$$\begin{aligned} \langle u_t(t), \varphi\rangle + a(u(t), \varphi) &= \langle f(t), \varphi\rangle \ \ \forall \varphi \in H_0^1(\Omega), \quad \text{a.e. } t \in (0, T], \\ u(0) &= u_0, \end{aligned} \tag{3.1.4}$$

where the bilinear form $a(\cdot, \cdot) : H_0^1(\Omega) \times H_0^1(\Omega) \longrightarrow \mathbb{R}$ is defined by

$$a(v, w) = \langle \beta \nabla v, \nabla w\rangle \quad \forall v, w \in H_0^1(\Omega). \tag{3.1.5}$$

The bilinear form $a(\cdot, \cdot)$ is bounded and coercive on $H_0^1(\Omega)$, i.e., $\exists \alpha_0, \gamma_0 > 0$ such that

$$|a(v, w)| \le \alpha_0 \, \|v\|_1 \|w\|_1 \quad \forall v, w \in H_0^1(\Omega), \tag{3.1.6}$$

and

$$a(v, v) \ge \ \gamma_0 \, \|v\|_1^2 \quad \forall v \in H_0^1(\Omega). \tag{3.1.7}$$

Let $\{\mathbb{S}^n\}_{0 \le n \le N}$ be a family of finite element spaces corresponding to the triangulation $\mathcal{T}_n$ and is defined by

$$\mathbb{S}^n := \left\{ \chi \in H_0^1(\Omega) \ \middle| \ \chi|_K \in \mathbb{P}_1(K) \ \text{ for all } \ K \in \mathcal{T}_n \right\},$$

where $\mathbb{P}_1(K)$ is the space of polynomials of degree less than or equal to 1 on K. The assumptions on the triangulations are detailed in Chapter 1. Let $f^n(x) := f(x, t_n)$. But in the sequel, we shall use the shorthand notation f^n for $f(x, t_n)$ and drop the space variable explicitly to avoid clutter in our notation .

The fully discrete backward Euler-Galerkin approximation of the problem (3.1.1) – (3.1.3) is stated as follows: Given $U^0 = I_h^0 u(0)$, seek $U^n \in \mathbb{S}^n$ $(1 \le n \le N)$ such that

$$\left\langle \frac{U^n - U^{n-1}}{k_n}, \chi_n \right\rangle + a(U^n, \chi_n) = \langle f^n, \chi_n\rangle \quad \forall \chi_n \in \mathbb{S}^n. \tag{3.1.8}$$

Here, the operator I_h^0 is a suitable projection operator from $H_0^1(\Omega)$ into $\mathbb{S}^0$.

Representation of the bilinear form. As in the spatially discrete case, for $v \in \mathbb{S}^n$, the bilinear form $a(\cdot,\cdot)$ can be represented in short form as

$$a(v,\varphi) \;=\; \langle (v)_{\mathrm{el}}, \varphi\rangle \;+\; \langle j[\beta v], \varphi\rangle_{\Sigma_n} \quad \forall \varphi \in H_0^1(\Omega), \tag{3.1.9}$$

and the symbols have the same meaning as before.

Discrete elliptic operator. The discrete elliptic operator associated with the bilinear form $a(\cdot,\cdot)$ and the finite element space $\mathbb{S}^n$ is the operator $\mathcal{A}_h^n : H_0^1(\Omega) \longrightarrow \mathbb{S}^n$ such that for $v \in H_0^1(\Omega)$ and $0 \le n \le N$,

$$\langle \mathcal{A}_h^n v,\ \chi_n\rangle \;=\; a(v,\chi_n) \quad \forall \chi_n \in \mathbb{S}^n. \tag{3.1.10}$$

Throughout this chapter, we shall use the following notation: For $1 \le n \le N$,

$$\partial v^n := \frac{v^n - v^{n-1}}{k_n}.$$

In the context of purely parabolic problems, *a posteriori* error analysis for the fully discrete backward Euler approximation has been studied by Picasso [86], Verfürth [101] and Lakkis and Makridakis [62]. The authors of [86, 101] have used the energy argument to obtain optimal order estimates in the $L^2(H^1)$-norm and suboptimal order estimates in the $L^\infty(L^2)$-norm. In [62], the elliptic reconstruction technique is adapted to restore optimality in the $L^\infty(L^2)$-norm using the energy argument.

In this chapter, we derive $L^\infty(L^2)$ *a posteriori* error bounds for the fully discrete backward Euler approximation of parabolic interface problem (3.1.1) – (3.1.3). *A posteriori* error analysis is based on the same principle as in [62], namely, an appropriate reconstruction operator and the energy argument. Moreover, new approximation results of the Clément-type interpolation operator also play a vital role in the analysis.

The layout of this chapter is as follows. In Section 3.2, elliptic reconstruction operator is introduced in the context of the fully discrete backward Euler approximation. In addition, optimal order *a posteriori* error bound in the $L^2(H^1)$-norm and almost optimal order bound in the $L^\infty(L^2)$-norm are derived for the fully discrete backward Euler approximation.

3.2 Abstract Error Analysis

In this section, we introduce an elliptic reconstruction operator and discuss the related *a posteriori* error analysis for the fully discrete backward Euler approximation.

Definition 3.2.1 (Elliptic reconstruction)**.** *For a fully discrete finite element solution $U^n \in \mathbb{S}^n$, we define the elliptic reconstruction $\mathcal{R}^n U^n \in H_0^1(\Omega)$ of $U^n \in \mathbb{S}^n$ as the solution of the following elliptic problem*

$$a(\mathcal{R}^n U^n, \varphi) = \langle \tilde{f}^n, \varphi \rangle \quad \forall \varphi \in H_0^1(\Omega), \tag{3.2.1}$$

where

$$\tilde{f}^n := \begin{cases} \mathcal{A}_h^0 U^0, & n = 0, \\ f^n - k_n^{-1}(U^n - U^{n-1}) \ , & 1 \le n \le N. \end{cases}$$

Note that $U^n - \mathcal{R}^n U^n$ is orthogonal to the finite dimensional subspace $\mathbb{S}^n$ of $H_0^1(\Omega)$ with respect to the bilinear form $a(\cdot, \cdot)$, i.e.,

$$a(U^n - \mathcal{R}^n U^n, \chi_n) = 0 \quad \forall \chi_n \in \mathbb{S}^n, \quad 0 \le n \le N,$$

which is called the Galerkin orthogonality property in the literature.

We now recall from Chapter 1 the following approximation properties of the Clément-type interpolation operator in the context of fully discrete approximation.

Proposition 3.2.1. *Let $\mathscr{J}_n : X \longrightarrow \mathbb{S}^n$ be the standard Clément-type interpolation operator defined by (2.2.1). Then, for the finite element polynomial space of degree ≤ 1, the following interpolation estimates hold: For $v \in H_0^1(\Omega)$, we have*

$$\begin{cases} \|v - \mathscr{J}_n v\| \ \le \mathcal{C}_{I,1} \ h_n \ \|v\|_1, \\ \|v - \mathscr{J}_n v\|_{\Sigma_n} \ \le \mathcal{C}_{I,2} \ h_n^{\frac{1}{2}} \ \|v\|_1, \end{cases} \tag{3.2.2}$$

and for $v \in X$,

$$\begin{cases} \|v - \mathscr{J}_n v\| \ \le \mathcal{C}_{I,3} \ h_n^2 \ |\log h_n|^{\frac{1}{2}} \ \|v\|_X, \\ \|v - \mathscr{J}_n v\|_{\Sigma_n} \ \le \mathcal{C}_{I,4} \ h_n^{\frac{3}{2}} \ |\log h_n|^{\frac{1}{2}} \ \|v\|_X, \end{cases} \tag{3.2.3}$$

where the constants $\mathcal{C}_{I,k}$, $k \in \{1, 2, 3, 4\}$ depend only on the shape-regularity of the family of triangulations.

Next, we state the Clément-type interpolation inequalities relative to the finest common coarsening of $\mathcal{T}_n$ and $\mathcal{T}_{n-1}$ which reflects the mesh change behaviour.

Proposition 3.2.2. *Let $\hat{\mathscr{J}}_n : X \longrightarrow \mathbb{S}^n \cap \mathbb{S}^{n-1}$ be the Clément type interpolation operator with respect to the finest common coarsening of $\mathcal{T}_n$ and $\mathcal{T}_{n-1}$, i.e., $\hat{\mathcal{T}}_n := \mathcal{T}_n \wedge \mathcal{T}_{n-1}$*

corresponding to the finite element space $\mathbb{S}^n \cap \mathbb{S}^{n-1}$ *with mesh size* $\hat{h}_n := max\{h_n, h_{n-1}\}$. *Then, for the finite element polynomial space of degree* ≤ 1, *the following is true for* $v \in X$*:*

$$\|v - \hat{\mathscr{I}}_n v\|_{\check{\Sigma}_n \setminus \hat{\Sigma}_n} \leq \mathcal{C}_{I,7}\, \hat{h}_n^{\frac{3}{2}}\, |\log \hat{h}_n|^{\frac{1}{2}}\, \|v\|_X,$$

where the constant $\mathcal{C}_{I,7}$ *depends on the shape regularity of the family of triangulations and on the number of steps required to move from* $\mathcal{T}_{n-1}$ *to* $\mathcal{T}_n$.

Further, the approximation properties (3.2.2) and (3.2.3) hold true in the finite element space $\mathbb{S}^n \cap \mathbb{S}^{n-1}$ *with* $\hat{h}_n$ *replacing* h_n.

The following lemma gives bounds on the elliptic reconstruction error.

Lemma 3.2.1. *For a finite element approximation* $U^n \in \mathbb{S}^n$ *of the elliptic equation (3.2.1), the following are true for* $0 \leq n \leq N$*:*

$$\|\mathcal{R}^n U^n - U^n\|_1 \leq \frac{\mathcal{C}_{I,1}}{\gamma_0}\, h_n\, \|\tilde{f}^n - (U^n)_{\text{el}}\| + \frac{\mathcal{C}_{I,2}}{\gamma_0}\, h_n^{\frac{1}{2}}\, \|j[\beta U^n]\|_{\Sigma_n}, \tag{3.2.4}$$

$$\begin{aligned}\|\mathcal{R}^n U^n - U^n\| \leq\ & \mathcal{C}_{I,5}\, h_n^2\, |\log h_n|^{\frac{1}{2}}\, \|\tilde{f}^n - (U^n)_{\text{el}}\| \\ & + \mathcal{C}_{I,6}\, h_n^{\frac{3}{2}}\, |\log h_n|^{\frac{1}{2}}\, \|j[\beta U^n]\|_{\Sigma_n},\end{aligned} \tag{3.2.5}$$

where the constants $\mathcal{C}_{I,j} (j = 1, 2, 3, 4)$ *are interpolation constants and* $\mathcal{C}_{I,5} := \mathcal{C}_{I,3}\, \mathcal{C}_R$ *and* $\mathcal{C}_{I,5} := \mathcal{C}_{I,3}\, \mathcal{C}_R$.

The proof of the above lemma is analogous to the proof of Lemma 2.3.1 and is therefore omitted here.

Now, we fix some notations for the subsequent use.

Let $U : [0, T] \longrightarrow H_0^1(\Omega)$ be a continuous piecewise linear approximation in time of $u(t)$ defined by

$$U(t) := l_{n-1}(t) U^{n-1} + l_n(t) U^n, \quad t \in I_n\ (n = 1 \ldots, N), \tag{3.2.6}$$

where for $1 \leq n \leq N$, the Lagrange hat functions $l_{n-1}(t)$ and $l_n(t)$ are defined by

$$l_{n-1}(t) := \frac{t_n - t}{k_n} \quad \text{and} \quad l_n(t) := \frac{t - t_{n-1}}{k_n} \quad \text{for } t \in I_n.$$

The linear space-time reconstruction $\Theta : [0, T] \longrightarrow H_0^1(\Omega)$ of U is defined as

$$\Theta(t) := l_{n-1}(t)\, \mathcal{R}^{n-1}\, U^{n-1} + l_n(t)\, \mathcal{R}^n\, U^n, \quad t \in I_n\ (n = 1 \ldots, N). \tag{3.2.7}$$

In the context of the fully discrete case we will also have two residual functions associated with equation (3.1.4), namely, the *element residual* and the *jump residual*.
The *element residual* is defined as

$$\begin{aligned}\mathbf{R}_0 &:= (U^0)_{\text{el}} - (\mathcal{A}_h^0 U^0), \\ \mathbf{R}_n &:= k_n^{-1}(U^n - U^{n-1}) + (U^n)_{\text{el}} - f^n, \quad \text{for} \quad n \in [1 : N],\end{aligned} \tag{3.2.8}$$

and the *jump residual* is defined as

$$\mathbf{J}_n := j[\beta U^n], \quad \text{for} \quad 0 \le n \le N. \tag{3.2.9}$$

A usual strategy in the error analysis is to split the total error by considering reconstruction as an intermediate object as follows:

$$e(t) := u(t) - U(t) = \rho(t) + \varepsilon(t), \quad t \in I_n. \tag{3.2.10}$$

Here, $\rho(t) := u(t) - \Theta(t)$ denotes the parabolic error and $\varepsilon(t) := \Theta(t) - U(t)$ refers to the elliptic reconstruction error. The second term $\varepsilon(t)$ is the error associate with the elliptic problem (3.2.1) can be handled via elliptic *a posteriori* bounds. Whereas, the first term can be bounded by an appropriate use of error equation and the energy argument.

Now, we state the main parabolic error equation.

Lemma 3.2.2 (Fully discrete error equation)**.** *Let $\rho(t)$ and $\varepsilon(t)$ be defined in (3.2.10), and let the space-time elliptic reconstruction $\Theta(t)$ be defined in (3.2.7). Then, for $1 \le n \le N$ and for each $\varphi \in H_0^1(\Omega)$, we have the following error equation for $\rho(t)$*

$$\langle \rho_t(t), \varphi\rangle + a(\rho(t), \varphi) = -\langle \varepsilon_t(t), \varphi\rangle - a(\Theta(t) - \Theta^n, \varphi) + \langle f(t) - f^n, \varphi\rangle, \ \ t \in I_n. \tag{3.2.11}$$

Proof. For all $\varphi \in H_0^1(\Omega)$, we use (3.1.4) and (3.2.1) to have

$$\begin{aligned}
\langle \rho_t(t), \varphi\rangle + a(\rho(t), \varphi) &= \langle (u(t) - \Theta(t))_t, \varphi\rangle + a(u(t) - \Theta(t), \varphi) \\
&= -\langle \Theta_t(t), \varphi\rangle - a(\Theta(t), \varphi) + \langle f(t), \varphi\rangle \\
&= -\langle \varepsilon_t(t), \varphi\rangle - \langle k_n^{-1}(U^n - U^{n-1}), \varphi\rangle - a(\Theta(t), \varphi) + \langle f, \varphi\rangle \\
&= -\langle \varepsilon_t(t), \varphi\rangle - a(\Theta(t) - \Theta^n, \varphi) + \langle f(t) - f^n, \varphi\rangle, \ \ t \in I_n,
\end{aligned}$$

and this completes the proof. □

Note that the right hand side of the error equation (3.2.11) comprises of three terms. The first term represents the *space-mesh error*, the second term refers to the *temporal error* and the third one is the *data approximation error*. To derive *a posteriori* bound for the parabolic error $\rho(t)$, we need to estimate the contribution of each error separately in a sequence of lemmas.

Lemma 3.2.3 (Space-mesh error estimate)**.** *For $1 \le n \le m$, let $\mathfrak{I}_{n,1}$ be given by*

$$\mathfrak{I}_{n,1} := \int_{t_{n-1}}^{t_n} |\langle \varepsilon_t(t), \rho(t)\rangle| dt.$$

Then the following is true:

$$\mathfrak{I}_{n,1} \le k_n \mathscr{M}_{\mathrm{BE},n} \max_{t \in \bar{I}_n} \|\rho(t)\|,$$

where $\mathscr{M}_{\mathrm{BE},n}$ is the spatial error estimator given by

$$\begin{aligned}\mathscr{M}_{\mathrm{BE},n} &:= \mathcal{C}_{I,5}\,\hat{h}_n^2\,|\log\hat{h}_n|^{\frac{1}{2}}\,\|\partial\mathbf{R}_n\| \;+\; \mathcal{C}_{I,6}\,\hat{h}_n^{\frac{3}{2}}\,|\log\hat{h}_n|^{\frac{1}{2}}\,\|\partial\mathbf{J}_n\|_{\hat{\Sigma}_n}\\ &\quad + \mathcal{C}_{I,8}\hat{h}_n^{\frac{3}{2}}\,|\log\hat{h}_n|^{\frac{1}{2}}\,\|\partial\mathbf{J}_n\|_{\check{\Sigma}_n\setminus\hat{\Sigma}_n}, \quad \mathcal{C}_{I,8}=\mathcal{C}_{I,7}\mathcal{C}_R. \end{aligned} \tag{3.2.12}$$

Proof. For $1\le n\le m$, we use (3.2.6) and (3.2.7) to have

$$\begin{aligned}\mathfrak{I}_{n,1} &= \int_{t_{n-1}}^{t_n} |\langle\varepsilon_t(t),\rho(t)\rangle|dt\\ &\le k_n^{-1}\max_{t\in\bar{I}_n}\|\rho(t)\|\int_{t_{n-1}}^{t_n}\|(\mathcal{R}^n-I)U^n-(\mathcal{R}^{n-1}-I)U^{n-1}\|dt\\ &= \max_{t\in\bar{I}_n}\|\rho(t)\|\,\|(\mathcal{R}^n-I)U^n-(\mathcal{R}^{n-1}-I)U^{n-1}\|. \end{aligned} \tag{3.2.13}$$

To bound the term $\|(\mathcal{R}^n-I)U^n-(\mathcal{R}^{n-1}-I)U^{n-1}\|$, we employ the well-known duality trick. For all $v\in H_0^1(\Omega)$, let $w:[0,T]\longrightarrow X$ be the solution of the following elliptic problem:

$$\begin{aligned} a(v,w(t)) &= \langle(\mathcal{R}^n-I)U^n-(\mathcal{R}^{n-1}-I)U^{n-1},v\rangle, \quad \text{a.e. } t\in[0,T],\\ w &= 0 \quad \text{on} \quad \partial\Omega,\\ [w] &= 0, \quad \left[\beta\frac{\partial w}{\partial\mathbf{n}}\right]=0 \text{ across } \Gamma, \end{aligned} \tag{3.2.14}$$

satisfying

$$\|w\|_X\le\mathcal{C}_R\,\|(\mathcal{R}^n-I)U^n-(\mathcal{R}^{n-1}-I)U^{n-1}\|. \tag{3.2.15}$$

Note that $\mathcal{R}^nU^n-U^n$ is orthogonal to $\mathbb{S}^n$ and hence, it follows that $(\mathcal{R}^n-I)U^n-(\mathcal{R}^{n-1}-I)U^{n-1}$ is orthogonal to $\mathbb{S}^n\cap\mathbb{S}^{n-1}$ with respect to $a(\cdot,\cdot)$. Set $v=(\mathcal{R}^n-I)U^n-(\mathcal{R}^{n-1}-I)U^{n-1}$ in (3.2.14). Using the Galerkin orthogonality property in the subspace $\mathbb{S}^n\cap\mathbb{S}^{n-1}$ and (3.2.1) we have

$$\begin{aligned}&\|(\mathcal{R}^n-I)U^n-(\mathcal{R}^{n-1}-I)U^{n-1}\|^2\\ &\quad= a\left((\mathcal{R}^n-I)U^n-(\mathcal{R}^{n-1}-I)U^{n-1},w(t)\right)\\ &\quad= a\left((\mathcal{R}^n-I)U^n-(\mathcal{R}^{n-1}-I)U^{n-1},w(t)-\hat{\mathscr{J}}_nw(t)\right)\\ &\quad= \left\langle\tilde{f}^n-\tilde{f}^{n-1}-(U^n)_{\mathrm{el}}+(U^{n-1})_{\mathrm{el}},\,w(t)-\hat{\mathscr{J}}_nw(t)\right\rangle\\ &\qquad-\left\langle j[\beta U^n]-j[\beta U^{n-1}],\,w(t)-\hat{\mathscr{J}}_nw(t)\right\rangle_{\check{\Sigma}_n}\\ &\quad= \left\langle-k_n\partial\mathbf{R}_n,\,w(t)-\hat{\mathscr{J}}_nw(t)\rangle-\langle k_n\partial\mathbf{J}_n,\,w(t)-\hat{\mathscr{J}}_nw(t)\right\rangle_{\check{\Sigma}_n}. \end{aligned}$$

We now use the Cauchy-Schwarz inequality and Proposition 3.2.1 (in the space $\mathbb{S}^n \cap \mathbb{S}^{n-1}$) and Proposition 3.2.2 to obtain

$$\begin{aligned}
&\|(\mathcal{R}^n - I)U^n - (\mathcal{R}^{n-1} - I)U^{n-1}\|^2 \\
&\quad \leq k_n \left\{ \mathcal{C}_{I,3}\, \hat{h}_n^2\, |\log \hat{h}_n|^{\frac{1}{2}}\, \|\partial \mathbf{R}_n\| + \mathcal{C}_{I,4}\, \hat{h}_n^{\frac{3}{2}}\, |\log \hat{h}_n|^{\frac{1}{2}} \|\partial \mathbf{J}_n\|_{\hat{\Sigma}_n} \right. \\
&\qquad \left. + \mathcal{C}_{\,I,7}\, \hat{h}_n^{\frac{3}{2}}\, |\log \hat{h}_n|^{\frac{1}{2}}\, \|\partial \mathbf{J}_n\|_{\tilde{\Sigma}_n \setminus \hat{\Sigma}_n} \right\} \|w(t)\|_X \\
&\quad \leq k_n\, \mathscr{M}_{\mathrm{BE},n}\, \|(\mathcal{R}^n - I)U^n - (\mathcal{R}^{n-1} - I)U^{n-1}\|,
\end{aligned}$$

where in the last inequality, we have used the elliptic regularity result (3.2.15). Thus, in view of (3.2.13), the desired result follows. □

Lemma 3.2.4 (Temporal error estimate)**.** *For $1 \leq n \leq m$, let $\mathfrak{I}_{n,2}$ be defined as*

$$\mathfrak{I}_{n,2} := \int_{t_{n-1}}^{t_n} |a(\Theta(t) - \Theta^n, \rho(t))| dt.$$

Then

$$\mathfrak{I}_{n,2} \leq k_n\, \mathscr{T}_{\mathrm{e,BE},n} \max_{t \in \bar{I}_n} \|\rho(t)\|,$$

where $\mathscr{T}_{\mathrm{e,BE},n}$ represents the temporal error estimator and is given by

$$\mathscr{T}_{\mathrm{e,BE},n} := \begin{cases} \frac{1}{2}\, \|\mathcal{A}_h^0 U^0 - f^1 + \partial U^1\|, & n = 1, \\ \frac{1}{2}\, k_n\, \|\partial(f^n - \partial U^n)\| \ , & 2 \leq n \leq N. \end{cases} \tag{3.2.16}$$

Proof. We use Definition 3.2.1 and (3.2.7) to obtain

$$\begin{aligned}
\mathfrak{I}_{n,2} &= \int_{t_{n-1}}^{t_n} |a(l_{n-1}(t)\mathcal{R}^{n-1}U^{n-1} + l_n(t)\mathcal{R}^n U^n - \mathcal{R}^n U^n, \rho(t))| dt \\
&= \int_{t_{n-1}}^{t_n} |l_{n-1}(t)|\, |a(\mathcal{R}^{n-1}U^{n-1}, \rho(t)) - a(\mathcal{R}^n U^n, \rho(t))| dt \\
&\leq \int_{t_{n-1}}^{t_n} |l_{n-1}(t)|\, \|\tilde{f}^{n-1} - \tilde{f}^n\|\, \|\rho(t)\| dt,
\end{aligned}$$

where in the second step we have used the fact that $l_{n-1}(t) + l_n(t) = 1$ for all $t \in I_n$.

$$\mathfrak{I}_{n,2} \leq k_n \max_{t \in \bar{I}_n} \|\rho(t)\|\, \|\tilde{f}^{n-1} - \tilde{f}^n\|, \tag{3.2.17}$$

and this completes the proof. □

Lemma 3.2.5 (Data approximation error estimate)**.** *For $1 \leq n \leq m$, let $\mathfrak{I}_{n,3}$ be defined by*

$$\mathfrak{I}_{n,3} := \int_{t_{n-1}}^{t_n} |\langle f(t) - f^n, \rho(t) \rangle| dt.$$

Then

$$\mathfrak{I}_{n,3} \leq k_n \max_{t\in \bar{I}_n} \|\rho(t)\| \mathscr{D}_{\mathrm{BE},n},$$

where the data approximation error estimator $\mathscr{D}_{\mathrm{BE},n}$ *for time is given by*

$$\mathscr{D}_{\mathrm{BE},n} := \frac{1}{k_n}\int_{t_{n-1}}^{t_n} \|f(t) - f^n\| dt. \tag{3.2.18}$$

Proof. We apply the Cauchy-Schwarz inequality to obtain

$$\begin{aligned} \mathfrak{I}_{n,3} &\leq \max_{t\in \bar{I}_n} \|\rho(t)\| \int_{t_{n-1}}^{t_n} \|f(t) - f^n\| \, dt \\ &= k_n \max_{t\in \bar{I}_n} \|\rho(t)\| \mathscr{D}_{\mathrm{BE},n}, \end{aligned}$$

and hence, the estimate follows. □

In order to obtain *a posteriori* error bound for the parabolic error, we have the following result.

Theorem 3.2.1. *Let* u *be the exact solution of (3.1.1)–(3.1.3) and let* U^n *be its finite element approximation obtained by the backward Euler fully discrete approximation (3.1.8). Then, for* $1 \leq m \leq N$*, the following estimate holds:*

$$\left(\max_{t\in[0,t_m]} \|\rho(t)\|^2 + \gamma_0 \int_0^{t_m} \|\rho(t)\|_1^2 dt\right)^{\frac{1}{2}} \leq \sqrt{2}\|\rho(0)\| + 4\sum_{n=1}^{m} k_n \left(\mathscr{M}_{\mathrm{BE},n} + \mathscr{T}_{\mathrm{e,BE},n} + \mathscr{D}_{\mathrm{BE},n}\right),$$

where the estimators $\mathscr{M}_{\mathrm{BE},n}$*,* $\mathscr{T}_{\mathrm{e,BE},n}$ *and* $\mathscr{D}_{\mathrm{BE},n}$ *are defined in (3.2.12), (3.2.16) and (3.2.18), respectively.*

Proof. Setting $\varphi = \rho(t)$ in the error equation (3.2.11) and using the coercivity of the bilinear form $a(\cdot,\cdot)$ we have

$$\frac{1}{2}\frac{d}{dt}\|\rho(t)\|^2 + \frac{\gamma_0}{2}\|\rho(t)\|_1^2 \leq |\langle \varepsilon_t(t), \rho(t)\rangle| + |a(\Theta(t) - \Theta^n, \rho(t))| + |\langle f^n - f(t), \rho(t)\rangle|, \tag{3.2.19}$$

which after integration on $[t_{n-1}, t_n]$ yields

$$\begin{aligned} \frac{1}{2}\|\rho(t_n)\|^2 - \frac{1}{2}\|\rho(t_{n-1})\|^2 + \frac{\gamma_0}{2}\int_{t_{n-1}}^{t_n} \|\rho(t)\|_1^2 dt \;\leq\; & \int_{t_{n-1}}^{t_n} \{|\langle \varepsilon_t(t), \rho(t)\rangle| + |a(\Theta(t) - \Theta^n, \rho(t))| \\ & + |\langle f^n - f(t), \rho(t)\rangle|\} \, dt. \end{aligned}$$

Summing up over $n = 1 : m$ we have that

$$\|\rho(t_m)\|^2 + \gamma_0 \int_0^{t_m} \|\rho(t)\|_1^2 dt \leq \|\rho(0)\|^2 + 2\sum_{n=1}^{m} \{\mathfrak{I}_{n,1} + \mathfrak{I}_{n,2} + \mathfrak{I}_{n,3}\}, \tag{3.2.20}$$

where $\mathfrak{I}_{n,i}(i = 1, 2, 3)$ are defined in Lemmas $3.2.3 - 3.2.5$. Since $\rho(t)$ is continuous in $[0, t_m]$, there exists $t_{0,m} \in [0, t_m]$ such that

$$\|\rho_{0,m}\| := \|\rho(t_{0,m})\| = \max_{t\in[0,t_m]} \|\rho(t)\|.$$

Again integrating (3.2.19) between the limits 0 to $t_{0,m}$ and observing that the integrands are non-negative, it follows that

$$\begin{aligned}
&\|\rho(t_{0,m})\|^2 + \gamma_0 \int_0^{t_{0,m}} \|\rho(t)\|_1^2 dt \\
&\quad \le \|\rho(0)\|^2 + 2\int_0^{t_{0,m}} |\langle \varepsilon_t(t), \rho(t)\rangle| dt + 2\int_0^{t_{0,m}} |a(\Theta(t) - \Theta^n, \rho(t))| dt \\
&\qquad + 2\int_0^{t_{0,m}} |\langle f^n - f(t), \rho(t)\rangle| dt \\
&\quad \le \|\rho(0)\|^2 + 2\sum_{n=1}^{m} \left\{ \int_{t_{n-1}}^{t_n} |\langle \varepsilon_t(t), \rho(t)\rangle| dt + \int_{t_{n-1}}^{t_n} |a(\Theta(t) - \Theta^n, \rho(t))|\, dt \right. \\
&\qquad \left. + \int_{t_{n-1}}^{t_n} |\langle f^n - f(t), \rho(t)\rangle| dt \right\} \\
&\quad = \|\rho(0)\|^2 + 2\sum_{n=1}^{m} \left\{ \mathfrak{I}_{n,1} + \mathfrak{I}_{n,2} + \mathfrak{I}_{n,3} \right\}. \qquad (3.2.21)
\end{aligned}$$

Now, combine (3.2.20) and (3.2.21) to have

$$\|\rho_{0,m}\|^2 + \gamma_0 \int_0^{t_m} \|\rho(t)\|_1^2 dt \le 2\|\rho(0)\|^2 + 4\sum_{n=1}^{m} \left\{ \mathfrak{I}_{n,1} + \mathfrak{I}_{n,2} + \mathfrak{I}_{n,3} \right\}.$$

Invoking Lemmas $3.2.3 - 3.2.5$, we obtain

$$\begin{aligned}
&\|\rho_{0,m}\|^2 + \gamma_0 \int_0^{t_m} \|\rho(t)\|_1^2 dt \\
&\qquad \le 2\|\rho(0)\|^2 + 4\|\rho_{0,m}\| \sum_{n=1}^{m} k_n \left(\mathscr{M}_{\mathrm{BE},n} + \mathscr{T}_{\mathrm{e,BE},n} + \mathscr{D}_{\mathrm{BE},n} \right).
\end{aligned}$$

To this end, we take

$$a_0 := \|\rho_{0,m}\|, \quad a_n := \left(\gamma_0 \int_{t_{n-1}}^{t_n} \|\rho(t)\|_1^2 \, dt \right)^{\frac{1}{2}}, \ (1 \le n \le m), \quad c := \sqrt{2}\|\rho(0)\|,$$

$$b_0 := 4\sum_{n=1}^{m} k_n \left(\mathscr{M}_{\mathrm{BE},n} + \mathscr{T}_{\mathrm{e,BE},n} + \mathscr{D}_{\mathrm{BE},n} \right), \quad b_n = 0, \ (1 \le n \le m),$$

and apply Lemma 1.2.3 to complete the rest of the proof. □

We are now ready to state the fully discrete backward Euler *a posteriori* error estimates in the $L^\infty(L^2)$ and $L^2(H^1)$ norms for the parabolic interface problem.

Theorem 3.2.2. *Let u be the exact solution of (3.1.1)–(3.1.3) and let U^n be its finite element approximation obtained by the backward Euler fully discrete approximation (3.1.8). Then, for each $1 \le m \le N$, the following a posteriori error estimates hold:*

$$\begin{aligned}\max_{t\in[0,t_m]} \|u(t)-U(t)\| &\le \sqrt{2}\,\|\mathcal{R}^0U^0-u(0)\| + 4\sum_{n=1}^{m} k_n\left(\mathscr{M}_{\mathrm{BE},n}+\mathscr{T}_{\mathrm{e,BE},n}+\mathscr{D}_{\mathrm{BE},n}\right)\\ &\quad +2\max_{0\le n\le m}\mathscr{O}_{\mathrm{BE},2,n},\end{aligned}$$

and

$$\begin{aligned}\left(\int_0^{t_m}\|u(t)-U(t)\|_1^2\right)^{\frac{1}{2}} &\le \frac{1}{\sqrt{\gamma_0}}\left\{\sqrt{2}\,\|\mathcal{R}^0U^0-u(0)\| + 4\sum_{n=1}^{m} k_n\left(\mathscr{M}_{\mathrm{BE},n}+\mathscr{T}_{\mathrm{e,BE},n}+\mathscr{D}_{\mathrm{BE},n}\right)\right\}\\ &\quad +\left\{\sum_{n=1}^{m} k_n\left(\mathscr{O}^2_{\mathrm{BE},1,n-1}+\mathscr{O}^2_{\mathrm{BE},1,n}\right)\right\}^{\frac{1}{2}}.\end{aligned}$$

In the above $\mathscr{O}_{\mathrm{BE},1,n}$ and $\mathscr{O}_{\mathrm{BE},2,n}$ are the elliptic reconstruction error estimators in the H^1 and the L^2-norms, respectively and are given by

$$\mathscr{O}_{\mathrm{BE},1,n} := \frac{\mathcal{C}_{I,1}}{\gamma_0}\,h_n\,\|\mathbf{R}_n\| + \frac{\mathcal{C}_{I,2}}{\gamma_0}\,h_n^{\frac{1}{2}}\,\|\mathbf{J}_n\|_{\Sigma_n}, \tag{3.2.22}$$

$$\mathscr{O}_{\mathrm{BE},2,n} := \mathcal{C}_{I,5}\,h_n^2\,|\log h_n|^{\frac{1}{2}}\,\|\mathbf{R}_n\| + \mathcal{C}_{I,6}\,h_n^{\frac{3}{2}}\,|\log h_n|^{\frac{1}{2}}\,\|\mathbf{J}_n\|_{\Sigma_n}, \tag{3.2.23}$$

and the estimators $\mathscr{M}_{\mathrm{BE},n}$, $\mathscr{T}_{\mathrm{e,BE},n}$ and $\mathscr{D}_{\mathrm{BE},n}$ are defined in (3.2.12), (3.2.16) and (3.2.18), respectively.

Proof. By the triangle inequality, we have

$$\|e(t)\| = \|u(t)-U(t)\| \le \|\rho(t)\| + \|\varepsilon(t)\|.$$

As $\max\limits_{t\in\bar{I}_n} l_n(t) = 1$, we have

$$\begin{aligned}\|\varepsilon(t)\| &= \|l_{n-1}(t)\varepsilon^{n-1} + l_n(t)\varepsilon^n\|, t\in I_n\\ &\le |l_{n-1}(t)|\,\|\varepsilon^{n-1}\| + |l_n(t)|\,\|\varepsilon^n\|\\ &\le 2\,\max\{\|\varepsilon^n\|,\|\varepsilon^{n-1}\|\}.\end{aligned}$$

Again, for $t\in[0,t_m]$, using Lemma 3.2.1 we obtain

$$\|\varepsilon(t)\| \le 2\max_{0\le n\le m}\|\varepsilon^n\| \le 2\max_{0\le n\le m}\mathscr{O}_{\mathrm{BE},2,n},$$

which together with Theorem 3.2.1 proves the first estimate. To prove the second estimate, we proceed as follows:

$$\begin{aligned}\int_0^{t_m} \|\varepsilon(t)\|_1^2 dt &= \int_0^{t_m} \|l_{n-1}(t)\varepsilon^{n-1} + l_n(t)\varepsilon^n\|_1^2 dt \\ &\leq \left(\sum_{n=1}^{m} k_n \|\varepsilon^{n-1}\|_1^2\right) + \left(\sum_{n=1}^{m} k_n \|\varepsilon^n\|_1^2\right) \\ &\leq \sum_{n=1}^{m} k_n \left(\mathscr{O}^2_{\mathrm{BE},1,n-1} + \mathscr{O}^2_{\mathrm{BE},1,n}\right), \qquad (3.2.24)\end{aligned}$$

where in the last inequality we have used Lemma 3.2.1. The rest of the proof follows from (3.2.24) and Theorem 3.2.1. □

Remark 3.2.1 (Comparison to the parabolic problems). (*i*) The *temporal error estimator* and the *data error estimator* appearing in Theorem 3.2.2 are similar to that of the parabolic problems (cf. [62]). The crucial difference between the *a posteriori* bounds for the parabolic problems and parabolic interface problems is reflected in the *elliptic reconstruction error estimator* in the L^2-norm and the *spatial error estimator*. For parabolic problems, both the estimators are of $O(h_n^2)$, whereas for the interface problems these estimators are of order $O(h_n^2|\log h_n|)$. The appearance of the factor $|\log h_n|$ in (3.2.23) and (3.2.12) is quite natural as the discontinuity of the diffusion coefficient reduces the regularity of the solution of interface problems.

(*ii*) We would like to emphasize the fact that the proposed analysis can easily be extended to treat more general parabolic interface problems in the presence of an interface function.

4

Fully Discrete Crank-Nicolson Error Analysis

This chapter is devoted to the *a posteriori* error analysis of the fully discrete Crank-Nicolson approximation for the linear parabolic interface problem (1.1.1) – (1.1.3). The discretization with respect to space is by the piecewise linear finite elements which are allowed to change in time, and in time we have applied the Crank-Nicolson approximation. We employ a space-time reconstruction that is piecewise quadratic in time to derive *a posteriori* error bound in the $L^\infty(L^2)$-norm. Our main results are proved using only the energy argument.

4.1 Introduction

We begin by stating the parabolic interface problem. Let Ω be a bounded convex polygonal domain in $\mathbb{R}^2$ with Lipschitz boundary $\partial\Omega$. Let Ω_1 be a subdomain of Ω with C^2 boundary $\partial\Omega_1 := \Gamma$. The interface Γ now divides the domain Ω into two subdomains Ω_1 and $\Omega_2 := \Omega \setminus \Omega_1$. Consider the linear parabolic interface problem of the form

$$u_t(x,t) - \mathrm{div}(\beta(x)\nabla u(x,t)) = f(x,t) \quad \text{in} \quad \Omega \times (0,T] \tag{4.1.1}$$

with prescribed initial and boundary conditions

$$u(x,0) = u_0(x) \quad \text{in} \quad \Omega; \qquad u = 0 \quad \text{on} \quad \partial\Omega \times [0,T] \tag{4.1.2}$$

and jump conditions on the interface

$$[u] = 0, \quad \left[\beta \frac{\partial u}{\partial \mathbf{n}}\right] = 0 \quad \text{across} \quad \Gamma \times [0,T], \tag{4.1.3}$$

where $[v]$ denotes the jump of a quantity v across the interface Γ, i.e., $[v](x) = v_1(x) - v_2(x)$, $x \in \Gamma$ with $v_i(x) = v(x)|_{\Omega_i}$, $i = 1, 2$ and $T < +\infty$. The symbol $\mathbf{n}$ denotes the unit

outward normal to the boundary $\partial\Omega_1 := \Gamma$. The diffusion coefficient $\beta(x)$ is assumed to be positive and piecewise constant on each subdomain, i.e.,

$$\beta(x) = \beta_i \quad \text{for} \quad x \in \Omega_i,\ i = 1, 2.$$

The initial function $u_0(x)$ and the forcing term $f(x,t)$ are real valued functions and assumed to be smooth.

For the purpose of the finite element approximation of $(4.1.1) - (4.1.3)$, we begin by writing the problem in weak form: Find $u \in L^\infty(0,T; H_0^1(\Omega))$ such that

$$\begin{aligned} \langle u_t(t), \varphi\rangle + a(u(t), \varphi) &= \langle f(t), \varphi\rangle \quad \forall \varphi \in H_0^1(\Omega), \quad \text{a.e. } t \in (0,T], \\ u(0) &= u_0. \end{aligned} \tag{4.1.4}$$

Here, $a(\cdot,\cdot)$ is a bilinear form on $H_0^1(\Omega)$ defined by

$$a(v,w) = \langle \beta \nabla v, \nabla w\rangle \quad \forall v, w \in H_0^1(\Omega).$$

The bilinear form $a(\cdot,\cdot)$ is bounded and coercive on $H_0^1(\Omega)$, i.e., $\exists \alpha_0, \gamma_0 > 0$ such that

$$|a(v,w)| \le \alpha_0 \, \|v\|_1 \|w\|_1 \quad \forall v, w \in H_0^1(\Omega), \tag{4.1.5}$$

$$\text{and} \quad a(v,v) \ge \gamma_0 \|v\|_1^2 \quad \forall v \in H_0^1(\Omega). \tag{4.1.6}$$

In order to discretize the problem $(4.1.1) - (4.1.3)$, we partition the time axis by $0 = t_0 < t_1 < \cdots < t_N = T$ and set $I_n := (t_{n-1}, t_n]$ with time steps $k_n := t_n - t_{n-1}$. Then for each $n = 0, \cdots, N$, we consider the finite element space $\mathbb{S}^n$ corresponding to the triangulation $\mathcal{T}_n$ as follows:

$$\mathbb{S}^n := \left\{ \chi \in H_0^1(\Omega) \ \middle|\ \chi|_K \in \mathbb{P}_1(K) \ \text{ for all } \ K \in \mathcal{T}_n \right\},$$

where $\mathbb{P}_1(K)$ is the space of polynomials of degree less than or equal to 1 on K. Hereafter, we shall use the following notations: For $1 \le n \le N$,

$$\partial v^n := \frac{v^n - v^{n-1}}{k_n}, \quad v^{n-\frac{1}{2}} := \frac{v^n + v^{n-1}}{2} \quad \text{and} \quad f^{n-\frac{1}{2}} := \frac{f^n + f^{n-1}}{2}.$$

The fully discrete Crank-Nicolson approximation of the problem $(4.1.1) - (4.1.3)$ associated with the finite element space $\mathbb{S}^n$ is stated as follows: Given $U^0 = I_h^0 u(0)$, seek $U^n \in \mathbb{S}^n$ for $1 \le n \le N$ such that

$$\left\langle \frac{U^n - U^{n-1}}{k_n}, \chi_n \right\rangle + a\left(U^{n-\frac{1}{2}}, \chi_n\right) = \left\langle f^{n-\frac{1}{2}}, \chi_n \right\rangle \quad \forall \chi_n \in \mathbb{S}^n. \tag{4.1.7}$$

Here I_h^0 is a suitable projection operator from $H_0^1(\Omega)$ into the finite dimensional subspace $\mathbb{S}^0$.

We now recall the following projection operators for later use.

Discrete elliptic operator. The discrete elliptic operator associated with the bilinear form $a(\cdot,\cdot)$ and the finite element space $\mathbb{S}^n$ is the operator $\mathcal{A}_h^n : H_0^1(\Omega) \longrightarrow \mathbb{S}^n$ such that for $v \in H_0^1(\Omega)$ and $0 \leq n \leq N$,

$$\langle \mathcal{A}_h^n v,\ \chi_n \rangle \ = \ a(v, \chi_n) \quad \forall \chi_n \in \mathbb{S}^n. \tag{4.1.8}$$

L^2-projection operator: The L^2-projection operator is a map $\Pi_0^n : L^2(\Omega) \longrightarrow \mathbb{S}^n$ such that for $v \in L^2(\Omega)$ and $0 \leq n \leq N$,

$$\langle \Pi_0^n\ v\ , \chi_n \rangle \ = \ \langle v,\ \chi_n \rangle \quad \forall \chi_n \in \mathbb{S}^n. \tag{4.1.9}$$

Using the above projections, (4.1.7) can be expressed in distributional form as

$$\frac{U^n - \Pi_0^n U^{n-1}}{k_n} + \frac{1}{2}(\mathcal{A}_h^n)U^n + \frac{1}{2}(\mathcal{A}_h^n)U^{n-1} = \Pi_0^n f^{n-\frac{1}{2}}.$$

For the parabolic problems, Bänsch *et al.* in [15] has observed that the discrete elliptic operator $\mathcal{A}_h^n$ on the finer mesh when applied to the coarse grid function U^{n-1} in the above may lead to oscillation during refinement. The same behaviour is naturally expected for the parabolic interface problems as well. Therefore, following the discussion of [15], we consider the following modified Crank-Nicolson approximation.

Modified Crank-Nicolson approximation. Given $U^0 = I_h^0 u(0)$, find $U^n \in \mathbb{S}^n$ ($1 \leq n \leq N$) such that

$$\frac{U^n - P_1^n U^{n-1}}{k_n} + \frac{1}{2}(\mathcal{A}_h^n U^n) + \frac{1}{2}P_2^n(\mathcal{A}_h^{n-1}U^{n-1}) = \Pi_0^n f^{n-\frac{1}{2}}, \tag{4.1.10}$$

where $P_1^n, P_2^n : \mathbb{S}^{n-1} \longrightarrow \mathbb{S}^n$ be any suitable projection operators. In particular ,one may choose $P_1^n = P_2^n = \Pi_0^n$.

Representation of the bilinear form. As before, for $v \in \mathbb{S}^n$, the bilinear form $a(\cdot,\cdot)$ can be represented in short form as

$$a(v,\varphi) \ = \ \langle (v)_{\rm el}, \varphi \rangle \ + \ \langle j[\beta v], \varphi \rangle_{\Sigma_n} \quad \forall \varphi \in H_0^1(\Omega), \tag{4.1.11}$$

where the symbols have their usual meaning.

A posteriori error bounds with the energy technique for the Crank-Nicolson method of the linear parabolic problems have been investigated by Verfürth [101], Akrivis *et al.* [4] and Bänsch *et al.* [15]. A continuous piecewise linear approximation in time has been used in [101] to obtain suboptimal error bound with respect to the time. Subsequently,

Akrivis *et al.* [4] have introduced a novel continuous piecewise quadratic (in time) Crank-Nicolson reconstruction to restore the optimal convergence (second order) in time for the linear and nonlinear parabolic problems. Recently, Bänsch *et al.* in [15] have proposed a continuous piecewise quadratic in time space-time reconstruction to obtain optimal order bound in the $L^\infty(L^2)$-norm. The authors of [15] have also considered the mesh-change effect in the error analysis.

In this chapter, an attempt has been made to carry over *a posteriori* error analysis for the Crank-Nicolson approximation of the parabolic problems(cf. [15]) to the interface problem (4.1.1) – (4.1.3). This is accomplished by an appropriate quadratic space-time Crank-Nicolson reconstruction of finite element solution and new Clément-type interpolation estimates. *A posteriori* bound of $O(k_n^2)$ in time and $O(h_n^2|\log h_n|)$ in space are derived in the $L^\infty(L^2)$-norm.

The rest of this chapter is planned as follows. In Section 4.2, we define quadratic space-time reconstruction for interface problem (4.1.1) – (4.1.3). Further, the abstract *a posteriori* analysis of the Crank-Nicolson approximation is also presented in this section.

4.2 Abstract Error Analysis

In this section, we first define space-time quadratic (in time) reconstruction for the Crank-Nicolson approximation (4.1.10). The later part of this section is devoted to the related *a posteriori* error analysis. For this purpose, we first define the elliptic reconstruction operator $\mathcal{R}^n$.

Definition 4.2.1 (elliptic reconstruction, [15]). *Let $v \in \mathbb{S}^n$. Then we define the elliptic reconstruction $\mathcal{R}^n : \mathbb{S}^n \longrightarrow H_0^1(\Omega)$ by*

$$a(\mathcal{R}^n v, \varphi) = \langle \mathcal{A}_h^n v, \varphi\rangle \quad \forall \varphi \in H_0^1(\Omega),\ 0 \le n \le N. \tag{4.2.1}$$

Note that $\mathcal{R}^n v - v$ is orthogonal to the finite dimensional subspace $\mathbb{S}^n$ of $H_0^1(\Omega)$ with respect to the bilinear form $a(\cdot,\cdot)$, i.e.,

$$a(\mathcal{R}^n v - v, \chi_n) = 0 \quad \forall \chi_n \in \mathbb{S}^n, \quad 0 \le n \le N,$$

which is called the Galerkin orthogonality property in the literature and plays a pivotal role in the derivation of residual-based *a posteriori* error estimates.

The following lemma gives the elliptic reconstruction error estimate in the L^2-norm. The proof essentially uses the idea of Lemma 2.3.1. But, for clarity of presentation we provide here the proof.

Lemma 4.2.1. *For any $v \in \mathbb{S}^n$ $(0 \leq n \leq N)$, the following is true:*

$$\|(\mathcal{R}^n - I)v\| \leq \mathcal{C}_{I,5}\, h_n^2\, |\log h_n|^{\frac{1}{2}} \|(\mathcal{A}_h^n)v - (v)_{\rm el}\| + \mathcal{C}_{I,6}\, h_n^{\frac{3}{2}}\, |\log h_n|^{\frac{1}{2}}\, \|j[\beta v]\|_{\Sigma_n},$$

where $\mathcal{C}_{I,5}$ and $\mathcal{C}_{I,6}$ are positive constants appearing due to the application of interpolation constants and the regularity constant.

Proof. The proof of the lemma will proceed by the duality argument. Let $w : [0,T] \longrightarrow X$ be the solution of the elliptic problem in the weak form as

$$\begin{aligned} a(z, w(t)) &= \langle (\mathcal{R}^n - I)v(t), z\rangle \quad \forall z \in H_0^1(\Omega), \quad \text{a.e. } t \in [0,T], \\ w &= 0 \text{ on } \partial\Omega, \\ [w] &= 0, \ \left[\beta \frac{\partial w}{\partial \mathbf{n}}\right] = 0 \text{ across } \Gamma. \end{aligned} \tag{4.2.2}$$

Further, the solution w satisfies the following regularity result

$$\|w\|_X \leq \mathcal{C}_R\, \|(\mathcal{R}^n - I)v\|, \tag{4.2.3}$$

where $\mathcal{C}_R$ refers to the regularity constant. Choose $z = (\mathcal{R}^n - I)v$ in (4.2.2). Then, using the fact that $(\mathcal{R}^n - I)v$ is orthogonal to $\mathbb{S}^n$ with respect to the bilinear form $a(\cdot,\cdot)$ and Definition 4.2.1 we have that

$$\begin{aligned} \|(\mathcal{R}^n - I)v\|^2 &= a((\mathcal{R}^n - I)v, w) \\ &= a(\mathcal{R}^n v - v, w - \mathscr{J}_n w) \\ &\leq |\, \langle (\mathcal{A}_h^n)v - (v)_{\rm el}, w - \mathscr{J}_n w\rangle - \langle j[\beta v], w - \mathscr{J}_n w\rangle\, |. \end{aligned}$$

To this end, using the Cauchy-Schwarz inequality, Proposition 3.2.1 and the regularity estimate (4.2.3) we obtain

$$\begin{aligned} &\|(\mathcal{R}^n - I)v\|^2 \\ &\quad \leq \left\{ \mathcal{C}_{I,3}\, h_n^2\, |\log h_n|^{\frac{1}{2}}\, \|(\mathcal{A}_h^n)v - (v)_{\rm el}\| + \mathcal{C}_{I,4}\, h_n^{\frac{3}{2}}\, |\log h_n|^{\frac{1}{2}} \|j[\beta v]\|_{\Sigma_n} \right\} \|w\|_X \\ &\quad \leq \left\{ \mathcal{C}_{I,5}\, h_n^2\, |\log h_n|^{\frac{1}{2}}\, \|(\mathcal{A}_h^n)v - (v)_{\rm el}\| + \mathcal{C}_{I,6}\, h_n^{\frac{3}{2}}\, |\log h_n|^{\frac{1}{2}} \|j[\beta v]\|_{\Sigma_n} \right\} \|(\mathcal{R}^n - I)v\|, \end{aligned}$$

which completes the proof of the lemma. □

We shall use the following notations for the subsequent analysis.

Let $U : [0,T] \longrightarrow H_0^1(\Omega)$ be a continuous piecewise linear approximation in time of $u(t)$ defined by

$$\begin{aligned} U(t) &:= l_{n-1}(t)U^{n-1} + l_n(t)U^n \\ &:= U^{n-\frac{1}{2}} + (t - t_{n-\frac{1}{2}})\partial U^n, \quad t \in I_n \ (n = 1, \ldots, N), \end{aligned} \tag{4.2.4}$$

where for $1 \leq n \leq N$, the Lagrange hat functions $l_{n-1}(t)$ and $l_n(t)$ are defined by

$$l_{n-1}(t) := \frac{t_n - t}{k_n} \quad \text{and} \quad l_n(t) := \frac{t - t_{n-1}}{k_n} \quad \text{for } t \in I_n. \tag{4.2.5}$$

Let $\Psi, \Theta : [0,T] \longrightarrow H_0^1(\Omega)$ be continuous piecewise linear functions in time defined by

$$\Psi(t) := l_{n-1}(t)\,(P_2^n(\mathcal{A}_h^{n-1}))\,U^{n-1} + l_n(t)\,(\mathcal{A}_h^n)\,U^n, \;\; t \in I_n \;(n = 1, \ldots, N) \tag{4.2.6}$$

and

$$\Theta(t) := l_{n-1}(t)\,\mathcal{R}^{n-1}\,U^{n-1} + l_n(t)\,\mathcal{R}^n\,U^n, \;\; t \in I_n \;(n = 1, \ldots, N), \tag{4.2.7}$$

respectively. Let $\tilde{\Phi} : [0,T] \longrightarrow H_0^1(\Omega)$ be a continuous piecewise linear approximation of $f(t)$ defined by

$$\tilde{\Phi}(t) := l_{n-1}(t)\,f^{n-1} + l_n(t)\,f^n, \quad t \in I_n \;\; (n = 1, \ldots, N). \tag{4.2.8}$$

Now, we rewrite the fully discrete Crank-Nicolson approximation to define the quadratic space-time reconstruction. Note that (4.1.10) can be rewritten in compact form as:

$$\frac{U^n - P_1^n U^{n-1}}{k_n} = H_1(t_{n-\frac{1}{2}}), \quad n \geq 1, \tag{4.2.9}$$

where

$$H_1(t_{n-\frac{1}{2}}) := \Pi_0^n f(t_{n-\frac{1}{2}}) - \Psi(t_{n-\frac{1}{2}}), \quad n \geq 1. \tag{4.2.10}$$

We also define $\tilde{H}_1 : [0,T] \longrightarrow H_0^1(\Omega)$ be a piecewise linear function in time defined as

$$\tilde{H}_1(t) := \Pi_0^n \tilde{\Phi}(t) - \Psi(t), \;\; t \in I_n \;(n = 1, \ldots, N). \tag{4.2.11}$$

Clearly, $\tilde{H}_1(\cdot)|_{I_n} \in \mathbb{P}_1(I_n)$ with $\tilde{H}_1(t_{n-\frac{1}{2}}) = H_1(t_{n-\frac{1}{2}})$.

Following the idea of [4, 15] we now define the space-time reconstruction for the Crank-Nicolson error analysis of the parabolic interface problem.

Definition 4.2.2 (space-time reconstruction)**.** *The quadratic space-time reconstruction* $\tilde{U} : [0,T] \longrightarrow H_0^1(\Omega)$ *of* U *is defined by*

$$\begin{aligned} \tilde{U}(t) \;\; := \;\; & \mathcal{R}^{n-1}U^{n-1} + {k_n}^{-1}\,(t - t_{n-1})\left\{(\mathcal{R}^n P_1^n)U^{n-1} - \mathcal{R}^{n-1}U^{n-1}\right\} \\ & + \int_{t_{n-1}}^{t} \mathcal{R}^n \tilde{H}_1(s)ds, \quad t \in I_n \;\; (n = 1, \ldots, N). \end{aligned}$$

Observe that $\tilde{U}(t_{n-1}) = \mathcal{R}^{n-1}U^{n-1}$. Further, evaluating the integral by the midpoint rule and recalling (4.1.10), we obtain $\tilde{U}(t_n) = \mathcal{R}^n U^n$. Thus, $\tilde{U}$ is a continuous function in time and satisfies the relation

$$\tilde{U}_t(t) = {k_n}^{-1}\left\{(\mathcal{R}^n P_1^n)U^{n-1} - \mathcal{R}^{n-1}U^{n-1}\right\} + \mathcal{R}^n\tilde{H}_1(t), \quad t \in I_n \ (n = 1, \ldots, N). \tag{4.2.12}$$

A usual strategy in the error analysis is to split the total error in such a way that each quantity can be bounded *a posteriori* in an optimal way. Following the idea of [15], we decompose the total error $e(t)$ as follows:

$$\begin{aligned} e(t) &:= u(t) - U(t) \\ &= \{u(t) - \tilde{U}(t)\} + \{\tilde{U}(t) - U(t)\} \\ &= \tilde{\rho}(t) + \tilde{\varepsilon}(t) \\ &= \tilde{\rho}(t) + \tilde{\sigma}(t) + \varepsilon(t), \quad t \in I_n. \end{aligned} \tag{4.2.13}$$

In the above $\tilde{\rho}(t) := u(t) - \tilde{U}(t)$ denotes the parabolic error, and $\tilde{\varepsilon}(t) := \tilde{U}(t) - U(t)$ represents the reconstruction error. Furthermore, the reconstruction error $\tilde{\varepsilon}(t)$ may be split into $\tilde{\varepsilon}(t) := \varepsilon(t) + \tilde{\sigma}(t)$, where $\varepsilon(t)$ is the elliptic reconstruction error or space discretization error defined by $\varepsilon(t) := \Theta(t) - U(t)$ and $\tilde{\sigma}(t)$ accounts for the time reconstruction error defined by $\tilde{\sigma}(t) := \tilde{U}(t) - \Theta(t)$. The *a posteriori* error bound on the main error is obtained by treating each term appearing in (4.2.13). To bound $\tilde{\rho}(t)$, the important step is to establish an appropriate error equation in $\tilde{\rho}$, which is stated in the following lemma.

Lemma 4.2.2. *For each $\varphi \in H_0^1(\Omega)$ and for $1 \le n \le N$, we have the following parabolic error equation*

$$\langle\tilde{\rho}_t(t), \varphi\rangle + a(\rho(t), \varphi) = \langle\mathscr{R}_1(t), \varphi\rangle, \quad t \in I_n, \tag{4.2.14}$$

with $\rho(t) := u(t) - \Theta(t)$ and

$$\begin{aligned} \mathscr{R}_1(t) &:= -\varepsilon_t(t) - (\mathcal{R}^n - I)\left\{\tilde{H}_1(t) - H_1(t_{n-\frac{1}{2}})\right\} + \left\{f(t) - \tilde{H}_1(t) - \Psi(t)\right\} \\ &\quad + \left\{l_{n-1}(t)(P_2^n - I)(\mathcal{A}_h^{n-1})U^{n-1} - k_n^{-1}(P_1^n - I)U^{n-1}\right\}, \end{aligned} \tag{4.2.15}$$

where the first, second, third and fourth terms in $\mathscr{R}_1(t)$ refer to the space-mesh error, space error, data approximation error and coarsening error, respectively.

Proof. Taking the L^2-inner product with $\varphi(t)$ in (4.2.12), for all $\varphi \in H_0^1(\Omega)$, we obtain

$$\left\langle\tilde{U}_t(t), \varphi\right\rangle = k_n^{-1}\left\langle\mathcal{R}^n P_1^n U^{n-1} - \mathcal{R}^{n-1}U^{n-1}, \varphi\right\rangle + \langle\mathcal{R}^n\tilde{H}_1(t), \varphi\rangle.$$

Subtracting the above relation from (4.1.4) we obtain

$$\begin{aligned}\langle\tilde{\rho}_t(t),\varphi\rangle + a(\rho(t),\varphi) &= \langle f(t),\varphi\rangle - a(\Theta(t),\varphi)\\ &\quad -k_n^{-1}\left\langle \mathcal{R}^n P_1^n U^{n-1} - \mathcal{R}^{n-1}U^{n-1},\varphi\right\rangle - \langle \mathcal{R}^n\tilde{H}_1(t),\varphi\rangle.\end{aligned}$$

In view of (4.2.7) and invoking (4.2.1) we obtain

$$\begin{aligned}&\langle\tilde{\rho}_t(t),\varphi\rangle + a(\rho(t),\varphi)\\ =\;& \langle f(t)-\tilde{H}_1(t),\varphi\rangle - \langle(\mathcal{R}^n - I)\tilde{H}_1(t),\varphi\rangle - l_{n-1}(t)\langle(\mathcal{A}_h^{n-1})U^{n-1},\varphi\rangle\\ &-l_n(t)\langle(\mathcal{A}_h^n)U^n,\varphi\rangle - k_n^{-1}\left\langle \mathcal{R}^n P_1^n U^{n-1} - \mathcal{R}^{n-1}U^{n-1},\varphi\right\rangle.\end{aligned}$$

Using (4.2.6), (4.2.9) - (4.2.10) and rearranging the above terms we finally lead to

$$\begin{aligned}&\langle\tilde{\rho}_t(t),\varphi\rangle + a(\rho(t),\varphi)\\ =\;& \left\langle f(t)-\tilde{H}_1(t)-\Psi(t),\varphi\right\rangle - \left\langle(\mathcal{R}^n-I)(\tilde{H}_1(t)-H_1(t_{n-\frac{1}{2}})),\varphi\right\rangle\\ &-k_n^{-1}\left\langle(\mathcal{R}^n-I)(U^n-P_1^nU^{n-1}),\varphi\right\rangle - k_n^{-1}\left\langle \mathcal{R}^nP_1^nU^{n-1}-\mathcal{R}^{n-1}U^{n-1},\varphi\right\rangle\\ &+l_{n-1}(t)\left\langle(P_2^n-I)(\mathcal{A}_h^{n-1})U^{n-1},\varphi\right\rangle\\ =\;& \left\langle f(t)-\tilde{H}_1(t)-\Psi(t),\varphi\right\rangle - \left\langle(\mathcal{R}^n-I)(\tilde{H}_1(t)-H_1(t_{n-\frac{1}{2}})),\varphi\right\rangle\\ &-k_n^{-1}\left\langle(\mathcal{R}^n-I)U^n-(\mathcal{R}^{n-1}-I)U^{n-1},\varphi\right\rangle - k_n^{-1}\left\langle(P_1^n-I)U^{n-1},\varphi\right\rangle\\ &+l_{n-1}(t)\left\langle(P_2^n-I)(\mathcal{A}_h^{n-1})U^{n-1},\varphi\right\rangle\\ =\;& -\langle\varepsilon_t(t),\varphi\rangle - \left\langle(\mathcal{R}^n-I)(\tilde{H}_1(t)-H_1(t_{n-\frac{1}{2}})),\varphi\right\rangle + \left\langle f(t)-\tilde{H}_1(t)-\Psi(t),\varphi\right\rangle\\ &+\left\langle l_{n-1}(t)(P_2^n-I)(\mathcal{A}_h^{n-1})U^{n-1} - k_n^{-1}(P_1^n-I)U^{n-1},\varphi\right\rangle,\end{aligned}$$

and this completes the proof. □

Now we shall summarize the notations of the various residual-based estimators as follows.

For $0 \le n \le N$, we define the *elliptic reconstruction error estimator:*

$$\mathscr{O}_{\mathrm{CN},n} := \mathcal{C}_{I,5}\; h_n^2\;|\log h_n|^{\frac{1}{2}}\;\|(\mathcal{A}_h^n)U^n - (U^n)_{\mathrm{el}}\| + \mathcal{C}_{I,6}\; h_n^{\frac{3}{2}}\;|\log h_n|^{\frac{1}{2}}\;\|j[\beta U^n]\|_{\Sigma_n}, \tag{4.2.16}$$

with $\mathcal{C}_{I,5} := \mathcal{C}_{I,3}\,\mathcal{C}_R$ and $\mathcal{C}_{I,6} := \mathcal{C}_{I,4}\,\mathcal{C}_R$.

For $1 \le n \le N$, we also define the following estimators.

The *space-mesh error estimator:*

$$\begin{aligned}\mathscr{M}_{\mathrm{CN},n} &:= \mathcal{C}_{I,5}\;\hat{h}_n^2\;|\log\hat{h}_n|^{\frac{1}{2}}\;\|k_n^{-1}\left\{(\mathcal{A}_h^n)U^n - (\mathcal{A}_h^{n-1})U^{n-1} - (U^n)_{\mathrm{el}} + (U^{n-1})_{\mathrm{el}}\right\}\|\\ &\quad + \mathcal{C}_{I,6}\;\hat{h}_n^{\frac{3}{2}}\;|\log\hat{h}_n|^{\frac{1}{2}}\;\|k_n^{-1}\left\{j[\beta U^n] - j[\beta U^{n-1}]\right\}\|_{\hat{\Sigma_n}}\\ &\quad + \mathcal{C}_{I,8}\;\hat{h}_n^{\frac{3}{2}}\;|\log\hat{h}_n|^{\frac{1}{2}}\;\|k_n^{-1}\left\{j[\beta U^n] - j[\beta U^{n-1}]\right\}\|_{\check{\Sigma_n}\setminus\hat{\Sigma_n}},\quad \mathcal{C}_{I,8} := \mathcal{C}_{I,7}\mathcal{C}_R.\end{aligned} \tag{4.2.17}$$

The *temporal reconstruction error estimator:*

$$\begin{aligned}\mathscr{T}_{\mathrm{re,CN},n} &:= \frac{k_n^2}{8}\Big\{\mathcal{C}_{I,5}\; h_n^2\;|\log h_n|^{\frac{1}{2}}\;\|(\mathcal{A}_h^n)\mathcal{Y}_n-(\mathcal{Y}_n)_{\mathrm{el}}\| \\ &\qquad + \mathcal{C}_{I,6}\; h_n^{\frac{3}{2}}\;|\log h_n|^{\frac{1}{2}}\;\|j[\beta\mathcal{Y}_n]\|_{\Sigma_n}+\|\mathcal{Y}_n\|\Big\},\end{aligned} \tag{4.2.18}$$

with

$$\mathcal{Y}_n := -\Pi_0^n\tilde{\Phi}_t(t)+\Psi_t(t).$$

The *space-error estimator:*

$$\begin{aligned}\mathscr{S}_{\mathrm{CN},n} &:= \frac{k_n}{4}\;\Big\{\mathcal{C}_{I,5}\; h_n^2\;|\log h_n|^{\frac{1}{2}}\;\|(\mathcal{A}_h^n)\mathcal{Y}_n-(\mathcal{Y}_n)_{\mathrm{el}}\| \\ &\qquad + \mathcal{C}_{I,6}\; h_n^{\frac{3}{2}}\;|\log h_n|^{\frac{1}{2}}\;\|j[\beta\mathcal{Y}_n]\|_{\Sigma_n}\Big\}.\end{aligned} \tag{4.2.19}$$

The *temporal error estimator:*

$$\begin{aligned}\mathscr{T}_{\mathrm{e,CN},n} &:= \frac{1}{\gamma_0}\sqrt{\frac{\alpha_0}{120}}\;k_n^2\;\{\mathcal{C}_{I,1}\,h_n\,\|(\mathcal{A}_h^n)\mathcal{Y}_n-(\mathcal{Y}_n)_{\mathrm{el}}\| \\ &\qquad + \mathcal{C}_{I,2}\,h_n^{\frac{1}{2}}\,\|j[\beta\mathcal{Y}_n]\|_{\Sigma_n}+\alpha_0\,\|\mathcal{Y}_n\|_1\Big\}.\end{aligned} \tag{4.2.20}$$

The *coarsening error estimator:*

$$\mathscr{C}_{\mathrm{CN},n} := k_n^{-1}\|(I-P_1^n)U^{n-1}\|+\frac{1}{2}\|(P_2^n-I)(\mathcal{A}_h^{n-1})U^{n-1}\|, \tag{4.2.21}$$

and the *data approximation error estimators:*

$$\begin{cases}\mathscr{D}_{\mathrm{CN},n,1} := \frac{1}{k_n}\int_{t_{n-1}}^{t_n}\|f(t)-\tilde{\Phi}(t)\|dt \\ \mathscr{D}_{\mathrm{CN},n,2} := \frac{1}{\sqrt{\gamma_0}}\,\mathcal{C}_{I,1}\,h_n\;\{\|(\Pi_0^n-I)f^{n-1}\|+\|(\Pi_0^n-I)f^n\|\}.\end{cases} \tag{4.2.22}$$

The following theorem gives *a posteriori* error bounds for the parabolic error $\tilde{\rho}$ in both the $L^2(H^1)$ and $L^\infty(L^2)$-norms.

Theorem 4.2.1. *Let u be the exact solution of (4.1.1)–(4.1.3) and let U^n be its finite element approximation obtained by the Crank-Nicolson approximation (4.1.10). Then, for $1\le m\le N$, the following is true:*

$$\begin{aligned}\left\{\max_{t\in[0,t_m]}\|\tilde{\rho}(t)\|^2+\gamma_0\int_0^{t_m}\|\tilde{\rho}(t)\|_1^2dt\right\}^{\frac{1}{2}} &\le \left\{2\left(\|\tilde{\rho}(0)\|^2+\sum_{n=1}^{m}k_n\mathscr{T}_{\mathrm{e,CN},n}^2\right)\right\}^{\frac{1}{2}} \\ &\quad +\left(\Lambda_{\mathrm{CN},m,1}^2+\Lambda_{\mathrm{CN},m,2}^2\right)^{\frac{1}{2}}\end{aligned}$$

with

$$\Lambda_{\mathrm{CN},m,1} := 4\sum_{n=1}^{m} k_n \left(\mathscr{M}_{\mathrm{CN},n} + \mathscr{S}_{\mathrm{CN},n} + \mathscr{D}_{\mathrm{CN},n,1} + \mathscr{C}_{\mathrm{CN},n}\right), \tag{4.2.23}$$

and

$$\Lambda_{\mathrm{CN},m,2} := 4\sum_{n=1}^{m} k_n^{\frac{1}{2}} \mathscr{D}_{\mathrm{CN},n,2}. \tag{4.2.24}$$

Here, $\mathscr{M}_{\mathrm{CN},n}$, $\mathscr{S}_{\mathrm{CN},n}$, $\mathscr{T}_{\mathrm{e,CN},n}$, $\mathscr{C}_{\mathrm{CN},n}$ and $\mathscr{D}_{\mathrm{CN},n,i}(i = 1, 2)$ are given by (4.2.17) and (4.2.19) −(4.2.22), respectively.

The proof of Theorem 4.2.1 essentially hinges on several lemmas. These lemmas provide bounds for the various errors by the appropriate estimators.

Lemma 4.2.3 (Temporal error estimate)**.** *Let $\mathfrak{I}_{n,1}$ $(1 \le n \le m)$ be defined by*

$$\mathfrak{I}_{n,1} := \alpha_0 \int_{t_{n-1}}^{t_n} \|\tilde{\sigma}(t)\|_1^2 dt.$$

Then

$$\mathfrak{I}_{n,1} \le k_n \, \mathscr{T}_{\mathrm{e,CN},n}^2,$$

where $\mathscr{T}_{\mathrm{e,CN},n}$ is given by (4.2.20).

Proof. The proof begins by first estimating $\tilde{\sigma}_t(t) := \tilde{U}_t(t) - \Theta_t(t)$. In view of (4.2.7) and (4.2.12) we have

$$\begin{aligned}
\tilde{\sigma}_t(t) &:= \frac{\mathcal{R}^n P_1^n U^{n-1} - \mathcal{R}^{n-1} U^{n-1}}{k_n} + \mathcal{R}^n \tilde{H}_1(t) - \frac{\mathcal{R}^n U^n - \mathcal{R}^{n-1} U^{n-1}}{k_n} \\
&= \mathcal{R}^n \left\{ \frac{P_1^n U^{n-1} - U^n}{k_n} + \tilde{H}_1(t) \right\} \\
&= \mathcal{R}^n \left\{ \tilde{H}_1(t) - H_1(t_{n-\frac{1}{2}}) \right\}. \qquad (4.2.25)
\end{aligned}$$

Integrate (4.2.25) from t_{n-1} to t. Using the fact that $\tilde{U}(t)$ and $\Theta(t)$ coincide at the nodal points, we obtain

$$\tilde{\sigma}(t) = \int_{t_{n-1}}^{t} \mathcal{R}^n \left\{ \tilde{H}_1(t) - H_1(t_{n-\frac{1}{2}}) \right\} dt. \tag{4.2.26}$$

From (4.2.10) and (4.2.11), it follows that

$$\tilde{H}_1(t) - H_1(t_{n-\frac{1}{2}}) := \Pi_0^n \left\{ \tilde{\Phi}(t) - \tilde{\Phi}(t_{n-\frac{1}{2}}) \right\} - \left\{ \Psi(t) - \Psi(t_{n-\frac{1}{2}}) \right\}. \tag{4.2.27}$$

Since $l_{n-1}(t) + l_n(t) = 1, t \in I_n$, a simple calculation now yields

$$\tilde{\Phi}(t) - \tilde{\Phi}(t_{n-\frac{1}{2}}) = (t - t_{n-\frac{1}{2}})\tilde{\Phi}_t(t)$$

and

$$\Psi(t) - \Psi(t_{n-\frac{1}{2}}) = (t - t_{n-\frac{1}{2}})\Psi_t(t).$$

Thus, in view of (4.2.27) we obtain

$$\tilde{H}_1(t) - H_1(t_{n-\frac{1}{2}}) = -(t - t_{n-\frac{1}{2}})\,\mathcal{Y}_n, \tag{4.2.28}$$

where

$$\mathcal{Y}_n := -\Pi_0^n \tilde{\Phi}_t(t) + \Psi_t(t). \tag{4.2.29}$$

Substituting (4.2.28) in (4.2.26) and evaluating the integral by the mid-point rule we have that

$$\begin{aligned} \tilde{\sigma}(t) &= -\int_{t_{n-1}}^{t} \mathcal{R}^n \left\{(t - t_{n-\frac{1}{2}})\mathcal{Y}_n\right\} \\ &= \frac{1}{2}(t - t_{n-1})(t_n - t)\mathcal{R}^n\mathcal{Y}_n. \end{aligned} \tag{4.2.30}$$

Using coercivity and continuity properties of the bilinear form $a(\cdot,\cdot)$, it follows that

$$\begin{aligned} \gamma_0\|\tilde{\sigma}(t)\|_1^2 &\leq a(\tilde{\sigma}(t), \tilde{\sigma}(t)) \\ &= \frac{1}{2}(t - t_{n-1})(t_n - t)\; a(\mathcal{R}^n\mathcal{Y}_n, \tilde{\sigma}(t)) \\ &= \frac{1}{2}(t - t_{n-1})(t_n - t)\,\{a((\mathcal{R}^n - I)\mathcal{Y}_n, \tilde{\sigma}(t)) + a(\mathcal{Y}_n, \tilde{\sigma}(t))\} \\ &\leq \frac{1}{2}(t - t_{n-1})(t_n - t)\;\{a((\mathcal{R}^n - I)\mathcal{Y}_n, \tilde{\sigma}(t)) + \alpha_0\|\mathcal{Y}_n\|_1\|\tilde{\sigma}(t)\|_1\}\,. \end{aligned} \tag{4.2.31}$$

We now apply the Galerkin orthogonality property of $\mathcal{R}^n$ and (4.2.1) to have

$$\begin{aligned} a((\mathcal{R}^n - I)\mathcal{Y}_n, \tilde{\sigma}(t)) &= a\left((\mathcal{R}^n - I)\mathcal{Y}_n, \tilde{\sigma}(t) - \mathscr{J}_n\tilde{\sigma}(t)\right) \\ &= |\langle(\mathcal{A}_h^n)\mathcal{Y}_n, \tilde{\sigma}(t) - \mathscr{J}_n\tilde{\sigma}(t)\rangle - \langle(\mathcal{Y}_n)_{\rm el}, \tilde{\sigma}(t) - \mathscr{J}_n\tilde{\sigma}(t)\rangle \\ &\quad -\langle j[\beta\mathcal{Y}_n], \tilde{\sigma}(t) - \mathscr{J}_n\tilde{\sigma}(t)\rangle_{\Sigma_n}|\,. \end{aligned}$$

Application of the Cauchy-Schwarz inequality and Proposition 3.2.1 yield

$$\begin{aligned} &a\left((\mathcal{R}^n - I)\mathcal{Y}_n, \tilde{\sigma}(t)\right) \\ &\quad\leq \|(\mathcal{A}_h^n)\mathcal{Y}_n - (\mathcal{Y}_n)_{\rm el}\|\,\|\tilde{\sigma}(t) - \mathscr{J}_n\tilde{\sigma}(t)\| + \|j[\beta\mathcal{Y}_n]\|_{\Sigma_n}\,\|\tilde{\sigma}(t) - \mathscr{J}_n\tilde{\sigma}(t)\|_{\Sigma_n} \\ &\quad\leq \left\{\mathcal{C}_{I,1}\,h_n\,\|(\mathcal{A}_h^n)\mathcal{Y}_n - (\mathcal{Y}_n)_{\rm el}\| + \mathcal{C}_{I,2}\,h_n^{\frac{1}{2}}\,\|j[\beta\mathcal{Y}_n]\|_{\Sigma_n}\right\}\|\tilde{\sigma}(t)\|_1, \end{aligned}$$

which combine with (4.2.31) leads to

$$\gamma_0 \, \|\tilde{\sigma}(t)\|_1 \leq \frac{1}{2}(t - t_{n-1})(t - t_n) \, \mathcal{G}_n,$$

where $\mathcal{G}_n := \mathcal{C}_{I,1} \, h_n \, \|(\mathcal{A}_h^n)\mathcal{Y}_n - (\mathcal{Y}_n)_{\rm el}\| + \mathcal{C}_{I,2} \, h_n^{\frac{1}{2}} \, \|j[\beta \mathcal{Y}_n]\|_{\Sigma_n} + \alpha_0 \|\mathcal{Y}_n\|_1$. Thus, we finally arrive at

$$\begin{aligned} \mathfrak{I}_{n,1} &\leq \frac{\alpha_0}{4\gamma_0^2} \, \mathcal{G}_n^2 \int_{t_{n-1}}^{t_n} (t - t_{n-1})^2 (t_n - t)^2 dt \\ &\leq k_n \mathscr{T}_{\rm e,CN,n}^2, \end{aligned}$$

where $\mathscr{T}_{\rm e,CN,n}^2 = \dfrac{1}{120} \, \dfrac{\alpha_0}{\gamma_0^2} \, k_n^4 \, \mathcal{G}_n^2$ and this completes the proof. □

Lemma 4.2.4 (Space-mesh error estimate)**.** *Let $\mathfrak{I}_{n,2}$ $(1 \leq n \leq m)$ be given by*

$$\mathfrak{I}_{n,2} := \int_{t_{n-1}}^{t_n} |\, \langle \varepsilon_t(t), \tilde{\rho}(t) \rangle \,| dt.$$

Then we have

$$\mathfrak{I}_{n,2} \leq k_n \, \mathscr{M}_{\rm CN,n} \max_{t \in \bar{I}_n} \|\tilde{\rho}(t)\|,$$

where $\mathscr{M}_{\rm CN,n}$ is given by (4.2.17).

Proof. For $1 \leq n \leq m$, we first observe that

$$\begin{aligned} \mathfrak{I}_{n,2} &= \int_{t_{n-1}}^{t_n} |\, \langle \tilde{\varepsilon}_t(t), \tilde{\rho}(t) \rangle \,| dt \\ &\leq k_n^{-1} \max_{t \in \bar{I}_n} \|\tilde{\rho}(t)\| \int_{t_{n-1}}^{t_n} \|(\mathcal{R}^n - I)U^n - (\mathcal{R}^{n-1} - I)U^{n-1}\| dt \\ &= \max_{t \in \bar{I}_n} \|\tilde{\rho}(t)\| \, \|(\mathcal{R}^n - I)U^n - (\mathcal{R}^{n-1} - I)U^{n-1}\|. \end{aligned} \tag{4.2.32}$$

In order to bound the term $\|(\mathcal{R}^n - I)U^n - (\mathcal{R}^{n-1} - I)U^{n-1}\|$, we use the well-known duality trick. For all $v \in H_0^1(\Omega)$, let $w : [0, T] \longrightarrow X$ be the solution of the following elliptic problem

$$\begin{aligned} a(v, w(t)) &= \langle (\mathcal{R}^n - I)U^n - (\mathcal{R}^{n-1} - I)U^{n-1}, v \rangle, \quad \text{a.e. } t \in [0, T], \\ w &= 0 \quad \text{on} \quad \partial\Omega, \\ [w] &= 0, \quad \left[\beta \frac{\partial w}{\partial \mathbf{n}}\right] = 0 \text{ across } \Gamma \end{aligned} \tag{4.2.33}$$

with

$$\|w\|_X \leq \mathcal{C}_R \, \|(\mathcal{R}^n - I)U^n - (\mathcal{R}^{n-1} - I)U^{n-1}\|. \tag{4.2.34}$$

Since $\mathcal{R}^n U^n - U^n$ is orthogonal to $\mathbb{S}^n$, it now follows that $(\mathcal{R}^n - I)U^n - (\mathcal{R}^{n-1} - I)U^{n-1}$ is orthogonal to $\mathbb{S}^n \cap \mathbb{S}^{n-1}$ with respect to $a(\cdot,\cdot)$. Set $v = (\mathcal{R}^n - I)U^n - (\mathcal{R}^{n-1} - I)U^{n-1}$ in (4.2.33). Using the Galerkin orthogonality property in the subspace $\mathbb{S}^n \cap \mathbb{S}^{n-1}$ and Definition 4.2.1 we obtain

$$\begin{aligned}
&\|(\mathcal{R}^n - I)U^n - (\mathcal{R}^{n-1} - I)U^{n-1}\|^2 \\
&\quad = a\left((\mathcal{R}^n - I)U^n - (\mathcal{R}^{n-1} - I)U^{n-1}, w(t)\right) \\
&\quad = a\left((\mathcal{R}^n - I)U^n - (\mathcal{R}^{n-1} - I)U^{n-1},\, w(t) - \hat{\mathscr{J}}_n w(t)\right) \\
&\quad = \left\langle (\mathcal{A}_h^n)U^n - (U^n)_{\text{el}},\, w(t) - \hat{\mathscr{J}}_n w(t)\right\rangle - \left\langle (\mathcal{A}_h^{n-1})U^{n-1} - (U^{n-1})_{\text{el}},\, w(t) - \hat{\mathscr{J}}_n w(t)\right\rangle \\
&\qquad - \left\langle j[\beta U^n] - j[\beta U^{n-1}],\, w(t) - \hat{\mathscr{J}}_n w(t)\right\rangle_{\check{\Sigma}_n}.
\end{aligned}$$

We now use the Cauchy-Schwarz inequality and Proposition 3.2.1 (in the subspace $\mathbb{S}^n \cap \mathbb{S}^{n-1}$) and Proposition 3.2.2 to obtain

$$\begin{aligned}
&\|(\mathcal{R}^n - I)U^n - (\mathcal{R}^{n-1} - I)U^{n-1}\|^2 \\
&\quad \le \Big\{ \mathcal{C}_{I,3}\, \hat{h}_n^2\, |\log \hat{h}_n|^{\frac{1}{2}}\, \|(\mathcal{A}_h^n)U^n - (\mathcal{A}_h^{n-1})U^{n-1} - (U^n)_{\text{el}} + (U^{n-1})_{\text{el}}\| \\
&\qquad + \mathcal{C}_{I,4}\, \hat{h}_n^{\frac{3}{2}}\, |\log \hat{h}_n|^{\frac{1}{2}} \|j[\beta U^n] - j[\beta U^{n-1}]\|_{\hat{\Sigma}_n} \\
&\qquad + \mathcal{C}_{\,I,7}\, \hat{h}_n^{\frac{3}{2}}\, |\log \hat{h}_n|^{\frac{1}{2}}\, \|j[\beta U^n] - j[\beta U^{n-1}]\|_{\check{\Sigma}_n \setminus \hat{\Sigma}_n} \Big\}\, \|w\|_X \\
&\quad \le k_n\, \mathscr{M}_{\text{CN},n}\, \|(\mathcal{R}^n - I)U^n - (\mathcal{R}^{n-1} - I)U^{n-1}\|, \qquad (4.2.35)
\end{aligned}$$

where in the last inequality we have used the elliptic regularity estimate (4.2.34). Now, use (4.2.32) and (4.2.35) to complete the proof. □

Lemma 4.2.5 (Space error estimate)**.** *Let $\mathfrak{I}_{n,3}$ $(1 \le n \le m)$ be defined as*

$$\mathfrak{I}_{n,3} := \int_{t_{n-1}}^{t_n} \left| \left\langle (\mathcal{R}^n - I)\left(\tilde{H}_1(t) - H_1(t_{n-\frac{1}{2}})\right), \tilde{\rho}(t)\right\rangle \right| dt.$$

Then

$$\mathfrak{I}_{n,3} \le\ k_n \mathscr{S}_{\text{CN},n}\ \max_{t \in \bar{I}_n} \|\tilde{\rho}(t)\|,$$

where $\mathscr{S}_{\text{CN},n}$ is defined in (4.2.19).

Proof. In view of (4.2.28), we note that

$$\tilde{H}_1(t) - H_1(t_{n-\frac{1}{2}}) = -(t - t_{n-\frac{1}{2}})\, \mathcal{Y}_n,$$

where $\mathcal{Y}_n$ is defined in (4.2.29). Then, using the Cauchy-Schwarz inequality we obtain

$$\begin{aligned}\mathfrak{I}_{n,3} &\leq \int_{t_{n-1}}^{t_n} \left|t - t_{n-\frac{1}{2}}\right| \|(\mathcal{R}^n - I)\mathcal{Y}_n\| \, \|\tilde{\rho}(t)\| dt \\ &\leq \frac{k_n^2}{4} \|(\mathcal{R}^n - I)\mathcal{Y}_n\| \max_{t\in\bar{I}_n} \|\tilde{\rho}(t)\| \\ &\leq k_n \, \mathscr{S}_{\mathrm{CN},n} \max_{t\in\bar{I}_n} \|\tilde{\rho}(t)\|,\end{aligned}$$

where we have used Lemma 4.2.1 and hence the result follows. □

Lemma 4.2.6 (Data approximation error estimate)**.** *Let $\mathfrak{I}_{n,4}$ $(1 \leq n \leq m)$ be defined as*

$$\mathfrak{I}_{n,4} := \int_{t_{n-1}}^{t_n} \left|\left\langle f(t) - \tilde{H}_1(t) - \Psi(t), \tilde{\rho}(t)\right\rangle\right| dt.$$

Then we have

$$\mathfrak{I}_{n,4} \leq k_n \, \mathscr{D}_{\mathrm{CN},n,1} \max_{t\in\bar{I}_n} \|\tilde{\rho}(t)\| + k_n^{\frac{1}{2}} \, \mathscr{D}_{\mathrm{CN},n,2} \left(\gamma_0 \int_{t_{n-1}}^{t_n} \|\tilde{\rho}(t)\|_1^2 dt\right)^{\frac{1}{2}},$$

where $\mathscr{D}_{\mathrm{CN},n,i}, i = 1, 2$ are given by (4.2.22).

Proof. Using (4.2.11), we obtain

$$\begin{aligned} f(t) - \tilde{H}_1(t) - \Psi(t) &= f(t) - \Pi_0^n \tilde{\Phi}(t) \\ &= \left(f(t) - \tilde{\Phi}(t)\right) - (\Pi_0^n - I)\tilde{\Phi}(t).\end{aligned}$$

Thus,

$$\begin{aligned}\mathfrak{I}_{n,4} &\leq \int_{t_{n-1}}^{t_n} \left|\left\langle f - \tilde{\Phi}(t), \tilde{\rho}(t)\right\rangle\right| dt + \int_{t_{n-1}}^{t_n} \left|\left\langle (\Pi_0^n - I)\tilde{\Phi}(t), \tilde{\rho}(t)\right\rangle\right| dt \\ &:= T_{1,n} + T_{2,n}. \qquad (4.2.36)\end{aligned}$$

Exploiting the orthogonality property of Π_0^n and Proposition 3.2.1 we have

$$\begin{aligned}\left\langle (\Pi_0^n - I)\tilde{\Phi}(t), \tilde{\rho}(t)\right\rangle &= \left\langle (\Pi_0^n - I)\tilde{\Phi}(t), \tilde{\rho}(t) - \mathscr{J}_n\tilde{\rho}(t)\right\rangle \\ &\leq \|(\Pi_0^n - I)\tilde{\Phi}(t)\| \, \|\tilde{\rho}(t) - \mathscr{J}_n\tilde{\rho}(t)\| \\ &\leq \mathcal{C}_{I,1} \, h_n \, \|(\Pi_0^n - I)\tilde{\Phi}(t)\| \, \|\tilde{\rho}(t)\|_1.\end{aligned}$$

As $\max_{t\in\bar{I}_n} |l_n(t)| = 1$ and $\max_{t\in\bar{I}_n} |l_{n-1}(t)| = 1$, it follows from (4.2.8) that

$$\begin{aligned}\|(\Pi_0^n - I)\tilde{\Phi}(t)\| &\leq \max_{t\in\bar{I}_n} |l_{n-1}(t)| \, \|(\Pi_0^n - I)f^{n-1}\| + \max_{t\in\bar{I}_n} |l_n(t)| \, \|(\Pi_0^n - I)f^n\| \\ &= \|(\Pi_0^n - I)f^{n-1}\| + \|(\Pi_0^n - I)f^n\|.\end{aligned}$$

Now, $T_{2,n}$ in (4.2.36) is estimated as

$$\begin{aligned} T_{2,n} &\leq \mathcal{C}_{I,1}\, h_n \left\{ \|(\Pi_0^n - I) f^{n-1}\| + \|(\Pi_0^n - I) f^n\| \right\} \int_{t_{n-1}}^{t_n} \|\tilde{\rho}(t)\|_1 dt \\ &\leq k_n^{\frac{1}{2}}\, \mathscr{D}_{\mathrm{CN},n,2} \left(\gamma_0 \int_{t_{n-1}}^{t_n} \|\tilde{\rho}(t)\|_1^2 dt \right)^{\frac{1}{2}}. \end{aligned}$$

Next for the term $T_{1,n}$, we use the Cauchy-Schwarz inequality to have

$$\begin{aligned} T_{1,n} &\leq \max_{t\in \bar{I}_n} \|\tilde{\rho}(t)\| \int_{t_{n-1}}^{t_n} \|f(t) - \tilde{\Phi}(t)\|\, dt \\ &= k_n\, \mathscr{D}_{\mathrm{CN},n,1} \max_{t\in \bar{I}_n} \|\tilde{\rho}(t)\|. \end{aligned}$$

Altogether these estimates complete the proof. □

Lemma 4.2.7 (Coarsening error estimate)**.** *Let $\mathfrak{I}_{n,5}$ $(1 \leq n \leq m)$ be defined as*

$$\mathfrak{I}_{n,5} := \int_{t_{n-1}}^{t_n} \left| \left\langle k_n^{-1}(I - P_1^n) U^{n-1} + l_{n-1}(t)(P_2^n - I)(\mathcal{A}_h^{n-1}) U^{n-1}, \tilde{\rho}(t) \right\rangle \right| dt.$$

Then

$$\mathfrak{I}_{n,5} \leq k_n\, \mathscr{C}_{\mathrm{CN},n} \max_{t\in \bar{I}_n} \|\tilde{\rho}(t)\|,$$

where $\mathscr{C}_{\mathrm{CN},n}$ is given by (4.2.21).

Proof. Applying the Cauchy-Schwarz inequality, we have

$$\begin{aligned} \mathfrak{I}_{n,5} &\leq \int_{t_{n-1}}^{t_n} k_n^{-1} \|(I - P_1^n) U^{n-1}\|\, \|\tilde{\rho}(t)\| dt \\ &\quad + \int_{t_{n-1}}^{t_n} \left| \frac{(t_n - t)}{k_n} \right| \|(P_2^n - I)(\mathcal{A}_h^{n-1}) U^{n-1}\|\, \|\tilde{\rho}(t)\| dt \\ &\leq \left\{ \|(I - P_1^n) U^{n-1}\| + \frac{k_n}{2} \|(P_2^n - I)(\mathcal{A}_h^{n-1}) U^{n-1}\| \right\} \max_{t\in \bar{I}_n} \|\tilde{\rho}(t)\| \\ &= k_n\, \mathscr{C}_{\mathrm{CN},n} \max_{t\in \bar{I}_n} \|\tilde{\rho}(t)\|, \end{aligned}$$

and hence we prove the desired result. □

Proof of Theorem 4.2.1. Setting $\varphi = \tilde{\rho}(t)$ in (4.2.14) we have that

$$\frac{1}{2}\frac{d}{dt}\|\tilde{\rho}(t)\|^2 + a\left(\rho(t), \tilde{\rho}(t)\right) = \left\langle \mathscr{R}_1(t), \tilde{\rho}(t) \right\rangle.$$

Recalling the identity $2a(v,w) = a(v,v) + a(w,w) - a(v-w, v-w) \quad \forall v, w \in H_0^1(\Omega)$ and using the continuity and coercitivity of the bilinear form $a(\cdot,\cdot)$, we arrive at

$$\frac{1}{2}\frac{d}{dt}\|\tilde{\rho}(t)\|^2 + \frac{\gamma_0}{2}\left(\|\rho(t)\|_1^2 + \|\tilde{\rho}(t)\|_1^2\right) \leq \frac{\alpha_0}{2}\|\tilde{\sigma}(t)\|_1^2 + |\left\langle \mathscr{R}_1(t), \tilde{\rho}(t) \right\rangle|. \tag{4.2.37}$$

Integrate (4.2.37) from t_{n-1} to t_n to have

$$\frac{1}{2}\|\tilde{\rho}(t_n)\|^2 - \frac{1}{2}\|\tilde{\rho}(t_{n-1})\|^2 + \frac{\gamma_0}{2}\int_{t_{n-1}}^{t_n}\left(\|\rho(t)\|_1^2 + \|\tilde{\rho}(t)\|_1^2\right)dt$$
$$\leq \frac{\alpha_0}{2}\int_{t_{n-1}}^{t_n}\|\tilde{\sigma}(t)\|_1^2 dt + \int_{t_{n-1}}^{t_n}|\langle \mathscr{R}_1(t), \tilde{\rho}(t)\rangle|dt.$$

Summing up over $n = 1 : m$ we have that

$$\|\tilde{\rho}(t_m)\|^2 + \gamma_0\int_0^{t_m}\left(\|\rho(t)\|_1^2 + \|\tilde{\rho}(t)\|_1^2\right)dt$$
$$\leq \|\tilde{\rho}(0)\|^2 + \sum_{n=1}^{m}\left\{\alpha_0\int_{t_{n-1}}^{t_n}\|\tilde{\sigma}(t)\|_1^2 dt + 2\int_{t_{n-1}}^{t_n}|\langle \mathscr{R}_1(t), \tilde{\rho}(t)\rangle|dt\right\}$$
$$= \|\tilde{\rho}(0)\|^2 + \sum_{n=1}^{m}\left\{\mathfrak{I}_{n,1} + 2\sum_{i=2}^{5}\mathfrak{I}_{n,i}\right\}, \tag{4.2.38}$$

where $\mathfrak{I}_{n,i}$ $(i = 1, ..., 5)$ are defined in Lemmas $4.2.3 - 4.2.7$, respectively.

Since $\tilde{\rho}(t)$ is continuous in $[0, t_m]$, there exists $t_{0,m} \in [0, t_m]$ such that

$$\|\tilde{\rho}_{0,m}\| := \|\tilde{\rho}(t_{0,m})\| = \max_{t\in[0,t_m]}\|\tilde{\rho}(t)\|.$$

Again integrating (4.2.37) between the limits 0 to $t_{0,m}$ and observing that the integrands are non-negative, it follows that

$$\|\tilde{\rho}(t_{0,m})\|^2 + \gamma_0\int_0^{t_{0,m}}\left(\|\rho(t)\|_1^2 + \|\tilde{\rho}(t)\|_1^2\right)dt$$
$$\leq \|\tilde{\rho}(0)\|^2 + \alpha_0\int_0^{t_{0,m}}\|\tilde{\sigma}(t)\|_1^2 dt + 2\int_0^{t_{0,m}}|\langle \mathscr{R}_1(t), \tilde{\rho}(t)\rangle|dt$$
$$\leq \|\tilde{\rho}(0)\|^2 + \sum_{n=1}^{m}\left\{\alpha_0\int_{t_{n-1}}^{t_n}\|\tilde{\sigma}(t)\|_1^2 dt + 2\int_{t_{n-1}}^{t_n}|\langle \mathscr{R}_1(t), \tilde{\rho}(t)\rangle|dt\right\}$$
$$= \|\tilde{\rho}(0)\|^2 + \sum_{n=1}^{m}\left\{\mathfrak{I}_{n,1} + 2\sum_{i=2}^{5}\mathfrak{I}_{n,i}\right\}. \tag{4.2.39}$$

Now combining (4.2.38) and (4.2.39) we finally obtain

$$\|\tilde{\rho}(t_{0,m})\|^2 + \gamma_0\int_0^{t_m}\|\tilde{\rho}(t)\|_1^2 dt \leq 2\|\tilde{\rho}(0)\|^2 + 2\sum_{n=1}^{m}\left\{\mathfrak{I}_{n,1} + 2\sum_{i=2}^{5}\mathfrak{I}_{n,i}\right\}.$$

Now, we apply Lemmas 4.2.3 – 4.2.7 to obtain

$$\begin{aligned}\|\tilde{\rho}_{0,m}\|^2 + \gamma_0 \int_0^{t_m} \|\tilde{\rho}(t)\|_1^2 \, dt &\leq 2\left\{\|\tilde{\rho}(0)\|^2 + \sum_{n=1}^{m} k_n \mathscr{T}_{\mathrm{e,CN},n}^2\right\} \\ &+ 4 \max_{t\in[0,t_m]} \|\tilde{\rho}(t)\| \sum_{n=1}^{m} k_n \left\{\mathscr{M}_{\mathrm{CN},n} + \mathscr{S}_{\mathrm{CN},n} + \mathscr{D}_{\mathrm{CN},n,1} + \mathscr{C}_{\mathrm{CN},n}\right\} \|\tilde{\rho}_{0,m}\| \\ &+ 4\sum_{n=1}^{m} k_n^{\frac{1}{2}} \mathscr{D}_{\mathrm{CN},n,2} \left(\gamma_0 \int_{t_{n-1}}^{t_n} \|\tilde{\rho}(t)\|_1^2 dt\right)^{\frac{1}{2}}.\end{aligned}$$

For $1 \leq n \leq m$, taking

$$a_0 := \|\tilde{\rho}_{0,m}\|, \quad a_n := \left(\gamma_0 \int_{t_{n-1}}^{t_n} \|\tilde{\rho}(t)\|_1^2 \, dt\right)^{\frac{1}{2}},$$

$$c := \left\{2\left(\|\tilde{\rho}(0)\|^2 + \sum_{n=1}^{m} k_n \mathscr{T}_{\mathrm{e,CN},n}^2\right)\right\}^{\frac{1}{2}},$$

$$b_0 := 4\sum_{n=1}^{m} k_n \left\{\mathscr{M}_{\mathrm{CN},n} + \mathscr{S}_{\mathrm{CN},n} + \mathscr{D}_{\mathrm{CN},n,1} + \mathscr{C}_{\mathrm{CN},n}\right\},$$

and

$$b_n := 4k_n^{\frac{1}{2}} \, \mathscr{D}_{\mathrm{CN},n,2},$$

in Lemma 1.2.3, the desired result follows. □

Now we present the main theorem of this chapter concerning the fully discrete Crank-Nicolson *a posteriori* error estimates in the $L^\infty(L^2)$ norm for the parabolic interface problem (4.1.1) – (4.1.3).

Theorem 4.2.2. *Let u be the exact solution of (4.1.1)–(4.1.3) and let U^n be its finite element approximation obtained by the Crank-Nicolson approximation (4.1.10). Then, for each $1 \leq m \leq N$, the following a posteriori error estimate holds:*

$$\begin{aligned}\max_{t\in[0,t_m]} \|u(t) - U(t)\| \quad &\leq \quad \sqrt{2}\,\|\mathcal{R}^0 U^0 - u(0)\| + \sqrt{2}\left(\sum_{n=1}^{m} k_n \mathscr{T}_{\mathrm{e,CN},n}^2\right)^{\frac{1}{2}} \\ &\quad + \left(\Lambda_{\mathrm{CN},m,1}^2 + \Lambda_{\mathrm{CN},m,2}^2\right)^{\frac{1}{2}} \\ &\quad + 2\max_{0\leq n\leq m} \mathscr{O}_{\mathrm{CN},n} + \max_{0\leq n\leq m} \mathscr{T}_{\mathrm{re,CN},n},\end{aligned}$$

where the symbols $\mathscr{O}_{\mathrm{CN},n}$, $\mathscr{T}_{\mathrm{re,CN},n}$, $\mathscr{T}_{\mathrm{e,CN},n}$, $\Lambda_{\mathrm{CN},m,1}$ and $\Lambda_{\mathrm{CN},m,2}$ are defined in (4.2.16), (4.2.18), (4.2.20), (4.2.23) and (4.2.24), respectively.

Proof. In view of (4.2.13), we apply the triangle inequality to have

$$\begin{aligned} \|u(t) - U(t)\| &\leq \|\tilde{\rho}(t)\| + \|\tilde{\sigma}(t)\| + \|\varepsilon(t)\|, \quad t \in I_n, \\ &\leq \max_{t\in[0,t_m]} \|\tilde{\rho}(t)\| + \max_{t\in[0,t_m]} \|\tilde{\sigma}(t)\| + \max_{t\in[0,t_m]} \|\varepsilon(t)\|. \end{aligned} \tag{4.2.40}$$

As $\max\limits_{t\in\bar{I}_n} l_n(t) = 1$, for $t \in I_n$, we have

$$\begin{aligned} \|\varepsilon(t)\| &= \|l_{n-1}(t)\varepsilon^{n-1} + l_n(t)\varepsilon^n\| \\ &\leq 2\max\{\|\varepsilon^{n-1}\|, \|\varepsilon^n\|\}. \end{aligned}$$

Therefore, for $t \in [0, t_m]$, using the Lemma 4.2.1, we obtain

$$\|\varepsilon(t)\| \leq 2 \max_{0\leq n\leq m} \|\varepsilon^n\| \leq 2 \max_{0\leq n\leq m} \mathscr{O}_{\mathrm{CN},n}. \tag{4.2.41}$$

Again, using (4.2.30) we have that

$$\begin{aligned} \|\tilde{\sigma}(t)\| &= \|\frac{1}{2}(t - t_{n-1})(t_n - t)\mathcal{R}^n\mathcal{Y}_n\| \\ &\leq \frac{1}{2}\max_{t\in\bar{I}_n}\{|(t - t_{n-1})(t_n - t)|\}\ (\|(\mathcal{R}^n - I)\mathcal{Y}_n\| + \|\mathcal{Y}_n\|) \\ &\leq \mathscr{T}_{\mathrm{re,CN},n}, \end{aligned} \tag{4.2.42}$$

where $\mathscr{T}_{\mathrm{re,CN},n}$ is defined in (4.2.18). Finally, we use (4.2.40) – (4.2.42) and Theorem 4.2.1 to complete the proof of the theorem. □

Remark 4.2.1 (Comparison to the parabolic problems). The crucial difference between the *a posteriori* bounds for the parabolic problems (cf. [15]) and the parabolic interface problems is reflected in the *elliptic reconstruction error estimator* in the L^2-norm, the *spatial-mesh error estimator* and the *spatial error estimator*. For parabolic problems, both the estimators are of $O(h_n^2)$ in the space variable, whereas for the interface problems these estimators are of order $O(h_n^2|\log h_n|)$. The appearance of the factor $|\log h_n|$ in (4.2.16), (4.2.17) and (4.2.19) is quite natural as the discontinuity of the diffusion coefficient reduces the regularity of the solution of interface problems. Note that the *temporal reconstruction error estimator* is of optimal order in time and nearly optimal order in space.

5

Fully Discrete BDF-2 Error Analysis

In the previous two chapters, we have considered the single step methods for the time discretizations of the linear parabolic interface problem. In this chapter, we discuss *a posteriori* error analysis of the two-step backward differentiation formula (BDF-2) method for the linear parabolic interface problem (1.1.1) – (1.1.3). We use the standard linear finite element spaces in space which are allowed to change in time and the two-step backward differentiation formula (BDF-2) approximation at equidistant time step is used for the time discretizations. The essential ingredients in the error analysis are the continuous piecewise quadratic space-time BDF-2 reconstruction and new Clément-type interpolation estimates. The error estimates of optimal order in time and almost optimal order in space are derived in the $L^\infty(L^2)$-norm using the energy method.

5.1 Introduction

To start with we first revisit the parabolic interface problem. Let Ω be a bounded convex polygonal domain in $\mathbb{R}^2$ with Lipschitz boundary $\partial\Omega$. Let Ω_1 be a subdomain of Ω with C^2 boundary $\partial\Omega_1 := \Gamma$. The interface Γ now divides the domain Ω into two subdomains Ω_1 and $\Omega_2 := \Omega \setminus \Omega_1$. Consider the linear parabolic interface problem of the form

$$u_t(x,t) - \mathrm{div}(\beta(x)\nabla u(x,t)) = f(x,t) \quad \text{in} \quad \Omega \times (0,T] \tag{5.1.1}$$

with prescribed initial and boundary conditions

$$u(x,0) = u_0(x) \quad \text{in} \quad \Omega; \qquad u = 0 \quad \text{on} \quad \partial\Omega \times [0,T] \tag{5.1.2}$$

and jump conditions on the interface

$$[u] = 0, \quad \left[\beta \frac{\partial u}{\partial \mathbf{n}}\right] = 0 \quad \text{across} \quad \Gamma \times [0,T], \tag{5.1.3}$$

where $[v]$ denotes the jump of a quantity v across the interface Γ, i.e., $[v](x) = v_1(x) - v_2(x)$, $x \in \Gamma$ with $v_i(x) = v(x)|_{\Omega_i}$, $i = 1, 2$ and $T < +\infty$. The symbol $\mathbf{n}$ denotes the unit outward normal to the boundary $\partial\Omega_1 := \Gamma$. The diffusion coefficient $\beta(x)$ is assumed to be positive and piecewise constant on each subdomain, i.e.,

$$\beta(x) = \beta_i \quad \text{for} \quad x \in \Omega_i,\ i = 1, 2.$$

The initial function $u_0(x)$ and the forcing term $f(x, t)$ are real valued functions and assumed to be smooth.

The weak formulation of the (5.1.1)−(5.1.3) may be stated as: Find $u \in L^\infty(0, T; H_0^1(\Omega))$ satisfying

$$\begin{aligned} \langle u_t(t), \varphi\rangle + a(u(t), \varphi) &= \langle f(t), \varphi\rangle \ \ \forall \varphi \in H_0^1(\Omega), \quad \text{a.e. } t \in (0, T], \\ u(0) &= u_0, \end{aligned} \tag{5.1.4}$$

where $a(\cdot, \cdot)$ is a bilinear form on $H_0^1(\Omega)$ defined by

$$a(v, w) = \langle \beta\nabla v, \nabla w\rangle \quad \forall v, w \in H_0^1(\Omega), \tag{5.1.5}$$

and ∇ denotes the spatial gradient. The bilinear form is bounded and coercive on $H_0^1(\Omega)$, i.e., $\exists \alpha_0, \gamma_0 > 0$ such that

$$|a(v, w)| \le \alpha_0 \, \|v\|_1 \|w\|_1 \quad \forall v, w \in H_0^1(\Omega), \tag{5.1.6}$$

and

$$a(v, v) \ge \ \gamma_0 \, \|v\|_1^2 \quad \forall v \in H_0^1(\Omega). \tag{5.1.7}$$

In this chapter, we consider partition of time axis with constant step-size, i.e., $\mathcal{P} := \{(t_{n-1}, t_n]\}_{n=1}^N$ is a partition of $[0, T]$ with $I_n := (t_{n-1}, t_n]$, and $k := t_n - t_{n-1} = \frac{T}{N}$ be the constant time step. Then, for each $n = 0, \cdots, N$, we consider the finite element space $\mathbb{S}^n$ corresponding to the triangulation $\mathcal{T}_n$ as follows:

$$\mathbb{S}^n := \left\{\chi \in H_0^1(\Omega) \ \middle|\ \chi|_K \in \mathbb{P}_1(K) \quad \text{for all} \quad K \in \mathcal{T}_n\right\},$$

where $\mathbb{P}_1(K)$ is the space of polynomials of degree less than or equal to 1 on K.

Henceforth, we shall use the following notations: For $1 \le n \le N$,

$$\bar\partial v^n := \frac{v^n - v^{n-1}}{k}, \qquad f^{n-\frac{1}{2}} := \frac{f^n + f^{n-1}}{2}.$$

The fully discrete BDF-2 approximation of the problem $(5.1.1)-(5.1.3)$ associated with the finite element space $\mathbb{S}^n$ is stated below. Given $U^0 = I_h^0 u(0)$, seek for a sequence of approximations $U^1, \ldots, U^n$ such that

$$
\begin{aligned}
(5.1.8) \qquad \langle \frac{1}{k}(U^1 - U^0), \chi_1 \rangle + a(\frac{1}{2}(U^0 + U^1), \chi_1) &= \langle f^{\frac{1}{2}}, \chi_1 \rangle \quad \forall \chi_1 \in \mathbb{S}^1, \\
\langle \frac{1}{k}(\frac{3}{2}U^n - 2U^{n-1} + \frac{1}{2}U^{n-2}), \chi_n \rangle + a\,(U^n, \chi_n) &= \langle f^n, \chi_n \rangle \quad \forall \chi_n \in \mathbb{S}^n,\ n \geq 2,
\end{aligned}
$$

where I_h^0 is a suitable projection operator from $H_0^1(\Omega)$ into the finite dimensional subspace $\mathbb{S}^0$. As BDF-2 is a two-step method we need two starting values U^0 and U^1. Given U^0, we perform one step with the Trapezoidal method to get U^1 and then apply BDF-2 method to obtain $U^2, \ldots, U^n$.

Remark 5.1.1. Since both U^0 and U^1 are needed to start the procedure, one may attempt to choose $U^0 = I_h^0 u(0)$ and compute U^1 by the backward Euler method, i.e.,

$$
(5.1.9) \qquad \langle \frac{1}{k}(U^1 - U^0), \chi_1 \rangle + a(U^1, \chi_1) = \langle f^1, \chi_1 \rangle \quad \forall \chi_1 \in \mathbb{S}^1.
$$

At this point we need to comment that although this equation is only first order accurate, but it is known from the BDF-2 *a priori* error analysis (cf. [97]) that (5.1.9) suffices to obtain a second order approximations U^m to $u(t_m)$. However, this procedure leads to suboptimal *a posteriori* error estimates for parabolic problem (cf. [3]) and hence, the Trapezoidal rule is used to compute U^1.

Representation of the bilinear form. As in the spatially discrete case for $v \in \mathbb{S}^n$, the bilinear form $a(\cdot, \cdot)$ can be represented in short form as

$$
(5.1.10) \qquad a(v, \varphi) \;=\; \langle (v)_{\text{el}}, \varphi \rangle \;+\; \langle j[\beta v], \varphi \rangle_{\Sigma_n} \quad \forall \varphi \in H_0^1(\Omega),
$$

and the symbols have the usual meaning as earlier.

Next, we recall the projection operators for our subsequent use.

Discrete elliptic operator. The discrete elliptic operator associated with the bilinear form $a(\cdot, \cdot)$ and the finite element space $\mathbb{S}^n$ is the operator $\mathcal{A}_h^n : H_0^1(\Omega) \longrightarrow \mathbb{S}^n$ such that for $v \in H_0^1(\Omega)$ and $0 \leq n \leq N$,

$$
(5.1.11) \qquad \langle \mathcal{A}_h^n v,\ \chi_n \rangle \;=\; a(v, \chi_n) \quad \forall \chi_n \in \mathbb{S}^n.
$$

L^2-projection operator: The L^2-projection operator is a map $\Pi_0^n : L^2(\Omega) \longrightarrow \mathbb{S}^n$ such that for $v \in L^2(\Omega)$ and $0 \leq n \leq N$,

$$
(5.1.12) \qquad \langle \Pi_0^n\ v\ , \chi_n \rangle \;=\; \langle v,\ \chi_n \rangle \quad \forall \chi_n \in \mathbb{S}^n.
$$

For $n = 1$, (5.1.8) can be written in the distributional form as

$$\frac{U^1 - \Pi_0^1 U^0}{k} + \frac{1}{2}(\mathcal{A}_h^1)U^1 + \frac{1}{2}(\mathcal{A}_h^1)U^0 = \Pi_0^1 f^{\frac{1}{2}}.$$

The discrete elliptic operator $\mathcal{A}_h^1$ on the finer mesh when applied to the coarse grid function in the above may lead to oscillation during refinement (cf. [15]). Therefore, in order to avoid such situation, we consider the modified BDF-2 approximation.

Modified BDF-2 approximation: For $0 \leq n \leq N$, seek $U^n \in \mathbb{S}^n$ as follows:

$$\text{(5.1.13)} \quad \begin{cases} U^0 = I_h^0 u(0), \\ \frac{1}{k}(U^1 - P_1^1 U^0) + \frac{1}{2}(P_2^1(\mathcal{A}_h^0))U^0 + \frac{1}{2}(\mathcal{A}_h^1)U^1 = \Pi_0^1 f^{\frac{1}{2}}, \\ \frac{1}{k}\left\{\frac{3}{2}U^n - 2P_1^n U^{n-1} + \frac{1}{2}(P_1^n P_1^{n-1})U^{n-2}\right\} + (\mathcal{A}_h^n)U^n = \Pi_0^n f^n, \quad n \geq 2, \end{cases}$$

where $P_1^n, P_2^n : \mathbb{S}^{n-1} \longrightarrow \mathbb{S}^n$ are suitable projection operators.

A posteriori error estimate of the BDF-2 approximation for the purely linear parabolic problems has been investigated by Akrivis and Chatzipantelidis in [3]. A continuous piecewise quadratic function so-called the BDF-2 reconstruction of the approximate solution U is introduced to obtain the second order convergence for the semidiscrete time discretization of the parabolic problems. The authors of [3] have shown that specific choices of the reconstructions lead to reconstruction based on approximation on one time interval (two-point reconstruction) as well as the reconstruction based on approximation on two time intervals (three-point reconstruction). However, the effect of mesh change is not considered in their analysis (cf. [3]).

In this chapter, an attempt has been made to derive *a posteriori* error bounds for the fully discrete BDF-2 approximation of the parabolic interface problem (5.1.1) – (5.1.3) in the $L^\infty(L^2)$-norm. Compared to the existing results in [3] for parabolic problems, our analysis also includes the effect of mesh modification strategy. Error analysis is based on the methodology developed in [15, 62] for space discretization and [3] for time approximations. The main key idea in the error analysis is the appropriate space-time BDF-2 reconstruction.

The rest of this chapter is organized as follows. In Section 5.2, we introduce a quadratic (in time) space-time BDF-2 reconstruction for the problem. In this section, we also point out that how BDF-2 reconstruction differs from the Crank-Nicolson reconstruction. Section 5.3 discusses the abstract *a posteriori* error analysis for the fully discrete BDF-2 approximation in the $L^\infty(L^2)$-norm.

5.2 Quadratic Space-time BDF-2 Reconstruction

In this section, we introduce a space-time quadratic reconstruction for the BDF-2 approximation (5.1.13). For this purpose we recall from [15] the following definition.

Definition 5.2.1 (Elliptic reconstruction)**.** *Let $v \in \mathbb{S}^n$. Then the elliptic reconstruction $\mathcal{R}^n : \mathbb{S}^n \longrightarrow H_0^1(\Omega)$ is defined as*

$$a(\mathcal{R}^n v, \varphi) = \langle \mathcal{A}_h^n v, \varphi \rangle \quad \forall \varphi \in H_0^1(\Omega),\ 0 \le n \le N. \tag{5.2.1}$$

Note that the elliptic reconstruction $\mathcal{R}^n$ satisfies the Galerkin orthogonality property.

Now, we fix the following notations for the introduction of quadratic reconstruction.

Let $U : [0,T] \longrightarrow H_0^1(\Omega)$ be a continuous piecewise linear approximation in time of $u(t)$ defined by

$$\begin{aligned} U(t) &:= l_{n-1}(t)U^{n-1} + l_n(t)U^n \\ &= U^{n-\frac{1}{2}} + (t - t_{n-\frac{1}{2}})\bar{\partial}U^n, \quad t \in I_n\ (n = 1, \ldots, N), \end{aligned} \tag{5.2.2}$$

where for $1 \le n \le N$, the Lagrange hat functions $l_{n-1}(t)$ and $l_n(t)$ are defined by

$$l_{n-1}(t) := \frac{t_n - t}{k} \quad \text{and} \quad l_n(t) := \frac{t - t_{n-1}}{k} \quad \text{for } t \in I_n. \tag{5.2.3}$$

Let $\Psi, \Theta : [0,T] \longrightarrow H_0^1(\Omega)$ be the continuous piecewise linear functions in time defined by

$$\Psi(t) := l_{n-1}(t)\,(P_2^n(\mathcal{A}_h^{n-1}))\,U^{n-1} + l_n(t)\,(\mathcal{A}_h^n)\,U^n, \quad t \in I_n\ (n = 1, \ldots, N), \tag{5.2.4}$$

and

$$\Theta(t) := l_{n-1}(t)\,\mathcal{R}^{n-1}\,U^{n-1} + l_n(t)\,\mathcal{R}^n\,U^n, \quad t \in I_n\ (n = 1, \ldots, N), \tag{5.2.5}$$

respectively.

To motivate the definition of the quadratic space-time BDF-2 reconstruction, we rewrite the fully discrete BDF-2 approximation (5.1.13) in compact form as

$$\begin{cases} U^0 = I_h^0 u(0), \\ \frac{1}{k}(U^1 - P_1^1 U^0) = H_2(t_1), \\ \frac{1}{k}\left(\frac{3}{2}U^n - 2P_1^n U^{n-1} + \frac{1}{2}(P_1^n P_1^{n-1})U^{n-2}\right) = H_2(t_n), \quad n \ge 2, \end{cases} \tag{5.2.6}$$

where

$$H_2(t_n) := \begin{cases} \Pi_0^1 f^{\frac{1}{2}} - \Psi(t_{\frac{1}{2}}), & n = 1, \\ \Pi_0^n f^n - \Psi(t_n), & n \geq 2. \end{cases} \tag{5.2.7}$$

Next, let $\hat{\Phi} : [0, T] \longrightarrow H_0^1(\Omega)$ be a piecewise linear approximation of $f(t)$ defined by

$$\hat{\Phi}(t) := (t - t_{n-\frac{1}{2}})\bar{\partial} f^n + \nu_n, \;\; t \in I_n \; (n = 1, \ldots, N), \tag{5.2.8}$$

where ν_n is a constant to be determined appropriately.

We also define $\hat{H}_2 : [0, T] \longrightarrow H_0^1(\Omega)$ be a piecewise linear function in time defined as

$$\hat{H}_2(t) := \Pi_0^n \hat{\Phi}(t) - \Psi(t), \;\; t \in I_n \; (n = 1, \ldots, N). \tag{5.2.9}$$

Clearly $\hat{H}_2(\cdot)|_{I_n} \in \mathbb{P}_1(I_n)$.

Definition 5.2.2 (Space-time reconstruction)**.** *The quadratic space-time BDF-2 reconstruction $\hat{U} : [0, T] \longrightarrow H_0^1(\Omega)$ of U is defined by*

$$\begin{aligned} \hat{U}(t) \;\; &:= \;\; \mathcal{R}^{n-1} U^{n-1} + k^{-1} (t - t_{n-1}) \left\{ (\mathcal{R}^n \Pi_0^n) U^{n-1} - \mathcal{R}^{n-1} U^{n-1} \right\} \\ &\quad + \int_{t_{n-1}}^{t} \mathcal{R}^n \hat{H}_2(s) ds, \;\; t \in I_n \; (n = 1, \ldots, N). \end{aligned} \tag{5.2.10}$$

Observe that $\hat{U}(t_{n-1}) = \mathcal{R}^{n-1} U^{n-1}$.

Furthermore, evaluating the integral in (5.2.10) by the midpoint rule and recalling (5.2.9), we obtain

$$\begin{aligned} \hat{U}(t_n) \;\; &= \;\; (\mathcal{R}^n \Pi_0^n) U^{n-1} + k \, \mathcal{R}^n \hat{H}_2 \left(t_{n-\frac{1}{2}} \right) \\ &= \;\; (\mathcal{R}^n \Pi_0^n) U^{n-1} + k \, \mathcal{R}^n \left\{ \Pi_0^n \nu_n - \Psi(t_{n-\frac{1}{2}}) \right\}. \end{aligned}$$

Then, $\hat{U}$ will interpolate $\mathcal{R}^n U^n$ at $t = t_n$ if and only if

$$\nu_n = \frac{U^n - \Pi_0^n U^{n-1}}{k} + \Psi(t_{n-\frac{1}{2}}). \tag{5.2.11}$$

Thus, $\hat{U}$ is a continuous function in time and satisfies the following relation

$$\hat{U}_t(t) = k^{-1} \left\{ (\mathcal{R}^n \Pi_0^n) U^{n-1} - \mathcal{R}^{n-1} U^{n-1} \right\} + \mathcal{R}^n \hat{H}_2(t), \;\; t \in I_n \; (n = 1, \ldots, N). \tag{5.2.12}$$

Remark 5.2.1. (i) In view of (5.2.8), (5.2.11) and recalling (5.1.13) we have,

$$\hat{\Phi}(t)|_{I_1} = \hat{I} f(t)|_{I_1} + (\Pi_0^1 - I) f^{\frac{1}{2}},$$

where $\hat{I}f(t)|_{I_n}$ is the piecewise linear interpolant of f at the nodes t_{n-1} and t_n. Similarly, for $n \geq 2$, we have that

$$\begin{aligned}\hat{\Phi}(t)|_{I_n} &= \hat{I}f(t)|_{I_n} + \frac{1}{2}(\Pi_0^n - I)f^n + \frac{1}{4k}\left\{U^n - (P_1^n P_1^{n-1})U^{n-2}\right\} \\ &\quad + \frac{1}{2}(P_2^n(\mathcal{A}_h^{n-1}))U^{n-2} - \frac{1}{2}f^{n-1}.\end{aligned}$$

The critical observation is that in contrary to the scenario in [4, 15], the piecewise linear approximation of $f(t)$, i.e., $\hat{\Phi}(t)$ is not a continuous function on $[0, T]$.

(ii) In the Crank-Nicolson error analysis, the function $\tilde{H}_1(t)$ is chosen in such a way that it interpolates $H_1(t)$ at $t = t_{n-\frac{1}{2}}$ (see, (4.2.11)). But in the case of BDF-2 method, $\hat{H}_2(t)$ and $H_2(t)$ do not coincide at the the nodal values and this is because of the choice of $\hat{\Phi}(t)$ in (5.2.8). The reason for this choice $\hat{\Phi}(t)$ in (5.2.8) is to make $\hat{U}(t)$ a continuous function in time.

5.3 Abstract Error Analysis

In this section, we derive residual-based *a posteriori* error estimates for the BDF-2 approximation.

Following the idea of [15], we decompose the total error $e(t)$ as $e(t) := u(t) - U(t) = \hat{\rho}(t) + \hat{\varepsilon}(t),\ t \in I_n$, where $\hat{\rho}(t) := u(t) - \hat{U}(t)$ denotes the parabolic error, and $\hat{\varepsilon}(t) := \hat{U}(t) - U(t)$ represents the reconstruction error. Furthermore, the reconstruction error $\hat{\varepsilon}(t)$ may be split into $\hat{\varepsilon}(t) := \varepsilon(t) + \hat{\sigma}(t)$, where $\varepsilon(t)$ is the elliptic reconstruction error or the space discretization error defined by $\varepsilon(t) := \Theta(t) - U(t)$ and $\hat{\sigma}(t)$ is the time reconstruction error defined by $\hat{\sigma}(t) := \hat{U}(t) - \Theta(t)$. Now, with the above splitting, the error $e(t)$ may be expressed as

$$e(t) = \hat{\rho}(t) + \hat{\sigma}(t) + \varepsilon(t),\ \ t \in I_n. \tag{5.3.1}$$

The *a posteriori* error bound on the main error is obtained by treating each term appearing in (5.3.1) separately.

To begin with, we shall recall from Chapter 4, the elliptic reconstruction error estimate in the L^2-norm.

Lemma 5.3.1. *For any $v \in \mathbb{S}^n$ $(0 \leq n \leq N)$, the following estimate holds:*

$$\|(\mathcal{R}^n - I)v\| \leq \mathcal{C}_{I,5}\, h_n^2\, |\log h_n|^{\frac{1}{2}} \|(\mathcal{A}_h^n)v - (v)_{\text{el}}\| + \mathcal{C}_{I,6}\, h_n^{\frac{3}{2}}\, |\log h_n|^{\frac{1}{2}}\, \|j[\beta v]\|_{\Sigma_n}.$$

The constant appeared are positive constants and depend on the interpolation and regularity constants.

To bound $\hat{\rho}(t)$, the first step is to derive an appropriate error equation, which is stated in the following lemma.

Lemma 5.3.2. *For each $\varphi \in H_0^1(\Omega)$ and for $1 \le n \le N$, we have the following parabolic error equation*

$$\langle \hat{\rho}_t(t), \varphi \rangle + a(\rho(t), \varphi) = \langle \mathscr{R}_2(t), \varphi \rangle, \quad t \in I_n \tag{5.3.2}$$

with $\rho(t) := u(t) - \Theta(t)$ and

$$\begin{aligned} \mathscr{R}_2(t) \;:=\; & -\varepsilon_t(t) - (\mathcal{R}^n - I)\left\{\hat{H}_2(t) - \left(\hat{\Phi}(t_{n-\frac{1}{2}}) - \Psi(t_{n-\frac{1}{2}})\right)\right\} + \left(f(t) - \hat{H}_2(t) - \Psi(t)\right) \\ & + k^{-1}(I - \Pi_0^n)U^{n-1} + l_{n-1}(t)(P_2^n - I)(\mathcal{A}_h^{n-1})U^{n-1}. \end{aligned}$$

Proof. Taking the L^2-inner product with $\varphi(t)$ in (5.2.12), we obtain for all $\varphi \in H_0^1(\Omega)$

$$\left\langle \hat{U}_t(t), \varphi \right\rangle = k^{-1} \left\langle \mathcal{R}^n \Pi_0^n U^{n-1} - \mathcal{R}^{n-1} U^{n-1}, \varphi \right\rangle + \left\langle \mathcal{R}^n \hat{H}_2(t), \varphi \right\rangle.$$

Subtracting the above relation from (5.1.4) we obtain

$$\begin{aligned} \langle \hat{\rho}_t(t), \varphi \rangle + a(\rho(t), \varphi) \;=\; & \langle f(t), \varphi \rangle - a(\Theta(t), \varphi) \\ & - k^{-1} \left\langle \mathcal{R}^n \Pi_0^n U^{n-1} - \mathcal{R}^{n-1} U^{n-1}, \varphi \right\rangle - \left\langle \mathcal{R}^n \hat{H}_2(t), \varphi \right\rangle. \end{aligned}$$

In view of (5.2.5) and invoking the definition of elliptic reconstruction (5.2.1), we obtain

$$\begin{aligned} \langle \hat{\rho}_t(t), \varphi \rangle \;+\; & a(\rho(t), \varphi) = \left\langle f(t) - \hat{H}_2(t), \varphi \right\rangle \\ & - \left\langle (\mathcal{R}^n - I)\hat{H}_2(t), \varphi \right\rangle - l_{n-1}(t) \left\langle (\mathcal{A}_h^{n-1})U^{n-1}, \varphi \right\rangle \\ & - l_n(t) \left\langle (\mathcal{A}_h^n)U^n, \varphi \right\rangle - k^{-1} \left\langle \mathcal{R}^n \Pi_0^n U^{n-1} - \mathcal{R}^{n-1} U^{n-1}, \varphi \right\rangle. \end{aligned}$$

Using (5.2.4), (5.2.8), (5.2.11) and rearranging the terms it finally leads to

$$\begin{aligned} & \langle \hat{\rho}_t(t), \varphi \rangle + a(\rho(t), \varphi) \\ = \; & \left\langle f(t) - \hat{H}_2(t) - \Psi(t), \varphi \right\rangle - \left\langle (\mathcal{R}^n - I)(\hat{H}_2(t) - \hat{\Phi}(t_{n-\frac{1}{2}})), \varphi \right\rangle \\ & - \left\langle (\mathcal{R}^n - I)\left\{k^{-1}(U^n - \Pi_0^n U^{n-1}) + \Psi(t_{n-\frac{1}{2}})\right\}, \varphi \right\rangle \\ & - k^{-1} \left\langle \mathcal{R}^n \Pi_0^n U^{n-1} - \mathcal{R}^{n-1} U^{n-1}, \varphi \right\rangle + l_{n-1}(t) \left\langle (P_2^n - I)(\mathcal{A}_h^{n-1})U^{n-1}, \varphi \right\rangle \\ = \; & \left\langle f(t) - \hat{H}_2(t) - \Psi(t), \varphi \right\rangle - \left\langle (\mathcal{R}^n - I)\left\{\hat{H}_2(t) - \hat{\Phi}(t_{n-\frac{1}{2}}) + \Psi(t_{n-\frac{1}{2}})\right\}, \varphi \right\rangle \\ & - k^{-1} \left\langle (\mathcal{R}^n - I)U^n - (\mathcal{R}^{n-1} - I)U^{n-1}, \varphi \right\rangle \\ & + k^{-1} \left\langle (I - \Pi_0^n)U^{n-1}, \varphi \right\rangle + l_{n-1}(t) \left\langle (P_2^n - I)(\mathcal{A}_h^{n-1})U^{n-1}, \varphi \right\rangle \\ = \; & - \langle \varepsilon_t(t), \varphi \rangle - \left\langle (\mathcal{R}^n - I)\left\{\hat{H}_2(t) - \left(\hat{\Phi}(t_{n-\frac{1}{2}}) - \Psi(t_{n-\frac{1}{2}})\right)\right\}, \varphi \right\rangle \\ & + \left\langle f(t) - \hat{H}_2(t) - \Psi(t), \varphi \right\rangle + \left\langle k^{-1}(I - \Pi_0^n)U^{n-1} + l_{n-1}(t)(P_2^n - I)(\mathcal{A}_h^{n-1})U^{n-1}, \varphi \right\rangle, \end{aligned}$$

and this completes the proof. □

The following theorem provides the *a posteriori* error bound for the parabolic error $\hat{\rho}(t)$ in the $L^\infty(L^2)$-norm.

Theorem 5.3.1. *Let u be the exact solution of (5.1.1)–(5.1.3) and let U^n be its finite element approximation obtained by the BDF-2 approximation (5.1.13). Then, for $1 \leq m \leq N$, the following estimate holds for $\hat{\rho}(t)$.*

$$\left\{\max_{t\in[0,t_m]} \|\hat{\rho}(t)\|^2 + \gamma_0 \int_0^{t_m} \|\hat{\rho}(t)\|_1^2 dt\right\}^{\frac{1}{2}} \leq \left\{2\left(\|\hat{\rho}(0)\|^2 + k\sum_{n=1}^{m} \mathscr{T}^2_{\mathrm{e,BDF},n}\right)\right\}^{\frac{1}{2}} + (\Lambda_{\mathrm{BDF},m,1} + \Lambda_{\mathrm{BDF},m,2})^{\frac{1}{2}},$$

where

$$\Lambda_{\mathrm{BDF},m,1} := 4\sum_{n=1}^{m} k\,(\mathscr{M}_{\mathrm{BDF},n} + \mathscr{S}_{\mathrm{BDF},n} + \mathscr{D}_{\mathrm{BDF},n,1} + \mathscr{C}_{\mathrm{BDF},n}) \tag{5.3.3}$$

and

$$\Lambda_{\mathrm{BDF},m,2} := 4\sum_{n=1}^{m} k^{\frac{1}{2}} \mathscr{D}_{\mathrm{BDF},n,2}. \tag{5.3.4}$$

Here, $\mathscr{T}_{\mathrm{e,BDF},n}$ is the temporal error estimator and is defined by

$$\begin{aligned}\mathscr{T}_{\mathrm{e,BDF},n} &:= \frac{1}{\gamma_0}\sqrt{\frac{\alpha_0}{120}}\,k^2\,\{\mathcal{C}_{I,1}\,h_n\,\|(\mathcal{A}_h^n)\mathcal{W}_n - (\mathcal{W}_n)_{\mathrm{el}}\| \\ &\qquad + \mathcal{C}_{I,2}\,h_n^{\frac{1}{2}}\,\|j[\beta\mathcal{W}_n]\|_{\Sigma_n} + \alpha_0\,\|\mathcal{W}_n\|_1\Big\}\end{aligned} \tag{5.3.5}$$

with $\mathcal{W}_n$ is an a posteriori quantity given by

$$\mathcal{W}_n := -\Pi_0^n\hat{\Phi}_t(t) + \Psi_t(t) = -(\hat{H}_2)_t(t). \tag{5.3.6}$$

$\mathscr{M}_{\mathrm{BDF},n}$ is the space-mesh error estimator defined by

$$\begin{aligned}\mathscr{M}_{\mathrm{BDF},n} &:= \mathcal{C}_{I,5}\,\hat{h}_n^2\,|\log\hat{h}_n|^{\frac{1}{2}}\,\|k^{-1}\{(\mathcal{A}_h^n)U^n - (\mathcal{A}_h^{n-1})U^{n-1} - (U^n)_{\mathrm{el}} + (U^{n-1})_{\mathrm{el}}\}\| \\ &\quad + \mathcal{C}_{I,6}\,\hat{h}_n^{\frac{3}{2}}\,|\log\hat{h}_n|^{\frac{1}{2}}\|k^{-1}\{j[\beta U^n] - j[\beta U^{n-1}]\}\|_{\hat{\Sigma}_n} \\ &\quad + \mathcal{C}_{I,8}\,\hat{h}_n^{\frac{3}{2}}\,|\log\hat{h}_n|^{\frac{1}{2}}\,\|k^{-1}\{j[\beta U^n] - j[\beta U^{n-1}]\}\|_{\check{\Sigma}_n\setminus\hat{\Sigma}_n}.\end{aligned} \tag{5.3.7}$$

$$\begin{aligned}\mathscr{S}_{\mathrm{BDF},n} &:= \frac{k}{4}\Big\{\mathcal{C}_{I,5}\,h_n^2\,|\log h_n|^{\frac{1}{2}}\,\|(\mathcal{A}_h^n)\mathcal{W}_n - (\mathcal{W}_n)_{\mathrm{el}}\| \\ &\qquad + \mathcal{C}_{I,6}\,h_n^{\frac{3}{2}}\,|\log h_n|^{\frac{1}{2}}\,\|j[\beta\mathcal{W}_n]\|_{\Sigma_n}\Big\}\end{aligned} \tag{5.3.8}$$

is the space error estimator with $\mathcal{W}_n$ is defined in (5.3.6).

Finally,

$$\mathscr{C}_{\mathrm{BDF},n} := k^{-1}\|(I-\Pi_0^n)U^{n-1}\| + \frac{1}{2}\|(P_2^n - I)(\mathcal{A}_h^{n-1})U^{n-1}\| \tag{5.3.9}$$

is the coarsening error estimator and $\mathscr{D}_{\mathrm{BDF},n,i}(i=1,2)$ *are the data approximation error estimators defined by*

$$\begin{cases} \mathscr{D}_{\mathrm{BDF},n,1} := \frac{1}{k}\int_{t_{n-1}}^{t_n} \|f(t) - \hat{\Phi}(t)\|dt \\ \mathscr{D}_{\mathrm{BDF},n,2} := \frac{1}{\sqrt{\gamma_0}}\,\mathcal{C}_{I,1}\,h_n \left\{ \|(\Pi_0^n - I)\frac{(f^n - f^{n-1})}{2}\| \right\}. \end{cases} \tag{5.3.10}$$

The constants $\mathcal{C}_{I,i}(i=1,\ldots,8)$ *appeared above are positive and independent of the discretization parameters, but depend upon the interpolation and the regularity constants.*

The proof of Theorem 5.3.1 needs some preparation. We note that the bound for $\hat{\rho}(t)$ essentially hinges on several auxiliary results which we shall discuss in detail below. We start by providing *a posteriori* error bound on the time discretization error.

Lemma 5.3.3 (Temporal error estimate)**.** *Let* $\mathfrak{I}_{n,1}$ *refer to the time discretization error term and be defined by*

$$\mathfrak{I}_{n,1} := \alpha_0 \int_{t_{n-1}}^{t_n} \|\hat{\sigma}(t)\|_1^2 dt.$$

Then the following a posteriori error bound holds:

$$\mathfrak{I}_{n,1} \leq k\,\mathscr{T}_{\mathrm{e,BDF},n}^2,$$

where $\mathscr{T}_{\mathrm{e,BDF},n}$ *is given by (5.3.5).*

Proof. In order to estimate $\hat{\sigma}(t)$, we first estimate $\hat{\sigma}_t(t) = \hat{U}_t(t) - \Theta_t(t)$. In view of (5.2.5) and (5.2.12), we have

$$\begin{aligned} \hat{\sigma}_t(t) &= \frac{\mathcal{R}^n\Pi_0^n U^{n-1} - \mathcal{R}^{n-1}U^{n-1}}{k} + \mathcal{R}^n\hat{H}_2(t) - \frac{\mathcal{R}^n U^n - \mathcal{R}^{n-1}U^{n-1}}{k} \\ &= \mathcal{R}^n\left\{\frac{\Pi_0^n U^{n-1} - U^n}{k} + \hat{H}_2(t)\right\} \\ &= \mathcal{R}^n\left\{\hat{H}_2(t) - \left(\hat{\Phi}(t_{n-\frac{1}{2}}) - \Psi(t_{n-\frac{1}{2}})\right)\right\}. \end{aligned}$$

Integrating from t_{n-1} to t and using the fact that $\hat{U}(t)$ and $\Theta(t)$ coincide at the nodal points, we obtain

$$\hat{U}(t) - \Theta(t) = \int_{t_{n-1}}^{t} \mathcal{R}^n\left\{\hat{H}_2(t) - \left(\hat{\Phi}(t_{n-\frac{1}{2}}) - \Psi(t_{n-\frac{1}{2}})\right)\right\} dt. \tag{5.3.11}$$

Using (5.2.4) and (5.2.8) – (5.2.9), the term within the bracket on the right hand side can be expressed as

$$\begin{aligned}\hat{H}_2(t) - \left\{\hat{\Phi}(t_{n-\frac{1}{2}}) - \Psi(t_{n-\frac{1}{2}})\right\} &= \left(\Pi_0^n\hat{\Phi}(t) - \Psi(t)\right) - \frac{U^n - \Pi_0^n U^{n-1}}{k} \\ &= \Pi_0^n\left\{(t-t_{n-\frac{1}{2}})\bar{\partial}f^n + \frac{U^n - \Pi_0^n U^{n-1}}{k} + \Psi(t_{n-\frac{1}{2}})\right\} \\ &\quad -\Psi(t) - \frac{U^n - \Pi_0^n U^{n-1}}{k} \\ &= (t-t_{n-\frac{1}{2}})\Pi_0^n\bar{\partial}f^n - \left\{\Psi(t) - \Psi(t_{n-\frac{1}{2}})\right\}, \qquad (5.3.12)\end{aligned}$$

where in the above we have used the fact that $(\Pi_0^n)^2 = \Pi_0^n$. Since $l_{n-1}(t)+l_n(t) = 1, t \in I_n$, a simple calculation implies

$$\Psi(t) - \Psi(t_{n-\frac{1}{2}}) = (t - t_{n-\frac{1}{2}})\,\Psi_t(t),$$

which combine with (5.3.12) leads to

$$\begin{aligned}\hat{H}_2(t) - (\hat{\Phi}(t_{n-\frac{1}{2}}) - \Psi(t_{n-\frac{1}{2}})) &= -(t-t_{n-\frac{1}{2}})\left\{-\Pi_0^n\bar{\partial}f^n + \Psi_t(t)\right\} \\ &= -(t-t_{n-\frac{1}{2}})\left\{-\Pi_0^n\hat{\Phi}_t(t) + \Psi_t(t)\right\} \\ &= -(t-t_{n-\frac{1}{2}})\,\mathcal{W}_n, \qquad (5.3.13)\end{aligned}$$

where $\mathcal{W}_n$ is given by (5.3.6). Now, substituting (5.3.13) in (5.3.11) and evaluating the integral by the midpoint rule we have that

$$\begin{aligned}\hat{U}(t) - \Theta(t) &= -\int_{t_{n-1}}^{t} \mathcal{R}^n\left\{(t-t_{n-\frac{1}{2}})\mathcal{W}_n\right\} \\ &= \frac{1}{2}(t-t_{n-1})(t_n - t)\mathcal{R}^n\mathcal{W}_n. \qquad (5.3.14)\end{aligned}$$

Using coercivity and continuity properties of the bilinear form $a(\cdot,\cdot)$, it follows that

$$\begin{aligned}\gamma_0\|\hat{\sigma}(t)\|_1^2 &\le a(\hat{\sigma}(t),\hat{\sigma}(t)) \\ &= \frac{1}{2}(t-t_{n-1})(t_n-t)\; a(\mathcal{R}^n\mathcal{W}_n,\hat{\sigma}(t)) \\ &= \frac{1}{2}(t-t_{n-1})(t_n-t)\left\{a((\mathcal{R}^n - I)\mathcal{W}_n,\hat{\sigma}(t)) + a(\mathcal{W}_n,\hat{\sigma}(t))\right\} \\ &\le \frac{1}{2}(t-t_{n-1})(t_n-t)\;\left\{a((\mathcal{R}^n - I)\mathcal{W}_n,\hat{\sigma}(t)) + \alpha_0\|\mathcal{W}_n\|_1\|\hat{\sigma}(t)\|_1\right\}. \qquad (5.3.15)\end{aligned}$$

We now apply the Galerkin orthogonality property of $\mathcal{R}^n$ and Definition 5.2.1 to have

$$\begin{aligned}a\left((\mathcal{R}^n - I)\mathcal{W}_n,\hat{\sigma}(t)\right) &= a\left((\mathcal{R}^n - I)\mathcal{W}_n,\hat{\sigma}(t) - \mathscr{J}_n\hat{\sigma}(t)\right) \\ &= \left|\langle\mathcal{A}_h^n\mathcal{W}_n,\hat{\sigma}(t) - \mathscr{J}_n\hat{\sigma}(t)\rangle - \langle(\mathcal{W}_n)_{\rm el},\hat{\sigma}(t) - \mathscr{J}_n\hat{\sigma}(t)\rangle\right. \\ &\quad \left. - \langle j[\beta\mathcal{W}_n],\hat{\sigma}(t) - \mathscr{J}_n\hat{\sigma}(t)\rangle_{\Sigma_n}\right|.\end{aligned}$$

An application of the Cauchy-Schwarz inequality and Proposition 3.2.1 yields

$$\begin{aligned} & a\left((\mathcal{R}^n - I)\mathcal{W}_n, \hat{\sigma}(t)\right) \\ & \quad \leq \|\mathcal{A}_h^n \mathcal{W}_n - (\mathcal{W}_n)_{\text{el}}\| \, \|\hat{\sigma}(t) - \mathscr{J}_n \hat{\sigma}(t)\| + \|j[\beta \mathcal{W}_n]\|_{\Sigma_n} \, \|\hat{\sigma}(t) - \mathscr{J}_n \hat{\sigma}(t)\|_{\Sigma_n} \\ & \quad \leq \left\{ \mathcal{C}_{I,1} \, h_n \, \|\mathcal{A}_h^n \mathcal{W}_n - (\mathcal{W}_n)_{\text{el}}\| + \mathcal{C}_{I,2} \, h_n^{\frac{1}{2}} \, \|j[\beta \mathcal{W}_n]\|_{\Sigma_n} \right\} \|\hat{\sigma}(t)\|_1. \end{aligned}$$

Now, in view of (5.3.15), we obtain

$$\gamma_0 \|\hat{\sigma}(t)\|_1^2 \leq \frac{1}{2}(t - t_{n-1})(t_n - t) \, \mathcal{B}_n \, \|\hat{\sigma}(t)\|_1,$$

where $\mathcal{B}_n := \mathcal{C}_{I,1} \, h_n \, \|\mathcal{A}_h^n \mathcal{W}_n - (\mathcal{W}_n)_{\text{el}}\| + \mathcal{C}_{I,2} \, h_n^{\frac{1}{2}} \, \|j[\beta \mathcal{W}_n]\|_{\Sigma_n} + \alpha_0 \|\mathcal{W}_n\|_1$. And hence,

$$\begin{aligned} \mathfrak{I}_{n,1} &\leq \frac{\alpha_0}{4\gamma_0^2} \, \mathcal{B}_n^2 \int_{t_{n-1}}^{t_n} (t - t_{n-1})^2 (t_n - t)^2 dt \\ &\leq k \mathscr{T}_{\text{e,BDF},n}^2, \end{aligned}$$

where $\mathscr{T}_{\text{e,BDF},n}^2 = \frac{1}{120} \, \frac{\alpha_0}{\gamma_0^2} \, k^4 \, \mathcal{B}_n^2$, and we thus complete the proof. □

The next lemma gives the *a posteriori* bounds for the space-mesh error.

Lemma 5.3.4 (Space-mesh error estimate)**.** *Let $\mathfrak{I}_{n,2}$ represent the space-mesh error term and be given by*

$$\mathfrak{I}_{n,2} := \int_{t_{n-1}}^{t_n} |\, \langle \varepsilon_t(t), \hat{\rho}(t) \rangle \,| dt.$$

Then the following is true:

$$\mathfrak{I}_{n,2} \leq k \, \mathscr{M}_{\text{BDF},n} \max_{t \in \bar{I}_n} \|\hat{\rho}(t)\|$$

with $\mathscr{M}_{\text{BDF},n}$ is defined in (5.3.7).

Proof. For $1 \leq n \leq m$, we first observe that

$$\begin{aligned} \mathfrak{I}_{n,2} &= \int_{t_{n-1}}^{t_n} |\, \langle \hat{\varepsilon}_t(t), \hat{\rho}(t) \rangle \,| dt \\ &\leq k^{-1} \max_{t \in \bar{I}_n} \|\hat{\rho}(t)\| \int_{t_{n-1}}^{t_n} \|(\mathcal{R}^n - I)U^n - (\mathcal{R}^{n-1} - I)U^{n-1}\| dt \\ &= \max_{t \in \bar{I}_n} \|\hat{\rho}(t)\| \, \|(\mathcal{R}^n - I)U^n - (\mathcal{R}^{n-1} - I)U^{n-1}\|. \end{aligned} \tag{5.3.16}$$

In order to bound the term $\|(\mathcal{R}^n - I)U^n - (\mathcal{R}^{n-1} - I)U^{n-1}\|$, we use the standard duality trick. For all $v \in H_0^1(\Omega)$, let $w : [0, T] \longrightarrow X$ be the solution of the following elliptic

problem:

$$
\begin{aligned}
(5.3.17)\quad a(v, w(t)) &= \langle (\mathcal{R}^n - I)U^n - (\mathcal{R}^{n-1} - I)U^{n-1}, v\rangle, \quad \text{a.e. } t \in [0, T], \\
w &= 0 \ \text{ on } \ \partial\Omega, \\
[w] &= 0, \quad \left[\beta \frac{\partial w}{\partial \mathbf{n}}\right] = 0 \ \text{ across } \ \Gamma
\end{aligned}
$$

with

$$
(5.3.18)\qquad \|w\|_X \leq \mathcal{C}_R \, \|(\mathcal{R}^n - I)U^n - (\mathcal{R}^{n-1} - I)U^{n-1}\|.
$$

Note that $(\mathcal{R}^n - I)U^n - (\mathcal{R}^{n-1} - I)U^{n-1}$ is orthogonal to $\mathbb{S}^n \cap \mathbb{S}^{n-1}$ with respect to $a(\cdot, \cdot)$. Set $v = (\mathcal{R}^n - I)U^n - (\mathcal{R}^{n-1} - I)U^{n-1}$ in (5.3.17). Using the Galerkin orthogonality property in the subspace $\mathbb{S}^n \cap \mathbb{S}^{n-1}$ and (5.2.1) we have

$$
\begin{aligned}
&\|(\mathcal{R}^n - I)U^n - (\mathcal{R}^{n-1} - I)U^{n-1}\|^2 \\
&\quad = a\left((\mathcal{R}^n - I)U^n - (\mathcal{R}^{n-1} - I)U^{n-1}, w(t)\right) \\
&\quad = a\left((\mathcal{R}^n - I)U^n - (\mathcal{R}^{n-1} - I)U^{n-1}, \, w(t) - \hat{\mathscr{I}}_n w(t)\right) \\
&\quad = \left\langle \mathcal{A}_h^n U^n - (U^n)_{\text{el}}, w(t) - \hat{\mathscr{I}}_n w(t)\right\rangle \\
&\qquad - \left\langle \mathcal{A}_h^{n-1} U^{n-1} - (U^{n-1})_{\text{el}}, \, w(t) - \hat{\mathscr{I}}_n w(t)\right\rangle \\
&\qquad - \left\langle j[\beta U^n] - j[\beta U^{n-1}], \, w(t) - \hat{\mathscr{I}}_n w(t)\right\rangle_{\hat{\Sigma}_n}.
\end{aligned}
$$

We now use the Cauchy-Schwarz inequality, Proposition 3.2.1 (in the subspace $\mathbb{S}^n \cap \mathbb{S}^{n-1}$), Proposition 3.2.2 and (5.3.18) to obtain

$$
\begin{aligned}
&\|(\mathcal{R}^n - I)U^n - (\mathcal{R}^{n-1} - I)U^{n-1}\|^2 \\
&\quad \leq \Big\{ \mathcal{C}_{I,3} \, \hat{h}_n^2 \, |\log \hat{h}_n|^{\frac{1}{2}} \, \|(\mathcal{A}_h^n)U^n - (\mathcal{A}_h^{n-1})U^{n-1} - (U^n)_{\text{el}} + (U^{n-1})_{\text{el}}\| \\
&\qquad + \mathcal{C}_{I,4} \, \hat{h}_n^{\frac{3}{2}} \, |\log \hat{h}_n|^{\frac{1}{2}} \|j[\beta U^n] - j[\beta U^{n-1}]\|_{\hat{\Sigma}_n} \\
&\qquad + \mathcal{C}_{I,7} \, \hat{h}_n^{\frac{3}{2}} \, |\log \hat{h}_n|^{\frac{1}{2}} \, \|j[\beta U^n] - j[\beta U^{n-1}]\|_{\hat{\Sigma}_n \setminus \check{\Sigma}_n} \Big\} \, \|w\|_X \\
&\quad \leq k \, \mathscr{M}_{\text{BDF},n} \, \|(\mathcal{R}^n - I)U^n - (\mathcal{R}^{n-1} - I)U^{n-1}\|,
\end{aligned}
$$

which together with (5.3.16) yields the desired estimate. □

The next lemma captures contributions of the error due to the spatial discretizations.

Lemma 5.3.5 (Space error estimate)**.** *Let the space error term $\mathfrak{I}_{n,3}$ be defined by*

$$
\mathfrak{I}_{n,3} := \int_{t_{n-1}}^{t_n} \left| \left\langle (\mathcal{R}^n - I)\left(\hat{H}_2(t) - \left(\hat{\Phi}(t_{n-\frac{1}{2}}) - \Psi(t_{n-\frac{1}{2}})\right)\right), \hat{\rho}(t)\right\rangle \right| dt.
$$

Then the following is true:

$$\mathfrak{I}_{n,3} \leq \; k\mathscr{S}_{\mathrm{BDF},n} \; \max_{t\in\bar{I}_n} \|\hat{\rho}(t)\|,$$

where the estimator $\mathscr{S}_{\mathrm{BDF},n}$ is defined in (5.3.8).

Proof. From (5.3.13), we observe that

$$\hat{H}_2(t) - (\hat{\Phi}(t_{n-\frac{1}{2}}) - \Psi(t_{n-\frac{1}{2}})) = -(t - t_{n-\frac{1}{2}})\,\mathcal{W}_n,$$

where $\mathcal{W}_n$ is defined in (5.3.6). Then, using the Cauchy- Schwarz inequality and Lemma 5.3.1 we obtain

$$\begin{aligned}
\mathfrak{I}_{n,3} &\leq \int_{t_{n-1}}^{t_n} |t - t_{n-\frac{1}{2}}| \, \|(\mathcal{R}^n - I)\mathcal{W}_n\| \, \|\hat{\rho}(t)\| dt \\
&\leq \frac{k^2}{4} \, \|(\mathcal{R}^n - I)\mathcal{W}_n\| \; \max_{t\in\bar{I}_n} \|\hat{\rho}(t)\| \\
&\leq k \; \mathscr{S}_{\mathrm{BDF},n} \; \max_{t\in\bar{I}_n} \|\hat{\rho}(t)\|.
\end{aligned}$$

□

The next lemma shows the contribution on the *a posteriori* bounds due to the data approximation error.

Lemma 5.3.6 (Data approximation error estimate)**.** *Let $\mathfrak{I}_{n,4}$ denote the data approximation error term and be defined as*

$$\mathfrak{I}_{n,4} := \int_{t_{n-1}}^{t_n} \left| \left\langle f(t) - \hat{H}_2(t) - \Psi(t), \hat{\rho}(t) \right\rangle \right| dt.$$

Then we have

$$\mathfrak{I}_{n,4} \leq k \, \mathscr{D}_{\mathrm{BDF},n,1} \max_{t\in\bar{I}_n} \|\hat{\rho}(t)\| + k^{\frac{1}{2}} \, \mathscr{D}_{\mathrm{BDF},n,2} \left(\gamma_0 \int_{t_{n-1}}^{t_n} \|\hat{\rho}(t)\|_1^2 dt \right)^{\frac{1}{2}},$$

where $\mathscr{D}_{\mathrm{BDF},n,1}$ and $\mathscr{D}_{\mathrm{BDF},n,2}$ are defined in (5.3.10).

Proof. In view of (5.2.9), we have

$$\begin{aligned}
f(t) - \hat{H}_2(t) - \Psi(t) &= f(t) - \Pi_0^n \hat{\Phi}(t) \\
&= \left(f(t) - \hat{\Phi}(t) \right) - (\Pi_0^n - I)\hat{\Phi}(t).
\end{aligned}$$

Thus,

$$\begin{aligned}
\mathfrak{I}_{n,4} &\leq \int_{t_{n-1}}^{t_n} \left| \left\langle f - \hat{\Phi}(t), \hat{\rho}(t) \right\rangle \right| dt + \int_{t_{n-1}}^{t_n} \left| \left\langle (\Pi_0^n - I)\hat{\Phi}(t), \hat{\rho}(t) \right\rangle \right| dt \\
&:= T_{1,n} + T_{2,n}. \qquad (5.3.19)
\end{aligned}$$

Exploiting the orthogonality property of Π_0^n and Proposition 3.2.1, we note that

$$\begin{aligned}\left\langle (\Pi_0^n - I)\hat{\Phi}(t), \hat{\rho}(t) \right\rangle &= \left\langle (\Pi_0^n - I)\hat{\Phi}(t), \hat{\rho}(t) - \mathscr{J}_n\hat{\rho}(t) \right\rangle \\ &\leq \|(\Pi_0^n - I)\hat{\Phi}(t)\| \, \|\hat{\rho}(t) - \mathscr{J}_n\hat{\rho}(t)\| \\ &\leq \mathcal{C}_{I,1}\, h_n \, \|(\Pi_0^n - I)\hat{\Phi}(t)\| \, \|\hat{\rho}(t)\|_1.\end{aligned}$$

As $\mathbb{S}^n \subset \mathrm{Ker}(\Pi_0^n - I)$, it follows that $(\Pi_0^n - I)(U^n - \Pi_0^n U^{n-1}) = 0$ and $(\Pi_0^n - I)\Psi(t_{n-\frac{1}{2}}) = 0$. Hence, we deduce that

$$\|(\Pi_0^n - I)\hat{\Phi}(t)\| = k^{-1} \, |t - t_{n-\frac{1}{2}}| \, \|(\Pi_0^n - I)(f^n - f^{n-1})\|.$$

Thus,

$$\begin{aligned}T_{2,n} &\leq \mathcal{C}_{I,1}\, h_n \, k^{-1} \|(\Pi_0^n - I)(f^n - f^{n-1})\| \, \max_{t\in\bar{I}_n} |t - t_{n-\frac{1}{2}}| \int_{t_{n-1}}^{t_n} \|\hat{\rho}(t)\|_1 dt \\ &\leq k^{\frac{1}{2}} \, \mathscr{D}_{\mathrm{BDF},n,2} \left(\gamma_0 \int_{t_{n-1}}^{t_n} \|\hat{\rho}(t)\|_1^2 dt \right)^{\frac{1}{2}}.\end{aligned}$$

Finally, to estimate the first term in (5.3.19), we use the Cauchy-Schwarz inequality to have

$$\begin{aligned}T_{1,n} &\leq \max_{t\in\bar{I}_n} \|\hat{\rho}(t)\| \int_{t_{n-1}}^{t_n} \|f(t) - \hat{\Phi}(t)\| \, dt \\ &= k \, \mathscr{D}_{\mathrm{BDF},n,1} \max_{t\in\bar{I}_n} \|\hat{\rho}(t)\|,\end{aligned}$$

and this completes the rest of the proof. □

The Coarsening error is estimated in the following lemma.

Lemma 5.3.7 (Coarsening error estimate)**.** *Let $\mathfrak{I}_{n,5}$ represent the coarsening error term and be defined by*

$$\mathfrak{I}_{n,5} := \int_{t_{n-1}}^{t_n} \left| \left\langle k^{-1}(I - \Pi_0^n)U^{n-1} + l_{n-1}(t)(P_2^n - I)(\mathcal{A}_h^{n-1})U^{n-1}, \hat{\rho}(t) \right\rangle \right| dt.$$

Then

$$\mathfrak{I}_{n,5} \leq k \, \mathscr{C}_{\mathrm{BDF},n} \max_{t\in\bar{I}_n} \|\hat{\rho}(t)\|,$$

where $\mathscr{C}_{\mathrm{BDF},n}$ is defined in (5.3.9).

Proof. Applying the Cauchy-Schwarz inequality, we have that

$$\begin{aligned}\mathfrak{I}_{n,5} &\leq \int_{t_{n-1}}^{t_n} k^{-1}\|(I-\Pi_0^n)U^{n-1}\|\,\|\hat{\rho}(t)\|dt \\ &\quad + \int_{t_{n-1}}^{t_n} \frac{(t_n-t)}{k}\,\|(P_2^n-I)(\mathcal{A}_h^{n-1})U^{n-1}\|\,\|\hat{\rho}(t)\|dt \\ &\leq \left\{\|(I-\Pi_0^n)U^{n-1}\| + \frac{k}{2}\|(P_2^n-I)(\mathcal{A}_h^{n-1})U^{n-1}\|\right\} \max_{t\in\bar{I}_n}\|\hat{\rho}(t)\| \\ &= k\,\mathscr{C}_{\mathrm{BDF},n}\,\max_{t\in\bar{I}_n}\|\hat{\rho}(t)\|,\end{aligned}$$

which completes the proof. □

Now, with the lemmas derived above we prove *a posteriori* bound for the parabolic error $\hat{\rho}(t)$.

Proof of Theorem 5.3.1. Set $\varphi = \hat{\rho}(t)$ in (5.3.2) to obtain

$$\frac{1}{2}\frac{d}{dt}\|\hat{\rho}(t)\|^2 + a(\rho(t),\hat{\rho}(t)) = \langle \mathscr{R}_2(t),\hat{\rho}(t)\rangle\,.$$

Use the fact

$$2a(v,w) = a(v,v) + a(w,w) - a(v-w,v-w) \quad \forall v,w\in H_0^1(\Omega),$$

together with the continuity and the coercivity of the bilinear form $a(\cdot,\cdot)$, we obtain

$$\frac{1}{2}\frac{d}{dt}\|\hat{\rho}(t)\|^2 + \frac{\gamma_0}{2}\left(\|\rho(t)\|_1^2 + \|\hat{\rho}(t)\|_1^2\right) \leq \frac{\alpha_0}{2}\|\hat{\sigma}(t)\|_1^2 + |\langle \mathscr{R}_2(t),\hat{\rho}(t)\rangle|\,. \tag{5.3.20}$$

Integrate the above from t_{n-1} to t_n to have

$$\begin{aligned}&\frac{1}{2}\|\hat{\rho}(t_n)\|^2 - \frac{1}{2}\|\hat{\rho}(t_{n-1})\|^2 + \frac{\gamma_0}{2}\int_{t_{n-1}}^{t_n}\left(\|\rho(t)\|_1^2 + \|\hat{\rho}(t)\|_1^2\right)dt \\ &\qquad \leq \frac{\alpha_0}{2}\int_{t_{n-1}}^{t_n}\|\hat{\sigma}(t)\|_1^2 dt + \int_{t_{n-1}}^{t_n}|\langle \mathscr{R}_2(t),\hat{\rho}(t)\rangle|\,dt.\end{aligned}$$

Summing up over $n = 1 : m$ we obtain

$$\begin{aligned}&\|\hat{\rho}(t_m)\|^2 + \gamma_0\int_0^{t_m}\left(\|\rho(t)\|_1^2 + \|\hat{\rho}(t)\|_1^2\right)dt \\ &\qquad \leq \|\hat{\rho}(0)\|^2 + \sum_{n=1}^{m}\left\{\alpha_0\int_{t_{n-1}}^{t_n}\|\hat{\sigma}(t)\|_1^2 dt + 2\int_{t_{n-1}}^{t_n}|\langle \mathscr{R}_2(t),\hat{\rho}(t)\rangle|\,dt\right\} \\ &\qquad = \|\hat{\rho}(0)\|^2 + \sum_{n=1}^{m}\left\{\mathfrak{I}_{n,1} + 2\sum_{i=2}^{5}\mathfrak{I}_{n,i}\right\},\end{aligned} \tag{5.3.21}$$

where $\mathfrak{I}_{n,i}$ $(i = 1,...,5)$ are defined in Lemmas 5.3.3 – 5.3.7, respectively.

Since $\hat{\rho}(t)$ is continuous in $[0, t_m]$, there exists $t_{0,m} \in [0, t_m]$ such that

$$\|\hat{\rho}_{0,m}\| := \|\hat{\rho}(t_{0,m})\| = \max_{t\in[0,t_m]} \|\hat{\rho}(t)\|.$$

Again integrating (5.3.20) between the limits 0 to $t_{0,m}$ and observing that the integrands are non-negative, it follows that

$$\begin{aligned}
&\|\hat{\rho}(t_{0,m})\|^2 + \gamma_0 \int_0^{t_{0,m}} \left(\|\rho(t)\|_1^2 + \|\hat{\rho}(t)\|_1^2\right) dt \\
&\qquad \le \|\hat{\rho}(0)\|^2 + \alpha_0 \int_0^{t_{0,m}} \|\hat{\sigma}(t)\|_1^2 dt + 2\int_0^{t_{0,m}} |\langle \mathscr{R}_2(t), \hat{\rho}(t)\rangle|\, dt \\
&\qquad \le \|\hat{\rho}(0)\|^2 + \sum_{n=1}^{m} \left\{ \alpha_0 \int_{t_{n-1}}^{t_n} \|\hat{\sigma}(t)\|_1^2 dt + 2\int_{t_{n-1}}^{t_n} |\langle \mathscr{R}_2(t), \hat{\rho}(t)\rangle|\, dt \right\} \\
&\qquad = \|\hat{\rho}(0)\|^2 + \sum_{n=1}^{m} \left\{ \mathfrak{I}_{n,1} + 2\sum_{i=2}^{5} \mathfrak{I}_{n,i} \right\}. \qquad (5.3.22)
\end{aligned}$$

Thus, combining (5.3.21) and (5.3.22) it finally leads to

$$\|\hat{\rho}(t_{0,m})\|^2 + \gamma_0 \int_0^{t_m} \|\hat{\rho}(t)\|_1^2 dt \le 2\|\hat{\rho}(0)\|^2 + 2\sum_{n=1}^{m} \left\{ \mathfrak{I}_{n,1} + 2\sum_{i=2}^{5} \mathfrak{I}_{n,i} \right\}.$$

Application of Lemmas 5.3.3 – 5.3.7 now yields

$$\begin{aligned}
\|\hat{\rho}_{0,m}\|^2 \;+\; \gamma_0 \int_0^{t_m} \|\hat{\rho}(t)\|_1^2 dt \;\le\; & 2\left(\|\hat{\rho}(0)\|^2 + k\sum_{n=1}^{m} \mathscr{T}_{\mathrm{e,BDF},n}^2 \right) \\
&+ 4k \max_{t\in[0,t_m]} \|\hat{\rho}(t)\| \sum_{n=1}^{m} \left(\mathscr{M}_{\mathrm{BDF},n} + \mathscr{S}_{\mathrm{BDF},n} + \mathscr{D}_{\mathrm{BDF},n,1} + \mathscr{C}_{\mathrm{BDF},n} \right) \\
&+ 4k^{\frac{1}{2}} \sum_{n=1}^{m} \mathscr{D}_{\mathrm{BDF},n,2} \left(\gamma_0 \int_{t_{n-1}}^{t_n} \|\hat{\rho}(t)\|_1^2 dt \right)^{\frac{1}{2}}.
\end{aligned}$$

Finally, for $1 \le n \le m$, we take

$$a_0 := \|\hat{\rho}_{0,m}\|, \quad a_n := \left(\gamma_0 \int_{t_{n-1}}^{t_n} \|\hat{\rho}(t)\|_1^2 \, dt \right)^{\frac{1}{2}},$$

$$c := \left\{ 2\left(\|\hat{\rho}(0)\|^2 + k\sum_{n=1}^{m} \mathscr{T}_{\mathrm{e,BDF},n}^2 \right) \right\}^{\frac{1}{2}},$$

$$b_0 := 4\sum_{n=1}^{m} k \left(\mathscr{M}_{\mathrm{BDF},n} + \mathscr{S}_{\mathrm{BDF},n} + \mathscr{D}_{\mathrm{BDF},n,1} + \mathscr{C}_{\mathrm{BDF},n} \right),$$

$$b_n := 4k^{\frac{1}{2}} \, \mathscr{D}_{\mathrm{BDF},n,2}$$

and apply Lemma 1.2.3 to complete the proof of the Theorem 5.3.1. □

We shall close this chapter with the fully discrete BDF-2 *a posteriori* error estimate in the $L^\infty(L^2)$ norm for the parabolic interface problem (5.1.1) – (5.1.3).

Theorem 5.3.2. *Let u be the exact solution of (5.1.1)–(5.1.3) and let U^n be its finite element approximation obtained by the BDF-2 approximation (5.1.13). Then, for each $1 \le m \le N$, the following a posteriori error estimate holds:*

$$\begin{aligned}\max_{t\in[0,t_m]} \|u(t)-U(t)\| \;\le\; & \sqrt{2}\,\|\mathcal{R}^0U^0-u(0)\| + \sqrt{2}\left(k\sum_{n=1}^{m}\mathscr{T}^2_{\mathrm{e,BDF},n}\right)^{\frac12} \\ & + \left(\Lambda^2_{\mathrm{BDF},m,1}+\Lambda^2_{\mathrm{BDF},m,2}\right)^{\frac12} \\ & + 2\max_{n\in[0:m]}\mathscr{O}_{\mathrm{BDF},n} + \max_{n\in[0:m]}\mathscr{T}_{\mathrm{re,BDF},n},\end{aligned}$$

where $\mathscr{O}_{\mathrm{BDF},n}$ is the elliptic reconstruction error estimator defined by

$$\mathscr{O}_{\mathrm{BDF},n} := \mathcal{C}_{I,5}\,h_n^2\,|\log h_n|^{\frac12}\,\|(\mathcal{A}_h^n)U^n-(U^n)_{\mathrm{el}}\| + \mathcal{C}_{I,6}\,h_n^{\frac32}\,|\log h_n|^{\frac12}\,\|j[\beta U^n]\|_{\Sigma_n}, \tag{5.3.23}$$

and

$$\begin{aligned}\mathscr{T}_{\mathrm{re,BDF},n} \;:=\; & \frac{k^2}{8}\Big\{\mathcal{C}_{I,5}\,h_n^2\,|\log h_n|^{\frac12}\,\|(\mathcal{A}_h^n)\mathcal{W}_n-(\mathcal{W}_n)_{\mathrm{el}}\| \\ & + \mathcal{C}_{I,6}\,h_n^{\frac32}\,|\log h_n|^{\frac12}\,\|j[\beta\mathcal{W}_n]\|_{\Sigma_n} + \|\mathcal{W}_n\|\Big\}\end{aligned} \tag{5.3.24}$$

is the temporal reconstruction error with $\mathcal{W}_n$ given by (5.3.6). Moreover, the estimators $\mathscr{T}_{\mathrm{e,BDF},n}$, $\Lambda_{\mathrm{BDF},m,1}$, $\Lambda_{\mathrm{BDF},m,2}$, $\mathscr{O}_{\mathrm{BDF},n}$ and $\mathscr{T}_{\mathrm{re,BDF},n}$ are defined in Theorem 5.3.1.

Proof. An application of the triangle inequality in (5.3.1) yields

$$\begin{aligned}\|e(t)\| &\le \|\hat\rho(t)\| + \|\hat\sigma(t)\| + \|\varepsilon(t)\|,\ t\in I_n \\ &\le \max_{t\in[0,t_m]}\|\hat\rho(t)\| + \max_{t\in[0,t_m]}\|\hat\sigma(t)\| + \max_{t\in[0,t_m]}\|\varepsilon(t)\|.\end{aligned}$$

For $t \in I_n$, we have

$$\begin{aligned}\|\varepsilon(t)\| &= \|l_{n-1}(t)\varepsilon^{n-1}+l_n(t)\varepsilon^n\| \\ &\le |l_{n-1}(t)|\,\|\varepsilon^{n-1}\| + |l_n(t)|\,\|\varepsilon^n\| \\ &\le 2\max\{\|\varepsilon^n\|,\|\varepsilon^{n-1}\|\}.\end{aligned}$$

Again, for $t \in [0, t_m]$, using Lemma 5.3.1 we obtain

$$\|\varepsilon(t)\| \le 2\max_{n\in[0:m]}\|\varepsilon^n\| \le 2\max_{n\in[0,m]}\mathscr{O}_{\mathrm{BDF},n}. \tag{5.3.25}$$

Also, in view of (5.3.14) we have

$$\begin{aligned} \|\hat{\sigma}(t)\| &= \|\frac{1}{2}(t-t_{n-1})(t_n-t)\mathcal{R}^n\mathcal{W}_n\| \\ &\leq \frac{1}{2}\max_{t\in\bar{I}_n}\{|(t-t_{n-1})(t_n-t)|\}\ \{\|(\mathcal{R}^n-I)\mathcal{W}_n\|+\|\mathcal{W}_n\|\} \\ &\leq \mathscr{T}_{\text{re,BDF},n}, \end{aligned} \tag{5.3.26}$$

where $\mathscr{T}_{\text{re,BDF},n}$ is defined in (5.3.24). Combine (5.3.25), (5.3.26) and Theorem 5.3.1 to obtain the desired result. □

6

Error Analysis of Semilinear Problems

This chapter is concerned with *a posteriori* error analysis of the semilinear parabolic interface problems. We shall restrict ourself to the case when only the forcing term is nonlinear. Both the backward Euler and the Crank-Nicolson approximations are considered for the time discretizations, whereas we have used the standard piecewise linear finite elements for the spatial discretizations. *A posteriori* estimate of optimal order in time and almost optimal order in space is derived in the $L^\infty(L^2)$-norm. The main technical tools used are the energy argument combined with the elliptic reconstruction technique. The forcing term is assumed to satisfy the Lipschitz condition.

6.1 Introduction

We shall start by formally introducing the semilinear parabolic interface problem. Let Ω be a bounded convex polygonal domain in $\mathbb{R}^2$ with Lipschitz boundary $\partial\Omega$. Let Ω_1 be a subdomain of Ω with C^2 boundary $\partial\Omega_1 := \Gamma$. The interface Γ now divides the domain Ω into two subdomains Ω_1 and $\Omega_2 := \Omega \setminus \Omega_1$. We consider the semilinear problem of the form

$$u_t(x,t) - \mathrm{div}(\beta(x)\nabla u(x,t)) = f(x,t,u) \quad \text{in} \quad \Omega \times (0,T] \tag{6.1.1}$$

with the prescribed initial and boundary conditions

$$u(x,0) = u_0(x) \quad \text{in} \quad \Omega; \qquad u = 0 \quad \text{on} \quad \partial\Omega \times [0,T] \tag{6.1.2}$$

and jump conditions on the interface

$$[u] = 0, \quad \left[\beta \frac{\partial u}{\partial \mathbf{n}}\right] = 0 \quad \text{across} \quad \Gamma \times [0,T], \tag{6.1.3}$$

where $0 < T < +\infty$ and $[v]$ denotes the jump of a quantity v across the interface Γ, i.e., $[v](x) = v_1(x) - v_2(x)$, $x \in \Gamma$ with $v_i(x) = v(x)|_{\Omega_i}$, $i = 1, 2$. The symbol $\mathbf{n}$ denotes

the unit outward normal to the boundary $\partial\Omega_1 := \Gamma$. The diffusion coefficient $\beta(x)$ is assumed to be positive and piecewise constant on each subdomain, i.e.,

$$\beta(x) = \beta_i \quad \text{for} \quad x \in \Omega_i,\ i = 1, 2.$$

The initial function $u_0(x)$ and the forcing term $f(x, t, u)$ are real valued functions and assumed to be smooth. We assume that $f : \bar{\Omega} \times [0, T] \times \mathbb{R} \longrightarrow \mathbb{R}$ satisfies the Lipschitz condition in the third argument, i.e., there exists a constant $\mathcal{C}_L > 0$ such that

$$|f(x, t, v) - f(x, t, w)| \leq \mathcal{C}_L |v - w| \quad \forall v, w \in \mathbb{R}. \tag{6.1.4}$$

Further, we shall call back the bilinear form $a(\cdot, \cdot) : H_0^1(\Omega) \times H_0^1(\Omega) \longrightarrow \mathbb{R}$ defined by

$$a(v, w) = \langle \beta \nabla v, \nabla w \rangle \quad \forall v, w \in H_0^1(\Omega). \tag{6.1.5}$$

The bilinear form $a(\cdot, \cdot)$ is bounded and coercive on $H_0^1(\Omega)$, i.e., $\exists \alpha_0, \gamma_0 > 0$ such that

$$|a(v, w)| \leq \alpha_0 \, \|v\|_1 \|w\|_1 \ \ \forall v, w \in H_0^1(\Omega), \tag{6.1.6}$$

and

$$a(v, v) \geq \ \gamma_0 \, \|v\|_1^2 \quad \forall v \in H_0^1(\Omega). \tag{6.1.7}$$

The weak formulation of the problem (6.1.1) – (6.1.3) is stated as follows: Find $u \in L^\infty(0, T; H_0^1(\Omega))$ such that

$$\begin{aligned} \langle u_t(t), \varphi \rangle + a(u(t), \varphi) &= \langle f(t, u), \varphi \rangle \ \ \varphi \in H_0^1(\Omega), \ \text{ a.e. } t \in (0, T], \\ u(0) &= u_0. \end{aligned} \tag{6.1.8}$$

Let $\mathcal{T}_n$ be a member of a family of triangulations $\{\mathcal{T}_n\}_{0 \leq n \leq N}$ of $\bar{\Omega}$ and let $\mathbb{S}^n$ be the corresponding finite dimensional space defined as

$$\mathbb{S}^n := \left\{ \chi \in H_0^1(\Omega) \ \middle| \ \chi|_K \in \mathbb{P}_1(K) \ \text{ for all } \ K \in \mathcal{T}_n \right\},$$

where $\mathbb{P}_1(K)$ is the space of polynomials of degree less than or equal to 1 on K. For $v \in \mathbb{S}^n$, let $f^n(v) := f(x, t_n, v)$. Henceforth, we shall use the following shorthand notations: For $1 \leq n \leq N$,

$$f^{n-\frac{1}{2}}(v^{n-\frac{1}{2}}) := \frac{f^n(v^n) + f^{n-1}(v^{n-1})}{2}, \ \ v^{n-\frac{1}{2}} := \frac{v^n + v^{n-1}}{2} \ \text{ and } \ \partial v^n := \frac{v^n - v^{n-1}}{k_n}.$$

Since both the backward Euler and the Crank-Nicolson approximations are analyzed, we first state these two methods below.

The fully discrete backward Euler approximation. The standard backward Euler approximation for problem (6.1.1) – (6.1.3) may be stated as follows: Given $U^0 = I_h^0 u(0)$, seek $U^n \in \mathbb{S}^n$ ($1 \leq n \leq N$) such that

$$\left\langle \frac{U^n - U^{n-1}}{k_n}, \chi_n \right\rangle + a(U^n, \chi_n) = \langle f^n(U^n), \chi_n \rangle \quad \forall \chi_n \in \mathbb{S}^n. \tag{6.1.9}$$

Here, the operator I_h^0 is a suitable projection from $H_0^1(\Omega)$ into the finite dimensional subspace $\mathbb{S}^0$.

The fully discrete Crank-Nicolson approximation. The fully discrete Crank-Nicolson approximation of the problem (6.1.1) – (6.1.3) is stated as follows: Let $U^0 = I_h^0 u(0)$, where I_h^0 is a suitable projection operator from $H_0^1(\Omega)$ into the finite dimensional subspace $\mathbb{S}^0$. Then, for $1 \leq n \leq N$, find $U^n \in \mathbb{S}^n$ such that

$$\left\langle \frac{U^n - U^{n-1}}{k_n}, \chi_n \right\rangle + a\left(U^{n-\frac{1}{2}}, \chi_n\right) = \left\langle f^{n-\frac{1}{2}}(U^{n-\frac{1}{2}}), \chi_n \right\rangle \quad \forall \chi_n \in \mathbb{S}^n. \tag{6.1.10}$$

We now recall the following projection operators for our subsequent use.

Discrete elliptic operator. The discrete elliptic operator associated with the bilinear form $a(\cdot, \cdot)$ and the finite element space $\mathbb{S}^n$ is the operator $\mathcal{A}_h^n : H_0^1(\Omega) \longrightarrow \mathbb{S}^n$ such that for $v \in H_0^1(\Omega)$ and $0 \leq n \leq N$,

$$\langle \mathcal{A}_h^n v, \ \chi_n \rangle \ = \ a(v, \chi_n) \quad \forall \chi_n \in \mathbb{S}^n. \tag{6.1.11}$$

L^2-projection operator: The L^2-projection operator is a map $\mathit{\Pi}_0^n : L^2(\Omega) \longrightarrow \mathbb{S}^n$ such that for $v \in L^2(\Omega)$ and $0 \leq n \leq N$,

$$\langle \mathit{\Pi}_0^n v, \chi_n \rangle \ = \ \langle v, \ \chi_n \rangle \quad \forall \chi_n \in \mathbb{S}^n. \tag{6.1.12}$$

Motivated by the discussion in Chapter 4, we rather consider the modified Crank-Nicolson approximation.

Modified Crank-Nicolson approximation. Given $U^0 = I_h^0 u(0)$, for $1 \leq n \leq N$ seek $U^n \in \mathbb{S}^n$ such that

$$\begin{aligned} &\frac{1}{k_n}(U^n - P_1^n U^{n-1}) + \frac{1}{2}(\mathcal{A}_h^n U^n) + \frac{1}{2} P_2^n (\mathcal{A}_h^{n-1} U^{n-1}) \\ &\qquad = \mathit{\Pi}_0^n f^{n-\frac{1}{2}}(U^{n-\frac{1}{2}}), \ 1 \leq n \leq N, \end{aligned} \tag{6.1.13}$$

where $P_1^n, P_2^n : \mathbb{S}^{n-1} \longrightarrow \mathbb{S}^n$ be any suitable projection operators.

Representation of the bilinear form. As before we represent the bilinear form $a(\cdot, \cdot)$ in short form as

$$a(v, \varphi) \ = \ \langle (v)_{\mathrm{el}}, \varphi \rangle \ + \ \langle j[\beta v], \varphi \rangle_{\Sigma_n} \quad \forall \varphi \in \ H_0^1(\Omega), \tag{6.1.14}$$

where the symbols have the same meaning as in Chapter 1.

A posteriori error estimates for the semilinear parabolic problems (in absence of interface) have been studied in the past by Kopteva and Linss [59], Kyza and Makridakis [60]. In [59], the authors have obtained maximum norm *a posteriori* error bounds using the elliptic reconstruction. Whereas, the error analysis of [60] is based on the reconstruction technique and the energy methods combined with the appropriate fixed point arguments. The *a posteriori* error analysis for a general nonlinear parabolic problems has been studied by Akrivis *et al.* in [4]. In [4], the authors have considered the Crank-Nicolson discretization in time only and have shown the second order convergence. The main aim of this chapter is to extend our previous methodology for linear interface problem to treat semilinear parabolic interface problems. We use only the energy technique combined with the reconstruction approach to derive *a posteriori* error estimators for (6.1.1) − (6.1.3). More precisely, for the backward Euler approximation, we use the piecewise linear space-time reconstruction (cf. [62]) whereas, the Crank-Nicolson analysis uses the quadratic space-time reconstruction (see, e.g., [15]) of finite element solution. Other worth mentioning technicalities for our analysis are the new approximation results of the Clément-type interpolation operator and the discrete version of Gronwall's lemma (Lemma 1.2.2). Optimal order estimates in time and almost optimal order estimates in space in the $L^\infty(L^2)$-norm are obtained for both the backward Euler and the Crank-Nicolson approximations.

The outline of this chapter is as follows. In Section 6.2, we derive *a posteriori* error estimates for the backward Euler approximation of the semilinear parabolic problem. Section 6.3 discusses the related *a posteriori* analysis for the Crank-Nicolson approximation.

6.2 Abstract Backward Euler Error Analysis

In this section, we first introduce the elliptic reconstruction operator and then discuss the related *a posteriori* error analysis for the backward Euler approximation.

Definition 6.2.1 (Elliptic reconstruction)**.** *For a fully discrete finite element solution $U^n \in \mathbb{S}^n$ obtained from (6.1.9), we define the elliptic reconstruction $\mathcal{R}_b^n U^n \in H_0^1(\Omega)$ of $U^n \in \mathbb{S}^n$ as the solution of the following elliptic problem written in the weak form as*

$$a(\mathcal{R}_b^n U^n, \varphi) = \langle \hat{f}^n, \varphi \rangle \ \ \forall \varphi \in H_0^1(\Omega), \tag{6.2.1}$$

where

$$\hat{f}^n := \begin{cases} \mathcal{A}_h^0 U^0, & n = 0, \\ f^n(U^n) - k_n^{-1}(U^n - U^{n-1}), & 1 \le n \le N. \end{cases}$$

Note that the operator $\mathcal{R}_b^n$ satisfies the Galerkin orthogonality property.

Now, we state the following elliptic reconstruction error bound for the fully discrete finite element approximation in the L^2-norm. Following the arguments used in deriving the estimates (3.2.5) the proof of lemma can be easily obtained. We therefore, refrain from giving the details.

Lemma 6.2.1. *For a finite element approximation $U^n \in \mathbb{S}^n$ of the elliptic equation (6.2.1), the following is true for $0 \le n \le N$:*

$$\|(\mathcal{R}_b^n - I)U^n\| \le \mathcal{C}_{I,5}\, h_n^2\, |\log h_n|^{\frac{1}{2}} \|\hat{f}^n - (U^n)_{\rm el}\| + \mathcal{C}_{I,6}\, h_n^{\frac{3}{2}}\, |\log h_n|^{\frac{1}{2}}\, \|j[\beta U^n]\|_{\Sigma_n},$$

where $\mathcal{C}_{I,5} := \mathcal{C}_{I,3}\mathcal{C}_R$ and $\mathcal{C}_{I,6} := \mathcal{C}_{I,4}\mathcal{C}_R$.

In order to derive the *a posteriori* error bound, we split the total error $e(t) := u(t) - U(t)$ by considering the reconstruction $\bar{\Theta}(t)$ as an intermediate object as follows:

$$e(t) := \bar{\rho}(t) - \bar{\varepsilon}(t), \quad t \in I_n \quad \text{where } \bar{\rho}(t) := u(t) - \bar{\Theta}(t),\ \bar{\varepsilon}(t) := \bar{\Theta}(t) - U(t), \tag{6.2.2}$$

where $U(t), t \in I_n$ is defined by

$$U(t) := l_{n-1}(t)U^{n-1} + l_n(t)U^n, \quad t \in I_n\ (n = 1\ldots, N). \tag{6.2.3}$$

The functions $l_{n-1}(t)$ and $l_n(t)$ are given by

$$l_{n-1}(t) := \frac{t_n - t}{k_n} \quad \text{and} \quad l_n(t) := \frac{t - t_{n-1}}{k_n} \ \text{ for } t \in I_n, \tag{6.2.4}$$

and $\bar{\Theta}$ is the piecewise linear interpolant of the reconstruction operator defined by

$$\bar{\Theta}(t) := l_{n-1}(t)\, \mathcal{R}_b^{n-1}\, U^{n-1} + l_n(t)\, \mathcal{R}_b^n\, U^n, \quad t \in I_n\ (n = 1\ldots, N). \tag{6.2.5}$$

In the above, $\bar{\rho}(t)$ refers to the parabolic error and $\bar{\varepsilon}(t)$ represents the elliptic reconstruction error.

With $\bar{\rho}(t)$ and $\bar{\varepsilon}(t)$ as above, for $1 \le n \le N$ and for each $\varphi \in H_0^1(\Omega)$, we have by simple calculation the following parabolic error equation:

$$\begin{aligned} \langle \bar{\rho}_t(t), \varphi\rangle + a(\bar{\rho}(t), \varphi) \;&=\; -\langle \bar{\varepsilon}_t(t), \varphi\rangle - a(\bar{\Theta}(t) - \bar{\Theta}^n, \varphi) \\ &\quad + \langle f(x,t,u) - f^n(U^n), \varphi\rangle, \quad t \in I_n. \end{aligned} \tag{6.2.6}$$

Now we define the following residual-based error estimators which will be used in the subsequent analysis of the fully discrete backward Euler approximation.

The elliptic reconstruction error estimator: For $0 \le n \le N$,

$$\mathscr{O}_{\mathrm{SBE},n} := \mathcal{C}_{I,5}\, h_n^2\, |\log h_n|^{\frac{1}{2}} \|\hat{f}^n - (U^n)_{\rm el}\| + \mathcal{C}_{I,6}\, h_n^{\frac{3}{2}}\, |\log h_n|^{\frac{1}{2}}\, \|j[\beta U^n]\|_{\Sigma_n}. \tag{6.2.7}$$

The space-mesh error estimator: For $1 \le n \le N$,

$$\begin{aligned} \mathscr{M}_{\mathrm{SBE},n} &:= \mathcal{C}_{I,5}\,\hat{h}_n^2\,|\log \hat{h}_n|^{\frac{1}{2}}\,\|\partial \hat{\mathbf{R}}_n\| + \mathcal{C}_{I,6}\,\hat{h}_n^{\frac{3}{2}}\,|\log \hat{h}_n|^{\frac{1}{2}}\|\partial \hat{\mathbf{J}}_n\|_{\hat{\Sigma}_n} \\ &\quad + \mathcal{C}_{I,8}\,\hat{h}_n^{\frac{3}{2}}\,|\log \hat{h}_n|^{\frac{1}{2}}\,\|\partial \hat{\mathbf{J}}_n\|_{\check{\Sigma}_n \setminus \hat{\Sigma}_n}, \quad \mathcal{C}_{I,8} = \mathcal{C}_{I,7}\mathcal{C}_R, \end{aligned} \tag{6.2.8}$$

where

$$\begin{aligned} \hat{\mathbf{R}}_0 &:= (U^0)_{\mathrm{el}} - (\mathcal{A}_h^0 U^0), \\ \hat{\mathbf{R}}_n &:= k_n^{-1}(U^n - U^{n-1}) + (U^n)_{\mathrm{el}} - \hat{f}^n \quad \text{for } 1 \le n \le N \end{aligned}$$

denote the *element residuals* and

$$\hat{\mathbf{J}}_n := j[\beta U^n] \quad \text{for} \quad 0 \le n \le N$$

refers to the *jump residual*.

The temporal error estimator: For $1 \le n \le N$,

$$\mathscr{T}_{\mathrm{e,SBE},n} := \begin{cases} \frac{1}{2}\,\|\mathcal{A}_h^0 U^0 - f^1(U^1) + \partial U^1\|, & n = 1, \\ \frac{1}{2}\,k_n\,\|\partial\,(f^n(U^n) - \partial U^n)\,\|, & 2 \le n \le N. \end{cases} \tag{6.2.9}$$

The data approximation error estimators: For $1 \le n \le N$,

$$\begin{cases} \mathscr{D}_{\mathrm{SBE},n,1} := \sqrt{\mathcal{C}_L}\,\max\{\|\bar{\varepsilon}^n\|, \|\bar{\varepsilon}^{(n-1)}\|\}, \\ \mathscr{D}_{\mathrm{SBE},n,2} := \frac{1}{k_n}\int_{t_{n-1}}^{t_n} \|f(x,t,U) - f^n(U^n)\|dt. \end{cases} \tag{6.2.10}$$

A posteriori error bound for the parabolic error $\bar{\rho}(t)$ relies on a sequence of auxiliary lemmas.

Below, we shall state first Lemmas 6.2.2 – 6.2.3 without proofs. The proofs follow the same line as in Chapter 3.

Lemma 6.2.2 (Space-mesh error estimate)**.** *With $\mathscr{M}_{\mathrm{SBE},n}$ as in (6.2.8), let $\mathfrak{I}_{n,1}$ represent the space-mesh error term and be given by*

$$\mathfrak{I}_{n,1} := \int_{t_{n-1}}^{t_n} |\langle \bar{\varepsilon}_t(t), \bar{\rho}(t)\rangle|\,dt.$$

Then we have

$$\mathfrak{I}_{n,1} \le k_n\,\mathscr{M}_{\mathrm{SBE},n}\,\max_{t\in \bar{I}_n} \|\bar{\rho}(t)\|.$$

Lemma 6.2.3 (Temporal error estimate)**.** *With $\mathscr{T}_{\mathrm{e,SBE},n}$ as in (6.2.9), let $\mathfrak{I}_{n,2}$ denote the temporal error term and be defined by*

$$\mathfrak{I}_{n,2} := \int_{t_{n-1}}^{t_n} \left| a\left(\bar{\Theta}(t) - \bar{\Theta}^n, \bar{\rho}(t)\right)\right| dt.$$

Then we have

$$\mathfrak{I}_{n,2} \leq k_n \ \mathscr{T}_{\mathrm{e,SBE},n} \ \max_{t\in\bar{I}_n} \|\bar{\rho}(t)\|.$$

Lemma 6.2.4 (Data approximation error estimate)**.** *With $\mathscr{D}_{\mathrm{SBE},n,1}$ and $\mathscr{D}_{\mathrm{SBE},n,2}$ as in (6.2.10), let the data approximation error term be represented by $\mathfrak{I}_{n,3}$ and be defined as*

$$\mathfrak{I}_{n,3} := \int_{t_{n-1}}^{t_n} |\langle f(x,t,u) - f^n(U^n), \bar{\rho}(t)\rangle| \, dt.$$

Then we have

$$\begin{aligned}\mathfrak{I}_{n,3} \ \leq \ & \frac{\sqrt{\mathcal{C}_L}}{2\epsilon}\, k_n \max_{t\in\bar{I}_n} \|\bar{\rho}(t)\|^2 + \frac{\epsilon\sqrt{\mathcal{C}_L}}{2} \int_{t_{n-1}}^{t_n} \|\bar{\rho}(t)\|_1^2 dt \\ & + k_n \, \mathscr{D}_{\mathrm{SBE},n,1} \max_{t\in\bar{I}_n} \|\bar{\rho}(t)\| + k_n \mathscr{D}_{\mathrm{SBE},n,2} \max_{t\in\bar{I}_n} \|\bar{\rho}(t)\|.\end{aligned}$$

Proof. We rewrite the integrand in $\mathfrak{I}_{n,3}$ as

$$\begin{aligned}\langle f(x,t,u) - f^n(U^n), \bar{\rho}(t)\rangle \ = \ & \left\langle f(x,t,u) - f(x,t,\bar{\Theta}(t)), \bar{\rho}(t)\right\rangle \\ & + \left\langle f(x,t,\bar{\Theta}(t)) - f(x,t,U(t)), \bar{\rho}(t)\right\rangle \\ & + \langle f(x,t,U(t)) - f^n(U^n), \bar{\rho}(t)\rangle \,.\end{aligned}$$

Then

$$\begin{aligned}\mathfrak{I}_{n,3} \ \leq \ & \int_{t_{n-1}}^{t_n} \left|\left\langle f(x,t,u) - f(x,t,\bar{\Theta}(t)), \bar{\rho}(t)\right\rangle\right| dt \\ & + \int_{t_{n-1}}^{t_n} \left|\left\langle f(x,t,\bar{\Theta}(t)) - f(x,t,U(t)), \bar{\rho}(t)\right\rangle\right| dt \\ & + \int_{t_{n-1}}^{t_n} |\langle f(x,t,U(t)) - f^n(U^n), \bar{\rho}(t)\rangle| \, dt \\ := \ & T_{n,1} + T_{n,2} + T_{n,3}. \end{aligned} \tag{6.2.11}$$

Using the Cauchy-Schwarz inequality, (6.1.4) and the Young's inequality, we obtain

$$\begin{aligned}\left|\left\langle f(x,t,u) - f(x,t,\bar{\Theta}(t)), \bar{\rho}(t)\right\rangle\right| \ & \leq \ \|f(x,t,u) - f(x,t,\bar{\Theta}(t))\|\|\bar{\rho}(t)\| \\ & \leq \ \sqrt{\mathcal{C}_L}\, \|\bar{\rho}(t)\| \, \|\bar{\rho}(t)\|_1 \\ & \leq \ \sqrt{\mathcal{C}_L} \left\{ \frac{\|\bar{\rho}(t)\|^2}{2\epsilon} + \frac{\epsilon}{2}\|\bar{\rho}(t)\|_1^2 \right\},\end{aligned}$$

where ϵ is any positive real number to be chosen appropriately.

Thus,

$$\begin{aligned} T_{n,1} &\leq \sqrt{\mathcal{C}_L}\int_{t_{n-1}}^{t_n}\left\{\frac{\|\bar{\rho}(t)\|^2}{2\epsilon}+\frac{\epsilon}{2}\|\bar{\rho}(t)\|_1^2\right\}dt \\ &\leq \frac{\sqrt{\mathcal{C}_L}}{2\epsilon}\,k_n\max_{t\in\bar{I}_n}\|\bar{\rho}(t)\|^2+\frac{\epsilon\sqrt{\mathcal{C}_L}}{2}\int_{t_{n-1}}^{t_n}\|\bar{\rho}(t)\|_1^2dt. \end{aligned} \tag{6.2.12}$$

To estimate the second term in (6.2.11), we use the Cauchy-Schwarz inequality and (6.1.4) to obtain

$$\left|\left\langle f(x,t,\bar{\Theta}(t))-f(x,t,U(t)),\bar{\rho}(t)\right\rangle\right|\leq\sqrt{\mathcal{C}_L}\,\|\bar{\Theta}(t)-U(t)\|\,\|\bar{\rho}(t)\|.$$

In view of (5.2.5), it follows that

$$\begin{aligned} &\left|\left\langle f(x,t,\bar{\Theta}(t))-f(x,t,U(t)),\bar{\rho}(t)\right\rangle\right| \\ &\quad\leq\sqrt{\mathcal{C}_L}\left\{\left|\frac{t_n-t}{k_n}\right|\,\|\mathcal{R}_b^{n-1}U^{n-1}-U^{n-1}\|+\left|\frac{t-t_{n-1}}{k_n}\right|\,\|\mathcal{R}_b^nU^n-U^n\|\right\}\|\bar{\rho}(t)\|. \end{aligned}$$

Therefore,

$$\begin{aligned} T_{n,2} &\leq \frac{\sqrt{\mathcal{C}_L}}{2}\,k_n\,\left\{\|\bar{\varepsilon}^{n-1}\|+\|\bar{\varepsilon}^n\|\right\}\max_{t\in\bar{I}_n}\|\bar{\rho}(t)\| \\ &= k_n\,\mathscr{D}_{\mathrm{SBE},n,1}\max_{t\in\bar{I}_n}\|\bar{\rho}(t)\|. \end{aligned} \tag{6.2.13}$$

Finally to estimate $T_{n,3}$, we use the Cauchy-Schwarz inequality to have

$$\begin{aligned} T_{n,3} &\leq \max_{t\in\bar{I}_n}\|\bar{\rho}(t)\|\int_{t_{n-1}}^{t_n}\|f(x,t,U(t))-f^n(U^n)\|\,dt \\ &= k_n\,\mathscr{D}_{\mathrm{SBE},n,2}\max_{t\in\bar{I}_n}\|\bar{\rho}(t)\|, \end{aligned} \tag{6.2.14}$$

which in conjunction with (6.2.12) and (6.2.13) complete the desired proof. □

Now, we apply the above lemmas to derive the *a posteriori* error bound for the parabolic error $\bar{\rho}(t)$ in the $L^\infty(L^2)$-norm.

Theorem 6.2.1. *Let u be the exact solution of (6.1.1)–(6.1.3) and let U^n be its finite element approximation obtained by the backward Euler approximation (6.1.9). Then, for $1\leq m\leq N$, the following a posteriori error bound holds:*

$$\begin{aligned} \left\{\max_{t\in[0,t_m]}\|\bar{\rho}(t)\|^2+\int_0^{t_m}\|\bar{\rho}(t)\|_1^2dt\right\}^{\frac{1}{2}} &\leq \left\{2\,\mathcal{C}_G(m)\,\|\bar{\rho}(0)\|^2\right\}^{\frac{1}{2}} \\ &\quad+4\,\mathcal{C}_G(m)\sum_{n=1}^{m}k_n\left\{\mathscr{M}_{\mathrm{SBE},n}+\mathscr{T}_{\mathrm{e,SBE},n}+\mathscr{D}_{\mathrm{SBE},n,1}+\mathscr{D}_{\mathrm{SBE},n,2}\right\}, \end{aligned}$$

where $\mathcal{C}_G(m)$ is a positive constant due to the Gronwall's lemma and the quantities $\mathscr{M}_{\mathrm{SBE},n}$, $\mathscr{T}_{\mathrm{e,SBE},n}$, $\mathscr{D}_{\mathrm{SBE},n,i}(i=1,2)$ are given in (6.2.8)–(6.2.10), respectively.

Proof. Setting $\varphi = \bar{\rho}(t)$ in (6.2.6) and using (6.1.7), we have

$$\begin{aligned}\frac{1}{2}\frac{d}{dt}\|\bar{\rho}(t)\|^2 + \frac{\gamma_0}{2}\|\bar{\rho}(t)\|_1^2 \;&\leq\; |\,\langle \bar{\varepsilon}_t(t), \bar{\rho}(t)\rangle\,| + |a(\bar{\Theta}(t) - \bar{\Theta}^n, \bar{\rho}(t))| \\ &\quad + |\,\langle f(x,t,u) - f^n(U^n), \bar{\rho}(t)\rangle\,|. \end{aligned} \tag{6.2.15}$$

Integrate the above from t_{n-1} to t_n to have

$$\frac{1}{2}\|\bar{\rho}(t_n)\|^2 - \frac{1}{2}\|\bar{\rho}(t_{n-1})\|^2 + \frac{\gamma_0}{2}\int_{t_{n-1}}^{t_n} \|\bar{\rho}(t)\|_1^2 dt \leq\; \mathfrak{I}_{n,1} + \mathfrak{I}_{n,2} + \mathfrak{I}_{n,3},$$

where $\mathfrak{I}_{n,i}(i = 1, 2, 3)$ are defined in Lemmas 6.2.2 – 6.2.4, respectively. Summing up over $n = 1 : m$ we have

$$\|\bar{\rho}(t_m)\|^2 + \gamma_0 \int_0^{t_m} \|\bar{\rho}(t)\|_1^2 dt \leq \|\bar{\rho}(0)\|^2 + 2\sum_{n=1}^{m} \{\mathfrak{I}_{n,1} + \mathfrak{I}_{n,2} + \mathfrak{I}_{n,3}\}. \tag{6.2.16}$$

Since $\bar{\rho}(t)$ is continuous in $[0, t_m]$, there exists $t_{0,m} \in [0, t_m]$ such that

$$\|\bar{\rho}_{0,m}\| := \|\bar{\rho}(t_{0,m})\| = \max_{t\in[0,t_m]} \|\bar{\rho}(t)\|.$$

Again, integrate (6.2.15) between the limits 0 to $t_{0,m}$ and note that the integrands are non-negative, it follows that

$$\|\bar{\rho}(t_{0,m})\|^2 + \gamma_0 \int_0^{t_{0,m}} \|\bar{\rho}(t)\|_1^2 dt \leq \|\bar{\rho}(0)\|^2 + 2\sum_{n=1}^{m} \{\mathfrak{I}_{n,1} + \mathfrak{I}_{n,2} + \mathfrak{I}_{n,3}\}. \tag{6.2.17}$$

Thus, combining (6.2.16) and (6.2.17) we finally lead to

$$\|\bar{\rho}(t_{0,m})\|^2 + \gamma_0 \int_0^{t_m} \|\bar{\rho}(t)\|_1^2 dt \leq 2\|\bar{\rho}(0)\|^2 + 4\sum_{n=1}^{m} \{\mathfrak{I}_{n,1} + \mathfrak{I}_{n,2} + \mathfrak{I}_{n,3}\}.$$

Now, using Lemmas 6.2.2 – 6.2.4, we obtain

$$\begin{aligned}\|\bar{\rho}_{0,m}\|^2 + \gamma_0 \int_0^{t_m} \|\bar{\rho}(t)\|_1^2 dt \;&\leq\; 2\|\bar{\rho}(0)\|^2 \\ &\quad + 4 \max_{t\in[0,t_m]} \|\bar{\rho}(t)\| \sum_{n=1}^{m} k_n \{\mathscr{M}_{\mathrm{SBE},n} + \mathscr{T}_{\mathrm{e,SBE},n} + \mathscr{D}_{\mathrm{SBE},n,1} + \mathscr{D}_{\mathrm{SBE},n,2}\} \\ &\quad + \frac{2\sqrt{\mathcal{C}_L}}{\epsilon} \sum_{n=1}^{m} k_n \max_{t\in\bar{I}_n} \|\bar{\rho}(t)\|^2 + 2\,\epsilon\,\sqrt{\mathcal{C}_L} \int_0^{t_m} \|\bar{\rho}(t)\|_1^2 dt. \end{aligned}$$

Therefore,

$$\begin{aligned}\max_{t\in[0,t_m]} \|\bar{\rho}(t)\|^2 \;&\leq\; 2\|\bar{\rho}(0)\|^2 + (2\,\epsilon\,\sqrt{\mathcal{C}_L} - \gamma_0) \int_0^{t_m} \|\bar{\rho}(t)\|_1^2 dt \\ &\quad + 4 \max_{t\in[0,t_m]} \|\bar{\rho}(t)\| \sum_{n=1}^{m} k_n \{\mathscr{M}_{\mathrm{SBE},n} + \mathscr{T}_{\mathrm{e,SBE},n} + \mathscr{D}_{\mathrm{SBE},n,1} + \mathscr{D}_{\mathrm{SBE},n,2}\} \\ &\quad + \frac{2\sqrt{\mathcal{C}_L}}{\epsilon} \sum_{n=1}^{m} k_n \max_{t\in[0,t_n]} \|\bar{\rho}(t)\|^2. \end{aligned}$$

Choose $\epsilon > 0$ be such that $(2\,\epsilon\,\sqrt{\mathcal{C}_L} - \gamma_0) > 0$ and use of the discrete Gronwall's Lemma 1.2.2 with

$$x_m := \max_{t\in[0,t_m]} \|\bar{\rho}(t)\|^2, \quad z_m := \frac{2\sqrt{\mathcal{C}_L}}{\epsilon}\, k_m,$$

$$\begin{aligned} y_m \;:=\; & 2\|\bar{\rho}(0)\|^2 + \int_0^{t_m} \|\bar{\rho}(t)\|_1^2 dt \\ & +4 \max_{t\in[0,t_m]} \|\bar{\rho}(t)\| \sum_{n=1}^{m} k_n \left\{\mathscr{M}_{\mathrm{SBE},n} + \mathscr{T}_{\mathrm{e,SBE},n} + \mathscr{D}_{\mathrm{SBE},n,1} + \mathscr{D}_{\mathrm{SBE},n,2}\right\}, \end{aligned}$$

to obtain

$$\begin{aligned} \max_{t\in[0,t_m]} \|\bar{\rho}(t)\|^2 + \mathcal{C}_G(m) \int_0^{t_m} \|\bar{\rho}(t)\|_1^2 dt \;\le\; & 2\,\mathcal{C}_G(m)\,\|\bar{\rho}(0)\|^2 \\ & + 4\,\mathcal{C}_G(m) \max_{t\in[0,t_m]} \|\bar{\rho}(t)\| \sum_{n=1}^{m} k_n \left\{\mathscr{M}_{\mathrm{SBE},n} + \mathscr{T}_{\mathrm{e,SBE},n} + \mathscr{D}_{\mathrm{SBE},n,1} + \mathscr{D}_{\mathrm{SBE},n,2}\right\}, \end{aligned}$$

where $\mathcal{C}_G(m) := 2\ \max\left\{1,\ \sum_{n=1}^{m} \frac{2\sqrt{\mathcal{C}_L}}{\epsilon}\, k_n\ \exp\{\frac{2\sqrt{\mathcal{C}_L}}{\epsilon}\ (\sum_{n<j<m} k_j)\}\right\}.$

Finally, we take

$$a_0 := \max_{t\in[0,t_m]} \|\bar{\rho}(t)\|, \quad a_n := \left\{\mathcal{C}_G(m) \int_{t_{n-1}}^{t_n} \|\bar{\rho}(t)\|_1^2\, dt\right\}^{\frac{1}{2}}\ (1 \le n \le m),$$

$$c := \left\{2\,\mathcal{C}_G(m)\,\|\bar{\rho}(0)\|^2\right\}^{\frac{1}{2}},$$

$$b_0 := 4\,\mathcal{C}_G(m) \sum_{n=1}^{m} k_n \left\{\mathscr{M}_{\mathrm{SBE},n} + \mathscr{T}_{\mathrm{e,SBE},n} + \mathscr{D}_{\mathrm{SBE},n,1} + \mathscr{D}_{\mathrm{SBE},n,2}\right\},$$

and

$$b_n := 0 (1 \le n \le m)$$

and invoke Lemma 1.2.3 to complete the proof. □

The following theorem presents the fully discrete backward Euler *a posteriori* error estimate in the $L^\infty(L^2)$-norm for the semilinear parabolic interface problem (6.1.1) – (6.1.3).

Theorem 6.2.2. *Let u be the exact solution of (6.1.1)–(6.1.3) and let U^n be its finite element approximation obtained by the backward Euler approximation (6.1.9). Then, for each $1 \le m \le N$, the following a posteriori error estimate holds:*

$$\begin{aligned} \max_{t\in[0,t_m]} \|u(t) - U(t)\| \le\; & \{2\,\mathcal{C}_G(m)\}^{\frac{1}{2}}\, \|\mathcal{R}^0 U^0 - u(0)\| \\ & + 4\,\mathcal{C}_G(m) \sum_{n=1}^{m} k_n \left\{\mathscr{M}_{\mathrm{SBE},n} + \mathscr{T}_{\mathrm{e,SBE},n} + \mathscr{D}_{\mathrm{SBE},n,1} + \mathscr{D}_{\mathrm{SBE},n,2}\right\} \\ & + 2 \max_{0\le n\le m} \mathscr{O}_{\mathrm{SBE},n}. \end{aligned}$$

The estimators $\mathscr{O}_{\mathrm{SBE},n}$, $\mathscr{M}_{\mathrm{SBE},n}$, $\mathscr{T}_{\mathrm{e,SBE},n}$ *and* $\mathscr{D}_{\mathrm{SBE},n,i}(i=1,2)$ *are given by* (6.2.7) – (6.2.10)*, respectively.*

Proof. By the triangle inequality, we have

$$\|e(t)\| = \|u(t) - U(t)\| \leq \|\bar{\rho}(t)\| + \|\bar{\varepsilon}(t)\|, \quad t \in I_n. \tag{6.2.18}$$

As $\max_{t\in\bar{I}_n} l_n(t) = 1$ we have

$$\begin{aligned} \|\bar{\varepsilon}(t)\| &= \|l_{n-1}(t)\bar{\varepsilon}^{(n-1)} + l_n(t)\bar{\varepsilon}^n\|, t \in I_n, \\ &\leq 2\max\{\|\bar{\varepsilon}^n\|, \|\bar{\varepsilon}^{(n-1)}\|\}. \end{aligned}$$

Again, for $t \in [0, t_m]$, using Lemma 6.2.1 we obtain

$$\|\bar{\varepsilon}(t)\| \leq 2 \max_{0\leq n\leq m} \mathscr{O}_{\mathrm{SBE},n},$$

which combine with Theorem 6.2.1 proves the desired result. □

6.3 Abstract Crank-Nicolson Error Analysis

For the purpose of the fully discrete Crank-Nicolson error analysis, we now define the space-time quadratic reconstruction for the Crank-Nicolson approximation (6.1.13). For this, we recall the definition of elliptic reconstruction from [15, 62].

Definition 6.3.1 (elliptic reconstruction)**.** *For* $v \in \mathbb{S}^n$*, we define the elliptic reconstruction* $\mathcal{R}_c^n v$ *of* v *as the solution of the following elliptic problem*

$$a(\mathcal{R}_c^n v, \varphi) = \langle \mathcal{A}_h^n v, \varphi\rangle \quad \forall \varphi \in H_0^1(\Omega),\ 0 \leq n \leq N. \tag{6.3.1}$$

Now, we shall introduce some notations for further use.

Let $\Psi : [0,T] \longrightarrow H_0^1(\Omega)$ be continuous piecewise linear function in time defined by

$$\Psi(t) := l_{n-1}(t)\,(P_2^n(\mathcal{A}_h^{n-1}))\,U^{n-1} + l_n(t)\,(\mathcal{A}_h^n)\,U^n, \quad t \in I_n\ (n = 1\ldots, N), \tag{6.3.2}$$

where $l_{n-1}(t)$ and $l_n(t)$ are given by (6.2.4).

Also, let $\breve{\Phi} : [0,T] \longrightarrow H_0^1(\Omega)$ be a continuous piecewise linear interpolant of $f(t)$ defined by

$$\breve{\Phi}(t) := l_{n-1}(t)\, f^{n-1}(U^{n-1}) + l_n(t)\, f^n(U^n), \quad t \in I_n\ (n = 1\ldots, N). \tag{6.3.3}$$

Next, to define space-time reconstruction we rewrite the fully discrete Crank-Nicolson approximation (6.1.13) in the compact form as:

$$\frac{U^n - P_1^n U^{n-1}}{k_n} = H_3(t_{n-\frac{1}{2}}), \quad n \geq 1, \tag{6.3.4}$$

where

$$H_3(t_{n-\frac{1}{2}}) := \Pi_0^n f^{n-\frac{1}{2}}(U^{n-\frac{1}{2}}) - \Psi(t_{n-\frac{1}{2}}), \quad n \geq 1. \tag{6.3.5}$$

We also define $\breve{H}_3 : [0,T] \longrightarrow H_0^1(\Omega)$ be a piecewise linear function in time defined as

$$\breve{H}_3(t) := \Pi_0^n \breve{\Phi}(t) - \Psi(t), \quad t \in I_n \ (n = 1, \ldots, N), \tag{6.3.6}$$

and $\breve{H}_3(t_{n-\frac{1}{2}}) = H_3(t_{n-\frac{1}{2}})$.

Inspired by the idea of [4, 15], we now define below the space-time Crank-Nicolson reconstruction $\breve{U}$ of the Crank-Nicolson finite element solution U.

Definition 6.3.2 (space-time reconstruction)**.** *The quadratic space-time reconstruction $\breve{U} : [0,T] \longrightarrow H_0^1(\Omega)$ of U is defined by*

$$\begin{aligned}\breve{U}(t) \ &:= \ \mathcal{R}_c^{n-1}U^{n-1} + {k_n}^{-1}(t - t_{n-1})\left\{(\mathcal{R}_c^n P_1^n)U^{n-1} - \mathcal{R}_c^{n-1}U^{n-1}\right\} \\ &\quad + \int_{t_{n-1}}^{t} \mathcal{R}_c^n \hat{H}_3(s)ds, \quad t \in I_n \ (n = 1, \ldots, N).\end{aligned}$$

Observe that $\breve{U}$ is a continuous function in time and satisfies the relation

$$\breve{U}_t(t) = {k_n}^{-1}\left\{(\mathcal{R}_c^n P_1^n)U^{n-1} - \mathcal{R}_c^{n-1}U^{n-1}\right\} + \mathcal{R}_c^n \breve{H}_3(t), \quad t \in I_n \ (n = 1, \ldots, N). \tag{6.3.7}$$

To derive the *a posteriori* estimates we decompose the total error $e(t) := u(t) - U(t)$ as

$$e(t) := \breve{\rho}(t) + \breve{\sigma}(t) + \breve{\varepsilon}(t), \quad t \in I_n, \tag{6.3.8}$$

where $\breve{\rho}(t) := u(t) - \breve{U}(t)$ denotes the parabolic error, $\breve{\sigma}(t) := \breve{U}(t) - \breve{\Theta}(t)$ refers to the time reconstruction error and $\breve{\varepsilon}(t) := \breve{\Theta}(t) - U(t)$ denotes the elliptic reconstruction error. Here, $\breve{\Theta}(t)$ is the continuous piecewise linear function in time defined by

$$\breve{\Theta}(t) := l_{n-1}(t)\,\mathcal{R}_c^{n-1}\,U^{n-1} + l_n(t)\,\mathcal{R}_c^n\,U^n, \quad t \in I_n \ (n = 1 \ldots, N). \tag{6.3.9}$$

Now, we shall state the following *a posteriori* error bounds for the elliptic reconstruction error $\breve{\varepsilon}(t)$. The proof follows exactly on the same line as in Lemma 4.2.1, and therefore, we refrain from doing proofs here.

Lemma 6.3.1. *For a finite element approximation $U^n \in \mathbb{S}^n$ of the elliptic equation (6.3.1), the following is true for $0 \leq n \leq N$:*

$$\|(\mathcal{R}_c^n - I)v\| \leq \mathcal{C}_{I,5}\, h_n^2\, |\log h_n|^{\frac{1}{2}} \|\mathcal{A}_h^n v - (v)_{\mathrm{el}}\| + \mathcal{C}_{I,6}\, h_n^{\frac{3}{2}}\, |\log h_n|^{\frac{1}{2}}\, \|j[\beta v]\|_{\Sigma_n},$$

where $\mathcal{C}_{I,5} := \mathcal{C}_{I,3}\mathcal{C}_R$ and $\mathcal{C}_{I,6} := \mathcal{C}_{I,4}\mathcal{C}_R$.

Now we define the various residual-based estimators for our subsequent use.

The elliptic reconstruction error estimator: For $0 \leq n \leq N$,

$$\mathscr{O}_{\mathrm{SCN},n} := \mathcal{C}_{I,5}\; h_n^2\; |\log h_n|^{\frac{1}{2}}\; \|(\mathcal{A}_h^n)U^n - (U^n)_{\mathrm{el}}\| + \mathcal{C}_{I,6}\; h_n^{\frac{3}{2}}\; |\log h_n|^{\frac{1}{2}}\; \|j[\beta U^n]\|_{\Sigma_n}. \tag{6.3.10}$$

The space-mesh error estimator: For $1 \leq n \leq N$,

$$\begin{aligned}\mathscr{M}_{\mathrm{SCN},n} \;:=\; & \mathcal{C}_{I,5}\; \hat{h}_n^2\; |\log \hat{h}_n|^{\frac{1}{2}}\; \|k_n^{-1}\left\{(\mathcal{A}_h^n)U^n - (\mathcal{A}_h^{n-1})U^{n-1} - (U^n)_{\mathrm{el}} + (U^{n-1})_{\mathrm{el}}\right\}\| \\ & + \mathcal{C}_{I,6}\; \hat{h}_n^{\frac{3}{2}}\; |\log \hat{h}_n|^{\frac{1}{2}}\; \|k_n^{-1}\left\{j[\beta U^n] - j[\beta U^{n-1}]\right\}\|_{\hat{\Sigma}_n} \\ & + \mathcal{C}_{I,8}\; \hat{h}_n^{\frac{3}{2}}\; |\log \hat{h}_n|^{\frac{1}{2}}\; \|k_n^{-1}\left\{j[\beta U^n] - j[\beta U^{n-1}]\right\}\|_{\check{\Sigma}_n \setminus \hat{\Sigma}_n}\end{aligned} \tag{6.3.11}$$

with $\mathcal{C}_{I,8} := \mathcal{C}_{I,7}\mathcal{C}_R$.

The temporal reconstruction error estimator:

$$\begin{aligned}\mathscr{T}_{\mathrm{re,SCN},n} \;:=\; & \frac{k_n^2}{8}\Big\{\mathcal{C}_{I,5}\; h_n^2\; |\log h_n|^{\frac{1}{2}}\; \|(\mathcal{A}_h^n)\mathcal{Z}_n - (\mathcal{Z}_n)_{\mathrm{el}}\| \\ & + \mathcal{C}_{I,6}\; h_n^{\frac{3}{2}}\; |\log h_n|^{\frac{1}{2}}\; \|j[\beta \mathcal{Z}_n]\|_{\Sigma_n} + \|\mathcal{Z}_n\|\Big\}\end{aligned} \tag{6.3.12}$$

with $\mathcal{Z}_n := -\Pi_0^n \breve{\Phi}_t(t) + \Psi_t(t)$.

The space-error estimator:

$$\begin{aligned}\mathscr{S}_{\mathrm{SCN},n} \;:=\; & \frac{k_n}{4}\Big\{\mathcal{C}_{I,5}\; h_n^2\; |\log h_n|^{\frac{1}{2}}\; \|(\mathcal{A}_h^n)\mathcal{Z}_n - (\mathcal{Z}_n)_{\mathrm{el}}\| \\ & + \mathcal{C}_{I,6}\; h_n^{\frac{3}{2}}\; |\log h_n|^{\frac{1}{2}}\; \|j[\beta \mathcal{Z}_n]\|_{\Sigma_n}\Big\}.\end{aligned} \tag{6.3.13}$$

The temporal error estimator:

$$\begin{aligned}\mathscr{T}_{\mathrm{e,SCN},n} \;:=\; & \frac{1}{\gamma_0}\sqrt{\frac{\alpha_0}{120}}\, k_n^2\; \{\mathcal{C}_{I,1}\; h_n\; \|(\mathcal{A}_h^n)\mathcal{Z}_n - (\mathcal{Z}_n)_{\mathrm{el}}\| \\ & + \mathcal{C}_{I,2}\; h_n^{\frac{1}{2}}\; \|j[\beta \mathcal{Z}_n]\|_{\Sigma_n} + \alpha_0\; \|\mathcal{Z}_n\|_1\Big\}.\end{aligned} \tag{6.3.14}$$

The coarsening error estimator:

$$\mathscr{C}_{\mathrm{SCN},n} := k_n^{-1}\|(I - \Pi_0^n)U^{n-1}\| + \frac{1}{2}\|(P_2^n - I)(-\Delta_h^{n-1})U^{n-1}\|. \tag{6.3.15}$$

The data approximation error estimators:

$$\begin{cases} \mathscr{D}_{\mathrm{SCN},n,1} := \frac{1}{12}\sqrt{\mathcal{C}_L}\; k_n^2\Big\{\mathcal{C}_{I,5}\; h_n^2\; |\log h_n|^{\frac{1}{2}}\; \|(\mathcal{A}_h^n)\mathcal{Z}_n - (\mathcal{Z}_n)_{\mathrm{el}}\| \\ \qquad\qquad + \mathcal{C}_{I,6}\; h_n^{\frac{3}{2}}\; |\log h_n|^{\frac{1}{2}}\; \|j[\beta \mathcal{Z}_n]\|_{\Sigma_n} + \|\mathcal{Z}_n\|\Big\}, \\ \mathscr{D}_{\mathrm{SCN},n,2} := \sqrt{\mathcal{C}_L}\; \max\{\|\breve{\varepsilon}^{n-1}\|, \|\breve{\varepsilon}^{n}\|\}, \\ \mathscr{D}_{\mathrm{SCN},n,3} := \frac{1}{k_n}\int_{t_{n-1}}^{t_n} \|f(x,t,U) - \breve{\Phi}(t)\|dt, \\ \mathscr{D}_{\mathrm{SCN},n,4} := \frac{1}{\sqrt{\gamma_0}}\,\mathcal{C}_{I,1}\, h_n\left\{\|(\Pi_0^n - I)\frac{\{f^n(U^n) - f^{n-1}(U^{n-1})\}}{2}\|\right\}. \end{cases} \tag{6.3.16}$$

Next, we state a series of lemmas to drive *a posteriori* error bounds for the parabolic error $\breve{\rho}(t)$.

Lemma 6.3.2 (Space-mesh error estimate). *With $\mathscr{M}_{\mathrm{SCN},n}$ as in (6.3.11), let $\mathcal{I}_{n,2}$ represent the space-mesh error term and be given by*

$$\mathcal{I}_{n,2} := \int_{t_{n-1}}^{t_n} |\langle \breve{\varepsilon}_t(t), \breve{\rho}(t)\rangle|\, dt.$$

Then the following is true:

$$\mathcal{I}_{n,2} \leq k_n\, \mathscr{M}_{\mathrm{SCN},n} \max_{t\in\bar{I}_n} \|\breve{\rho}(t)\|.$$

Lemma 6.3.3 (Space error estimate). *With $\mathscr{S}_{\mathrm{SCN},n}$ as in (6.3.13), let $\mathcal{I}_{n,3}$ denote the space error term and be defined as*

$$\mathcal{I}_{n,3} := \int_{t_{n-1}}^{t_n} \left| \left\langle (\mathcal{R}_c^n - I)\left(\breve{H}_3(t) - H_3(t_{n-\frac{1}{2}})\right), \breve{\rho}(t)\right\rangle \right| dt.$$

Then

$$\mathcal{I}_{n,3} \leq\ k_n \mathscr{S}_{\mathrm{SCN},n} \max_{t\in\bar{I}_n} \|\breve{\rho}(t)\|.$$

Lemma 6.3.4 (Coarsening error estimate). *With $\mathscr{C}_{\mathrm{SCN},n}$ as in (6.3.15), let $\mathcal{I}_{n,5}$ denote the coarsening error term and be defined as*

$$\mathcal{I}_{n,5} := \int_{t_{n-1}}^{t_n} \left|\left\langle k_n^{-1}(I - \Pi_0^n)U^{n-1} + l_{n-1}(t)(P_2^n - I)(-\Delta_h^{n-1})U^{n-1}, \breve{\rho}(t)\right\rangle\right| dt.$$

Then

$$\mathcal{I}_{n,5} \leq k_n\, \mathscr{C}_{\mathrm{SCN},n} \max_{t\in\bar{I}_n} \|\breve{\rho}(t)\|.$$

The proofs of Lemmas 6.3.2 – 6.3.4 can be treated in a similar manner as Lemmas 4.2.4 – 4.2.7 of Chapter 4 and hence, the details are omitted.

The following lemma gives the *a posteriori* error bound for the temporal error $\breve{\sigma}(t)$.

Lemma 6.3.5 (Temporal error estimate). *With $\mathscr{T}_{\mathrm{e,SCN},n}$ as in (6.3.14), let $\mathcal{I}_{n,1}$ refer to the error term due to time discretization and is defined by*

$$\mathcal{I}_{n,1} := \alpha_0 \int_{t_{n-1}}^{t_n} \|\breve{\sigma}(t)\|_1^2 dt.$$

Then

$$\mathfrak{I}_{n,1} \leq k_n\, \mathscr{T}_{\mathrm{e,SCN},n}^2.$$

Proof. In order to estimate $\breve{\sigma}(t)$ we first estimate $\breve{\sigma}_t(t) := \breve{U}_t(t) - \breve{\Theta}_t(t)$. In view of (6.3.7) and (6.3.9) we have

$$\begin{aligned}\breve{\sigma}_t(t) &= \mathcal{R}_c^n \left\{ \frac{P_1^n U^{n-1} - U^n}{k_n} + \breve{H}_3(t) \right\} \\ &= \mathcal{R}_c^n \left\{ \breve{H}_3(t) - H_3(t_{n-\frac{1}{2}}) \right\}.\end{aligned}$$

Integrating from t_{n-1} to t and using the fact that $\breve{U}(t)$ and $\breve{\Theta}(t)$ coincide at the nodal points, it now leads to

$$\breve{\sigma}(t) = \int_{t_{n-1}}^{t} \mathcal{R}_c^n \left\{ \breve{H}_3(t) - H_3(t_{n-\frac{1}{2}}) \right\} dt. \tag{6.3.17}$$

Now, using (6.3.5) – (6.3.6) and a simple calculation yields

$$\begin{aligned}\breve{H}_3(t) - H_3(t_{n-\frac{1}{2}}) &= \Pi_0^n \left\{ \breve{\Phi}(t) - \breve{\Phi}(t_{n-\frac{1}{2}}) \right\} - \left\{ \Psi(t) - \Psi(t_{n-\frac{1}{2}}) \right\} \\ &= \Pi_0^n \left\{ (t - t_{n-\frac{1}{2}})\, \breve{\Phi}_t(t) \right\} - \left\{ (t - t_{n-\frac{1}{2}})\, \Psi_t(t) \right\} \\ &= -(t - t_{n-\frac{1}{2}})\, \mathcal{Z}_n \qquad (6.3.18)\end{aligned}$$

with

$$\mathcal{Z}_n := -\Pi_0^n \breve{\Phi}_t(t) + \Psi_t(t). \tag{6.3.19}$$

Substituting (6.3.18) in (6.3.17) and evaluating the integral by the midpoint rule we have that

$$\begin{aligned}\breve{\sigma}(t) &= -\int_{t_{n-1}}^{t} \mathcal{R}_c^n \left\{ (t - t_{n-\frac{1}{2}}) \mathcal{Z}_n \right\} \\ &= \frac{1}{2}(t - t_{n-1})(t_n - t) \mathcal{R}_c^n \mathcal{Z}_n. \qquad (6.3.20)\end{aligned}$$

Using the coercivity and continuity properties of the bilinear form $a(\cdot, \cdot)$, it follows that

$$\begin{aligned}\gamma_0 \|\breve{\sigma}(t)\|_1^2 &\leq a(\breve{\sigma}(t), \breve{\sigma}(t)) \\ &= \frac{1}{2}(t - t_{n-1})(t_n - t)\; a(\mathcal{R}_c^n \mathcal{Z}_n, \breve{\sigma}(t)) \\ &\leq \frac{1}{2}(t - t_{n-1})(t_n - t)\; \left\{ a((\mathcal{R}_c^n - I)\mathcal{Z}_n, \breve{\sigma}(t)) + \alpha_0 \|\mathcal{Z}_n\|_1 \|\breve{\sigma}(t)\|_1 \right\}. \qquad (6.3.21)\end{aligned}$$

We now apply the Galerkin orthogonality property of $\mathcal{R}_c^n$ and (6.3.1) to have

$$a((\mathcal{R}_c^n - I)\mathcal{Z}_n, \breve{\sigma}(t)) = |\langle (\mathcal{A}_h^n)\mathcal{Z}_n - (\mathcal{Z}_n)_{\text{el}}, \breve{\sigma}(t) - \mathscr{J}_n \breve{\sigma}(t) \rangle| + |\langle j[\beta \mathcal{Z}_n], \breve{\sigma}(t) - \mathscr{J}_n \breve{\sigma}(t) \rangle_{\Sigma_n}|.$$

An application of the Cauchy-Schwarz inequality and Proposition 3.2.1 yields

$$\begin{aligned} & a\left((\mathcal{R}_c^n - I)\mathcal{Z}_n, \breve{\sigma}(t)\right) \\ & \quad \leq \|(\mathcal{A}_h^n)\mathcal{Z}_n - (\mathcal{Z}_n)_{\text{el}}\| \, \|\breve{\sigma}(t) - \mathscr{J}_n\breve{\sigma}(t)\| + \|j[\beta\mathcal{Z}_n]\|_{\Sigma_n} \, \|\breve{\sigma}(t) - \mathscr{J}_n\breve{\sigma}(t)\|_{\Sigma_n} \\ & \quad \leq \left\{\mathcal{C}_{I,1}\, h_n \, \|(\mathcal{A}_h^n)\mathcal{Z}_n - (\mathcal{Z}_n)_{\text{el}}\| + \mathcal{C}_{I,2}\, h_n^{\frac{1}{2}} \, \|j[\beta\mathcal{Z}_n]\|_{\Sigma_n}\right\} \|\breve{\sigma}(t)\|_1. \end{aligned}$$

Thus, in view of (6.3.21), we obtain

$$\gamma_0 \, \|\breve{\sigma}(t)\|_1^2 \leq \frac{1}{2}(t - t_{n-1})(t - t_n) \, \mathcal{D}_n \, \|\breve{\sigma}(t)\|_1,$$

where $\mathcal{D}_n := \left\{\mathcal{C}_{I,1}\, h_n \, \|(\mathcal{A}_h^n)\mathcal{Z}_n - (\mathcal{Z}_n)_{\text{el}}\| + \mathcal{C}_{I,2}\, h_n^{\frac{1}{2}} \, \|j[\beta\mathcal{Z}_n]\|_{\Sigma_n} + \alpha_0\|\mathcal{Z}_n\|_1\right\}$. Thus, we finally arrive at

$$\begin{aligned} \mathcal{I}_{n,1} &\leq \frac{\alpha_0}{4\gamma_0^2} \, \mathcal{D}_n^2 \int_{t_{n-1}}^{t_n} (t - t_{n-1})^2 (t_n - t)^2 dt \\ &\leq k_n \mathscr{T}_{\text{e,SCN},n}^2, \end{aligned}$$

where $\mathscr{T}_{\text{e,SCN},n}^2 = \frac{1}{120} \, \frac{\alpha_0}{\gamma_0^2} \, k_n^4 \, \mathcal{D}_n^2$ and we thus complete the proof. □

Lemma 6.3.6 (Data approximation error estimate)**.** *With $\mathscr{D}_{\text{SCN},n,i} (i = 1, \ldots, 4)$ as in (6.3.16), let $\mathcal{I}_{n,4}$ denote the data approximation error term and be defined as*

$$\mathcal{I}_{n,4} := \int_{t_{n-1}}^{t_n} \left| \left\langle f(x,t,u) - \breve{H}_3(t) - \Psi(t), \breve{\rho}(t) \right\rangle \right| dt.$$

Then we have

$$\begin{aligned} \mathcal{I}_{n,4} \leq \; & \frac{\sqrt{\mathcal{C}_L}}{2\,\epsilon} \, k_n \, \max_{t \in \bar{I}_n} \|\breve{\rho}(t)\|^2 + \frac{\epsilon\sqrt{\mathcal{C}_L}}{2} \int_{t_{n-1}}^{t_n} \|\breve{\rho}(t)\|_1^2 dt \\ & + k_n \left\{\mathscr{D}_{\text{SCN},n,1} + \mathscr{D}_{\text{SCN},n,2} + \mathscr{D}_{\text{SCN},n,3}\right\} \max_{t \in \bar{I}_n} \|\breve{\rho}(t)\| \\ & + k_n^{\frac{1}{2}} \, \mathscr{D}_{\text{SCN},n,4} \left(\gamma_0 \int_{t_{n-1}}^{t_n} \|\breve{\rho}(t)\|_1^2 dt\right)^{\frac{1}{2}}. \end{aligned}$$

Proof. With an aid of (6.3.6), we first rewrite the integrand in $\mathcal{I}_{n,4}$ as

$$\begin{aligned} f(x,t,u) - \breve{H}_3(t) - \Psi(t) &= f(x,t,u) - \Pi_0^n \breve{\Phi}(t) \\ &= \left(f(x,t,u) - \breve{\Phi}(t)\right) - (\Pi_0^n - I)\breve{\Phi}(t). \end{aligned} \tag{6.3.22}$$

Further, we split the first term of (6.3.22) to obtain

$$\begin{aligned}\mathcal{I}_{n,4} &\leq \int_{t_{n-1}}^{t_n} \left|\left\langle f(x,t,u) - f(x,t,\breve{U}), \breve{\rho}(t)\right\rangle\right| dt \\ &\quad + \int_{t_{n-1}}^{t_n} \left|\left\langle f(x,t,\breve{U}) - f(x,t,\breve{\Theta}(t), \breve{\rho}(t)\right\rangle\right| dt \\ &\quad + \int_{t_{n-1}}^{t_n} \left|\left\langle f(x,t,\breve{\Theta}(t)) - f(x,t,U(t)), \breve{\rho}(t)\right\rangle\right| dt \\ &\quad + \int_{t_{n-1}}^{t_n} \left|\left\langle f(x,t,U(t)) - \breve{\Phi}(t), \breve{\rho}(t)\right\rangle\right| dt \\ &\quad + \int_{t_{n-1}}^{t_n} \left|\left\langle (\Pi_0^n - I)\breve{\Phi}(t), \breve{\rho}(t)\right\rangle\right| dt \\ &:= T_1^n + T_2^n + T_3^n + T_4^n + T_5^n.\end{aligned}$$

Then using the Cauchy-schwarz inequality and the Young's inequality, we have

$$\begin{aligned}\left|\left\langle f(x,t,u) - f(x,t,\breve{U}), \breve{\rho}(t)\right\rangle\right| &\leq \sqrt{\mathcal{C}_L}\, \|\breve{\rho}(t)\|\, \|\breve{\rho}(t)\|_1 \\ &\leq \sqrt{\mathcal{C}_L}\left(\frac{1}{2\,\epsilon}\|\breve{\rho}(t)\|^2 + \frac{\epsilon}{2}\|\breve{\rho}(t)\|_1^2\right),\end{aligned}$$

and hence,

$$T_1^n \leq \frac{\sqrt{\mathcal{C}_L}}{2\,\epsilon}\, k_n \max_{t\in\bar{I}_n}\|\breve{\rho}(t)\|^2 + \frac{\epsilon\,\sqrt{\mathcal{C}_L}}{2}\int_{t_{n-1}}^{t_n}\|\breve{\rho}(t)\|_1^2 dt.$$

Again, using the Cauchy-schwarz inequality once more and (6.3.20) we obtain

$$\begin{aligned}&\left|\left\langle f(x,t,\breve{U}) - f(x,t,\breve{\Theta}(t), \breve{\rho}(t)\right\rangle\right| \\ &\leq \|f(x,t,\breve{U}) - f(x,t,\breve{\Theta}(t)\|\, \|\breve{\rho}(t)\| \\ &\leq \sqrt{\mathcal{C}_L}\, \|\breve{\sigma}(t)\|\, \|\breve{\rho}(t)\| \\ &\leq \frac{1}{2}\,\sqrt{\mathcal{C}_L}\, |t-t_{n-1}|\, |t_n - t|\, \{\|(\mathcal{R}_c^n - I)\mathcal{Z}_n\| + \|\mathcal{Z}_n\|\}\ \|\breve{\rho}(t)\|.\end{aligned}$$

Therefore,

$$\begin{aligned}T_2^n &\leq \frac{k_n^3}{12}\sqrt{\mathcal{C}_L}\ \{\|(\mathcal{R}_c^n - I)\mathcal{Z}_n\| + \|\mathcal{Z}_n\|\}\ \max_{t\in\bar{I}_n}\|\breve{\rho}(t)\| \\ &= k_n\, \mathscr{D}_{\mathrm{SCN},n,1}\ \max_{t\in\bar{I}_n}\|\breve{\rho}(t)\|.\end{aligned}$$

Exactly following the same argument of (6.2.13), we have

$$T_3^n \leq k_n\, \mathscr{D}_{\mathrm{SCN},n,2}\ \max_{t\in\bar{I}_n}\|\breve{\rho}(t)\|.$$

Again, invoking the Cauchy-schwarz inequality it follows that

$$\begin{aligned} T_4^n &\leq \max_{t\in\bar{I}_n}\|\breve{\rho}(t)\|\int_{t_{n-1}}^{t_n}\|f(x,t,U(t))-\breve{\Phi}(t)\| \\ &= k_n\,\mathscr{D}_{\mathrm{SCN},n,3}\,\max_{t\in\bar{I}_n}\|\breve{\rho}(t)\|. \end{aligned}$$

Finally to estimate T_5^n, we exploit the orthogonality property of Π_0^n and Proposition 3.2.1 to have

$$\begin{aligned} \left\langle(\Pi_0^n-I)\breve{\Phi}(t),\breve{\rho}(t)\right\rangle &= \left\langle(\Pi_0^n-I)\breve{\Phi}(t),\breve{\rho}(t)-\mathscr{J}_n\breve{\rho}(t)\right\rangle \\ &\leq \|(\Pi_0^n-I)\breve{\Phi}(t)\|\,\|\breve{\rho}(t)-\mathscr{J}_n\breve{\rho}(t)\| \\ &\leq \mathcal{C}_{I,1}\,h_n\,\|(\Pi_0^n-I)\breve{\Phi}(t)\|\,\|\breve{\rho}(t)\|_1. \end{aligned}$$

As $\max_{t\in\bar{I}_n}|l_n(t)|=1$ and $\max_{t\in\bar{I}_n}|l_{n-1}(t)|=1$, it follows from (6.3.3) that

$$\begin{aligned} \|(\Pi_0^n-I)\breve{\Phi}(t)\| &\leq \max_{t\in\bar{I}_n}|l_{n-1}(t)|\,\|(\Pi_0^n-I)f^{n-1}\|+\max_{t\in\bar{I}_n}|l_n(t)|\,\|(\Pi_0^n-I)f^n\| \\ &= \|(\Pi_0^n-I)f^{n-1}\|+\|(\Pi_0^n-I)f^n\|, \end{aligned}$$

and hence,

$$T_5^n \leq k_n^{\frac{1}{2}}\,\mathscr{D}_{\mathrm{SCN},n,4}\left(\gamma_0\int_{t_{n-1}}^{t_n}\|\breve{\rho}(t)\|_1^2dt\right)^{\frac{1}{2}},$$

and this completes the proof of the lemma. □

As a consequence of the above lemmas we derive the *a posteriori* error bound for the parabolic error $\breve{\rho}(t)$ in the following theorem.

Theorem 6.3.1. *Let u be the exact solution of (6.1.1)–(6.1.3) and let U^n be its finite element approximation obtained by the Crank-Nicolson approximation (6.1.13). Then, for $1\leq m\leq N$, the following is true:*

$$\begin{aligned} \left\{\max_{t\in[0,t_m]}\|\breve{\rho}(t)\|^2+\int_0^{t_m}\|\breve{\rho}(t)\|_1^2dt\right\}^{\frac{1}{2}} &\leq \left\{2\,\mathcal{C}_G(m)\left(\|\breve{\rho}(0)\|^2+\sum_{n=1}^m k_n\mathscr{T}_{\mathrm{e,SCN},n}^2\right)\right\}^{\frac{1}{2}} \\ &\quad+\left(\Upsilon_{m,1}^2+\Upsilon_{m,2}^2\right)^{\frac{1}{2}}, \end{aligned}$$

where

$$\begin{aligned} \Upsilon_{m,1} &:= 4\mathcal{C}_G(m)\sum_{n=1}^m k_n\,(\mathscr{M}_{\mathrm{SCN},n}+\mathscr{S}_{\mathrm{SCN},n}+\mathscr{D}_{\mathrm{SCN},n,1}+\mathscr{D}_{\mathrm{SCN},n,2} \\ &\qquad \mathscr{D}_{\mathrm{SCN},n,3}+\mathscr{C}_{\mathrm{SCN},n}), \end{aligned} \tag{6.3.23}$$

and

$$\Upsilon_{m,2} := 4\mathcal{C}_G(m)\sum_{n=1}^{m} k_n^{\frac{1}{2}}\mathscr{D}_{\mathrm{SCN},n,4}. \tag{6.3.24}$$

$\mathscr{M}_{\mathrm{SCN},n}$, $\mathscr{S}_{\mathrm{SCN},n}$, $\mathscr{T}_{\mathrm{e,SCN},n}$, $\mathscr{C}_{\mathrm{SCN},n}$, $\mathscr{D}_{\mathrm{SCN},n,i}(i = 1,\ldots,4)$ *are defined in (6.3.11) and (6.3.13)−(6.3.16), respectively.*

Proof. For each $\varphi \in H_0^1(\Omega)$ and for $1 \le n \le N$, using (6.3.7), (6.1.8) and rearranging the terms we have the following error equation for $\breve{\rho}(t)$

$$\langle \breve{\rho}_t(t),\varphi\rangle + a(\rho(t),\varphi) = \langle \mathscr{R}_3(t),\varphi\rangle, \quad t \in I_n, \tag{6.3.25}$$

where $\rho(t) := u(t) - \breve{\Theta}(t)$ and

$$\begin{aligned}\mathscr{R}_3(t) \;:=\; & -\breve{\varepsilon}_t(t) - (\mathcal{R}_c^n - I)\left(\breve{H}_3(t) - H_3(t_{n-\frac{1}{2}})\right) + \left(f(x,t,u) - \breve{H}_3(t) - \Psi(t)\right)\\ & + l_{n-1}(t)(P_2^n - I)(\mathcal{A}_h^{n-1})U^{n-1} - k_n^{-1}(P_1^n - I)U^{n-1}.\end{aligned}$$

Setting $\varphi = \breve{\rho}(t)$ in (6.3.25), we have

$$\frac{1}{2}\frac{d}{dt}\|\breve{\rho}(t)\|^2 + a\left(\rho(t),\breve{\rho}(t)\right) = \left\langle \mathscr{R}_3(t),\breve{\rho}(t)\right\rangle.$$

Using the fact that $2a(v,w) = a(v,v) + a(w,w) - a(v-w,v-w) \quad \forall v,w \in H_0^1(\Omega)$ and using the properties (6.1.6) and (6.1.7) of the bilinear form $a(\cdot,\cdot)$, we arrive at

$$\frac{1}{2}\frac{d}{dt}\|\breve{\rho}(t)\|^2 + \frac{\gamma_0}{2}\left(\|\rho(t)\|_1^2 + \|\breve{\rho}(t)\|_1^2\right) \le \frac{\alpha_0}{2}\|\breve{\sigma}(t)\|_1^2 + \left|\langle \mathscr{R}_3(t),\breve{\rho}(t)\rangle\right|. \tag{6.3.26}$$

Integrating the above from t_{n-1} to t_n and summing up over $n = 1 : m$, we obtain

$$\begin{aligned}&\|\breve{\rho}(t_m)\|^2 + \gamma_0\int_0^{t_m}\left(\|\rho(t)\|_1^2 + \|\breve{\rho}(t)\|_1^2\right)dt \le \|\breve{\rho}(0)\|^2\\ &+\sum_{n=1}^{m}\left\{\alpha_0\int_{t_{n-1}}^{t_n}\|\breve{\sigma}(t)\|_1^2 dt + 2\int_{t_{n-1}}^{t_n}\left|\langle \mathscr{R}_3(t),\breve{\rho}(t)\rangle\right|dt\right\}\\ &= \|\breve{\rho}(0)\|^2 + \sum_{n=1}^{m}\left\{\mathcal{I}_{n,1} + 2\sum_{i=2}^{5}\mathcal{I}_{n,i}\right\},\end{aligned} \tag{6.3.27}$$

where $\mathcal{I}_{n,i}$ $(i = 1,...,5)$ are defined in Lemmas 6.3.2 − 6.3.6.

Since $\breve{\rho}(t)$ is continuous in $[0,t_m]$, there exists $t_{0,m} \in [0,t_m]$ such that

$$\|\breve{\rho}_{0,m}\| := \|\breve{\rho}(t_{0,m})\| = \max_{t\in[0,t_m]}\|\breve{\rho}(t)\|.$$

Again, integrating (6.3.26) between the limits 0 to $t_{0,m}$ and observing that the integrands are non-negative, it follows that

$$\begin{aligned}
&\|\breve{\rho}(t_{0,m})\|^2 + \gamma_0 \int_0^{t_{0,m}} \left(\|\rho(t)\|_1^2 + \|\breve{\rho}(t)\|_1^2\right) dt \\
&\leq \|\breve{\rho}(0)\|^2 + \sum_{n=1}^{m} \left\{ \alpha_0 \int_{t_{n-1}}^{t_n} \|\breve{\sigma}(t)\|_1^2 dt + 2 \int_{t_{n-1}}^{t_n} |\langle \mathscr{R}_3(t), \breve{\rho}(t)\rangle| \, dt \right\} \\
&= \|\breve{\rho}(0)\|^2 + \sum_{n=1}^{m} \left\{ \mathcal{I}_{n,1} + 2 \sum_{i=2}^{5} \mathcal{I}_{n,i} \right\}. \qquad (6.3.28)
\end{aligned}$$

Thus, combining (6.3.27) and (6.3.28), we finally lead to

$$\|\breve{\rho}(t_{0,m})\|^2 + \gamma_0 \int_0^{t_m} \|\breve{\rho}(t)\|_1^2 dt \leq 2\|\breve{\rho}(0)\|^2 + 2 \sum_{n=1}^{m} \left\{ \mathcal{I}_{n,1} + 2 \sum_{i=2}^{5} \mathcal{I}_{n,i} \right\}.$$

Using Lemmas 6.3.2 – 6.3.6, we obtain

$$\begin{aligned}
&\|\breve{\rho}(t_{0,m})\|^2 + \gamma_0 \int_0^{t_m} \|\breve{\rho}(t)\|_1^2 \, dt \;\leq\; 2 \left\{ \|\breve{\rho}(0)\|^2 + \sum_{n=1}^{m} k_n \mathscr{T}_{\mathrm{e,SCN},n}^2 \right\} \\
&+4 \max_{t\in[0,t_m]} \|\breve{\rho}(t)\| \sum_{n=1}^{m} k_n \{ \mathscr{M}_{\mathrm{SCN},n} + \mathscr{S}_{\mathrm{SCN},n} + \mathscr{D}_{\mathrm{SCN},n,1} + \mathscr{D}_{\mathrm{SCN},n,2} \\
&+\mathscr{D}_{\mathrm{SCN},n,3} + \mathscr{C}_{\mathrm{SCN},n} \} + \; 4 \sum_{n=1}^{m} k_n^{\frac{1}{2}} \mathscr{D}_{\mathrm{SCN},n,4} \left(\gamma_0 \int_{t_{n-1}}^{t_n} \|\breve{\rho}(t)\|_1^2 dt \right)^{\frac{1}{2}} \\
&+ \frac{2\sqrt{\mathcal{C}_L}}{\epsilon} \sum_{n=1}^{m} k_n \max_{t\in\bar{I}_n} \|\breve{\rho}(t)\|^2 + 2\,\epsilon\,\sqrt{\mathcal{C}_L} \int_0^{t_m} \|\breve{\rho}(t)\|_1^2 dt.
\end{aligned}$$

Therefore,

$$\begin{aligned}
&\max_{t\in[0,t_m]} \|\breve{\rho}(t)\|^2 \;\leq\; 2 \left\{ \|\breve{\rho}(0)\|^2 + \sum_{n=1}^{m} k_n \mathscr{T}_{\mathrm{e,SCN},n}^2 \right\} + (2\,\epsilon\,\sqrt{\mathcal{C}_L} - \gamma_0) \int_0^{t_m} \|\breve{\rho}(t)\|_1^2 dt \\
&+ 4 \max_{t\in[0,t_m]} \|\breve{\rho}(t)\| \sum_{n=1}^{m} k_n \{ \mathscr{M}_{\mathrm{SCN},n} + \mathscr{S}_{\mathrm{SCN},n} + \mathscr{D}_{\mathrm{SCN},n,1} + \mathscr{D}_{\mathrm{SCN},n,2} \\
&+\mathscr{D}_{\mathrm{SCN},n,3} + \mathscr{C}_{\mathrm{SCN},n} \} + \; 4 \sum_{n=1}^{m} k_n^{\frac{1}{2}} \mathscr{D}_{\mathrm{SCN},n,4} \left(\gamma_0 \int_{t_{n-1}}^{t_n} \|\breve{\rho}(t)\|_1^2 dt \right)^{\frac{1}{2}} \\
&+ \frac{2\sqrt{\mathcal{C}_L}}{\epsilon} \sum_{n=1}^{m} k_n \max_{t\in[0,t_n]} \|\breve{\rho}(t)\|^2.
\end{aligned}$$

Choose $\epsilon > 0$ to be such that $(2\,\epsilon\,\sqrt{\mathcal{C}_L} - \gamma_0) > 0$ and invoking Lemma 1.2.2 with

$$x_m := \max_{t\in[0,t_m]} \|\rho(t)\|^2, \quad z_m := \frac{2\sqrt{\mathcal{C}_L}}{\epsilon}\, k_m,$$

$$
\begin{aligned}
y_m \;:=\; & 2\left\{\|\breve{\rho}(0)\|^2+\sum_{n=1}^{m}k_n\mathscr{T}^2_{\mathrm{e,SCN},n}\right\}+\int_0^{t_m}\|\breve{\rho}(t)\|_1^2dt\\
& +4\max_{t\in[0,t_m]}\|\breve{\rho}(t)\|\sum_{n=1}^{m}k_n\left\{\mathscr{M}_{\mathrm{SCN},n}+\mathscr{S}_{\mathrm{SCN},n}+\mathscr{D}_{\mathrm{SCN},n,1}+\mathscr{D}_{\mathrm{SCN},n,2}\right.\\
& \left.+\mathscr{D}_{\mathrm{SCN},n,3}+\mathscr{C}_{\mathrm{SCN},n}\right\}+4\sum_{n=1}^{m}k_n^{\frac{1}{2}}\mathscr{D}_{\mathrm{SCN},n,4}\left(\gamma_0\int_{t_{n-1}}^{t_n}\|\breve{\rho}(t)\|_1^2dt\right)^{\frac{1}{2}},
\end{aligned}
$$

we obtain

$$
\begin{aligned}
\max_{t\in[0,t_m]}\|\breve{\rho}(t)\|^2+\int_0^{t_m}\|\breve{\rho}(t)\|_1^2dt \;\le\; & 2\,\mathcal{C}_G(m)\left\{\|\breve{\rho}(0)\|^2+\sum_{n=1}^{m}k_n\mathscr{T}^2_{\mathrm{e,SCN},n}\right\}\\
& +\;4\,\mathcal{C}_G(m)\max_{t\in[0,t_m]}\|\breve{\rho}(t)\|\sum_{n=1}^{m}k_n\left\{\mathscr{M}_{\mathrm{SCN},n}+\mathscr{S}_{\mathrm{SCN},n}+\mathscr{D}_{\mathrm{SCN},n,1}+\mathscr{D}_{\mathrm{SCN},n,2}\right.\\
& \left.+\mathscr{D}_{\mathrm{SCN},n,3}+\mathscr{C}_{\mathrm{SCN},n}\right\}+4\mathcal{C}_G(m)\,k_n^{\frac{1}{2}}\mathscr{D}_{\mathrm{SCN},n,4}\left(\gamma_0\int_{t_{n-1}}^{t_n}\|\breve{\rho}(t)\|_1^2dt\right)^{\frac{1}{2}},
\end{aligned}
$$

where $\mathcal{C}_G(m):=2\;\max\left\{1,\;\sum_{n=1}^{m}\dfrac{2\sqrt{\mathcal{C}_L}}{\epsilon}\,k_n\;\exp\{\dfrac{2\sqrt{\mathcal{C}_L}}{\epsilon}\;(\sum_{n<j<m}k_j)\}\right\}$.

Finally, we take

$$
a_0:=\max_{t\in[0,t_m]}\|\breve{\rho}(t)\|,\quad a_n:=\left\{\mathcal{C}_G(m)\;(\gamma_0-2\,\epsilon\,\sqrt{\mathcal{C}_L})\int_{t_{n-1}}^{t_n}\|\breve{\rho}(t)\|_1^2\;dt\right\}^{\frac{1}{2}}\;(1\le n\le m),
$$

$$
c:=\left\{2\,\mathcal{C}_G(m)\;\left(\|\breve{\rho}(0)\|^2+\sum_{n=1}^{m}k_n\mathscr{T}^2_{\mathrm{e,SCN},n}\right)\right\}^{\frac{1}{2}},
$$

$$
b_0:=4\,\mathcal{C}_G(m)\sum_{n=1}^{m}k_n\left\{\mathscr{M}_{\mathrm{SCN},n}+\mathscr{S}_{\mathrm{SCN},n}+\mathscr{D}_{\mathrm{SCN},n,1}+\mathscr{D}_{\mathrm{SCN},n,2}+\mathscr{D}_{\mathrm{SCN},n,3}+\mathscr{C}_{\mathrm{SCN},n}\right\},
$$

$$
b_n:=4\,\mathcal{C}_G(m)\;k_n^{\frac{1}{2}}\;\mathscr{D}_{\mathrm{CN},n,2}\;(1\le n\le m),
$$

and invoke Lemma 1.2.3 to complete the rest of the proof. □

We are now prepared to state the fully discrete Crank-Nicolson *a posteriori* error estimate in the $L^\infty(L^2)$ norm for the semilinear parabolic interface problem (6.1.1) – (6.1.3).

Theorem 6.3.2. *Let u be the exact solution of (6.1.1)–(6.1.3) and let U^n be its finite element approximation obtained by the Crank-Nicolson approximation (6.1.13). Then,*

for each $1 \leq m \leq N$, the following a posteriori error estimate holds:

$$\begin{aligned}\max_{t\in[0,t_m]} \|u(t)-U(t)\| \;\leq\; & \left\{2\,\mathcal{C}_G(m)\left(\|\mathcal{R}^0U^0-u(0)\|^2+\sum_{n=1}^{m} k_n\mathscr{T}^2_{\mathrm{e,SCN},n}\right)\right\}^{\frac{1}{2}} \\ & +\left(\Upsilon^2_{m,1}+\Upsilon^2_{m,2}\right)^{\frac{1}{2}}+2\max_{0\leq n\leq m}\mathscr{O}_{\mathrm{SCN},n}+\max_{0\leq n\leq m}\mathscr{T}_{\mathrm{re,SCN},n},\end{aligned}$$

where the estimators are given in Theorem 6.3.1.

Proof. By the triangle inequality, we have for $t \in I_n$

$$\|e(t)\| \leq \max_{t\in[0,t_m]}\|\breve{\rho}(t)\|+\max_{t\in[0,t_m]}\|\breve{\sigma}(t)\|+\max_{t\in[0,t_m]}\|\breve{\epsilon}(t)\|.$$

As $\max\limits_{t\in\bar{I}_n} l_n(t)=1$, we have

$$\begin{aligned}\|\breve{\varepsilon}(t)\| &= \|l_{n-1}(t)\breve{\varepsilon}^{n-1}+l_n(t)\breve{\varepsilon}^{n}\| \\ &\leq |l_{n-1}(t)|\,\|\breve{\varepsilon}^{n-1}\|+|l_n(t)|\,\|\breve{\varepsilon}^{n}\| \\ &\leq 2\,\max\{\|\breve{\varepsilon}^{n}\|,\|\breve{\varepsilon}^{n-1}\|\},\quad t\in I_n.\end{aligned}$$

Again for $t \in [0, t_m]$, using Lemma 6.3.1, we obtain

$$\|\breve{\varepsilon}(t)\| \leq 2\max_{0\leq n\leq m}\|\breve{\varepsilon}^{n}\| \leq 2\max_{0\leq n\leq m}\mathscr{O}_{\mathrm{SCN},n}. \tag{6.3.29}$$

In view of (6.3.20), we have that

$$\begin{aligned}\|\breve{\sigma}(t)\| &= \|\frac{1}{2}(t-t_{n-1})(t_n-t)\mathcal{R}^n_c\mathcal{Z}_n\| \\ &\leq \frac{1}{2}\max_{t\in\bar{I}_n}\{|(t-t_{n-1})(t_n-t)|\}\;(\|(\mathcal{R}^n_c-I)\mathcal{Z}_n\|+\|\mathcal{Z}_n\|) \\ &\leq \mathscr{T}_{\mathrm{re,SCN},n}, \qquad (6.3.30)\end{aligned}$$

which in combination with (6.3.29) and Theorem 6.3.1 completes the proof. □

7

Numerical Assessments

This chapter reports the numerical results for a two dimensional test problem to validate the theoretical findings. Our main objective is to understand the asymptotic behaviour of the various estimators. We perform numerical tests on uniform meshes with uniform time-steps. All computations are carried out using MATLAB-7.8. Bisection algorithm [6, 104] is used to generate the refined triangulations. In the first section, we present the behaviour of the estimators of Chapter 3. In Section 7.2, we discuss the behaviour of the estimators of Chapter 4. Finally, Section 7.3 is devoted to study the behaviour of the estimators of Chapter 5.

7.1 Results for Backward Euler Approximation

In this section, the asymptotic behaviour of the error estimators obtained in Theorem 3.2.2 for the backward Euler approximation is studied for the following test problem.

Example 7.1.1. We shall solve the parabolic interface problem (1.1.1) – (1.1.3) in a domain $\Omega = (0,2) \times (0,1) \subset \mathbb{R}^2$. The interface occurs at $x = 1$ so that we choose $\Omega_1 = (0,1) \times (0,1)$, $\Omega_2 = (1,2) \times (0,1)$ and the interface $\Gamma = \bar{\Omega}_1 \cap \bar{\Omega}_2$. We shall consider the following problem in Ω:

$$\begin{aligned} u_t(x,y,t) - \mathrm{div}(\beta(x,y)\nabla u(x,y,t)) &= f(x,y,t) \quad \text{in} \quad \Omega \times (0,T], \\ u(x,y,0) &= u_0(x,y) \quad \text{in} \quad \Omega, \\ u(x,y,t) &= 0 \quad \text{on} \quad \partial\Omega \times [0,T], \\ [u] = 0, \quad \left[\beta \frac{\partial u}{\partial \mathbf{n}}\right] &= 0 \quad \text{across} \quad \Gamma \times [0,T], \end{aligned}$$

where $\mathbf{n}$ denotes the unit outer normal vector on Γ and ∇ denotes the spatial gradient.

We choose

$$\beta(x,y) = \begin{cases} 1 & \text{if} \quad (x,y) \in \Omega_1, \\ \frac{1}{2} & \text{if} \quad (x,y) \in \Omega_2. \end{cases}$$

We select the forcing term f such that the exact solution is given by

$$u(x,y,t) = \begin{cases} \exp(\sin(t))\sin(\pi x)\sin(\pi y) & \text{in} \quad \Omega_1 \times T, \\ -\exp(\sin(t))\sin(2\pi x)\sin(\pi y) & \text{in} \quad \Omega_2 \times T. \end{cases}$$

.

Let $\{\mathcal{T}_n\}_{0\le n\le N}$ be a family of conforming triangulations of $\bar{\Omega}$ at the time level t_n. Then for each $n = 0, \cdots, N$, we consider the finite element space $\mathbb{S}^n$ corresponding to the triangulation $\mathcal{T}_n$ as follows:

$$\mathbb{S}^n := \left\{ \chi \in H_0^1(\Omega) \;\middle|\; \chi|_K \in \mathbb{P}_1(K) \;\text{ for all }\; K \in \mathcal{T}_n \right\},$$

where $\mathbb{P}_1(K)$ is the space of polynomials of degree less than or equal to 1 on K. For

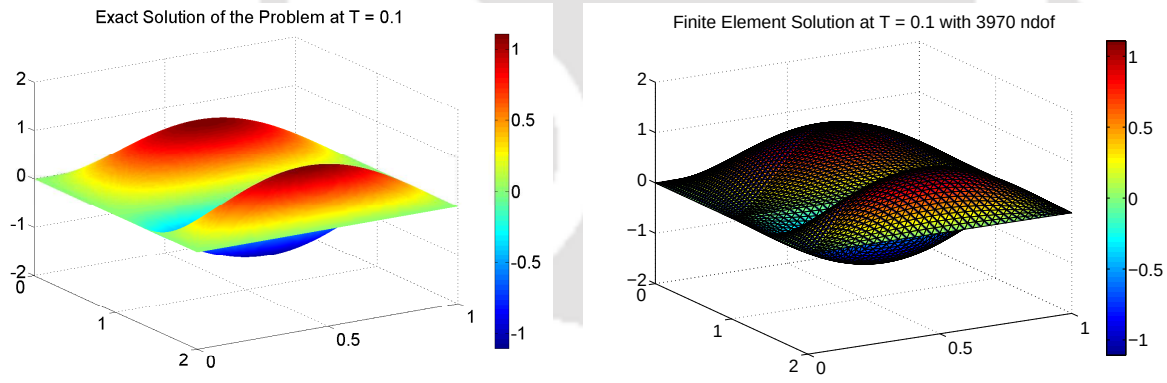

Figure 7.1: *The first plot shows the exact solution and the second one corresponds to the backward Euler FEM solution. FEM solution is computed using* $\mathbb{P}_1$ *elements with* 3970 *free nodes at* $T = 0.1$ *corresponding to* $k = 0.015625$.

each numerical experiment, we choose a sequence of mesh sizes $(h(i) : i \in [1 : l])$ to which we couple a sequence of time steps $(k(i) : i \in [1 : l])$, $k(i) = 0.1 \times h(i)$. Here, l denotes the number of runs ranging from 1 to 4 in each of the experiment. For each run, the spatial mesh size becomes half of the previous mesh size.

For each run $i \in [1 : l]$, we compute the following quantities of interest at the final time point $t_N = T = 0.1$.

- The *elliptic reconstruction error estimators*:

$$\max_{0\le n\le N} \mathscr{O}_{\mathrm{BE},2,n} \quad \text{and} \quad \left(\sum_{n=1}^{N} k_n \mathscr{O}_{\mathrm{BE},1,n}\right)^{1/2}.$$

- The *space error estimator*:

$$\sum_{n=1}^{N} k_n \mathscr{M}_{\mathrm{BE},n}.$$

- The *temporal error estimator*:

$$\sum_{n=1}^{N} k_n \mathscr{T}_{\mathrm{e,BE},n}.$$

We have dropped the *data approximation estimator* from study. The experiment is carried out with $\mathbb{P}_1$ elements. All the constants involved in the estimators are taken to be 1.

For each quantities of interest we observe its experimental order of convergence (EOC). The EOC is defined as follows: For a given finite sequence of successive runs (indexed by i), the EOC of the corresponding sequence of quantities of interest $E(i)$ (estimator or part of an estimator) itself is a sequence defined by

$$EOC(E(i)) = \frac{log(E(i+1)/E(i))}{log(h(i+1)/h(i))},$$

where $h(i)$ denotes the mesh size of the run i. The value of EOC of a given estimator indicates its order.

The numerical results at the final time point $t_N = T = 0.1$ are shown in the Tables 7.1 – 7.4.

Table 7.1: *Backward Euler elliptic reconstruction error estimator in the L^2-norm.*

l(runs)	h	k	$\max_{0\le n\le N}\mathscr{O}_{\mathrm{BE},2,n}$	EOC
1	0.125000	0.0125000	4.42127e-01	-
2	0.062500	0.0062500	1.30997e-01	1.7
3	0.031250	0.0031250	3.68663e-02	1.8
4	0.015625	0.0015625	1.01123e-02	1.8

Table 7.2: *Backward Euler elliptic reconstruction error estimator in the H^1-norm.*

l(runs)	h	k	$(\sum_{n=1}^{N} k_n \mathscr{O}_{\mathrm{BE},1,n})^{1/2}$	EOC
1	0.125000	0.0125000	8.38003e-01	-
2	0.062500	0.0062500	7.08467e-01	0.2
3	0.031250	0.0031250	3.51657e-01	1.0
4	0.015625	0.0015625	1.74902e-01	1.0

Table 7.3: *Backward Euler space error estimator.*

l(runs)	h	k	$\sum_{n=1}^{N} k_n \mathscr{M}_{\mathrm{BE},n}$	EOC
1	0.125000	0.0125000	2.92903e-01	-
2	0.062500	0.0062500	7.39044e-02	1.9
3	0.031250	0.0031250	1.86888e-02	1.9
4	0.015625	0.0015625	4.72710e-03	1.9

Table 7.4: *Backward Euler temporal error estimator.*

l(runs)	h	k	$\sum_{n=1}^{N} k_n \mathscr{T}_{\mathrm{e,BE},n}$	EOC
1	0.125000	0.0125000	1.00924e-01	-
2	0.062500	0.0062500	4.98260e-02	1.0
3	0.031250	0.0031250	2.47862e-02	1.0
4	0.015625	0.0015625	1.23662e-02	1.0

7.2 Results for Crank-Nicolson Approximation

We shall consider the same example as in Section 7.1 with $T = 0.5$. In this section, we examine the numerical behaviour of the error estimators presented in Theorem 4.2.2 for

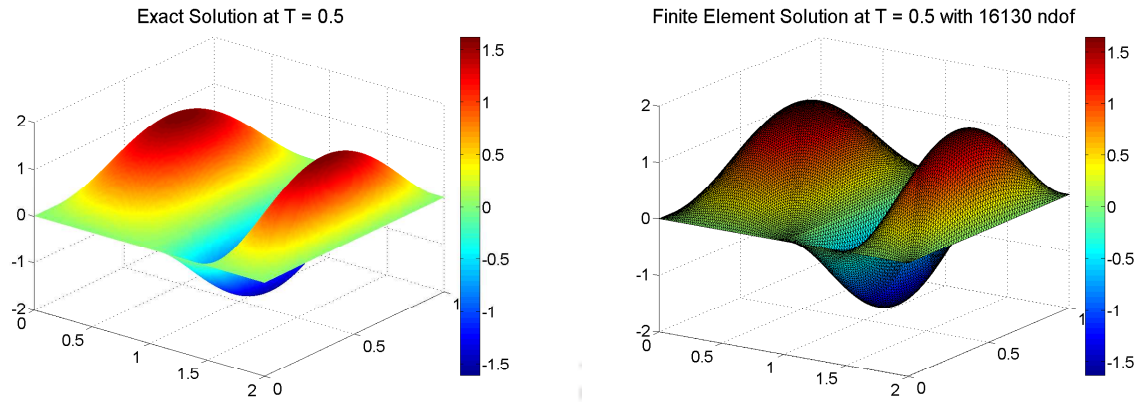

Figure 7.2: *The first plot shows the exact solution and the second one corresponds to the Crank-Nicolson FEM solution. FEM solution is computed using* $\mathbb{P}_1$ *elements with 16130 free nodes at* $T = 0.5$ *corresponding to* $k = 0.015625$.

the Crank-Nicolson approximation. We choose a sequence of mesh sizes $(h(i) : i \in [1 : l])$ to which we couple a sequence of time steps $(k(i) : i \in [1 : l])$, $k(i) = h(i)$. Here, l denotes the number of runs in each of the experiment. For each run, the spatial mesh size becomes half of the previous mesh size. For each run $i \in [1 : l]$, we compute the following quantities of interest:

- The *elliptic reconstruction error estimator*:

$$2 \max_{0 \le n \le N} \mathscr{O}_{\mathrm{CN},n}.$$

- The *space-mesh error estimator*:

$$\sum_{n=1}^{N} k_n \, \mathscr{M}_{\mathrm{CN},n}.$$

- The *temporal reconstruction error estimator*:

$$\max_{0 \le n \le N} \mathscr{T}_{\mathrm{re,CN},n}.$$

- The *space error estimator*:

$$\sum_{n=1}^{N} k_n \, \mathscr{S}_{\mathrm{CN},n}.$$

- The *temporal error estimator*:

$$\left(2 \sum_{n=1}^{N} k_n \, \mathscr{T}^2_{\mathrm{e,CN},n} \right)^{1/2}.$$

We dropped the *data approximation estimators* and *coarsening estimator* from study. The experiment is carried out with $\mathbb{P}_1$ elements. For each quantities of interest we observe its experimental order of convergence (EOC). The numerical results at the final time point $t_N = T = 0.5$ is shown in the following tables.

Table 7.5: *Crank-Nicolson elliptic reconstruction error estimator for the L^2 norm.*

l(runs)	h	k	$2\max_{0\leq n\leq N}\mathscr{O}_{\mathrm{CN},n}$	EOC
1	0.125000	0.125000	7.12016e-01	-
2	0.062500	0.062500	2.01035e-01	1.8
3	0.031250	0.031250	5.52205e-02	1.8
4	0.015625	0.015625	1.49632e-02	1.8

Table 7.6: *Crank-Nicolson space-mesh error estimator.*

l(runs)	h	k	$\sum_{n=1}^{N} k_n\,\mathscr{M}_{\mathrm{CN},n}$	EOC
1	0.125000	0.125000	6.74251e-01	-
2	0.062500	0.062500	1.81810e-01	1.8
3	0.031250	0.031250	4.89326e-02	1.8
4	0.015625	0.015625	1.31191e-02	1.8

Table 7.7: *Crank-Nicolson temporal reconstruction error estimator.*

l(runs)	h	k	$\max_{0\leq n\leq N}\mathscr{T}_{\mathrm{re},\mathrm{CN},n}$	EOC
1	0.125000	0.125000	2.51878e-01	-
2	0.062500	0.062500	3.41547e-02	2.8
3	0.031250	0.031250	6.43236e-03	2.1
4	0.015625	0.015625	1.45975e-03	2.1

Table 7.8: *Crank-Nicolson space error estimator.*

l(runs)	h	k	$\sum_{n=1}^{N} k_n \mathscr{S}_{\mathrm{CN},n}$	EOC
1	0.125000	0.125000	1.29627	-
2	0.062500	0.062500	1.87101e-01	2.7
3	0.031250	0.031250	2.61481e-02	2.8
4	0.015625	0.015625	3.58048e-03	2.8

Table 7.9: *Crank-Nicolson temporal error estimator.*

l(runs)	h	k	$2\sum_{n=1}^{N} k_n \mathscr{T}^2_{\mathrm{e,CN},n})^{1/2}$	EOC
1	0.125000	0.125000	2.63965e-01	-
2	0.062500	0.062500	4.54763e-02	2.5
3	0.031250	0.031250	8.80471e-03	2.2
4	0.015625	0.015625	1.88063e-03	2.2

7.3 Results for BDF-2 Approximation

We continue our experiment with the same Example 7.1.1 with $T = 1$ for the BDF-2 approximation and discuss the behaviour of the estimators presented in Theorem 5.3.2.

We choose a sequence of mesh sizes $(h(i) : i \in [1 : l])$ to which we couple a sequence of time steps $(k(i) : i \in [1 : l])$, $k(i) = h(i)$. Here, l denotes the number of runs in each of the experiment. For each run, the spatial mesh size becomes half of the previous mesh size. For each run $i \in [1 : l]$, we compute the following quantities of interest:

- The *elliptic reconstruction error estimator*:

$$2 \max_{0 \le n \le N} \mathscr{O}_{\mathrm{BDF},n}.$$

- The *space-mesh error estimator*:

$$k \sum_{n=1}^{N} \mathscr{M}_{\mathrm{BDF},n}.$$

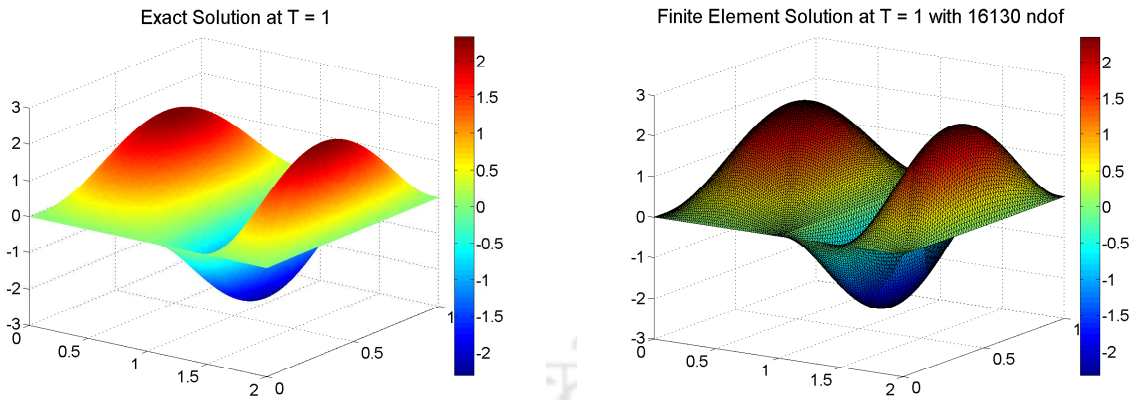

Figure 7.3: *The first plot shows the exact solution and the second one corresponds to the BDF-2 FEM solution. FEM solution is computed using* $\mathbb{P}_1$ *elements with* 16130 *free nodes at* $T = 1$ *corresponding to* $k = 0.015625$.

- The *temporal reconstruction error estimator*:

$$\max_{0\leq n\leq N} \mathscr{T}_{\mathrm{re,BDF},n}.$$

- the *space error estimator*:

$$k\sum_{n=1}^{N} \mathscr{S}_{\mathrm{BDF},n}.$$

- The *temporal error estimator*:

$$\left(2k\sum_{n=1}^{N} \mathscr{T}^2_{\mathrm{e,BDF},n}\right)^{1/2}.$$

We dropped the *data approximation estimators* and *coarsening estimator* from study. For each quantities of interest we observe its experimental order of convergence (EOC). The numerical results at the final time point $t_N = T = 1$ is shown in the following tables.

Table 7.10: *BDF-2 elliptic reconstruction error estimator.*

l(runs)	h	k	$2\max_{0\leq n\leq N}\mathscr{O}_{\mathrm{BDF},n}$	EOC
1	0.125000	0.125000	9.74194e-01	-
2	0.062500	0.062500	2.82299e-01	1.7
3	0.031250	0.031250	7.84522e-02	1.8
4	0.015625	0.015625	2.13764e-02	1.8

Table 7.11: *BDF-2 space-mesh error estimator.*

l(runs)	h	k	$k\sum_{n=1}^{N}\mathscr{M}_{\mathrm{BDF},n}$	EOC
1	0.125000	0.125000	9.60257e-01	-
2	0.062500	0.062500	2.62328e-01	1.8
3	0.031250	0.031250	7.08575e-02	1.8
4	0.015625	0.015625	1.89977e-02	1.8

Table 7.12: *BDF-2 temporal reconstruction error estimator.*

l(runs)	h	k	$\max_{0\leq n\leq N}\mathscr{T}_{\mathrm{re,BDF},n}$	EOC
1	0.125000	0.125000	2.02147e-01	-
2	0.062500	0.062500	2.72313e-02	2.8
3	0.031250	0.031250	5.10425e-03	2.1
4	0.015625	0.015625	1.15608e-03	2.1

Table 7.13: *BDF-2 space error estimator.*

l(runs)	h	k	$k\sum_{n=1}^{N}\mathscr{S}_{\mathrm{BDF},n}$	EOC
1	0.125000	0.125000	2.09685	-
2	0.062500	0.062500	3.02654e-01	2.7
3	0.031250	0.031250	4.22972e-02	2.8
4	0.015625	0.015625	5.79179e-03	2.8

Table 7.14: *BDF-2 temporal error estimator.*

l(runs)	h	k	$(2k\sum_{n=1}^{N}\mathscr{T}^2_{\mathrm{e,BDF},n})^{1/2}$	EOC
1	0.125000	0.125000	4.23807e-01	-
2	0.062500	0.062500	7.27666e-02	2.5
3	0.031250	0.031250	1.40435e-02	2.2
4	0.015625	0.015625	2.99236e-03	2.2

Numerical results for the backward Euler approximation reveal that the *elliptic reconstruction* and the *space error estimators* (Table 7.1 and Table 7.3) have nearly optimal rates of convergence in the L^2-norm. From Tables 7.2 and 7.4, we observe that the *elliptic reconstruction error estimator* in the H^1-norm and the *temporal error estimator* have optimal rates of convergence which matches with that of the error's norm.

For the Crank-Nicolson approximation, numerical results for the *elliptic reconstruction* and the *space-mesh error estimators* show the nearly optimal order convergence (cf. Table 7.5 and Table 7.6) whereas EOC shows that the *temporal reconstruction error estimator* (cf. Table 7.7), the *space error estimator* (cf. Table 7.8) and *temporal error estimator* (cf. Table 7.9) decreases with optimal order.

Finally, the numerical experiment for the BDF-2 approximation indicates nearly optimal order convergence for the *elliptic reconstruction estimator* (Table 7.10) and the *space-mesh estimator* (Table 7.11). From Tables 7.12 − 7.14, EOC of BDF-2 *temporal reconstruction error estimator*, the *space error estimator* and the *temporal error estimator* show optimal rates of convergence.

8

Conclusions and Extensions

This chapter is devoted to the critical assessment of the results highlighting the contributions made by this thesis and techniques used in deriving these. We conclude by providing some information for the scope of possible extensions and future investigations.

8.1 Critical Review of the Results

In this thesis, we have studied residual-based *a posteriori* error estimates for both the linear and semilinear parabolic interface problems in a bounded convex polygonal domain in $\mathbb{R}^2$. The interfaces are assumed to be of arbitrary shape but are smooth for our purpose. *A posteriori* error bounds in the $L^\infty(L^2)$-norm are derived for various space-time discretization methods for the parabolic interface problems. The derivation of residual-based *a posteriori* error bounds mainly rely on the approximation properties of the Clément-type interpolation operator. However, in the present case due to the discontinuity of the coefficient along the interface Γ, the solution of the parabolic interface problem is only in $H^1(\Omega)$ globally. For a higher order approximation properties of such type of operator, the analysis of [92] require $v \in H^r(\Omega), r \geq 2$ and hence the standard results can not be applied directly. One of the main focal point of this thesis is the derivation of new Clément-Type interpolation estimates (cf. Theorem 2.2.2) with low regularity condition on the function. We comment that this new approximation properties of the Clément-type interpolation operator can be used to derive *a posteriori* error bound for a wider class of time-dependent interface problems in the $L^\infty(L^2)$-norm. The critical review of the results of each chapter is presented below.

Chapter 2 studies *a posteriori* error analysis for the spatially discrete approximation for parabolic interface problem (1.1.1) – (1.1.3) in a bounded convex polygonal domain in $\mathbb{R}^2$. The essential tool used in the error analysis is the appropriate elliptic reconstruction operator. It should be mentioned that in contrast to [76] we have defined elliptic

reconstruction operator via the spatially discrete approximation (2.1.8). The elliptic reconstruction of finite element solution is used as an intermediate object to split the total error into two parts, namely the parabolic error and the elliptic error. Then the $L^\infty(L^2)$-norm *a posteriori* error bound for the main error (cf. Theorem 2.3.2) is obtained by estimating each term separately. As pointed out before, due to the low global regularity of the solution the standard approximation properties of the Clément-type interpolation operator can not be applied directly here. However, if the interface is smooth then one can expect higher local regularity property of the solution operator (cf. [33]). This higher local regularity property along with the extension results and the Sobolev embedding theorem are exploited to establish new approximation properties for the Clément-type interpolation operator. As a result of these new Clément-type approximation properties we are able to prove a reconstruction error estimates in the L^2 norm (see Lemma 2.3.1) which plays a key role in deriving *a posteriori* error bounds in the $L^\infty(L^2)$ norm for the parabolic interface problems. This reconstruction error bound permits us to obtain naturally L^2-norm *a posteriori* error bound for the elliptic interface problems. More importantly, our analysis relies only on the energy technique. Almost optimal error estimate in the $L^\infty(L^2)$-norm is established. The proposed *a posteriori* error analysis can easily be extended to treat more general parabolic interface problems.

In Chapter 3, we have studied *a posteriori* error analysis for the fully discrete backward Euler approximation for the linear parabolic interface problem (1.1.1) – (1.1.3). The essential components used in the analysis are: (i) The appropriate elliptic reconstruction of finite element solution obtained by the backward Euler approximation, and (ii) the approximation results of the Clément-type interpolation operator. We use only the energy argument to establish *a posteriori* error estimates with optimal order convergence in the $L^2(H^1)$-norm and almost optimal order in the $L^\infty(L^2)$-norms (cf. Theorem 3.2.2).

Chapter 4 is devoted to the *a posteriori* error analysis of the fully discrete Crank-Nicolson approximation for the problem (1.1.1) – (1.1.3). The space discretization uses the standard piecewise linear finite elements while we have used the Crank-Nicolson approximation for the time discretization. The *a posteriori* error estimate thus obtained is optimal in time and almost optimal order in space with respect to the $L^\infty(L^2)$-norm (cf. Theorem 4.2.2). The main technical tools used are new approximation properties of the Clémet-type interpolation operator and the quadratic (in time) space-time Crank-Nicolson reconstruction.

Chapter 5 deals with *a posteriori* error analysis for the BDF-2 approximation. In contrast to the Crank-Nicolson reconstruction, quadratic space-time BDF-2 reconstruc-

tion is nontrivial. The main crucial part is to define a linear approximation to $f(t)$ in such a way that it ultimately gives a continuous piecewise quadratic reconstruction in time (cf. (5.2.10)). Optimal order estimate in time and nearly optimal order estimate in space are established in the $L^\infty(L^2)$-norm (cf. Theorem 5.3.2). The proposed error analysis also extends the work of Akrivis *et al.* [3] for the parabolic problems with mesh modification strategy.

Chapter 6 studies *a posteriori* error estimates for the semilinear parabolic interface problems. The space discretization uses the standard piecewise linear finite elements while we have used both the backward Euler and the Crank-Nicolson approximations for the time discretization. The *a posteriori* error estimates are derived which are optimal in time and almost optimal order in space with respect to the $L^\infty(L^2)$-norm (cf. Theorem 6.2.2 and Theorem 6.3.2). The main crucial part in the error analysis is to handle the forcing term appropriately by *a posteriori* quantity. A key argument of our proof is the appropriate elliptic reconstruction operator combined with the energy technique. Other worth mentioning technicalities for our analysis are the approximation results of the Clément-type interpolation operator and a discrete version of Gronwall's lemma. The forcing term is assumed to satisfy the Lipschitz condition.

Chapter 7 is concerned with numerical assessment of the proposed estimators of Chapters $3-5$. All computations are carried out using the software MATLAB 7.8. The main emphasis is to observe the asymptotic behaviour of the estimators presented in Theorem 3.2.2, Theorem 4.2.2 and Theorem 5.3.2. Numerical experiments reveal that the estimators decrease with nearly optimal order in space and optimal order in time which validate our theoretical findings.

8.2 Extensions and Remarks

Interface problems have a wide variety of applications in science and engineering and arise naturally when two dissimilar materials interact across an interface. Despite being common, they remain intensely difficult to tackle as the discontinuity of the diffusion coefficient reduces the regularity of the solution. Therefore, the convergence analysis of these problems are some of the greatest challenges in computational mathematics today and has attracted a lot of attention over the past years. To the best of our knowledge the results presented in this thesis are reported for the first time in the context of parabolic interface problems. Now, we shall briefly outline some interesting aspects for future developments.

Interface problem in presence of an interface function. In this thesis, we have considered the problems with zero jump conditions on the interface. However, many

physical problems are characterized by interface problems with nonzero jump condition. More precisely, consider the following problem

$$u_t(x,t) - \mathrm{div}(\beta(x)\nabla u) = f(x,t) \quad \text{in} \quad \Omega \times (0,T] \tag{8.2.1}$$

with prescribed initial and boundary conditions

$$u(x,0) = u_0(x) \quad \text{in} \quad \Omega; \qquad u = 0 \quad \text{on} \quad \partial\Omega \times [0,T] \tag{8.2.2}$$

and jump conditions on the interface

$$[u] = 0, \quad \left[\beta \frac{\partial u}{\partial \mathbf{n}}\right] = g(x,t) \quad \text{across} \quad \Gamma \times [0,T]. \tag{8.2.3}$$

The existence and uniqueness of the solution of this problem can be found in [33, 61]. The main challenge in the *a posteriori* error analysis is to obtain the approximation property for the interface function $g(x,t)$. A natural extension of our work is to study *a posteriori* error analysis of (8.2.1) – (8.2.3) for various space-time finite element approximations. We believe that this new approximation properties of the Clément-type interpolation operator will play a vital role in the error analysis.

Nonlinear interface problem. Let Ω be a bounded domain in $\mathbb{R}^2$ with smooth boundary $\partial\Omega$. We consider the following nonlinear parabolic interface problem

$$u_t(x,t) + \mathcal{L}u = f(x,t) \quad \text{in} \quad \Omega \times (0,T] \tag{8.2.4}$$

with prescribed initial and boundary conditions

$$u(x,0) = u_0(x), \quad x \in \Omega; \quad u = 0 \quad \text{on} \quad \partial\Omega \times [0,T], \tag{8.2.5}$$

where the operator $\mathcal{L}$ is of the form

$$\mathcal{L}u = -\nabla \cdot (\beta(x,u)\nabla u) + a_0(x,u)u. \tag{8.2.6}$$

The functions $\beta, a_0 : \Omega \times \mathbb{R} \to \mathbb{R}$ are such that the operator $\mathcal{L}$ is strongly monotone and Lipschitz continuous. We assume that a is of the form

$$\beta(x,\xi) = \beta_k(x,\xi), \qquad x \in \Omega_k, \ \xi \in \mathbb{R}\,(k = 1,2),$$

where $\beta_k : \Omega_k \times \mathbb{R} \to \mathbb{R}$ are continuous, Ω_1 is a subset of Ω with sufficiently smooth boundary Γ and $\Omega_2 = \Omega \setminus (\Omega_1 \cup \Gamma)$. In this case, equation (8.2.4) is satisfied only for $x \in \Omega_k$, $(k = 1,2)$, and on the interface Γ the following interface conditions are prescribed

$$\begin{aligned} u_1(x,t) &= u_2(x,t), \\ \beta_1(x,u_1)\mathbf{n_1}(x) - \beta_2(x,u_2)\mathbf{n_2}(x) &= g(x,t), \end{aligned}$$

across Γ, where $u_k(x,t) = u(x,t)\mid_{\Omega_k},\ k = 1,2$ and $(\mathbf{n_1}, \mathbf{n_2})$ is the unit outer normal to interface Γ.

It will be interesting and challenging to extend the analysis of the linear interface problems to the nonlinear problems. Although some investigations concerning *a priori* error analysis have been made for the nonlinear elliptic interface problems [44, 105], but the *a posteriori* error analysis of such problem remains unexplored. The nonlinear case is far more complicated and certainly requires additional effort. We would like to explore this issue in future.

***A posteriori* error analysis of unfitted FEM.** A further extension of the present *a posteriori* analysis could be the analysis of the unfitted finite element method. In the thesis, we have only considered fitted finite element method where the discretization is done in such a way that grid points lie on the interface. Currently, one of the most difficult problem in computational science is the moving interface problems. The moving interface problems are frequently encountered in many physical applications, for instance, the Stefans problem for simulating temperature distribution undergoing a phase transition such as ice melting into water [12], modeling of the island dynamics in epitaxial growth [14], incompressible Stokes flow problems with moving interfaces [64, 99] and many more. Biological fluid dynamics is an another rich source of problems with complex geometry and frequently the interaction of fluids with moving elastic structures, e.g., the study of blood flow in the heart [84]. Different methods have been developed to tackle the situation when the interfaces changes its topology in time. One of the well known method is the unfitted finite element method. The unfitted grid methods are usually preferred as it avoids the expensive remeshing required for fitted methods to tackle moving interface problems.

***A*nisotropic *a posteriori* error analysis.** In Chapters $2-6$, *a posteriori* error bounds are derived in the isotropic setting. In an isotropic finite element method, the aspect ratio (ratio of the diameters of the circumscribed and inscribed circles of a finite element) is bounded by a constant. But, the recent literature survey reveals that this restriction on mesh can be relaxed and one can achieve a given level of accuracy with reduced degrees of freedom using anisotropic mesh [46, 72]. For this attractive features, anisotropic *a posteriori* error estimates have recently received much attention. The basic principle behind this method is to apply some postprocessing technique to approach the error gradient. Among the techniques available in the literature, Zienkiewicz-Zhu (ZZ) estimator is one of the most popular in practice. However, for interface problems it has been shown in [82, 83] through various examples that these type of estimator over-refine regions where there are no errors, and hence fails to reduce the global error. In

[28], the authors have pointed out that the gradient recovery technique is not practical for interface problems. Therefore, it seems promising to recover flux in the $H(\mathrm{div})$ conforming finite element spaces space via mixed finite element method to derive *a posteriori* error bound for parabolic interface problems using anisotropic finite element discretizations.

Computational aspect. The only omission with in the realm of this thesis is numerical study of the behaviour of the estimators of semilinear parabolic interface problems. The implementation of the estimators derived in Chapters $3-6$ in devising adaptive algorithm will be an interesting future project.

Bibliography

[1] R. A. Adams and J. J. F. Fournier, *Sobolev Spaces*, vol. 140 of Pure and Applied Mathematics, Elsevier, Amsterdam, second ed., 2003.

[2] M. Ainsworth and J. T. Oden, *A Posteriori Error Estimation in Finite Element Analysis*, Pure and Applied Mathematics, Wiley-Interscience, New York, 2000.

[3] G. Akrivis and P. Chatzipantelidis, *A posteriori error estimates for the two-step backward differentiation formula method for parabolic equations*, SIAM J. Numer. Anal., 48 (2010), pp. 109–132.

[4] G. Akrivis, C. Makridakis, and R. H. Nochetto, *A posteriori error estimates for the Crank-Nicolson method for parabolic equations*, Math. Comp., 75 (2006), pp. 511–531.

[5] G. D. Akrivis and V. A. Dougalis, *Finite difference discretizations of some initial and boundary value problems with interface*, Math. Comp., 56 (1991), pp. 505–522.

[6] J. Alberty, C. Carstensen, and S. A. Funken, *Remarks around 50 lines of matlab: short finite element implementation*, Numerical Algorithms, 20 (1999), pp. 117–137.

[7] A. Aldroubi and M. Renardy, *Energy methods for a parabolic-hyperbolic interface problem arising in electromagnetism*, Z. Angew. Math. Phys., 39 (1988), pp. 931–936.

[8] I. Babuška, *The finite element method for elliptic equations with discontinuous coefficients*, Computing, 5 (1970), pp. 207–213.

[9] I. Babuška and W. C. Rheinboldt, *A-posteriori error estimates for the finite element method*, Int. J. Numer. Meth. in Engng., 12 (1978), pp. 1597–1615.

[10] I. Babuška and W. C. Rheinboldt, *Error estimates for adaptive finite element computations*, SIAM J. Numer. Anal., 15 (1978), pp. 736–754.

[11] I. Babuška and W. C. Rheinboldt, *A posteriori error analysis of finite element solutions for one-dimensional problems*, SIAM J. Numer. Anal., 18 (1981), pp. 565–589.

[12] C. Bandle, H. Berestycki, B. Brighi, A. Brillard, M. Chipot, J.-M. Coron, C. Sbordone, I. Shafrir, V. Valente, and G. V. Caffarelli, *Elliptic and Parabolic Problems*, Progress in Nonlinear Differential Equations and their Applications, 63, Birkhäuser Verlag, Basel, 2005.

[13] R. E. Bank and A. Weiser, *Some a posteriori error estimators for elliptic partial differential equations*, Math. Comp., 44 (1985), pp. 283–301.

[14] E. Bänsch, F. Hausser, O. Lakkis, B. Li, and A. Voigt, *Finite element method for epitaxial growth with attachment-detachment kinetics*, J. Comput. Phys., 194 (2004), pp. 409–434.

[15] E. Bänsch, F. Karakatsani, and C. Makridakis, *A posteriori error control for fully discrete Crank-Nicolson schemes*, SIAM J. Numer. Anal., 50 (2012), pp. 2845–2872.

[16] J. W. Barrett and C. M. Elliott, *Fitted and unfitted finite-element methods for elliptic equations with smooth interfaces*, IMA J. Numer. Anal., 7 (1987), pp. 283–300.

[17] J. Becker, *A second order backward difference method with variable steps for a parabolic problem*, BIT, 38 (1998), pp. 644–662.

[18] A. Bergam, C. Bernardi, and Z. Mghazli, *A posteriori analysis of the finite element discretization of some parabolic equations*, Math. Comp., 74 (2005), pp. 1117–1138.

[19] C. Bernardi and R. Verfürth, *Adaptive finite element methods for elliptic equations with non-smooth coefficients*, Numer. Math., 85 (2000), pp. 579–608.

[20] S. Berrone, *Robust a posteriori error estimates for finite element discretizations of the heat equation with discontinuous coefficients*, M2AN Math. Model. Numer. Anal., 40 (2006), pp. 991–1021.

[21] D. R. Bojović and B. S. Jovanović, *Convergence of a finite difference method for solving 2D parabolic interface problems*, J. Comput. Appl. Math., 236 (2012), pp. 3605–3612.

[22] J. H. Bramble and J. T. King, *A finite element method for interface problems in domains with smooth boundaries and interfaces*, Adv. Comput. Math., 6 (1996), pp. 109–138.

[23] J. H. Bramble, J. E. Pasciak, P. H. Sammon, and V. Thomée, *Incomplete iterations in multistep backward difference methods for parabolic problems with smooth and nonsmooth data*, Math. Comp., 52 (1989), pp. 339–367.

[24] S. C. Brenner and L. R. Scott, *The Mathematical Theory of Finite Element Methods*, vol. 15 of Texts in Applied Mathematics, Springer, New York, third ed., 2008.

[25] M. Brera, J. W. Jerome, Y. Mori, and R. Sacco, *A conservative and monotone mixed-hybridized finite element approximation of transport problems in heterogeneous domains*, Comput. Methods Appl. Mech. Engrg., 199 (2010), pp. 2709–2770.

[26] F. Brezzi, J. Rappaz, and P.-A. Raviart, *Finite-dimensional approximation of nonlinear problems. I. Branches of nonsingular solutions*, Numer. Math., 36 (1980), pp. 1–25.

[27] Z. Cai, X. Ye, and S. Zhang, *Discontinuous Galerkin finite element methods for interface problems: a priori and a posteriori error estimations*, SIAM J. Numer. Anal., 49 (2011), pp. 1761–1787.

[28] Z. Cai and S. Zhang, *Recovery-based error estimator for interface problems: Conforming linear elements*, SIAM J. Numer. Anal., 47 (2009), pp. 2132–2156.

[29] A. Cangiani, E. H. Georgoulis, and M. Jensen, *Discontinuous Galerkin methods for mass transfer through semipermeable membranes*, SIAM J. Numer. Anal., 51 (2013), pp. 2911–2934.

[30] A. Cangiani and R. Natalini, *A spatial model of cellular molecular trafficking including active transport along microtubules*, J. Theoret. Biol., 267 (2010), pp. 614–625.

[31] C. Carstensen, *Interface problems in viscoplasticity and plasticity*, SIAM J. Math. Anal., 25 (1994), pp. 1468–1487.

[32] Z. Chen and J. Feng, *An adaptive finite element algorithm with reliable and efficient error control for linear parabolic problems*, Math. Comp., 73 (2004), pp. 1167–1193.

[33] Z. Chen and J. Zou, *Finite element methods and their convergence for elliptic and parabolic interface problems*, Numer. Math., 79 (1998), pp. 175–202.

[34] K. Chrysafinos and L. S. Hou, *Error estimates for semidiscrete finite element approximations of linear and semilinear parabolic equations under minimal regularity assumptions*, SIAM J. Numer. Anal., 40 (2002), pp. 282–306.

[35] P. G. Ciarlet, *The Finite Element Method for Elliptic Problems*, vol. 40 of Classics in Applied Mathematics, SIAM, Philadelphia, 2002.

[36] R. Dautray and J.-L. Lions, *Mathematical Analysis and Numerical Methods for Science and Technology, Evolution problems. I*, Springer-Verlag, Berlin, 1992. Vol. 5.

[37] B. Deka and R. K. Sinha, *$L^\infty(L^2)$ and $L^\infty(H^1)$ norms error estimates in finite element method for linear parabolic interface problems*, Numer. Funct. Anal. Optim., 32 (2011), pp. 267–285.

[38] W. Dörfler and M. Rumpf, *An adaptive strategy for elliptic problems including a posteriori controlled boundary approximation*, Math. Comp., 67 (1998), pp. 1361–1382.

[39] K. Eriksson and C. Johnson, *An adaptive finite element method for linear elliptic problems*, Math. Comp., 50 (1988), pp. 361–383.

[40] ——, *Adaptive finite element methods for parabolic problems. I. A linear model problem*, SIAM J. Numer. Anal., 28 (1991), pp. 43–77.

[41] ——, *Adaptive finite element methods for parabolic problems. II. Optimal error estimates in $L_\infty(L_2)$ and $L_\infty(L_\infty)$*, SIAM J. Numer. Anal., 32 (1995), pp. 706–740.

[42] ——, *Adaptive finite element methods for parabolic problems. IV. Nonlinear problems*, SIAM J. Numer. Anal., 32 (1995), pp. 1729–1749.

[43] R. S. Falk and S. W. Walker, *A mixed finite element method for EWOD that directly computes the position of the moving interface*, SIAM J. Numer. Anal., 51 (2013), pp. 1016–1040.

[44] M. Feistauer and A. Ženíšek, *Finite element solution of nonlinear elliptic problems*, Numer. Math., 50 (1987), pp. 451–475.

[45] H. Feng and L.-j. Shen, *The finite element method for semilinear parabolic equations with discontinuous coefficients*, J. Comput. Mathematics, 17 (1999), pp. 191–198.

[46] L. Formaggia and S. Perotto, *New anisotropic a priori error estimates*, Numer. Math., 89 (2001), pp. 641–667.

[47] D. Gilbarg and N. S. Trudinger, *Elliptic Partial Differential Equations of Second Order*, Springer-Verlag, Berlin-New York, 1977.

[48] V. Girault and P.-A. Raviart, *Finite Element Methods for Navier-Stokes Equations*, vol. 5 of Springer Series in Computational Mathematics, Springer-Verlag, Berlin, 1986.

[49] Y. Gong, B. Li, and Z. Li, *Immersed-interface finite-element methods for elliptic interface problems with nonhomogeneous jump conditions*, SIAM J. Numer. Anal., 46 (2008), pp. 472–495.

[50] P. Grisvard, *Elliptic Problems in Nonsmooth Domains*, vol. 24 of Monographs and Studies in Mathematics, Pitman, Boston, MA, 1985.

[51] W. Hackbusch, *Elliptic Differential Equations*, vol. 18 of Springer Series in Computational Mathematics, Springer-Verlag, Berlin, 1992.

[52] A. Hansbo and P. Hansbo, *An unfitted finite element method based on Nitsche's method for elliptic interface problems*, Comput. Methods Appl. Mech. Engrg., 191 (2002), pp. 5537–5552.

[53] G. H. Hardy, J. E. Littlewood, and G. Pólya, *Inequalities*, Cambridge Mathematical Library, Cambridge University Press, Cambridge, 1988.

[54] S. Hou and X.-D. Liu, *A numerical method for solving variable coefficient elliptic equation with interfaces*, J. Comput. Phys., 202 (2005), pp. 411–445.

[55] J. Huang and J. Zou, *Some new a priori estimates for second-order elliptic and parabolic interface problems*, J. Differential Equations, 184 (2002), pp. 570–586.

[56] B. S. Jovanović and L. G. Vulkov, *Finite difference approximation of strong solutions of a parabolic interface problem on disconnected domains*, Publ. Inst. Math. (Beograd) (N.S.), 84(98) (2008), pp. 37–48.

[57] ——, *Formulation and analysis of a parabolic transmission problem on disjoint intervals*, Publ. Inst. Math. (Beograd) (N.S.), 91(105) (2012), pp. 111–123.

[58] R. B. Kellogg, *On the Poisson equation with intersecting interfaces*, Applicable Anal., 4 (1974/75), pp. 101–129.

[59] N. Kopteva and T. Linss, *Maximum norm a posteriori error estimation for parabolic problems using elliptic reconstructions*, SIAM J. Numer. Anal., 51 (2013), pp. 1494–1524.

[60] I. Kyza and C. Makridakis, *Analysis for time discrete approximations of blow-up solutions of semilinear parabolic equations*, SIAM J. Numer. Anal., 49 (2011), pp. 405–426.

[61] O. A. Ladyženskaja, V. A. Solonnikov, and N. N. Ural′ceva, *Linear and Quasilinear Equations of Parabolic Type*, Translated from the Russian by S. Smith. Translations of Mathematical Monographs, Vol. 23, American Mathematical Society, 1968.

[62] O. Lakkis and C. Makridakis, *Elliptic reconstruction and a posteriori error estimates for fully discrete linear parabolic problems*, Math. Comp., 75 (2006), pp. 1627–1658.

[63] M.-N. Le Roux, *Semidiscretization in time for parabolic problems*, Math. Comp., 33 (1979), pp. 919–931.

[64] R. J. LeVeque and Z. Li, *Immersed interface methods for Stokes flow with elastic boundaries or surface tension*, SIAM J. Sci. Comput., 18 (1997), pp. 709–735.

[65] R. J. LeVeque and Z. L. Li, *The immersed interface method for elliptic equations with discontinuous coefficients and singular sources*, SIAM J. Numer. Anal., 31 (1994), pp. 1019–1044.

[66] J. Li, H. Yang, and E. Machorro, *Recent Advances in Scientific Computing and Applications*, vol. 586 of Contemporary Mathematics, American Mathematical Society, 2013.

[67] Z. Li and K. Ito, *Maximum principle preserving schemes for interface problems with discontinuous coefficients*, SIAM J. Sci. Comput., 23 (2001), pp. 339–361.

[68] ——, *The immersed Interface Method*, vol. 33 of Frontiers in Applied Mathematics, SIAM, Philadelphia, PA, 2006.

[69] Z. Li, T. Lin, and X. Wu, *New Cartesian grid methods for interface problems using the finite element formulation*, Numer. Math., 96 (2003), pp. 61–98.

[70] Z. Li, W.-C. Wang, I.-L. Chern, and M.-C. Lai, *New formulations for interface problems in polar coordinates*, SIAM J. Sci. Comput., 25 (2003), pp. 224–245.

[71] X.-D. Liu, R. P. Fedkiw, and M. Kang, *A boundary condition capturing method for Poisson's equation on irregular domains*, J. Comput. Phys., 160 (2000), pp. 151–178.

[72] A. Lozinski, M. Picasso, and V. Prachittham, *An anisotropic error estimator for the Crank-Nicolson method: application to a parabolic problem*, SIAM J. Sci. Comput., 31 (2009), pp. 2757–2783.

[73] G. Lumer and L. Weis, *Evolution Equations and Their Applications in Physical and Life sciences*, vol. 215 of Lecture Notes in Pure and Applied Mathematics, New York, 2001.

[74] M. Luskin and R. Rannacher, *On the smoothing property of the Crank-Nicolson scheme*, Applicable Anal., 14 (1983), pp. 117–135.

[75] R. C. MacCamy and M. Suri, *A time-dependent interface problem for two-dimensional eddy currents*, Quart. Appl. Math., 44 (1987), pp. 675–690.

[76] C. Makridakis and R. H. Nochetto, *Elliptic reconstruction and a posteriori error estimates for parabolic problems*, SIAM J. Numer. Anal., 41 (2003), pp. 1585–1594.

[77] J. T. Marti, *Introduction to Sobolev Spaces and Finite Element Solution of Elliptic Boundary Value Problems*, Computational Mathematics and Applications, Academic Press, London, 1986.

[78] R. Massjung, *An unfitted discontinuous Galerkin method applied to elliptic interface problems*, SIAM J. Numer. Anal., 50 (2012), pp. 3134–3162.

[79] W. McLean and V. Thomée, *Numerical solution of an evolution equation with a positive-type memory term*, J. Austral. Math. Soc. Ser. B, 35 (1993), pp. 23–70.

[80] T. Miyazaki, *Water Flow in Soils*, CRC Press, 2006.

[81] B. F. Nielsen, *Finite element discretizations of elliptic problems in the presence of arbitrarily small ellipticity: an error analysis*, SIAM J. Numer. Anal., 36 (1999), pp. 368–392.

[82] J. S. Ovall, *Fixing a " bug" in recovery-type a posteriori error estimators, technical report 25*, Max-Planck-Institute fur Mathematick in den Naturwissenschaften, Bonn, Germany, (2006).

[83] ——, *Two dangers to avoid when using gradient recovery methods for finite element error estimation and adaptivity, technical report 6*, Max-Planck-Institute fur Mathematick in den Naturwissenschaften, Bonn, Germany, (2006).

[84] C. S. Peskin, *Numerical analysis of blood flow in the heart*, J. Computational Phys., 25 (1977), pp. 220–252.

[85] D. Peterseim, *Composite finite elements for elliptic interface problems*, Math. Comp., 83 (2014), pp. 2657–2674.

[86] M. Picasso, *Adaptive finite elements for a linear parabolic problem*, Comput. Methods Appl. Mech. Engrg., 167 (1998), pp. 223–237.

[87] A. Quarteroni and A. Valli, *Numerical Approximation of Partial Differential Equations*, vol. 23 of Springer Series in Computational Mathematics, Springer-Verlag, Berlin, 1994.

[88] R. Rannacher, *Adaptive Galerkin finite element methods for partial differential equations*, J. Comput. Appl. Math., 128 (2001), pp. 205–233.

[89] X. Ren and J. Wei, *On a two-dimensional elliptic problem with large exponent in nonlinearity*, Trans. Amer. Math. Soc., 343 (1994), pp. 749–763.

[90] A. Reusken and T. H. Nguyen, *Nitsche's method for a transport problem in two-phase incompressible flows*, J. Fourier Anal. Appl., 15 (2009), pp. 663–683.

[91] A. Schmidt and K. G. Siebert, *ALBERT—software for scientific computations and applications*, Acta Math. Univ. Comenian. (N.S.), 70 (2000), pp. 105–122.

[92] L. R. Scott and S. Zhang, *Finite element interpolation of nonsmooth functions satisfying boundary conditions*, Math. Comp., 54 (1990), pp. 483–493.

[93] R. K. Sinha and B. Deka, *Optimal error estimates for linear parabolic problems with discontinuous coefficients*, SIAM J. Numer. Anal., 43 (2005), pp. 733–749.

[94] ——, *An unfitted finite-element method for elliptic and parabolic interface problems*, IMA J. Numer. Anal., 27 (2007), pp. 529–549.

[95] ——, *Finite element methods for semilinear elliptic and parabolic interface problems*, Appl. Numer. Math., 59 (2009), pp. 1870–1883.

[96] E. M. Stein, *Singular Integrals and Differentiability Properties of Functions*, Princeton Mathematical Series, No. 30, Princeton University Press, Princeton,, 1970.

[97] V. Thomée, *Galerkin Finite Element Methods for Parabolic Problems*, vol. 25 of Springer Series in Computational Mathematics, Springer-Verlag, Berlin, second ed., 2006.

[98] V. Thomée and L. Wahlbin, *On Galerkin methods in semilinear parabolic problems*, SIAM J. Numer. Anal., 12 (1975), pp. 378–389.

[99] C. Tu and C. S. Peskin, *Stability and instability in the computation of flows with moving immersed boundaries: a comparison of three methods*, SIAM J. Sci. Statist. Comput., 13 (1992), pp. 1361–1376.

[100] R. Verfürth, *A Review of A Posteriori Error Estimation and Adaptive Mesh-Refinement Techniques*, Wiley and Teubner Mathematics, 1996.

[101] R. Verfürth, *A posteriori error estimates for finite element discretizations of the heat equation*, Calcolo, 40 (2003), pp. 195–212.

[102] H. Wei, L. Chen, Y. Huang, and B. Zheng, *Adaptive mesh refinement and superconvergence for two-dimensional interface problems*, SIAM J. Sci. Comput., 36 (2014), pp. A1478–A1499.

[103] M. F. Wheeler, *A priori L_2 error estimates for Galerkin approximations to parabolic partial differential equations*, SIAM J. Numer. Anal., 10 (1973), pp. 723–759.

[104] P. Wissgott, *A Space-Time Adaptive Algorithm for Linear Parabolic Problems*, Diploma Thesis, TU Vienna, 2007.

[105] A. Ženíšek, *The finite element method for nonlinear elliptic equations with discontinuous coefficients*, Numer. Math., 58 (1990), pp. 51–77.

[106] Q. Zhang and W. Sun, *A numerical study of air-vapor-heat transport through textile materials with a moving interface*, J. Comput. Appl. Math., 236 (2011), pp. 819–833.